The Stable Isotopic Variations and the Hydrogeology of the Coronet Peak Skifield, Queenstown.

A thesis
submitted in partial fulfilment
of the requirements for the degree
of
Master of Science in Engineering Geology
at the
University of Canterbury
by

DANNIELLE MARIE BELCHER

Frontispiece: A photo of Coronet Peak looking towards the north, taken from the Coronet Peak road on 20/07/2009.

Abstract

This study aims to investigate the stable isotopic characteristics of meteoric and ground waters, and to obtain spring flow rates in the Coronet Peak Skifield, Queenstown. Spring flows were gathered during the winters of 2008 and 2009, whilst water samples were collected from precipitation, springs, reservoirs and groundwater during July, August and September 2009. The spring flows were examined and the water samples were analysed for δD and $\delta^{18}O$ values using the CF-IRMS at the University of Canterbury.

A database has been gathered from all natural water sources to give a local meteoric water line (LMWL) for the area that fits clearly with the global meteoric water line. The LMWL has an R^2 value of 0.97 and the equation is $\delta D = 8\ \delta^{18}O + 10$. An understanding of evaporation as it occurs in the water storage reservoirs of the mountain has also been obtained, giving rise to a local evaporation line.

The stable isotope ratios of hydrogen and oxygen within precipitation have been used extensively to characterise the hydrogeology with emphasis on altitude effects, storm duration and variations in storm track trajectories. Of these three phenomena, it is the trajectory of the storm track that is best shown to affect the composition of precipitation in this area. The air masses advancing on the study area from the north being more depleted in their isotopic signatures, with approximate δD and $\delta^{18}O$ values of –130‰ and -16‰. The air masses approaching from a southerly direction are more positive in comparison, having approximate δD and $\delta^{18}O$ values of –65‰ and -9‰.

The altitude effect in precipitation on the Skifield has led to an altitude gradient being found: for every 100-metre increase in elevation, $\delta^{18}O$ decreases by 0.71‰. However there were some inconsistencies. The influence on precipitation from storm duration is also inconsistent in this area. The R^2 values range from 0.14 to 0.99, but this method does not take into account the position of the individual samples. Some samples did not plot in the expected order that is governed by a decrease in stable isotopic ratios with storm duration.

The stable isotopic compositions within meteoric waters can be used as tracers of water sources. The isotope date of the springs also infers an altitude effect. The

springs gave an altitude gradient of a decrease –0.43‰ with each 100-metre increase in elevation. This indicates that precipitation is the main influence on the stable isotopic composition of the springs in this area. However, data shows differences between the current precipitation and the groundwater compositions, indicating that present precipitation is not flowing from the springs, past precipitation is. The stable isotopic compositions of the springs have also been correlated with groundwater isotope data and suggest the sources of the springs are groundwater dominated. Although some springs compositions indicate an influence by current precipitation. This is shown by a negative stable isotopic trend in the precipitation sampled in August, corresponding with a relatively negative stable isotopic composition in some springs during this time period.

Monitoring of spring flows on Coronet Peak have led to an average winter flow rate being established of 26.5 litres per second. Spring flow rates range from 0.25 – 6 litres per second. This monitoring has indicated the springs of the greatest yield that are not already being utilised on the Skifield. It is these springs that should be further investigated as to whether they would provide a sustainable source of water on the mountain. This locally derived water would then be utilised for the purposes of artificial snowmaking and other activities and amenities that are currently operated by NZ Ski on Coronet Peak.

List of Figures

List of Tables

List of Equations

Acknowledgments

I would like to thank everyone that had a role to play in the completion of this thesis. Especially:

To my supervisors David Bell and Travis Horton, who provided encouragement throughout my thesis and who also bestowed unparalleled advice and showed great patience whilst editing my chapters. Also my sincerest thanks goes to the administration staff in the Department of Geology, Pat and Janet, and in the College of Science, for always being willing to help a poor student deal with the paper work, especially in the case of the suspension of my thesis. The technical team also came to my aid many times with last minute equipment requests, which were all dealt with kindly and efficiently, I always had everything I needed, with special thanks going to Vanessa Tappenden, Cathy Higgins and Chris Grimshaw. I would also like to thank Travis Horton once again, for the very precise stable isotope analyses of my water samples.

Thank you to my office mates during the past two years, especially to Hanna Donders for your invaluable input, and Angela Doherty, you both made this whole experience worthwhile and kept me sane at the same time. Also to, Jeremy O'Brien, Matthew Clark and Matthew Fitzmaurice, for putting up with my increasing silence over the last few months.

To the staff of NZ Ski working on the Coronet Peak Skifield, thank you for all of your help and support over the duration of this thesis, especially to Nick Edwards, Peter Duart, Garry Steedman and those of you who monitored the springs for me. Thank you to James Hadley and Will Oswald of Hadley Consultants Limited, Queenstown, and to Royden Thomson, for the use of your resources and the help you gave me during this experience. Also to the managers Jo and Buzz, and the owners of the Gobblers Lodge up on the mountain, thank you for accommodating me during my visits to Coronet Peak, it was the best thing to come back after a day of slogging through the snow to a nice warm fire and a friendly face.

Last and not least, I would like to thank my family for all of the support and encouragement they gave me during the last two years, especially mum and dad, you

have always helped me grow in every way, allowing me to stand on my own two feet, but then also letting me lean on you when things became difficult. To my best friend Genevieve Taylor, thank you for all of your unending support and willingness to drink with me when it needed to be done. Thank you to my other flatmates, Patrick, Julia and Ronald, who never complained when I was hardly there and if I was there I would be in my room trying to do some work, the way you guys made me laugh has been such a gift during this stressful time. And last of all I'd like to give a special thanks to James Tod, for putting up with me even though it may have seemed that I was going a little crazy, you played the biggest part in keeping me sane and helped me to laugh at myself, thank you.

Table of Contents

Chapter One:

Introduction

1.1. Background Statement

Coronet Peak Skifield is located 18 kilometres from Queenstown, New Zealand, as shown in Figure 1.1. The skifield is approximately 280 hectares in area. The skifield itself has a range in elevation from 1100 to 1651 metres above sea level located on Coronet Peak itself. This is relatively low for a skifield at this latitude, and requires water storage for artificial snowmaking. The skifield is owned and managed by NZ Ski Limited, and the ski season normally extends from June to early September.

Figure 1.1: Map of the South Island of New Zealand with the area of Coronet Peak located by the white square; the inset is a zoom in of the area (main satellite image from NASA, 2007, insert from Google, 2009).

The basement rocks of the area of metamorphic in origin, namely schist and gneiss of varying grades: the bedrock of Coronet Peak being schist. The Coronet Peak Skifield is located almost entirely on the Coronet Peak Landslide (Figure 1.2). The volume of the landslide is estimated to be 1 x 10^9 cubic metres. The Coronet Peak Landslide is a foliation-controlled failure in low rank chlorite schist, with thicknesses of the order of 60-70 metres. The hummocky terrain (shown in Figure 1.3) is characterised by springs and large schist blocks forming depressions, which makes this environment suited to be a skifield. Below the skifield to an approximate elevation of 880 metres above sea level is the Recreation Reserve See Figure 1.4. Below this point the mountain becomes farmland.

Figure 1.2. The Coronet Peak Landslide, the black lines represent a rough outline of the landslide, the white lines represent the toe of the slide, whilst the red lines show prominent scarps (adapted from Willetts, 2000).

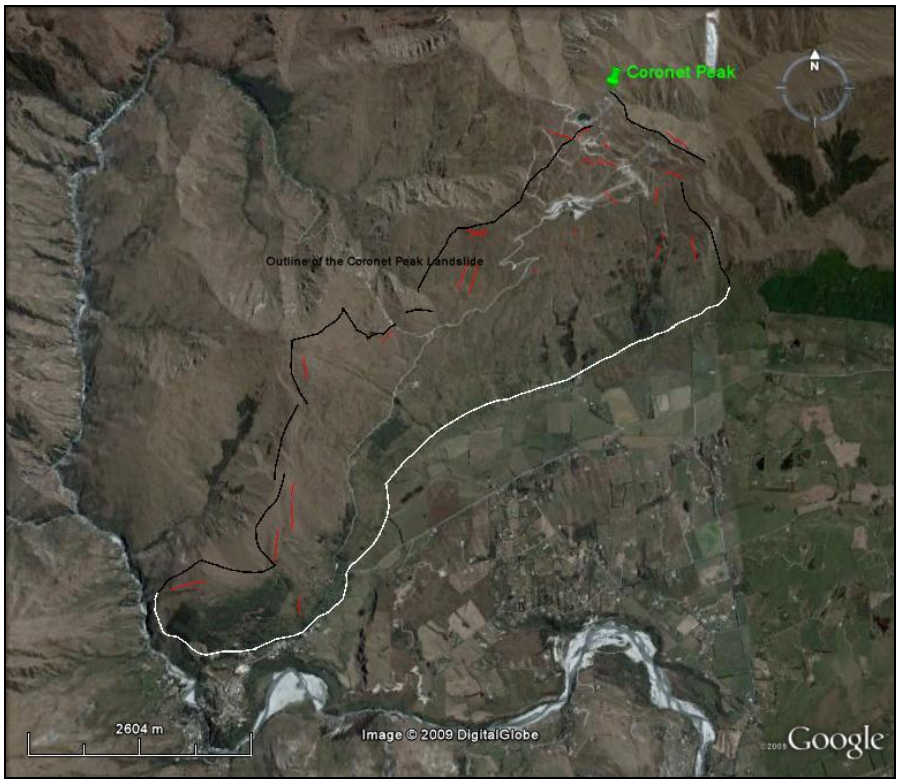

Figure 1.3. The hummocky terrain of Coronet Peak. A) Looking up towards to skifield in a north-easterly direction. B) Looking south-west down onto the lower slopes of the Coronet Peak Landslide beyond the skifield, Coronet Peak Road is located in the foreground. Both photos taken on the 03/03/2008.

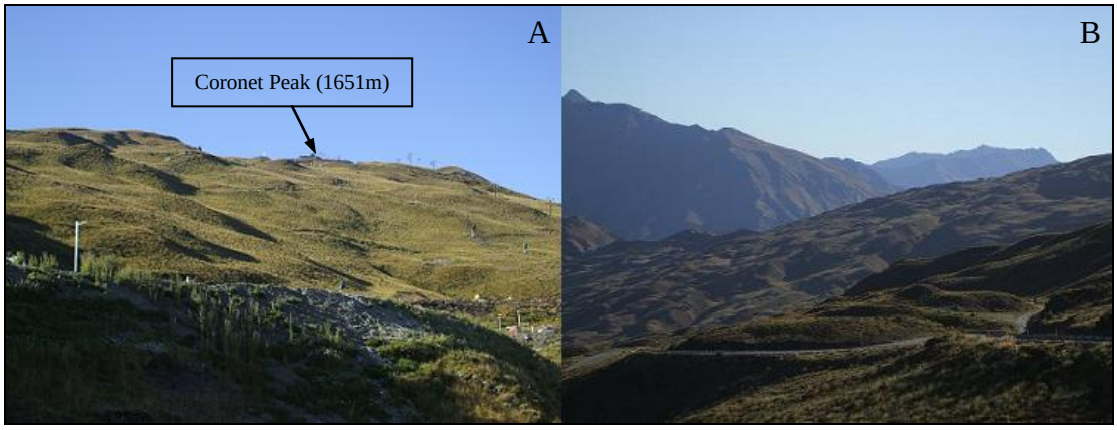

Figure 1.4. A Google Earth image of the Coronet Peak Skifield area boundary (green outline) and the Recreation Reserve (above the white line).

The aquifers present within the Coronet Peak Landslide beneath the Skifield and Recreation Reserve are interpreted to be located in areas where groundwater can accumulate and flow freely into. Groundwater has been located via a drilling program at three depths beneath Coronet Peak: approximately 40, 56-63 and 130 metres below

the level of the ground where has drilling occurred. Therefore, it is interpreted that there are three aquifers beneath Coronet Peak, two within the landslide and one under it (the deepest). The main recharge mechanism for the upper two aquifers is the infiltration of precipitation. The aquifer within the in situ bedrock is most likely comprised of deep groundwater, however there will be some interaction with and through the landslide interface: recharge could also occur this way through small faults that act as passageways for water. The groundwater within the bedrock may flow through defects and accumulate within the schist.

The surface waters of Coronet Peak consist of springs and water storage reservoirs. The springs exist as the discharge points of groundwater at the surface, indicating a healthy aquifer system. The reservoirs store water for the purposes of snowmaking and are mostly composed of groundwater, with some spring and precipitation contributions. Figure 1.5 below indicates the meteoric waters from all available sources on Coronet Peak and which contribute to the reservoirs.

Figure 1.5. The meteoric water sources that contribute to the water storage reservoirs.

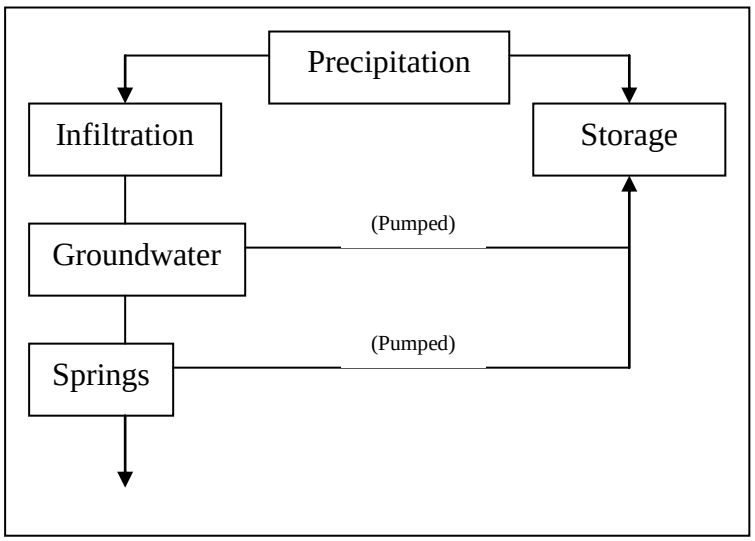

Since 2007, the Coronet Peak Skifield has been undergoing a developing program in which water reservoirs have been built in order to provide adequate water supply to a newly built Base Hut and other services, as well as the new snow guns (installation was completed in 2008). This development has allowed the Coronet Peak Skifield to compete in an ever-changing global and local climate with the other, higher altitude skifields in the area, like the Remarkables, Cardrona and Mt Aspiring.

The stable isotopes of hydrogen and oxygen within the meteoric waters of Coronet Peak can be used to better understand the relationship between the surface and groundwater of the area. Using the stable isotope technique of Isotope Ratio Mass Spectrometry, the ratios of these two elements, δD and $\delta^{18}O$, have been identified within the precipitation that falls on Coronet Peak, the springs located on the mountain, the groundwater collected from the two pumping bores of the skifield and the five surface reservoirs used for water storage. This information can help NZ Ski Limited by attaining a better understanding of the hydrogeology of Coronet Peak. This will allow the maximum utilisation of the natural water resources available to the Skifield for artificial snowmaking. The use of snow guns can extend the ski season by increasing the thickness and quality of the snow base on the Skifield.

1.2. Thesis Objectives

The primary objectives for this thesis are:

a) To determine the stable isotopic signatures and trends of the precipitation that falls during the period of July to September 2009 over Coronet Peak, including the skifield, Recreational Reserve and down to the base of the mountain.
b) To analyse and critically review the isotopic composition using δD and $\delta^{18}O$ of the natural springs that occur on the mountain and the groundwater collected from boreholes.
c) To create a Local Meteoric Water Line for the Coronet Peak area using the stable isotopic data collected from all water sources of Coronet Peak.
d) To link stable isotopic signatures of precipitation events on Coronet Peak with specific storm track trajectories.
e) To identify long-term management requirements for artificial snowmaking in terms of water sources and variability.

1.3. Description of Study Area

1.3.1. *Topography*

The topography of the Coronet Peak Skifield is very hummocky, typical of a landslide environment. The highest point in the study area is the very top of the peak that houses a viewing tower as well as meteorological equipment. The lowest point of spring sampling occurs at the beginning of the Coronet Peak Recreation Reserve at 879 metres, however, there is one precipitation sampling site at a lower elevation that this at 450 metres above sea level (the base of the mountain). The slopes of the Skifield are typically between 15-25°, with the scarps being subdued. The streams are incised and often impeded; they therefore follow the contours of schist blocks within the landslide debris (Willetts, 2000). A good example of this is the Tussock Spring; a photo showing the clear dog-leg in the spring flow is located in Appendix E.

1.3.2. *Climate*

The climate of Coronet Peak is one of extremes. The mountain has an average summer (December 2008 to February 2009) temperature of 14.6˚ where the skifield has been recently turned into a mountain bike park, it then drops to an average winter (June to August 2008) temperature of 4.8˚ when Coronet Peak becomes a world famous skifield. The annual rainfall is 730 millimetres. Temperatures and rainfall are an average of data collected by NIWA, 2009 (National Institute for Water and Atmospheric Research) over the last 30 years. Some of the precipitation will infiltrate the ground surface to feed the aquifers and springs, though this will possibly not happen during the winter and early spring as the ground will be frozen. It is also at this time where Coronet Peak Skifield staff believe some of the springs stop flowing because they are also frozen, however only the higher elevation springs stop flowing entirely.

The prevailing wind direction for New Zealand is a westerly, this is due to the atmospheric circulation of heat and moisture and the position of New Zealand on the globe. During the summer months is south-westerly or westerly, while in winter the wind blows predominantly from the north-east. The Queenstown Airport is located at an elevation of 358 metres above sea level and experiences mainly light winds, less than 10 knots, due to the sheltered nature of the area (New Zealand Meteorological Service, 1983). However wind speeds increase exponentially with altitude and

therefore Coronet Peak would experience much faster wind speeds than this (Whiteman, 2000).

1.3.3. *Vegetation*

The vegetation on Coronet Peak ranges from forest covered slopes (lower mountain) to sparse alpine vegetation with few trees and mostly tussocks. Any vegetation that occurs within the Coronet Peak Skifield and Recreation Reserve other than tussock tends to occur in close proximity to the springs located here where water is abundant and is typically small shrubs and bushes. The vegetation on Coronet Peak can be an indicator of spring locations or near surface water sources as seen in the Figure 1.6 below.

Figure 1.6: Vegetation around the ponding area of the flows from the Cattlestop and Swamp Springs, and the flow from the Wired Spring is also picked out by vegetation (image created using Google Earth, 2009).

1.3.4. *Existing landuse on the mountain*

The existing landuse of Coronet Peak is varied. The lower part of the peak (below 880 metres) is generally utilised as farm land, typically sheep farming, with two houses built close to Coronet Peak Road and another two are proposed and are in consultation with the local council. Above this height it becomes the Coronet Peak Recreation Reserve and above this at approximately 1100 metres elevation it becomes the Coronet Peak Skifield. Here, there are a variety of users of the area, skiers for the most part however only in winter, mountain bikers use the skifield during the summer months, while walkers and paragliders use the mountain all year round. There are also five ski huts built within the skifield that can be used throughout the year to house approximately 75 people at one time.

There are areas within the Coronet Peak Skifield that are suited to store water because of the natural topography of the Coronet Peak Landslide. The hummocky landscape the landslide provides has allowed NZ Ski (the operator of the skifield) to construct water reservoirs on the mountain. There are currently five reservoirs on Coronet Peak that store meteoric water. The water is pumped through subterranean pipes to the snow guns on the skifield to create artificial snow. The snow guns are utilised in times where the natural snowfall is not enough to allow the skifield to remain open. Table 1 below shows the volume of each of the reservoirs situated on Coronet Peak, Queenstown.

Table 1.1. Reservoir storage volumes within Coronet Peak Skifield.

Reservoir	Volume (m^3)
1 - Main	80,000
1b -Elephant Pit	19,000
2 - Lower	4,000
3 - Rocky Gully	93,000
5 - Sarah Sue	47,000
Total	**243,000**

1.4. Background Geology: Wakatipu Basin Setting.

Coronet Peak is located on the borders of the Wakatipu Basin where the basement rock is the Otago Schist.

Fig. 1.7. Photo of Otago Schist collected from Coronet Peak (04/11/2009).

The Otago Schist consists of different facies, namely pelitic, greenschist (chlorite) and quartzofeldspathic lithologies, and is a sub-group of the more copious Haast Schist. Schists are a metamorphic rock, where the type of foliation that gives them their name, schistosity, dominates them. The schistosity can be seen in the above figure by the parallel banding.

The specific lithologies of metamorphic rocks are determined by the parent rock they are formed from. The parent rock of the Otago Schist is a group sedimentary rocks composed of intermittent sandstones and mudstones with a small component of volcanic material. These sedimentary rocks are known as the Torlesse and Caples Terranes, which can only be distinguished from each other within the Haast Schist by geochemistry (Craw, 1984). The Torlesse and Caples Terranes were formed between the Permian and the Cretaceous periods (approximately between 270 – 60 million years ago). Metamorphism began in the Permian with the first phase of the Rangitata Orogeny due to the collision of the Torlesse and Caples Terranes (Wood, 1978). There have been several episodes of metamorphism, both local and regional in nature, giving rise to very complex metamorphic imprints in the Haast Schist. See figure 1.8 below for a geological map of the region.

Figure 1.8. Geological map, 1:250,000 map number 18, “Wakatipu”, Turnbull, 2000. For a full key, see Turnbull, 2000, main rock types for study are: **Q1a**-Peat swamp deposits with interbedded sand, mud and gravels, alluvial fans and valley alluvium, and modern to post glacial flood plains. **Q2t**-Undifferentiated till. **Q2a**-Associated outwash gravel from valley glaciers, associated fan gravels and alluvium in low terraces in non-glaciated catchments. **Yai**-Pelitic schist, variable segregated veined and foliated includes extensive greenschist bands and thinner horizons (**Yag**). **Yc**-Volcaniclastic sandstone and siltstone, undifferentiated.

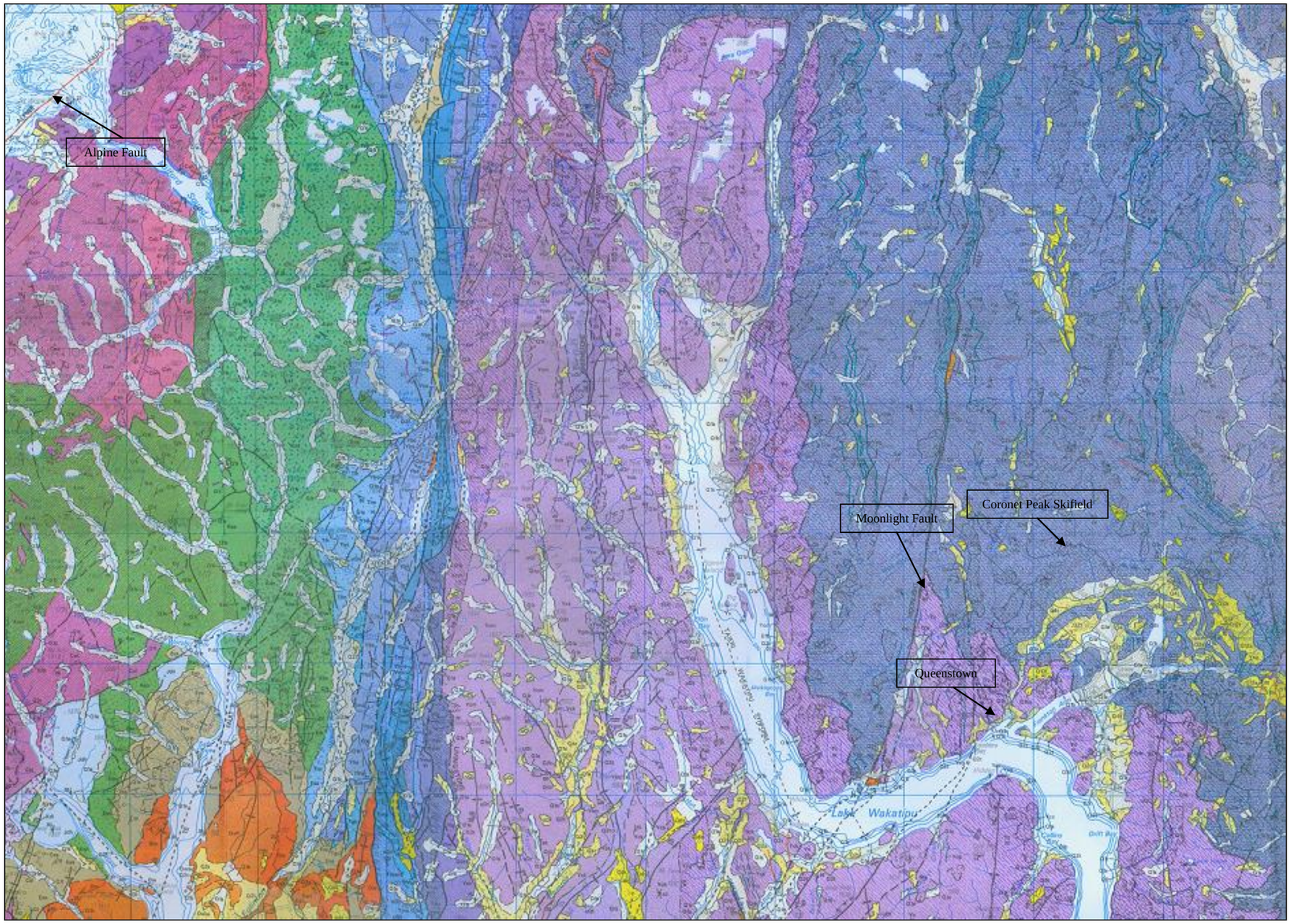

The area that is the Wakatipu Basin between the end of the second phase of the Rangitata Orogeny and the mid-Tertiary, approximate ages of 105 and 30 million years ago respectively, was eroded to a near flat surface forming a peneplain. This peneplain was later deformed tectonically forming high ranges and depressions in the Miocene during the Kaikoura Orogeny, (Willets, 2000). The formation and consequent movement of the Alpine Fault is responsible for the local deformation. In the Quaternary (within the last 2.5 million years) the Wakatipu Basin and greater area was subjected to periods of cooler temperatures know as 'glacials'. The periods of warmer weather are known as 'inter-glacials'. There have possibly been 20 glacial periods within the Quaternary with evidence of four in the Wakatipu Basin occurring within the last 500,000 years. The 'glacial' periods are characterised by widespread snow accumulation in high elevation areas resulting in glaciers spreading down the valleys. The glaciers moving down these valleys have produced the 'U-shaped' valleys that can be typically seen in the Wakatipu Basin and any other glaciated area.

Landslides dominate Central Otago's mountainous landscape; this is due to the inherent instability of the basement rock of the area, the Otago Schist. Figure 1.9 below shows the landslides with an area in excess of one square kilometre. Failure within schists generally occurs due to the schistosity of the rock.

Fig. 1.9. Landslides in the Wakatipu Area, (Turnbull, 2000, p52).

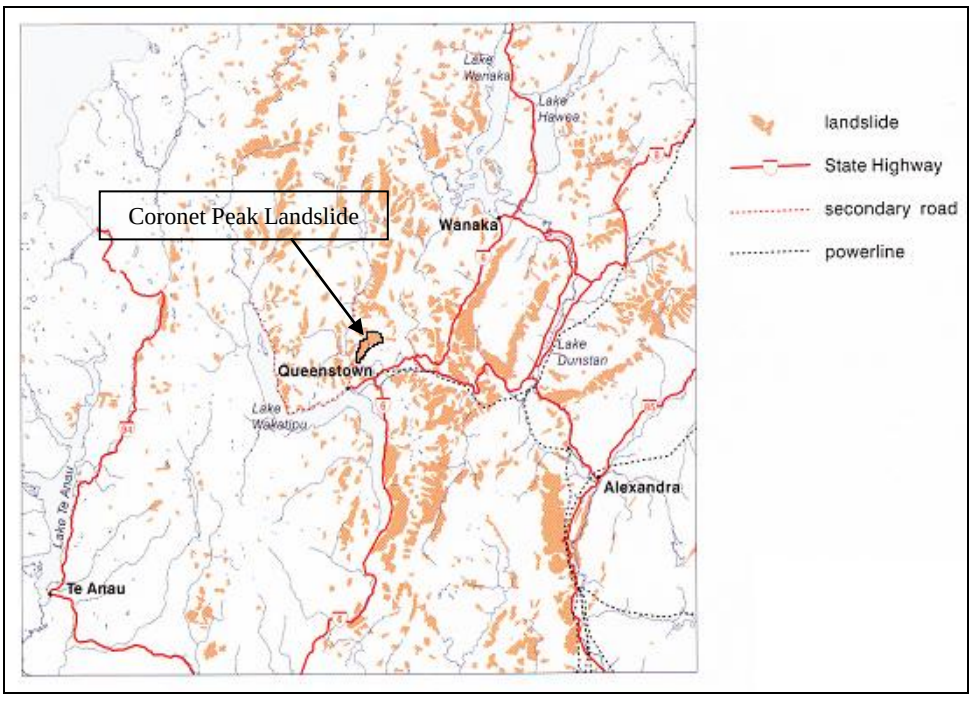

The Coronet Peak Landslide has been outlined in Figure 1.9 above, and is dated to have failed between 135,000 (Waimean Glaciation) and 23,000 (Otiran Glaciation) years ago. The failure mechanism for the landslide is interpreted as the undercutting of the slope by the Shotover River and glaciers during the Waimean Glaciation (Penultimate Glaciation). It is the consequent retreat of the glaciers at this time creating the instability (Willetts, 2000). There have been some reactivations in areas of the Coronet Peak Landslide, however the site on which the Coronet Peak Skifield is located is thought to be stable as there have been no reactivations in this area and there is no removal mechanism (like a river or glacier as in the other reactivated events). Though the whole of the landslide is thought to be moving at a rate of a few millimetres a year.

There are two faults in close vicinity to Coronet Peak which may when activated cause some instability within the mass of the landslide, these can be seen in Figure 1.8. The Moonlight Fault, located to the west and formed approximately 40 million years ago, and the Nevis-Cardrona Fault to the east which is approximately Pliocene in age (2.5 – 5 million years ago), with respective probabilities of occurrence within the next 150 years of 4-21% and <4%. Both faults have similar recurrence intervals of approximately 4,000 years (Willetts, 2000). However with the skifield showing no sign of reactivation in the past, it is possible this area of the Coronet Peak Landslide may be stable enough to withstand the earthquakes associated with these faults, or there may have been reactivations within the skifield area that there is no or little identifiable evidence for.

1.5. Thesis Methodology

The methodology for this thesis began with collecting meteoric water samples from precipitation, springs, boreholes and water storage reservoirs on Coronet Peak. These samples were then analysed by the isotope ratio mass spectrometer at the University of Canterbury, to attain the ratios of δD and $\delta^{18}O$. The results obtained were then critically reviewed to discover the relationships between δD and $\delta^{18}O$ within the meteoric waters of the study area. Using this information to determine the effects of the relationships discovered on the water usage of the Coronet Peak Skifield.

1.6. Thesis Format

- Chapter Two: Is an introduction to the stable isotopes of hydrogen and oxygen in water and their relationship with each other in meteoric waters.
- Chapter Three: Is the methodology under which the sampling for this thesis was undertaken, also showing the locations of each sampling site.
- Chapter Four: Determines the Local Meteoric Water Line for the Coronet Peak area, as well as a Local Evaporation Line for the surface waters on the skifield.
- Chapter Five: Looks at the relationship of the isotopes of water and their variation with altitude, storm duration and storm track trajectory.
- Chapter Six: Indicates the flow rates of the springs on the mountain and which springs show the most promise for future utilisation.
- Chapter Seven: Determines that stable isotopic composition of the springs and groundwater sources.
- Chapter Eight: Emphasises the summaries and conclusions made in this thesis.

Chapter Two:

The Stable Isotopes of Hydrogen and Oxygen

2.1. Introduction

The study of isotopes is based on the tendency of certain elements to separate into light and heavy fractions. The separation of isotopes into relatively heavier and lighter fractions is called mass dependent fractionation (Hiscock, 2005). Isotopes are variations of the same element and are differentiated from each other by variations in their neutron number, giving each isotope a different atomic mass. It is these variations in mass that give rise to fractionation between isotopes as this directly impacts on the isotopic/atomic vibrational frequency and bond strength.

In nature isotopes can be both stable and radioactive. The radioactive isotopes being unstable and decay over time, the stable isotopes do not decay. Stable isotopes can be traced through many systems, including the hydrologic system, giving information on the origin of meteoric waters, information on temperatures and atmospheric concentrations of gases in paleoclimates. Therefore the stable isotopes are considered the best form of isotope tracers as they are generally considered environmentally friendly as they are readily found in nature and do not require any input of radioactive materials. For a full introduction to stable isotopes see Appendix A.

2.2. Isotopic Composition of Water

Hydrogen and oxygen stable isotopes participate in most geochemical and biochemical processes that take place on Earth. Hydrogen is the most abundant element that occurs in the universe, while oxygen is the most abundant element that exists within the Earths' crust (Faure and Mensing, 2005). Both hydrogen and oxygen are compared to the international standard of VSMOW and display similar patterns of isotope fractionation; because of this these two elements cannot be separated easily and so are explained in conjunction with one another (Eby, 2004).

Water is composed of hydrogen and oxygen isotopes. These two elements have differing neutron numbers within their nuclei that create both stable and unstable

isotopes. As we are only concerned with the stable species here, they are the ones that we refer to. The elements of hydrogen and oxygen have two and three stable isotopes respectively, therefore there are nine different stable molecules (isotopologues) of water that occur in nature, these are shown below in Table 2.1 (Sharp, 2007).

Table 2.1: The isotopes of hydrogen and oxygen and the isotopologues of water.

Hydrogen Isotopes	**Oxygen Isotopes**	**Isotopologues**
^{1}H	^{16}O	$^{1}H_2{}^{16}O$, $^{1}H_2{}^{17}O$, $^{1}H_2{}^{18}O$
^{2}H	^{17}O	$^{1}HD^{16}O$, $^{1}HD^{17}O$, $^{1}HD^{18}O$
	^{18}O	$D_2{}^{16}O$, $D_2{}^{17}O$, $D_2{}^{18}O$

The isotopologues listed above are in the order of the lightest molecule ($^{1}H_2{}^{16}O$) to the heaviest molecule ($D_2{}^{18}O$). Each element has a specific atomic mass that changes with each isotopic variation of that element. The mass of an isotope is noted in the unit amu, the atomic mass unit, which is based on the carbon isotope, ^{12}C, having an exact amu of 12, all other isotopes are compared to this. Using the ratio of an elements isotope ratio ($^{2}H/^{1}H$ or $^{18}O/^{16}O$), found by mass spectrometry, and multiplying it by 12, the amu can be found for that isotope (Eby, 2004). Table 2.2 below lists the abundance and each isotope of hydrogen and oxygen, the lightest isotope of each element is also the most abundant and the mass difference between hydrogen and oxygen (Faure and Mensing, 2005). From Table 2.2 we can see that D is 100% heavier than ^{1}H and ^{18}O is 12.5% heavier than ^{16}O.

Table 2.2: Isotopic mass and abundance for hydrogen and oxygen (Faure and Mensing, 2005).

Element	**Isotope**	**Mass (amu)**	**Relative Mass Difference (%)**	**Abundance (%)**
Hydrogen	H	1.007825	100 (δD)	99.985
	D	2.0140		0.0155
Oxygen	^{16}O	15.994915	12.5 ($\delta^{18}O$)	99.759
	^{17}O	16.999131		0.037
	^{18}O	17.999160		0.204

The use of a standard to which both hydrogen and oxygen are referenced back to V-SMOW gives rise to the δ values (Faure and Mensing, 2005). Where a δ value is:

$$\frac{(Ratio_{sample} - Ratio_{standard})}{Ratio_{standard}} \cdot 1000 \qquad \text{Eq. 2.1.}$$

The delta ratio for the stable isotope of oxygen is $\delta^{18}O$. For the purpose of stable isotope water geochemistry the delta ratio used does not take into account the abundance of ^{17}O. This is due to the ratio being conventionally written as the rare, heavy isotope (^{18}O) to the more abundant, light isotope (^{16}O), giving the ratio used to calculate the δ value in Equation 2.4 of $^{18}O/^{16}O$ the oxygen (Sharp, 2007). On the other hand, the ratio for hydrogen can only be $^{2}H/^{1}H$ or D/H as these are the only stable isotopes of this particular element. However, ^{3}H or tritium, was used in the 1950's and 1960's as an artificial tracer of the water systems around the globe. Tritium became a global tracer due to its release into the atmosphere in large quantities by thermonuclear weapons testing in the 1950's (Aggarwal, et al. 2005). Tritium is radioactive and has a half-life of approximately 12.3 years. However, tritium is not used as commonly as it was in the 1960's because of its short half life and also because the signal has weakened over time due to the cessation of weapons testing. It may be useful though to follow its daughter product in shallow groundwater. Artificial tracers have been deemed environmentally unfriendly due to the introduction of radioactive materials into the water cycle, they have been replaced by 'environmental' tracers that can be both natural and anthropogenic in origin, for example δD and $\delta^{18}O$ ratios (Sharp, 2007). However, tritium can be used to determine the age of modern water, as there are still trace amounts in the atmosphere. The concentration of tritium in the atmosphere is known since the testing of nuclear weapons and once the sample is tested for it's own tritium levels it can then be compared to these known levels and the age determined.

The monitoring of tritium in the hydrologic cycle resulted in an exponential increase in the number and geographic distribution of stable isotope measurement stations. This lead to the formation of the Global Network of Isotopes in Precipitation (GNIP) in 1966 that is governed by the International Atomic Energy Agency (IAEA) (Aggarwal et al. 2005). One of the focuses for the IAEA is to investigate freshwater resources using the nuclear technique of isotope hydrology to better understand this

resource to allow sustainable use of the freshwater around the world today and in the future (IAEA, 2002).

When analysed using a mass spectrometer, both hydrogen isotopes (D/H or δD) and oxygen isotopes ($^{18}O/^{16}O$ or $\delta^{18}O$) are compared to the Standard Mean Ocean Water (SMOW), where δD and $\delta^{18}O$ in SMOW are equal to zero. Negative values of δD and $\delta^{18}O$ show samples that are depleted in the heavy isotopes of hydrogen and oxygen, positive values indicate enrichment in the heavy isotopes (Faure, 1986). Typically heavy water isotopologues tend to remain in the denser phases of the water cycle, either the liquid or solid phases, due to their preferential conversion into water droplets and ice crystals during condensation. Light water molecules are preferentially evaporated from water bodies over the heavier isotopologues (Araguas-Araguas, 2000). Commonly SMOW is known as V-SMOW, the Vienna Standard Mean Ocean Water, named after the location where the International Atomic Energy Agency gather to establish protocols for stable isotope analysis. V-SMOW is now used to reassure workers and readers that the δD and $\delta^{18}O$ samples were analysed using the proper reference standard, as in the past SMOW has been defined slightly differently, therefore V-SMOW eases ambiguity. The reference standard of V-SMOW can be calibrated even further than just giving a δD value of zero. V-SMOW can be analysed with the δD ratio of the Standard Light Antarctic Precipitation (SLAP), which according to the International Reference Standard of VSMOW the difference between the V-SMOW and SLAP ratios of δD must be -428‰. This comparison is used as an additional reference standard when calibrating the individual analytical tools for stable isotope studies, known as mass spectrometers. If the difference between VSMOW and SLAP when analysed on the same mass spectrometer is not -428‰ then a stretching factor needs to be applied to the data. The stretching factor is found by determining the ratio of the accepted difference between the two standards and the measured difference of the two standards (Δ accepted/ Δ measured). All measurements are then multiplied by this factor to get $\Delta D_{SLAP\text{-}VSMOW}$ = -428‰ (Sharp, 2007).

2.3. Evaporation and Condensation

The fractionation of hydrogen and oxygen isotopes is very similar. The main reactions that take place within the water cycle are the processes of evaporation and condensation, and will be concentrated on in this chapter.

Evaporation is a process that occurs due to kinetic isotope effects, whilst condensation is an equilibrium process. Many factors influence the isotopic fractionation associated with evaporation, however only temperature needs to be considered for equilibrium reactions (condensation) (Sharp, 2007).

As water molecules move through the transition of liquid to vapour phase (fractionate), known as evaporation, the molecules will exit the liquid phase when they have enough energy (vibrational) to allow the electrostatic attraction that binds the molecules together in the liquid phase to be overcome (Eby, 2004). Figure 2.1 is a schematic of the process of evaporation. Due to the differences in the masses of the isotopes of the elements of hydrogen and oxygen, some isotopes wills preferentially move 'rattle free' into the 'lighter' phase of that molecule than others. The 'lighter' isotopes, ^{1}H and ^{16}O, need less energy to overcome the electrostatic attraction than the 'heavier' isotopes, D and ^{18}O. Evaporation is a kinetic, unidirectional process; the back exchanges between the departing vapour and the remaining liquid are prohibited due to under-saturated vapour (humidity is less than 100%). This would be an equilibrium process if the vapour above the oceans were saturated (humidity equal to 100%) and there was no wind, this would create no net evaporation, as evaporation would equal condensation. However, this does not occur and so is a kinetic process with the main determinants being temperature and humidity. The temperature of the atmosphere has a great effect on evaporation; higher temperatures give rise to higher evaporation rates.

Figure 2.1: A simple schematic showing how during evaporation with the addition of temperature (T) and humidity (H) the composition of the liquid becomes isotopically heavier, as indicated by the dominance of the blue circles in the right-hand side of the diagram, as the lighter isotopologues are preferentially evaporated into the atmosphere, the orange circles.

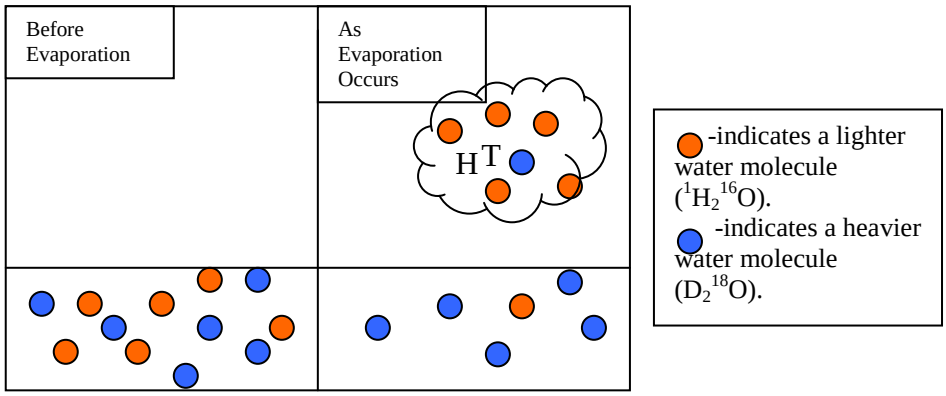

Condensation on the other hand is an equilibrium process. As air masses move away from their source and rise, their temperature drops. If supersaturation (an excess of a dissolved substance due to cooling) of the air mass occurs, condensation and precipitation will occur. Figure 2.2 is a schematic of the process of condensation. In an open system where condensate is continuously removed, back exchange reactions are restricted as they can only occur in closed systems, this process is known as the Rayleigh distillation process or Rayleigh fractionation. The liquid condenses in isotopic equilibrium with the parent vapour and then is removed from the system as precipitation. During condensation, 'heavy' water is continuously removed; therefore the δ value of the remaining vapour becomes lighter (more negative when compared to V-SMOW) with increasing degrees of condensation. Therefore, the δ value of the newly formed condensate from the already 'light' water vapour will also become correspondingly lighter, more negative. In a closed system, condensation is governed by the Batch Model of fractionation, however in an open system, Rayleigh fractionation occurs which is responsible for most of the stable isotopic variation that occurs in precipitation from air masses. The Rayleigh equation is as follows:

$$\frac{R}{R_0} = f^{(\alpha - 1)} \qquad \text{Eq. 2.2.}$$

Where R is the $^{18}O/^{16}O$ ratio of the remaining vapour, R_0 is the $^{18}O/^{16}O$ ratio of the vapour before evaporation, f is the fraction of vapour remaining in the air mass and α is the fractionation factor for oxygen (R_{liquid}/R_{vapour}) (Faure, 1986). Rayleigh distillation processes can also be used to explain other processes where a newly formed phase is separated or removed from its parent, crystals precipitated from a magma is an example of this (Sharp, 2007). The Rayleigh Fractionation Process can be seen in Figure 2.6 on page 26, where as air masses undergo cycles of precipitation as they move across continents, the hydrogen and oxygen isotopes values become progressively more negative as the air mass becomes progressively lighter.

Figure 2.2: A simple schematic displaying the effect of condensation the ratio of heavy to light isotopologues of water. The left hand side indicates an air mass that has not reached supersaturation, whilst the right-hand side of the diagram is showing condensation once the vapour has reached supersaturation (S).

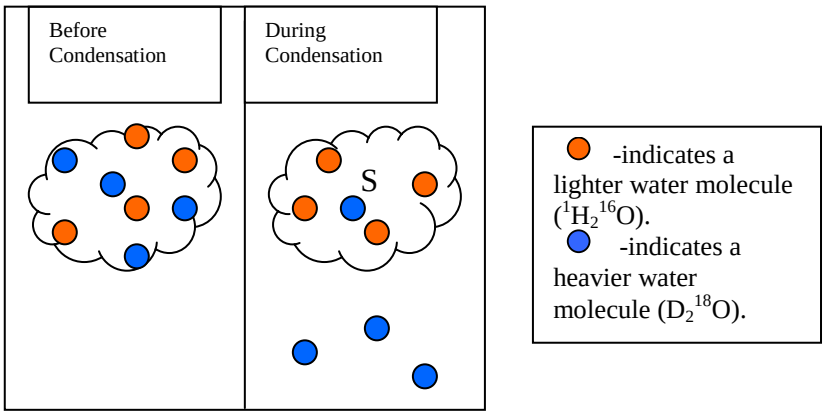

2.4. Meteoric Waters.

The stable isotopic ratios of D/H and $^{18}O/^{16}O$ vary throughout the Earth's natural waters. Oceanic waters do not vary as much when compared to precipitation and have a global average for δD and $\delta^{18}O$ values known as the Standard Mean Ocean Water (SMOW), with the reference material for all hydrogen and oxygen isotopes in any water reservoir being SMOW where δD and $\delta^{18}O$ values are equal to zero. Meteoric precipitation has a global correlation between hydrogen and oxygen as they undergo evaporation and condensation very similarly, known as the Global Meteoric Water Line (GMWL) (Sharp, 2007). However, the δD and $\delta^{18}O$ values can vary

greatly around the world depending on the latitude, the proximity to a water source, amount of rainfall that has taken place, the altitude and the season. These factors lead to the formation of Local Meteoric Water Lines (LMWL), which are specific to a given locality. Lakes and rivers are also influenced by the aforementioned factors, but are more complicated due to their extended exposure to the atmosphere and specifically the processes of evaporation and condensation. Groundwater is a much simpler water resource in terms of the stable isotopes of hydrogen and oxygen. When water is underground, it experiences very little to no evaporation and condensation under most conditions, therefore the δD and $\delta^{18}O$ values do not change and are a record of the source water for that groundwater reservoir, however when this water is heated by geothermal processes the ratios do alter (Sharp, 2007).

2.4.1. *Oceanic Waters*

Oceanic water varies slightly around the world, with D and ^{18}O content in ocean water that has not been contaminated with a fresh water resource (river, ice melt) only varying of ±1 ppm (parts per million) (Dansgaard, 1961). The abundance of the stable isotope ^{18}O in the ocean also varies with depth. Water samples taken from the surface of the ocean are slightly enriched in this 'heavy' isotope of oxygen (a positive δ value) due to the kinetic process of evaporation. On the other hand, samples taken from depth should be even more enriched in ^{18}O due to the gravitation of the heavy components but Dansgaard in 1960 showed no great difference between ^{18}O samples from depths of 4000 metres and 10,000 metres, this is due to the ocean not being stagnant. (Dansgaard, 1961). The δD and $\delta^{18}O$ values may also be slightly different at the equator in the short term because of the higher temperatures associated with this region and the lower rates of evaporation as one moves polewards due to cooler temperatures, there are also differences due to the salinity of ocean water too, however, these variations are slight due to ocean circulation.

All hydrogen and oxygen samples are compared to V-SMOW, the Vienna Standard Mean Ocean Water, this is pure water and does not consider any other substances found in ocean water, for example salt (Sharp, 2007).

The absolute isotopic composition of V-SMOW is:

$$\delta D = 155.76 \pm 0.1 \text{ ppm} \quad \text{Eq. 2.3.}$$

$$\delta^{18}O = 2005.20 \pm 0.43 \text{ ppm} \quad \text{Eq. 2.4.}$$

The compositions above are in parts per million (ppm). However for comparative purposes both δD and $\delta^{18}O$ ratios are described as relative differences to the V-SMOW standard, the δD and $\delta^{18}O$ ratios of V-SMOW are set to zero, therefore any variations from this standard, that is negative or positive correlations, can be easily seen and analysed (Faure, 1986).

2.4.2. *Meteoric Precipitation*

The hydrogen and oxygen isotopic ratios in meteoric precipitation vary significantly; however there is a global relationship that can be seen when comparing these two elements with each other due to the similarity of fractionation processes between them, the Global Meteoric Water Line (GMWL). Figure 2.3 shows the GMWL as indicated by Craig, 1961. This relationship between the stable isotopes of hydrogen (D and ^{1}H) and oxygen (^{18}O and ^{16}O) is a useful tool in determining whether a water sample sits on or off the GMWL, that is, whether the sample is an average one or not.

Figure 2.3: Global Meteoric Water Line (Craig, 1961).

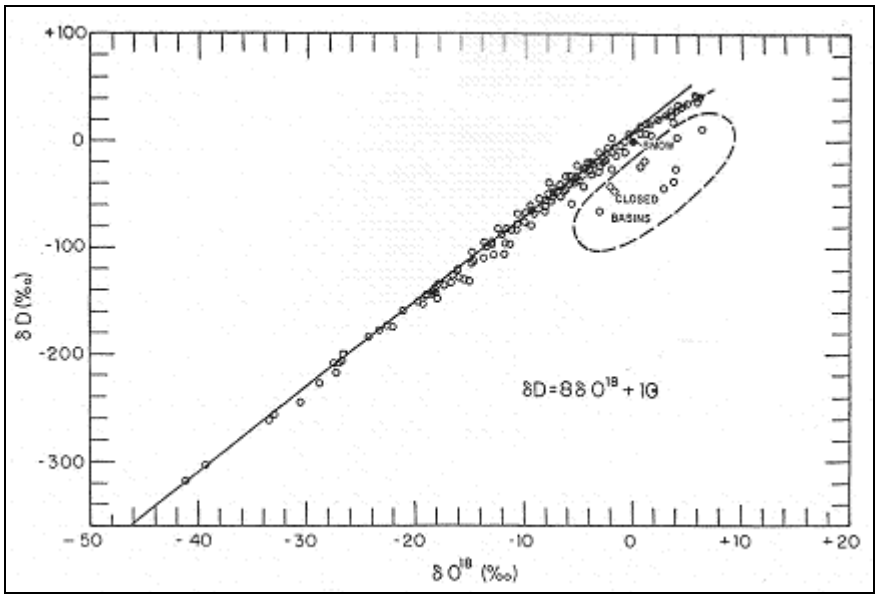

The GMWL is defined as:

$$\delta D = 8\delta^{18}O + 10 \qquad \text{Eq. 2.5.}$$

This trend is based on a global survey of non-evaporated freshwaters, and was first inferred by H. Craig in 1961. Deviations from this tendency of hydrogen and oxygen for a specific locality are known as Local Meteoric Water Lines (LMWL) and are due to the variations in the delta ratios of these stable isotopes. Samples differing from the GMWL are generally due to certain phenomena, often termed 'effects' observed within atmospheric precipitation. These are listed below.

- The Latitude Effect
- The Continental Effect
- The Amount Effect
- The Altitude Effect
- The Seasonal Effect

The Latitude Effect on the stable isotopic ratios of hydrogen and oxygen can also be thought of as a temperature effect. The variations in the ratios are due to the temperature changes associated with changing latitudes, and how this effects the fractionation of the hydrogen and oxygen isotopes. As water is evaporated from the oceans, the ratios are dependent on the temperature of the environment. When moving from lower latitudes to higher latitudes there is a measured decrease in the concentration of the heavy isotopes in precipitation, or the precipitation gradually becomes 'lighter' with increasing latitude (Jä ger and Hunziker, 1979). Figure 2.4 below adapted from Jä ger and Hunziker 1979, demonstrates the effect that latitude and mean annual air temperature have on $\delta^{18}O$ values (orange bars). Increasing latitude occurs from left to right, beginning with Barbados at 13°N and ending with Byrd Station, Antarctica with latitude of 82°S. As with increasing latitude from left to right there is also a corresponding decrease in annual mean air temperatures (blue bars) from 23° C to -28° C.

Figure 2.4: Annual mean values of $\delta^{18}O$ vs. air temperature (adapted from Jä ger and Hunziker, 1979).

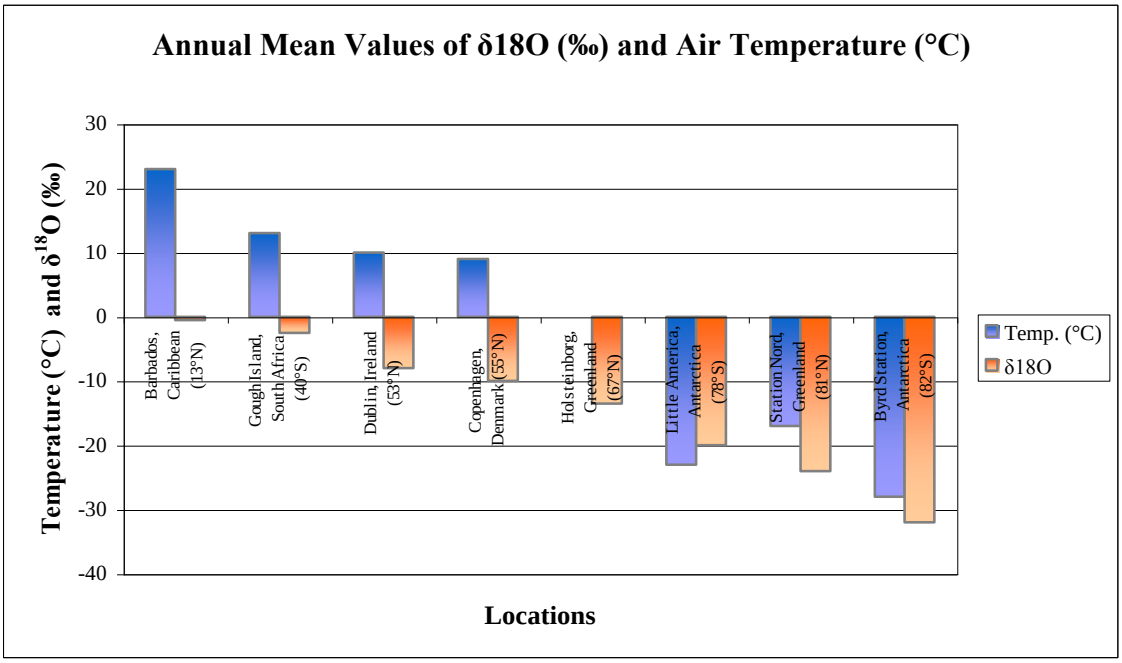

However, there is no linear relationship with Latitude Effects, this is due to differing topographic and local climate conditions. Also, global atmospheric circulation patterns are not constant all over the Earth's surface; these patterns vary over oceans and continents (Sharp, 2007). Figure 2.5 from Araguas-Araguas et al, 2000, below demonstrates this clearly. With latitude on the x-axis and the contour spacing at 5‰ of $\delta^{18}O$ values, the variations of $\delta^{18}O$ with latitude are evident, as well as the areas where this relationship is not wholly true due to the factors mentioned above, these areas include southern Africa and the western seaboard of South America, with a large band over Indonesia running in an approximate north-south direction, including New Zealand.

Figure 2.5: Global $\delta^{18}O$ values vs. latitude (latitude is plotted on the y-axis and longitude on the x-axis. The isotherms join locations where the $\delta^{18}O$ values are equal. The points show the locations of all stations included in the Global Network of Isotopes in Precipitation that is jointly operated by the International Atomic Energy Agency (IAEA) and the World Meteorological Organisation (WMO) (Araguas-Araguas et al, 2000).

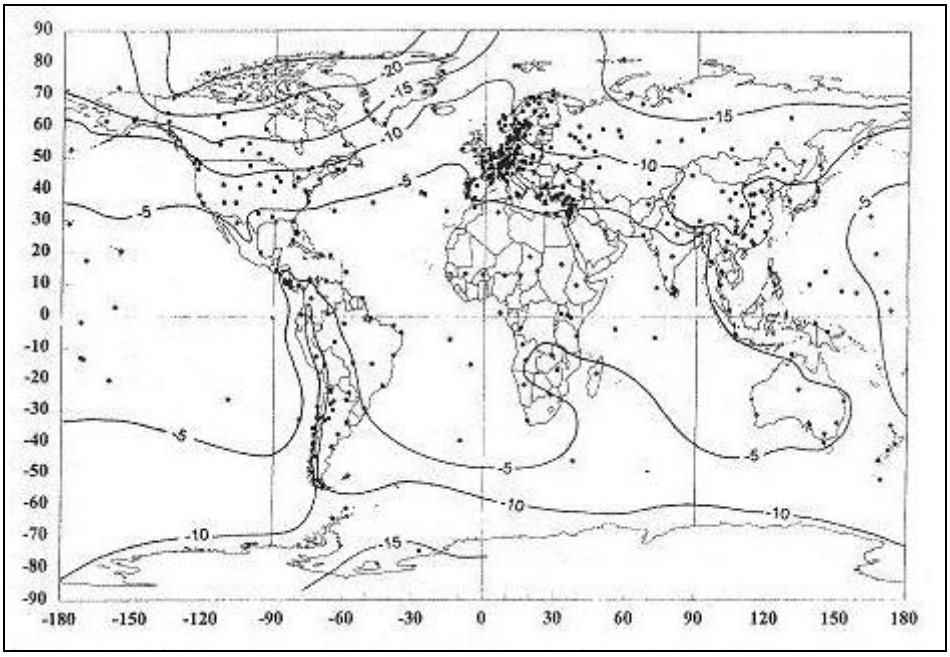

The Continental Effect is the change of the isotopic compositions of δD and $\delta^{18}O$ due to the movement of an air mass away from its water source, usually the ocean, towards the centre of a continent where a water source is typically further away. The ratios of hydrogen and oxygen decrease as an air mass moves further away from its water source. This is due to the air mass having undergone several cycles of precipitation as it moves over a continent, becoming isotopically 'lighter' (Sharp, 2007). Figure 2.6 below is a schematic of the atmospheric water cycle, where the $\delta^{18}O$ values become more negative as the air mass moves inland. This is also called the Rainout Effect or the Outraining Effect, as the heavy isotopes are rained out first and the air mass becomes progressively lighter and lighter, as well as the corresponding precipitation (Jä ger and Huniker, 1979).

Figure 2.6: Atmospheric water cycle showing the continental effect of $\delta^{18}O$ (Jä ger and Huniker, 1979).

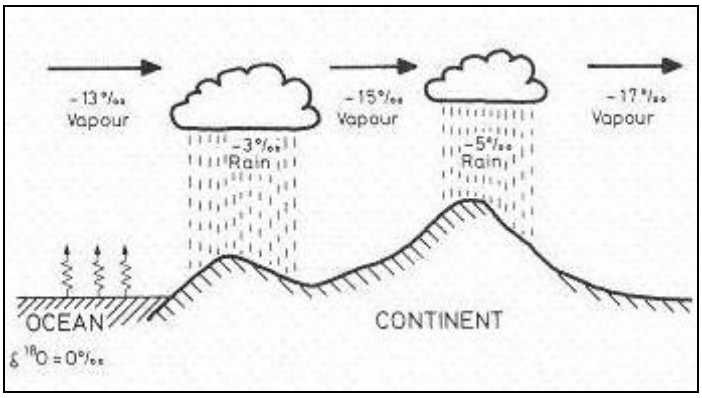

The Amount Effect is only a factor influencing meteoric precipitation in the tropical regions of the world. It is the correlation between the isotopic composition of rainfall and the amount of rainfall that has been precipitated in a given month. High δD and $\delta^{18}O$ values occur in months where there has been little rainfall, whilst in months of high precipitation the values are lower, more negative. This can also be thought of as a Rainout Effect, in a month of increased rainfall, the isotopic compositions will become more negative as the heavy isotopes are 'rained out' (Sharp, 2007). Below in Figure 2.7 the Amount Effect is shown for the city of Binza, Democratic Republic of Congo, there is a distinct relationship with decreasing $\delta^{18}O$ values and the amount of precipitation that occurs during one month. Figure 2.8 also shows the Amount Effect, though generally used in tropical areas, it does show the right correlation in Norfolk, England. It also shows the relationship between rainfall and $\delta^{18}O$ values that occur over the duration of a year instead of over a month as in Figure 2.7.

Figure 2.7: Amount Effect in Binza, Democratic Republic of Congo (adapted values from Sharp, 2007)

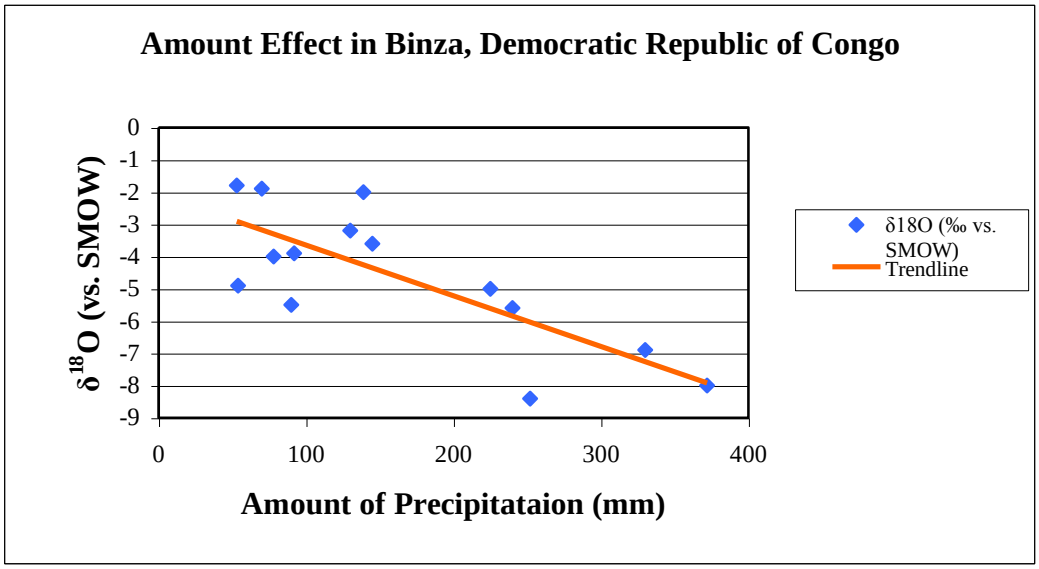

Figure 2.8: Rainfall vs. $\delta^{18}O$ from Norfolk, England for the year 1995/1996, (adapted from Hiscock, 2005).

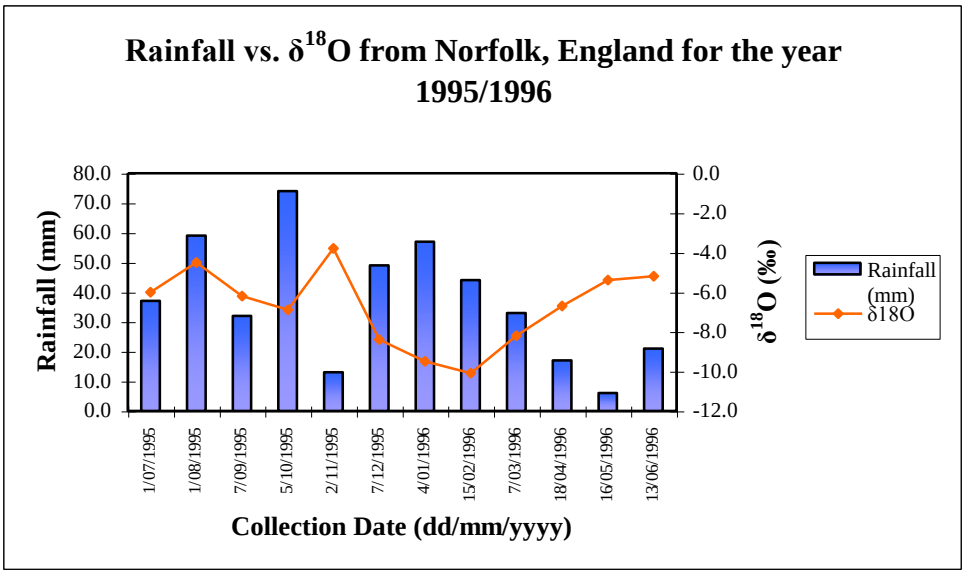

The Altitude Effect refers to the changes in the isotopic ratios of atmospheric precipitation corresponding with changes in height above sea level with which it is falling. The ratios of δD and $\delta^{18}O$ decrease with increasing altitude. This is due to the decrease in temperature at elevation and also because air masses hold less moisture at altitude. Figure 2.9 below demonstrates this principle, showing three stations in the Swiss Alps with varying altitudes and their corresponding $\delta^{18}O$ values that have been averaged over the years 1970 to 1976, month 1 being January an month 12 being december (Jä ger and Huniker, 1979).

Figure 2.9: $\delta^{18}O$ monthly samples vs. altitude in metres above sea level (m.s.a.l.) (adapted from Jä ger and Huniker, 1979).

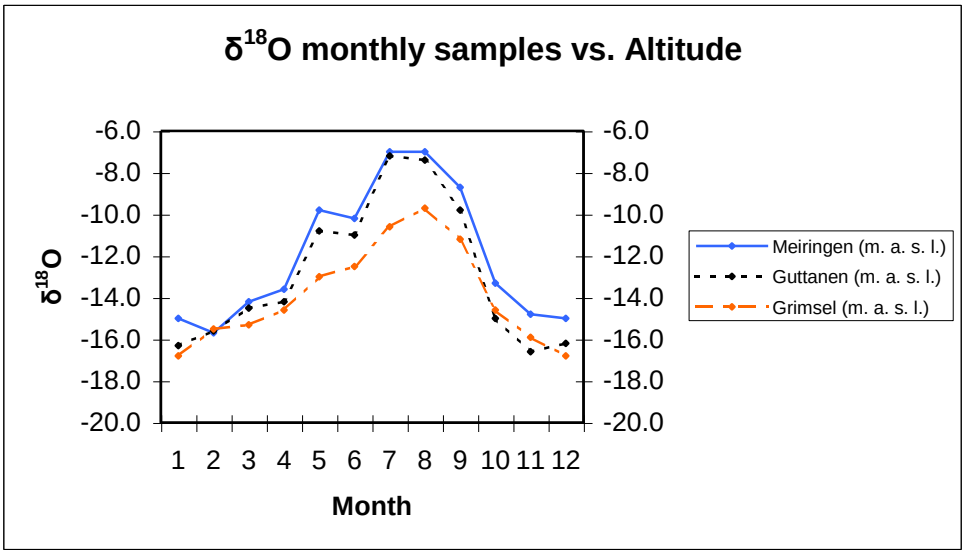

Figure 2.10 also shows the Altitude Effect, but with $\delta^{18}O$ data compiled from world wide studies against net elevation from sea level in metres. An altitude gradient can be derived from this data below. The equation of the line (below in Eq. 2.6) giving a 3.5 ‰ decrease in $\delta^{18}O$ for every 1000 metre increase in altitude.

$$y=-0.0025x +0.968 \qquad \text{Eq. 2.6.}$$

There is also a difference depending on the relief of the land in which the air mass is flowing over. If the relief is high, like a mountain range, then the water vapour will decrease more rapidly compared to a gentler slope (Sharp, 2007). Therefore, in

mountainous areas of high altitude there will be an even greater decrease in the heavy isotopes of hydrogen and oxygen, compared to areas of high altitude that have a gentler relief, for example, a high plateau.

Figure 2.10: Changes in $\delta^{18}O$ ($\Delta\ \delta^{18}O$) vs. net elevation in metres (Sharp, 2007).

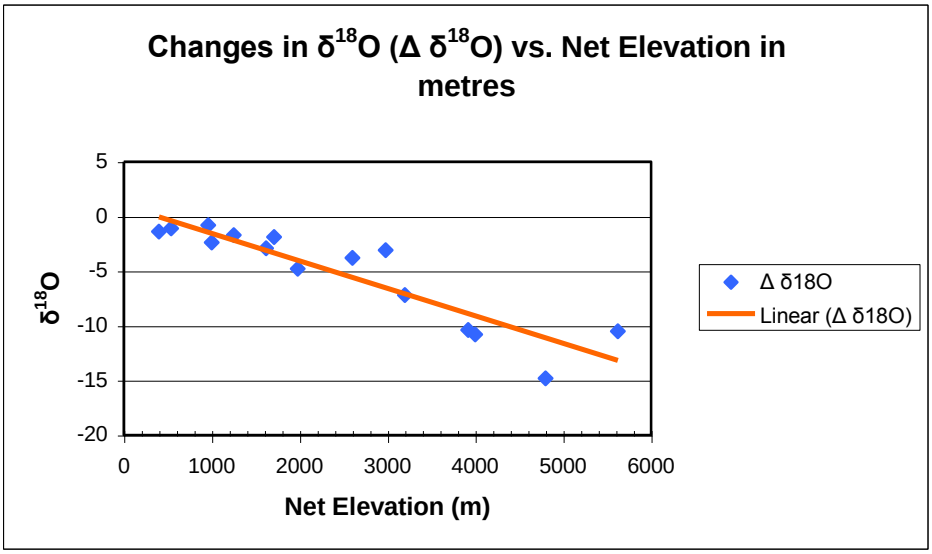

The Seasonal Effect is also shown in Figure 2.9 on the previous page (data from the Swiss Alps) from Jä ger and Huniker, 1979, and can furthermore be known as a temperature effect too, like the Latitude Effect. In these mountainous areas, during the summer months (June and July), they experience very high precipitation that leads to a decrease in the $\delta^{18}O$ values compared to the times of lower rainfall (winter in the northern hemisphere). This phenomenon has the same impact on the isotopic ratios of hydrogen and oxygen with increasing latitude. As temperature decreases, there is a corresponding decrease in δD and $\delta^{18}O$. The Seasonal Effect influences all the above factors, however there is less of an effect in the tropics because there is little temperature change in this area. The Seasonal Effects on δD and $\delta^{18}O$ values of precipitation over Albuquerque, USA is also shown in Figure 2.11 for the period of 1998-1999. During the winter months, December, January and February, the high rainfall leads to a depletion of both δD and $\delta^{18}O$ values. There is also a large variation shown in the wide range of δD and $\delta^{18}O$ values given for individual storm events, not only due to 'rainout' but also due to the direction of the storm track, the duration of the storm and the temperature.

Figure 2.11: Seasonal Effects on δD and $\delta^{18}O$ values of precipitation over Albuquerque, USA for 1998-1999. (Sharp, 2007).

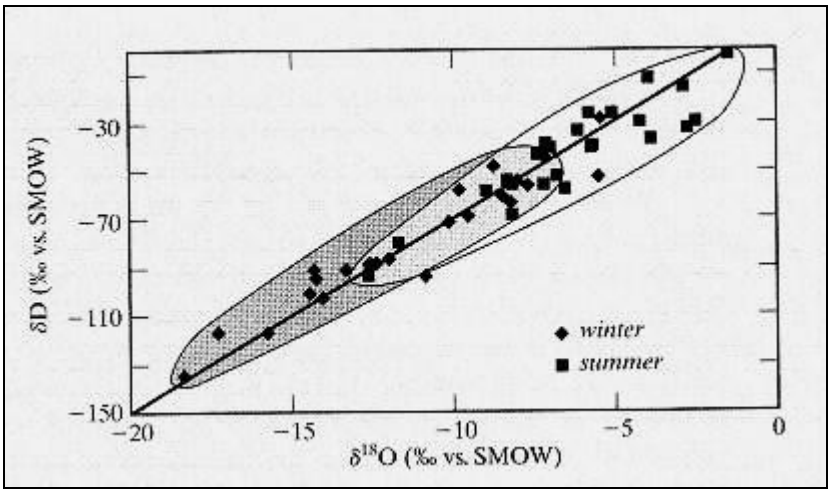

It is these five main factors that differ depending on their location around the world and these deviations from the Global Meteoric Water Line (GMWL) by locality give rise to Local Meteoric Water Lines (LMWL). As mentioned previously the GMWL has a slope equal to 8 and can be defined as:

$$\text{GMWL: } \delta D = 8\delta^{18}O + 10 \qquad \text{Eq. 2.7.}$$

Local Meteoric Water Lines that have a slope less than 8 may be due to the partial evaporation of raindrops as they fall in a dry atmosphere, giving rise to even more negative delta ratios. Craig, 1961, indicated that evaporated water gave a slope of approximately 5, as he observed in the waters sampled from East African rivers and lakes. Deviations that have a slope above 8 are most likely due to seasonal variations in the sources and origins of precipitation (Araguas-Araguas et al, 2000).

The Global Meteoric Water Line can also be written as:

$$\delta D = 8\delta^{18}O + d \qquad \text{Eq. 2.8.}$$

Where ‘d’ is the Deuterium Excess (Eby, 2004). The Deuterium Excess is “a measure of the deviation of any given data point from a line with a slope equal to 8 that goes through V-SMOW” (Araguas-Araguas et al, 2000, P1350). The Deuterium Excess allows the possibility of characterising the interaction of different air masses and their evolution throughout time to be understood. Figure 2.12 below shows the GMWL as evaporation occurs, during this process what remains of the liquid water reservoir becomes enriched in the ‘heavy’ stable isotopes of hydrogen and oxygen, therefore the δD and $\delta^{18}O$ values move to the right. However, the water vapour that has just been created from the liquid reservoir will be isotopically ‘light’ and therefore will plot to the left of the GMWL.

Figure 2.12: The deuterium excess parameter. Water begins on the GMWL, as evaporation occurs, the residual water moves to the right of the GMWL, whilst the vapour moves to the left.

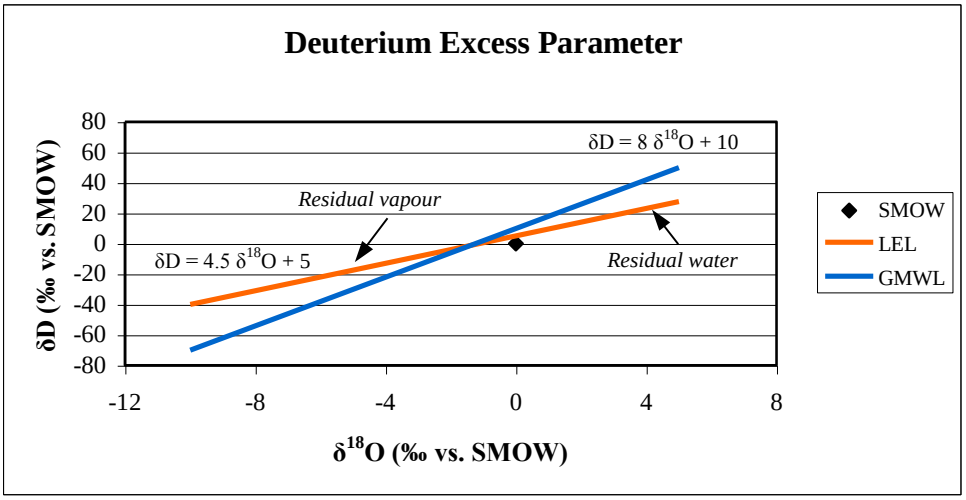

When the d-excess value is equal to 10‰ it indicates the sample is from an intertropical oceanic area, when the temperature is 25 degrees celcius and the humidity is at 80%. This value tends to fit most of the samples worldwide taken from modern times, which is why often instead of using d, for the Deuterium Excess, it is simply written as 10. A d-excess value less than 10‰ can indicate secondary evaporation processes where the temperature is 25 degrees celcius and the humidity is at 80% (Araguas-Araguas et al, 2000). D-excess values less than 10‰ give rise to another type of relationship within meteoric water samples, the Local Evaporation

Line (LEL), showing the effects of evaporation, this can be seen in Figure 2.12 above as the evaporation trend line (Iqbal, 2008).

Local Evaporation Lines (LEL) plot to the right of the GMWL as shown in Figure 2.12 and have a slope less than that of the GMWL. These lines are helpful in the fact that they can identify the reason for stable isotope variations of samples from the GMWL. Figure 2.13 below is the GMWL from Craig 1961, here he has plotted stable isotope ratios from nay different meteoric water sources, including lakes, rivers, rain and snow. However, there is a noticeable deviation from the GMWL at the top of the curve that is shown by a dotted line with a slope less than the GMWL. These samples represent samples collected from rivers and lakes in East Africa indicating that they have undergone evaporation (Dansgaard, 1961).

The Global Meteoric Water Line does not pass through V-SMOW where the δD and $\delta^{18}O$ ratios are both equal to zero. This is because as liquid water is evaporated from the oceans and becomes water vapour, the transition is a kinetic fractionation process rather than an equilibrium one, where the liquid and vapour are not in equilibrium here, therefore, GMWL cannot pass through V-SMOW at $\delta D = 0$ and $\delta^{18}O = 0$. If evaporation were solely an equilibrium process, the GMWL would have to pass through V-SMOW at zero (Jä ger and Hunziker, 1979). It must also be noted that as the isotopic composition of liquid water moves to the right and the composition of the water vapour moves to the left on Figure 2.11, that the enrichment or depletion of the oxygen isotopes is affected more by the process of evaporation and other processes governed by fractionation than hydrogen. According to the Global Meteoric Water Line, for every $\delta^{18}O$ value, there are 8 δD values indicating an abundance of hydrogen over oxygen. Because of this, we see a much more pronounced change in $\delta^{18}O$ values during evaporation than we do in the δD values. This is also shown in Figure 2.13 below, where samples are plotted on the graph depicting the GMWL. This graph shows the difference in the abundance of δD and $\delta^{18}O$ values well because it has samples collected from the South Pole that are extremely depleted in the heavy stable isotopes, with a δD value being approximately eight times more negative than the $\delta^{18}O$ value.

Figure 2.13: Global Meteoric Water Line (Craig, 1961).

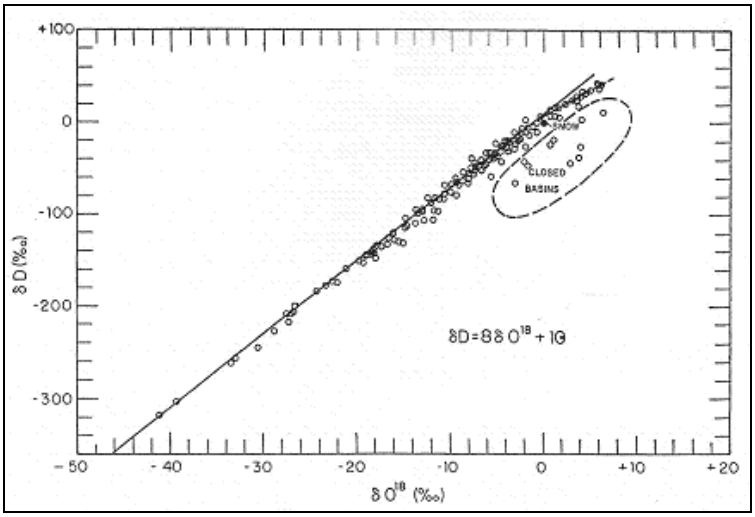

Local Meteoric Water Lines are specific for each locality. Figure 2.14 shows LMWLs for five states in the USA in comparison with the GMWL. There is a close relationship between the LMWLs and the GMWL, however, the slope of each of the American states own LMWL is less than 8 (the slope of the GMWL) (Sharp, 2007).

Figure 2.14: Local Meteoric Water Lines in five States of the USA. (Sharp, 2007, p70).

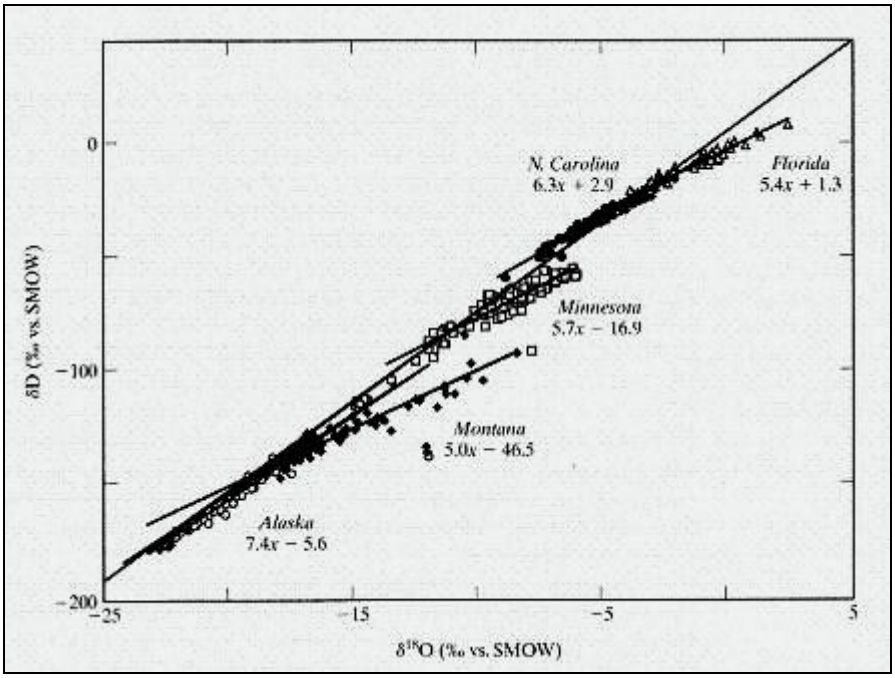

LMWLs may change for a specific location depending on the scope of the stable isotopic study. For example, a study of the stable isotopes of hydrogen and oxygen in atmospheric precipitation for a particular site over a one-month period will give a different LMWL than a study of that same area with duration of one year. This in turn would be different from a study that was undertaken over a ten-year period. These differences are due to the five main effects explained above and this is why it is important to have a very large database for stable isotope studies. Also a large database enables the opportunity to look at changes in the trends of stable isotopes in meteoric water and analysis for the reasons for these changes, for example, climate change may be affecting the stable isotopic composition of water. Without detailed studies, both large and small to create a database, these analyses would not be possible.

There are other factors that affect the stable isotopic composition of precipitation, which will be discussed in later chapters. These are the influences of the duration of a storm event as well as the variations in trajectory the air mass takes to reach the study area. These two factors impact on the stable isotopes in basically the same way; they are both 'rain out' effects. Where as precipitation continues, the heavy isotopes are rained out and so the composition of the precipitation becomes progressively more negative, or depleted in the heavy isotopes. On the other hand, the direction an air mass travels to reach a certain location determines the stable isotopic signature of the precipitation falling from that air mass, differing directions lead to differences in temperature, terrain and the height of the air mass.

2.5. Groundwater

The isotopic composition of groundwater typically remains unchanged whilst the water is underground, as here there is limited evaporation and therefore the hydrogen and oxygen ratios remain the same or very similar. The composition stays the same as when it entered the groundwater system, therefore the stable isotopic ratios depend on the location of the entry point of the surface water into the underground pathways. This intrinsic property of water has been used to determine where groundwater pathways are recharged by the isotopic signatures found within the groundwater. Elevated recharge areas are depleted in the heavy isotopes, as are inland source areas, whereas recharge areas near the coast and at lower altitudes are

enriched in the heavy isotopes. Groundwater flow paths can also be found by matching the hydrogen and oxygen ratios with source areas and other underground reservoirs. For example, groundwater in Missouri, USA, has been found to originate in the Front Range, Colorado, over 1000 kilometres away by similar isotopic signatures (Sharp, 2007).

The isotopic signatures can change whilst underground, but this tends to involve high temperatures in geothermal areas. The higher temperatures allow the groundwater to mix and boil, whilst becoming contaminated with dissolved solids from the rocks in which it is travelling though, like silica, as well as exchanging isotopes with minerals. In most cases there is little change in the δD ratios because rocks tend to have little hydrogen in them. However, the ratio changes in $\delta^{18}O$ can be significant as rocks are comprised of approximately 50% oxygen atoms, oxygen is the most abundant element in the Earths crust (Aggarwal et al, 2005). This variation in the oxygen isotopes is known as an 'oxygen shift'. In geothermal systems that are hot, young, have fresh rock and little throughput of water, the oxygen shift will be greater than a system that is old where the rock has already been shifted to be in equilibrium with the water (Aggarwal et al, 2005).

2.6. Other

2.6.1. *Lakes and Rivers*

The Latitude, Continental, Amount, Altitude and Seasonal Effects are the chief phenomena that have an impact on the isotopic ratios of hydrogen and oxygen in atmospheric precipitation. These relationships all measure the degrees of 'rainout' of moisture transported in air masses from source regions, usually intertropical oceanic regions, to the site of precipitation (Araguas-Araguas et al, 2000). However, they also have an impact on freshwater bodies in the natural landscape.

The isotopic compositions of freshwater lakes and rivers follow along with these relationships. Lakes and rivers at high altitudes are depleted in the heavy isotopes compared to lakes and rivers situated at lower altitudes, as these are enriched in the heavy isotopes as precipitation is less 'rained out' here. Freshwater reservoirs in cooler climes (generally at higher latitudes) will be depleted in the heavy isotopes compared to those bodies in warmer climates or closer to the equator. However, the

δD and $\delta^{18}O$ ratios can become complicated as lakes undergo many cycles of rainfall and evaporation. Therefore there will be variations due to local climatic conditions.

2.6.2. *Glacial Ice*

Glacial ice constitutes a very important and large global freshwater reservoir. A glacier is a great block of ice that is composed of layer upon layer of frozen precipitation that has accumulated over thousands of years (Dansgaard, 1961). Glaciers form in areas of high latitude and high altitude; therefore they have isotopic compositions of δD and $\delta^{18}O$ ratio that are very 'light'. That is, glaciers are depleted in the heavy isotopes with the greatest factor influencing the stable isotopic composition of glacial ice is temperature.

Throughout history there have been periods of cooler temperatures known as glacials, where glaciers cover a large area of land, interspersed with warmer periods known as interglacials (today). It is during these glacial climates that the oceans were significantly enriched in the δD and $\delta^{18}O$ ratios in comparison to todays oceans due to the fact that large quantities of the 'light' hydrogen and oxygen isotopes were locked in glaciers on land (Sharp, 2007).

It was first postulated by Dansgaard in 1954 that there was the possibility to determine variations in past climates over a period of several hundred years by observing the stable isotopes of hydrogen and oxygen in ice cores from the Greenland Ice Cap (Dansgaard, 1954). However, Dansgaard underestimated the scope of this area of research by several orders of magnitude. In 1972, Greenland and Antarctic ice cores offered an unbroken record of precipitation in excess of 100,000 years (Sharp, 2007).

2.7. Stable Isotope Analysis

In this thesis, stable isotopes are being utilised to help to determine the origin of the water sourced on Coronet Peak. The stable isotopes of hydrogen and oxygen have been analysed using the CF-IRMS (continuous flow-isotope ratio mass spectrometer) at the University of Canterbury Stable Isotope Laboratory under the supervision of Dr Travis Horton, the samples were collected from precipitation, springs, surface water storage reservoirs and groundwater sampled from boreholes.

For details on how a CF-IRMS works, see Appendix A. These meteoric water samples have been analysed using this technique, the results will be discussed in later chapters.

2.8. Summary

To summarise, the elements of hydrogen and oxygen when undergoing fractionation due to phase changes in the water cycle, do so very similarly that they can be analysed and interpreted together and form a very important relationship with regard to meteoric water, known as the Global Meteoric Water Line (GMWL). Variations of meteoric water samples from the GMWL are due to changes in temperature via the effects of latitude, continent, altitude, amount and season give rise to Local Meteoric Water Lines (LMWL), and in turn Local Evaporation Lines (LEL) when evaporation occurs. The variations in the stable isotopic composition of precipitation lead to variations in all freshwater reservoirs on Earth.

It is the study of these variations in stable isotopic composition of meteoric waters using mass spectrometry that gives rise to the area of research known as Stable Isotope Hydrology where many avenues can be explored. In this thesis the main focus is on stable isotopic variation in precipitation, springs and groundwater, with emphasis on the relationship between these three aspects of the hydrogeological cycle on Coronet Peak. Better knowledge of the water systems on Coronet Peak will help to utilise this resource as best as possible to allow the impact on this resource in the future to be minimised and therefore be enjoyed by generations to come.

The locations of the precipitation, spring, borehole and water storage reservoir sample sites are shown on Google Earth images in Chapter Three. Here, the sampling methodology is also laid out, describing each step taken to collect the samples and indicating the problems associated with these methods.

Chapter Three:

Methodology of Stable Isotopic Sampling on Coronet Peak

3.1. Introduction

The hydrological components of Coronet Peak consist of precipitation that falls on the mountain, see Figure 3.1 for sampling site locations and Table 3.2 for GPS co-ordinates and elevations. Aquifers that are accessed by boreholes, and springs see Figure 3.2, and man-made surface reservoirs, see Figure 3.3. Each of these water bodies has been sampled to determine the stable isotope composition of each of these water sources. Stable isotopes can determine relationships between surface and ground waters, because the stable isotopic composition of the groundwater is not altered once precipitation enters the underground system. Using this technique the composition of each water source on Coronet Peak can be defined and explained in terms of it's relative importance and influence to better understand the hydrogeology (groundwater) and hydrology (surface water including precipitation) of Coronet Peak.

Figure 3.1. Google Earth image of the five precipitation sampling sites on Coronet Peak.

Figure 3.2. Google Earth image showing the locations of the springs and boreholes (blue icons) on Coronet Peak.

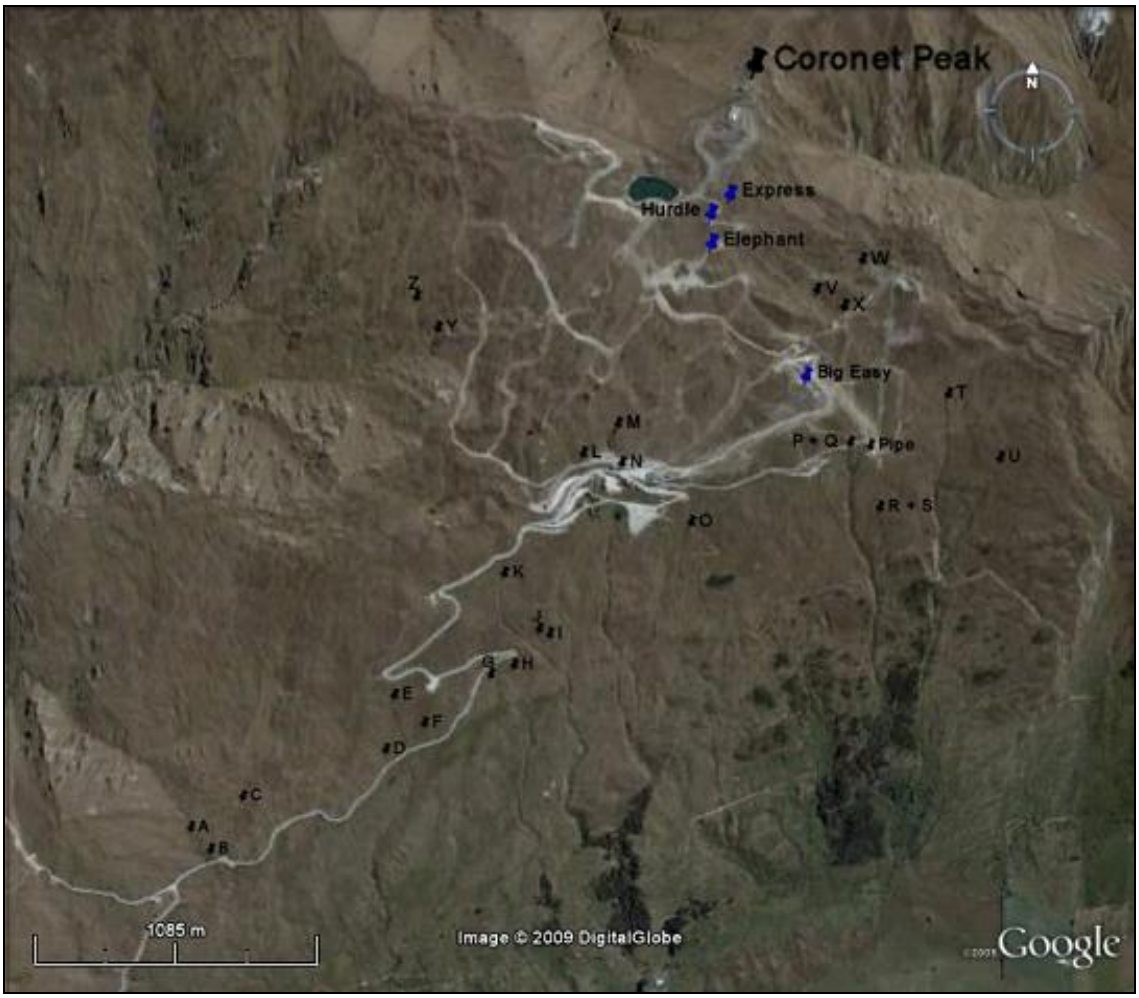

Table 3.1. Spring GPS co-ordinates, elevation and corresponding letters to Figure 3.2.

	Springs	Min-max Flows	Easting	Northing	Elevation (m)
A	Cattlestop	0.05-0.9	2171763	5576564	913
B	Swamp	0.05-0.6	2171821	5576500	879
C	Wired	0.05-1.0	2171871	5576637	968
D	Pond	0.5-2.5	2172541	5576933	977
E	Bramble	0.2-0.6	2172520	5577230	1059
F	Coronet Peak Rd	0.2-1.6	2172750	5577088	1010
G	Multiple	0.1-0.6	2172972	5577252	975
H	Hairpin	1.5-2.5	2173083	5577273	966
I	Grassy	0.25-0.7	2173246	5577489	1003
J	Twin	0.25-2.0	2173272	5577497	982
K	Tussock	0.25-5.6	2172992	5577653	1128
L	Gobblers	0.3-1.2	2173238	5578104	1200

M	**Wall St**	0.25-1.6	2173340	5578209	1256
N	**Water Supply**	2.0-3.2	2173440	5578112	1161
O	**Station**	0.1-0.9	2173651	5577906	1133
P	**Moss**	0.15-2.0	2174410	5577966	1120
Q	**McMullan #2**	0.5-1.5	2174405	5577961	1112
R	**Heidi's**	1.0-6.0	2174249	5578196	1208
S	**Danni's)**	0.1-1.2	2174223	5578163	1184
T	**Waterfall**	1.0-2.2	2174559	5578372	1279
U	**Grasshopper**	0.25-1.6	2174782	5578145	1231
V	**Lunch Rocks**	-	2174057	5578726	1381
W	**Rocky Gully**	-	2174076	5578718	1368
X	**Easy Rider**	-	2174175	5578607	1358
-	**Pipe at Heidi's hut**	0.3-0.5			
Y	**Dirty Four**	1.6-6.0	2172556	5578469	1265
Z	**Dirty Creek**	0.3-6.0	2172595	5578726	1380
-	**Express (Hurdles 3)**	-	2173766	5578925	1378
-	**Hurdle (Hurdles 2)**	-	2173704	5578863	1364
-	**Elephant (Hurdles 1)**	-	2173661	5578722	1357
-	**Big Easy**	-	2174065	5578420	1198

Figure 3.3. Google Earth image showing the locations of the water storage reservoirs on Coronet Peak. The red icon indicates the settlement pond, not a reservoir.

There are 26 known springs located on Coronet Peak, most of which are contact springs, although not all could be sampled on each occasion due to inaccessibility. The other springs are of the nature of fracture, depression and artesian springs, or a combination of these. Contact Springs occur when a permeable water-bearing formation overlies a less permeable formation that intersects the ground surface. Depression Springs form where the ground surface intersects the water table. Artesian Springs result from the release of water under pressure at outcrop or through a confining bed. Whilst fracture springs result where fracture controlled flow is dominant in the rock mass. Each of these spring types are shown in Figure 3.4.

Figure 3.4. Diagrams of the common spring types on Coronet Peak, with water flow indicated by the arrows.

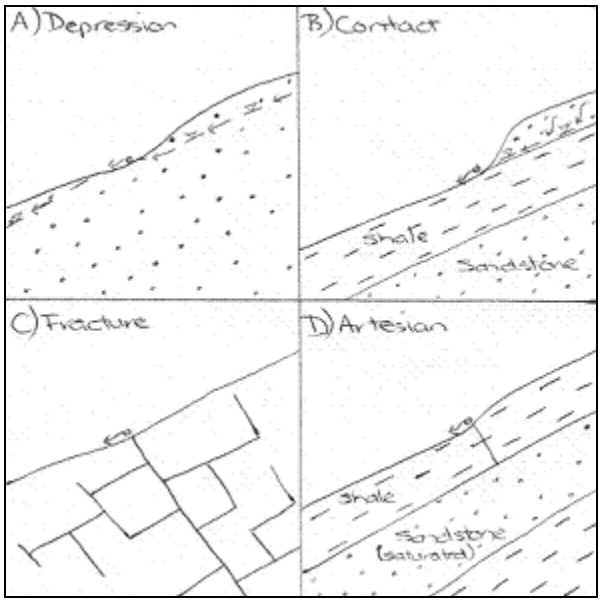

The groundwater of Coronet Peak is located within three different aquifers, which have been deduced from boreholes. There had been 14 boreholes drilled previous to February 2008 to depths between 25 and 174 metres. The three pumping bores indicate the water-bearing intervals at the base of the vertical line drawn in Figure 3.5, where the cross-section line is shown in Figure 3.6. The three aquifers accessed by these pumping bores are at approximately 40, 60 and 130 metres below ground level, the water level in this bore rose to approximately 85 metres indicating a confined aquifer that is sub-artesianing. Bore logs can be found in Appendix B.

Figure 3.5. Elevations (in metres above sea level) of the aquifers beneath Coronet Peak Skifield. The aquifers are located at the base of the vertical blue lines (boreholes).

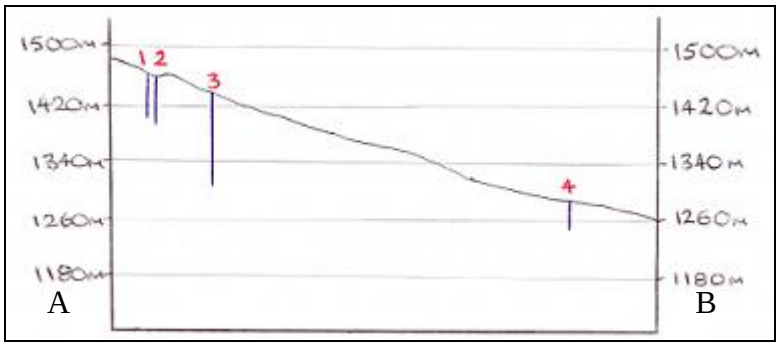

Figure 3.6. Google Earth image of the line used in the above cross-section.

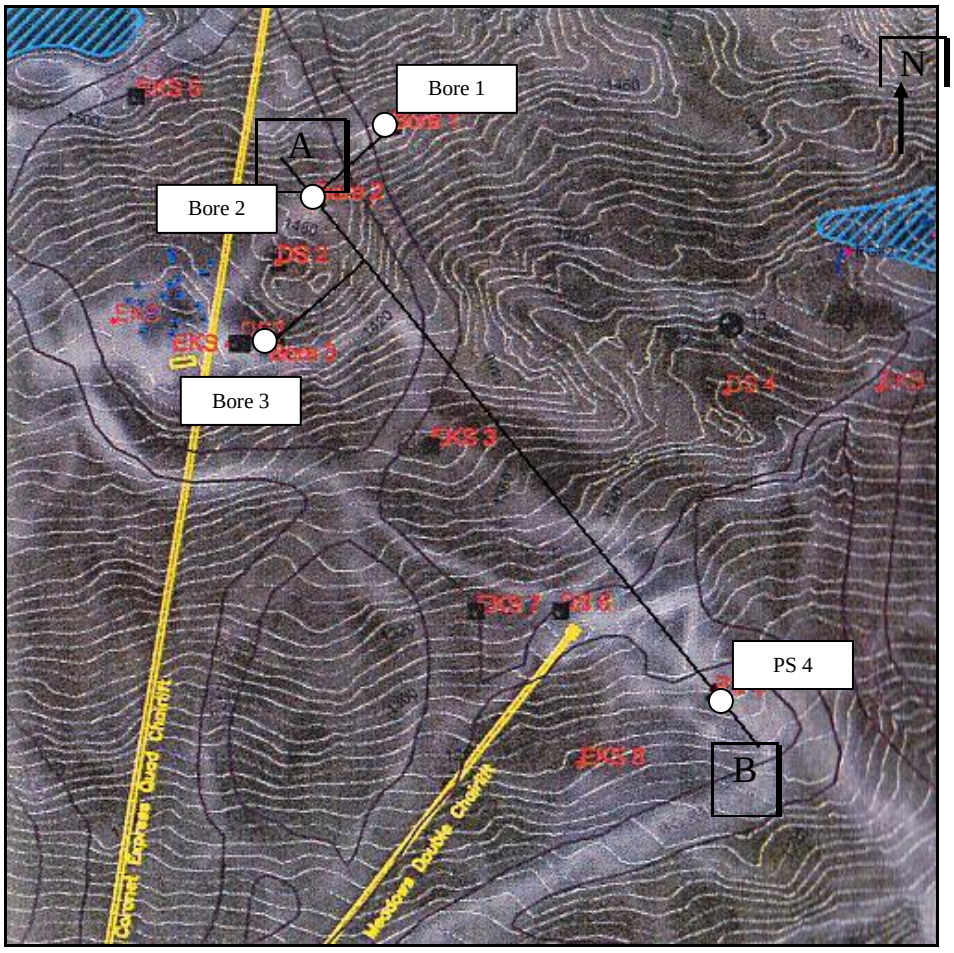

There are five water reservoirs that have been constructed to store water that can be pumped around the mountain to the 141 snow guns on the Coronet Peak Skifield. These reservoirs are located at various elevations on the skifield, 1130 metres (RSVR 2), 1255 metres (RSVR 5), 1390 metres (RSVR 3), 1430 metres (RSVR 1b) and 1490 metres (RSVR 1). Each reservoir has a different volume, the largest being the Reservoir 3 (Rocky Gully) at 90,000 cubic metres, with a total capacity of all five reservoirs being approximately 243,000 cubic metres.

The annual precipitation for Queenstown is 729 millimetres; this is the average of 30 years of precipitation data collected by NIWA, the National Institute for Water and Atmospheric Research, at the Queenstown Airport. The annual precipitation on Coronet Peak will be much greater than this, however the precipitation is only measured on the mountain during the ski season and the only available data to this thesis was recorded between the 1st of July and the 5th of August 2008, where 69 millimetres fell on the top of the mountain. However, precipitation data was not taken every day, there were 16 days with no data. This precipitation data can be found in Appendix B, the NIWA precipitation data can also be found here.

Water samples were collected from each of these water sources; 23 springs and one pipe where spring flow was collected from some springs that could not be sampled directly. Two boreholes, one of these samples collected water from three borehole sources, also from five man-made water storage reservoirs. Precipitation was collected from five different sites of various elevations on Coronet Peak. The samples were then stored in a chilly bin in the field, and a fridge in the University, the optimal temperature for storage being approximately fridge temperature (4° celsius). There they were stored until they could be analysed using the CF-IRMS of the University of Canterbury to determine the δD and $\delta^{18}O$ values of the water sources on Coronet Peak.

3.2. Method for sampling precipitation

The method for sampling precipitation involved setting up five different sampling stations at different elevations, see Table 3.3, on Coronet Peak where a plastic bottle is held in a ring clamp to collect precipitation. Five sites were chosen because in a mountainous area the stable isotope composition of the precipitation falling can vary dramatically, both in a spatial and temporal sense.

3.2.1. *Location of precipitation sampling stations*

The stations were initially only to be set up on the Coronet Peak Skifield and Recreation Reserve, however a more complete picture of the stable isotope composition of the precipitation in this area would be obtained with an increase in the number of sites sampled, and also with a greater elevation profile. Therefore five sites were chosen as sampling stations, three of the five stations fall along the Coronet Peak Road. The other two stations are on the Coronet Peak Skifield itself. The Meadows Station or Site 4 is located at the top of the small double chairlift, and the last sampling station is located at the top of the main chairlift, the Express Chairlift, known as the Express Station or Site 5, this is the highest sampling station on the mountain at 1621 metres above sea level.

The five sites can be seen in Figure 3.1. Table 3.2 gives the elevations above sea level for each site as well as the GPS co-ordinates. Table 3.3 shows the date of the seven precipitation events sampled with their start and end times. At the end of each period of fieldwork all stations were dismantled and packed in case of damage, but were replaced in the same position when the next round of fieldwork began.

Table 3.2. Precipitation sampling site GPS co-ordinates and elevations (metres above sea level).

Sampling Site	Easting	Northing	Elevation
1	2170262	5572244	450
2	2171906	5576470	867
3	2173314	5578031	1164
4	2173934	5578453	1300
5	2173660	5579237	1621

Table 3.3. Summary of precipitation events sampled.

Event	Date	Start time	End time
A	15/07/2009	02:45	14:45
B	18-19/07/2009	19:00	03:00
C	21/07/2009	04:00	20:00
D	11/08/2009	07:30	10:30
E	12/08/2009	00:00	16:00
F	21-22/09/2009	14:00	10:00
G	23/09/2009	03:00	07:00

3.2.2. *Method of Meteoric Precipitation Sampling*

To obtain a complete overview of the variations in stable isotopic composition of the meteoric precipitation over Coronet Peak five stations were set up in different locations at various elevations on the mountain (Figure 3.3). These stations comprised a stand and base that was able to be dug into the ground or covered by snow or rocks in order to minimise the possibility of toppling over. Attached to the stands were a series of two clamps, one, a double ended clamp that was secured tightly around the stand and the other was a single clamp whose end was attached to the double ended clamp also but the clamp itself was left free to hold a plastic bottle for precipitation sample collection, below Figure 3.7 shows the Meadows/Site 4 sampling station. The clamps were all tightened as much as possible and the clean and dry sample bottles connected. Each bottle had a funnel sitting in the neck, the diametre of the funnel was approximately 8cm. This size was selected as it would collect enough precipitation to be sampled but would also minimise the amount of debris that could enter the bottle. The funnel was then attached to the bottle using duct tape so that the bottle would not blow away.

Figure 3.7. Precipitation Site 4 (14/07/2009). The stand base was covered in snow to anchor the station in high winds. The two clamps can be seen connected the bottle and the cross bar to the main stand. The safety tape was used to deter people from disturbing the site.

During the process of setting up the bottle for sample collection, the inside and the top of the bottle was not touched to minimise contamination by contact with skin. At one station known as the Gobblers station or site 3, there were also smaller plastic vials used in conjunction with the one-litre bottles for sample collection. These vials were 50 millilitres in volume and between four and five vials were attached to the two stands at this location with clamps as above. Figure 3.8 below, shows Site 3 with the one-litre bottle and the five smaller, 50 millilitre bottles.

Figure 3.8. Photo of Site 3 showing both the one-litre bottle and 50 millilitre vials (14/07/2009). Set up is very similar to the station at Site 4 in Figure 3.7, but here the smaller vials are clamped to the main stands as well as the larger bottles. There were typically five 50-millilitre vials out at any one time.

The five one-litre bottles at the five stations were left out to collect precipitation samples (both rain and snow fall) during a precipitation event, the lengths of events can be seen in Table 3.4. After each event the bottles were collected, capped and five new one were put out for the next event. The 50 millilitre vials at Site 3 also collected precipitation from the same event as the one litre bottle at this site, but these vials were collected and replaced after every four hours during a precipitation event. The vials were capped and stored in a chilly bin filled with snow to limit evaporation. This way, the stable isotopic compositional changes during the precipitation event could be quantified whilst the one-litre bottle collected precipitation from the entire event.

There were a total of seven precipitation events sampled; the dates and durations are shown in the following chapters. For each of the events, a one-litre bottle was collected at each site, and at Site 3 the smaller, 50 millilitre vials were also collected, the number of these depending on the length of the precipitation event.

3.3. Reporting of precipitation results.

The δD and $\delta^{18}O$ values that are found from analysing the water samples collected with a CF-IRMS were graphed using Excel so that any relationships can be shown and analysed. Generally the hydrogen isotope and oxygen isotope data values are plotted on a scatter graph where δD values are plotted versus the $\delta^{18}O$ values. However in some it is more prudent to plot the δD values and $\delta^{18}O$ values alone against altitude or time to better show the relationships of the stable isotopes with these variables.

Statistical methods were also applied to this data to demonstrate how well the data expresses these correlations between the stable isotopes of hydrogen and oxygen and the main variables of altitude and the duration of the precipitation event. The correlation of determination (R^2) can be used to show the amount of variability accounted for in the relationship between two variables and provides a means to measure how well future outcomes are likely to be predicted by the current model of the data set. Values close to 1 show a good relationship between the variables, where values near 0 indicate a very poor correlation (Salkind, 2007).

3.4. Critical review of precipitation method

The sampling method applied to meteoric precipitation collection may be problematic. The main issue being that samples may evaporate in their bottles before they could be collected and kept in a cool environment, thus minimising the likelihood of evaporation. Coronet Peak is a mountain with a height range of approximately 1201 metres (450 to 1651 metres above sea level); therefore precipitation may not be occurring all at once over the entire mountain. Because of this possibility, there is a chance that some samples may be exposed to the sun where they can heat up and evaporation may occur, whilst others may be still collecting precipitation. Water can evaporate at any temperature if left long enough, but with increased temperatures the rate of evaporation increases and the liquid water in the sample bottles gains enough energy to cross the phase threshold and convert from a liquid to a gas.

Another problem with this method of sampling is the time it takes to transport the samples to the laboratory for analysis. The precipitation samples once collected are kept in a fridge or chilly bin filled with snow until they can be taken for analysis. As long as the samples are kept cool, the effects of evaporation should be minimised. Evidence of evaporation could be seen in the bottles that had 'misted up'. Some samples were more prone to evaporation than others, the larger sample bottles. The samples that were least liable to this were the samples that were completely filled to the brim of the bottle or vial. Being filled to the very top leaves no room for evaporation to take place, this was the case with the spring, reservoir and borehole samples.

However, none of the precipitation samples filled their sample bottles to the top, allowing room for evaporation to transpire. How much the bottles were filled depended entirely upon the amount of precipitation that had occurred. Therefore the sample bottles for precipitation events that were of short duration, or produced a small amount of precipitation were more likely to be affected by evaporation. To try to negate this factor, towards the end of the field sample collection the precipitation that was collected in the one-litre bottles were transferred to either a 50 or 25 millilitre plastic vial (depending on sample size) once they were brought in from the field. It was hoped that this would counteract the effects of evaporation of the samples. A better way and one that would be used in any future studies in the stable isotopes of meteoric waters would be to use an oil that would sit on the surface of the sample not allowing it to react with the air and evaporate.

The effect the large one-litre bottles had on the precipitation collected inside them can be seen in precipitation event B. Four samples were collected for this event, from Sites 1, 2, 3 and 4 (sample for Site 5 was lost on the mountain due to high wind speeds) precipitation for this event occurred over an eight-hour period on the 18-19 of July 2009, though created very little precipitation. The precipitation collected was left in the one litre bottles until analysis could occur, however when they were to be analysed only one bottle had any sample left, Site 2, the sample in the other three bottles had been completely evaporated away.

3.5. Sampling of boreholes, springs, and reservoirs

There are 14 boreholes that have been drilled on Coronet Peak to better understand the groundwater situation beneath the skifield. This information is required so that the skifield can utilise this resource in artificial snowmaking. However, only four are pumped from, these are the Big Easy Bore, the Elephant Bore, the Hurdles Bore and the Express Bore, brief logs are shown in Appendix B. The other boreholes were not pumped from due to a lack of groundwater found when drilling occurred.

The Big Easy Bore pumps water from a depth of approximately 40 metres, the Elephant Bore from 130 metres, the Hurdles Bore from 58 metres and the Express Bore from 65 metres. This is the information that implies that there are three aquifers beneath Coronet Peak. The shallower aquifer at 40 metres below ground level, another at approximately 58 to 65 metres, which coincides with the base of the Coronet Peak Landslide, and the deepest aquifer at 130-m depth. There are only two borehole samples collected on Coronet Peak, these being the Big Easy Bore and the Hurdles Bore. However, the staff on Coronet Peak have pumped all water from the Elephant, Hurdles and Express Bores into a collection tank together, and this is where the sample is collected as the boreholes themselves cannot be accessed. Therefore the stable isotope data from the 'Hurdles Bore' is an amalgamation of three boreholes from differing depths and ranging between two aquifers. The data is still useful however, as these bores all collect water from beneath the Big Easy Bore and so are all of a deeper groundwater source. This groundwater source is most likely two different aquifers or two different water-bearing layers within the rock. As seen in Figure 3.5 Bores 1 and 2 indicate water flow at very similar depths (56 and 63 metres respectively) and therefore may be related, whilst Bore 3 had initial flow depths at 130 metres, indicating no relation to the other water sources.

During the winter months when sampling was undertaken some springs became inaccessible due to snow cover or their location. Two of these springs, known as the Dirty Four and Dirty Creek springs, were inaccessible due to avalanche danger during August 2009. An avalanche occurred on Coronet Peak in the beginning of August 2009 and a snow boarder was killed outside the skifield boundary. The location of these two springs was very close to that of the avalanche and it was

advised not to go off piste, however these springs were later sampled in September 2009.

Three springs were sampled indirectly, these were the Lunch Rocks, Rocky Gully and Easy Rider Springs, all located within the central northern area of the Coronet Peak Skifield. They were sampled from a pipe that is used to collect flow from these three springs and divert to a collection area. When the stable isotopic composition of the 'pipe at Heidi's Hut' is mentioned it refers to all three spring compositions. The sampling times are shown in Table 3.4, each date given is the Monday of the week when sampling was undertaken.

Table 3.4. Spring sampling dates.

2008	2009
14/04/2008	13/07/2009
21/04/2008	10/08/2009
09/06/2008	21/09/2009
07/07/2008	-
21/07/2008	-
11/08/2008	-
01/09/2008	-
15/09/2008	-

The locations of the reservoirs on Coronet Peak are also shown in Figure 3.3, and all five reservoirs were sampled for their stable isotopic content.

The springs, reservoirs and boreholes were sampled very simply. Using a 25 millilitre plastic vial, they were filled from a tap from the pump-houses of the boreholes, dipped into the spring flows and reservoirs. The vials were filled to the top to discourage evaporation whilst inside the vial and during transportation to the laboratory. Plastic vials were preferred over glass to minimise breaking of the vials in transport from field area to laboratory. The vials were handled very carefully whilst sampling in order to negate contamination. Whilst the samples were being taken, the top of the vial did not come into contact with anything other than the water sampled and its lid. The vials were labelled with name and date of collection after they were

filled so the water would not affect them. The tops were checked on the vials to make sure they were done up tight and then the vials were placed in a chilly bin that was filled with snow to keep the samples cool. Once the samples were back at the University of Canterbury they were kept cool in a fridge until they could be analysed using the continuous flow-isotope ratio mass spectrometer. The process of analysing the samples in general is discussed in Appendix A.

3.6. CF-IRMS analysis of water samples

The Stable Isotope Laboratory at the University of Canterbury uses a isotope ratio mass spectrometer to determine the δD and $\delta^{18}O$ values in water samples. As the science of mass spectrometers has evolved, from the first mass spectrometer in 1912 to today, there have been great advances in the areas of sensitivity, detection limits and the diversity of the applications in which this technique can be utilised (Hoffman and Stroobant, 2002). A mass spectrometer will always have the same basic elements, as seen in Figure 3.9. More detailed information on this analysis can be found in Appendix A.

Figure 3.9. Basic diagram of a mass spectrometer (Hoffman and Stroobant, 2002).

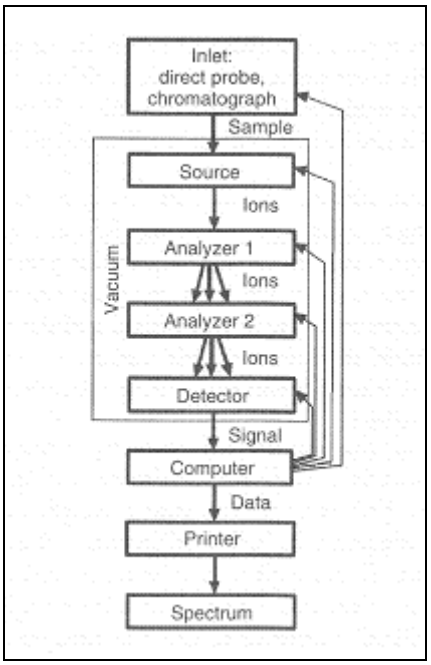

Water samples were analysed by the Thermo-finnigan temperature conversion elemental analyser (TC-EA) connected to a Thermo-finnigan Delta V Plus isotope ratio mass spectrometer. During this process the samples were under continuous flow conditions (helium stream). The stable isotope data produced was automatically entered into a computer where it can be interpreted.

The data obtained from the CF-IRMS at the University of Canterbury is very high quality, accurate to ± 1.0‰ for δD values and ±0.2‰ for $\delta^{18}O$. These results are based on replicate analyses of the IAEA (International Atomic Energy Agency) standards SMOW2 (n=20) and GISP (Greenland Ice Sheet Project) (n=20) certified materials analysed in the same analytical sequence. This data was then normalised to the V-SMOW using certified GISP δD and $\delta^{18}O$ values of –189.73‰ and –23.784‰ respectively and SMOW δD and $\delta^{18}O$ values of 0.00‰ and 0.00‰ respectively. The results obtained allowed the conclusions in the following chapters to be drawn.

Chapter Four:

Isotopic Characterisation of Local Waters for the Coronet Peak Area

4.1. Introduction

The local meteoric water line (LMWL) is a line determined by the stable isotopic composition of meteoric sources (natural waters that have been derived from meteoric water) in a specific region or locality. This line is created by plotting the stable isotopic values for each water sample collected on a graph of δD versus $\delta^{18}O$, and is typically very similar to the global meteoric water line (GMWL). The GMWL is derived from all the stable isotopic data that has been collected from meteoric water and plotted on a δD versus $\delta^{18}O$ graph. The resulting global relationship between hydrogen and oxygen isotopes in meteoric waters was first proposed by Craig (1961), and the initial linear relationship was first suggested by both Epstein and Mayeda. (1953) and Friedman (1953), who worked with the stable oxygen and hydrogen isotope composition of meteoric waters respectively. Craig used this idea and compared the ratios of oxygen and hydrogen in meteoric waters together, defining the GMWL by the following equation:

$$\delta D = 8\ \delta^{18}O + 10 \qquad \text{Eq. 4.1.}$$

This relationship is characterised by a slope of 8 with a y-intercept of 10. LMWLs will show a very similar equation to this, but they tend to a have a slope that is slightly lower or shallower than the GMWL (Figure 4.1). If this is the case, it suggests that the processes forming the precipitation in the Coronet Peak area "occurred under isotopic equilibrium conditions between both the condensate and the corresponding vapour", and that the stable isotopic content was not altered by evaporation during the descent of the precipitation (Nijitchoua et al. 1999, p17). Neither the GMWL nor the LMWL pass through V-SMOW (δD=0 and $\delta^{18}O$=0) due to the kinetic processes involved during evaporation of the water molecules from the oceans (Jager and Huniker, 1979). Figure 4.1 shows the variations with location (LMWL) from the GMWL in five states in the USA.

Figure 4.1. Local Meteoric Water Lines in five States of the USA. (Sharp, 2007, p70).

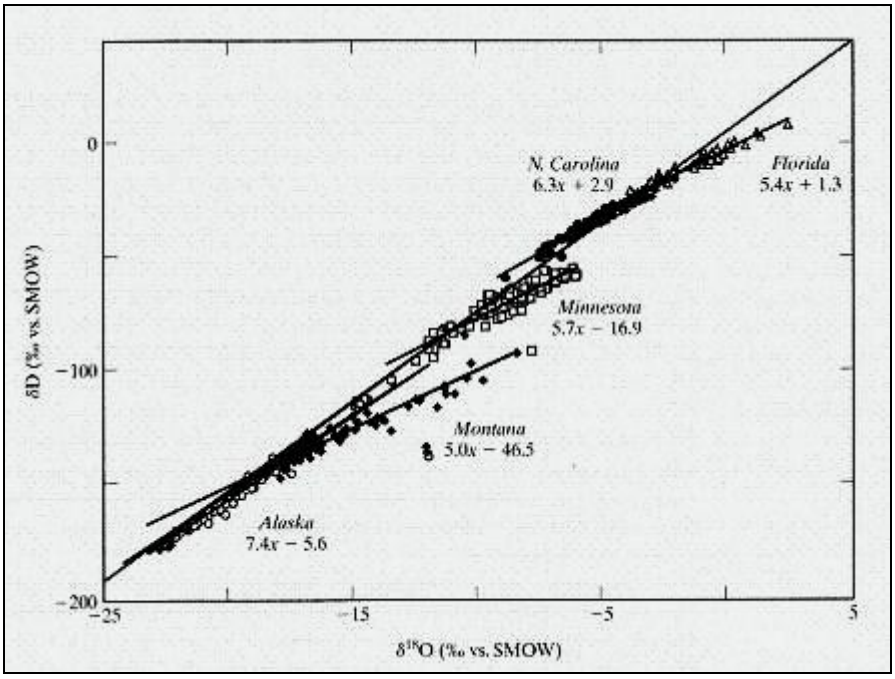

The y-intercept of the LMWL is otherwise known as the deuterium excess or d-excess value. This is a ‘measure of deviation of any given point from the line with a slope equal to 8 that goes through V-SMOW’, a line with a y-intercept of 0 (Araguas-Araguas, et al. 2000, p1350). The precipitation parameter of deuterium excess is a ‘powerful tool to estimate the evaporative admixture from ground sources to the atmosphere’ (Iqbal, 2008, p4612). For modern meteoric water, a d-excess value equal to 10‰ is the average global value as indicated by the GMWL. On the other hand, a d-excess value less than 10‰ indicates that secondary evaporation has occurred, with values greater than 10‰ suggesting that there has been moisture returned from the surface or a mixed air moisture source. Studies done by the International Atomic Energy Agency (IAEA) and other organisations from around the globe have indicated that most modern precipitation falls between d-excess values of 0 and 20‰, and that any values that are outside this range should signify a considerable alteration either by evaporation or from a secondary moisture source (Iqbal, 2008).

Typically groups of samples that have been evaporated will plot on a variation of the LMWL, with the equation of the line giving a y-intercept or d-excess value less than 10‰. When this happens, instead of labelling it a LMWL, even though it does

indicate the variations within natural meteoric waters on a regional scale, a more appropriate name would be to call it a Local Evaporation Line (LEL).

Figure 4.2. The deuterium excess parameter. Water begins on the GMWL with a ratio of δ0. As evaporation occurs, the residual water moves to the right of the GMWL, whilst the vapour moves to the left.

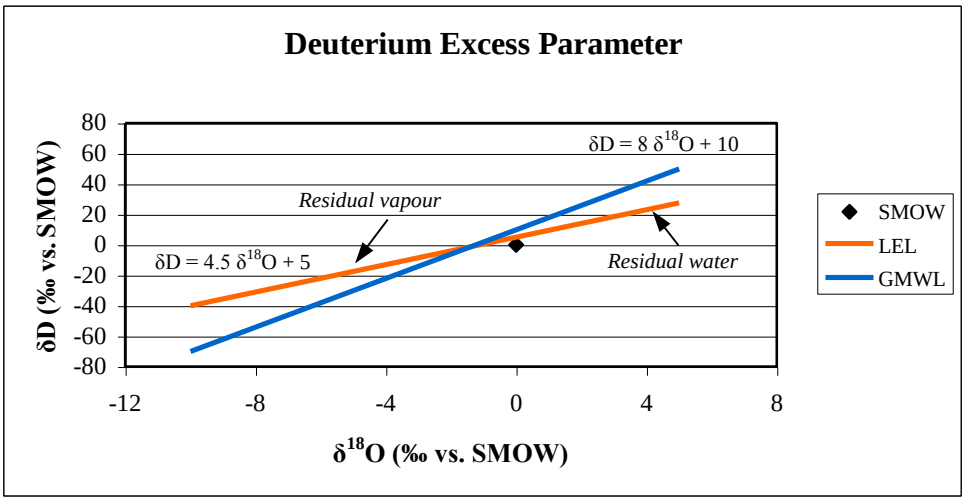

Unevaporated meteoric water sits on or very close to the GMWL, however as shown in Figure 4.2 above, when evaporation occurs the slope of the line decreases. This is now known as the LEL, as the water samples move below and to the right of the GMWL, whilst the remaining vapour in the air mass moves above and to the left of the GMWL. This relationship is extremely useful as it can indicate the explanation for the variability in the stable isotope data, in that some or all of the samples have undergone evaporation.

LMWLs and LELs are only possible due to the variables associated with temperature within the atmosphere that affect the stable isotopic composition of meteoric waters. For example the effects of altitude, latitude, continent, amount and season (described in Chapter Two) give rise to the deviations from the GMWL. These influences on the stable isotopic composition of meteoric water are diverse and vary spatially and temporally, and lead to the creation of LMWLs. LELs are a variant of LMWLs and indicate that evaporation has had a significant impact on the water samples collected.

4.2. Meteoric water samples

All of the samples collected on Coronet Peak and the adjacent area are meteoric water samples; ie they have all been derived from meteoric water, unlike some waters that can be derived from igneous activities. These meteoric water samples were collected from precipitation, spring, borehole and reservoir sources. Sampling of the Coronet Peak area took place during the months of July, August and September 2009; all of the sample locations are shown below in the Google Earth image of Figure 4.3, with the location names shown in Table 4.1.

Figure 4.3. Google Earth image of the sample sites on Coronet Peak.

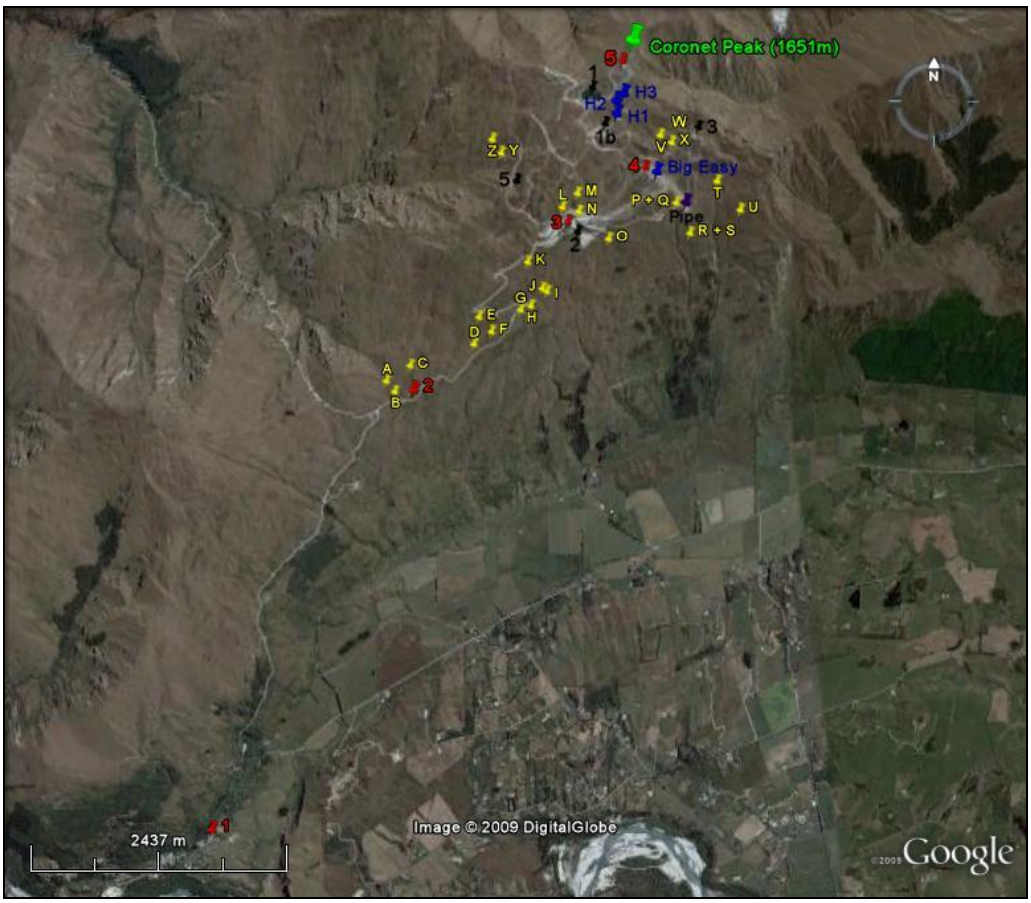

Table 4.1. Corresponding sample location names with the letters and numbers from Figure 4.3. Yellow/orange letters are spring locations, black are reservoirs, red are precipitation sites, and blue are boreholes.

Symbol	Location Name	Symbol	Location Name
A	Cattlestop	U	Grasshopper
B	Swamp	V	Lunch Rocks
C	Wired	W	Rocky Gully
D	Pond	X	Easy Rider
E	Bramble	Y	Dirty Four
F	Coronet Peak Rd	Z	Dirty Creek
G	Multiple	Pipe	Pipe at Heidi's Hut
H	Hairpin	1	Main Reservoir
I	Grassy	1b	Elephant Pit
J	Twin	2	Lower Reservoir
K	Tussock	3	Rocky Gully
L	Gobblers	5	Sarah Sue
M	Wall St	1	Precipitation Site 1
N	Water Supply	2	Precipitation Site 2
O	Station	3	Precipitation Site 3
P	Danni's	4	Precipitation Site 4
Q	Heidi's	5	Precipitation Site 5
R	Moss	Big Easy	Big Easy Bore
S	McMullan #2	H1	Elephant Bore
T	Waterfall	H2	Hurdle Bore
		H3	Express Bore

Groundwater pumped from the Elephant (H1), Hurdle (H2) and Express (H3) bores has all been diverted to a combined collection tank, such that the individual bores could not be sampled. Although the above figure shows all three borehole locations, it must be noted that the Hurdles Bore sample is a combination of all three boreholes and represents groundwater from approximately 58m depth and greater.

The Big Easy Bore, in contrast, accesses water from approximately 40m below ground level. Samples were collected from all of these sites where possible for each sampling period in July, August and September 2009, and were then analysed using the continuous flow-isotope ratio mass spectrometer. The δD and $\delta^{18}O$ values were determined and plotted on a δD versus $\delta^{18}O$ graph to identify any relationships between them, and to determine a LMWL for each month of sampling and a total LMWL for the Coronet Peak area (Figures 4.4 to 4.7). A LEL for Coronet Peak is also presented on graphs of δD versus $\delta^{18}O$ (Figures 4.8 to 4.11), where only the water located on the surface of the mountain (ie the reservoirs) is plotted. These are theoretically the only waters to have been under the influence of evaporation for an extended period of time.

4.3. Local Meteoric Water Line

To create a LMWL for the Coronet Peak area, all of the water samples collected (see Figure 4.3 above for locations and Appendix C for all stable isotope data) were plotted on a graph of δD versus $\delta^{18}O$, and then compared to the GMWL. Data for each month has been graphed individually to determine any difference between them in Figures 4.4 (July), 4.5 (August) and 4.6 (September), and then graphed together in Figure 4.7, to give a Local Meteoric Water Line for the Coronet Peak area in the winter of 2009.

The stable isotope data all fit the regression/trend lines given well. Table 4.2 displays the R^2 values for all of the LMWLs for the Coronet Peak area. Each R^2 value is greater than 0.9, indicating that there is little variability within the data. The main outside variable is evaporation affecting the samples, which could explain the deviation of the data from this trend.

The equations of each of the LMWLs for the months of July, August and September 2009, as well as the total LMWL for the Coronet Peak area, are shown on the corresponding graphs (Figures 4.4 to 4.7). The slope of each line for the monthly LMWLs are all very close that of the GMWL slope of 8.0, with the total LMWL giving a slope of 8.0009. The data also show a y-intercept of 10.178. The monthly LMWL y-intercepts vary between –1.7674 and +13.463, these generally fall within

Table 4.2. R^2 values for the LMWLs of the Coronet Peak area.

LMWL	**R^2 value**
July 2009	0.98
August 2009	0.97
September 2009	0.91
Total 2009	0.97

The accepted values for deuterium excess are between 0‰ and 20‰ (Iqbal, 2008). The reason for the month of September having a negative y-intercept may be due to some samples being affected by evaporation more than in the previous two months. From the graphs provided, it can be seen that this month has a greater variability than the other months, and this is also shown by the lowest R^2 value of 0.91 (Table 4.2). The reservoir samples are certainly all affected by evaporation, as discussed later.

4.4. Local Evaporation Line

Local evaporation lines indicate the relationship between δD and $\delta^{18}O$ in evaporated waters, and for Coronet Peak data has been plotted only for surface waters. The stable isotopic data used in these LELs is from the five surface water storage reservoirs that are located on the Coronet Peak Skifield, and their locations are shown in Figure 4.8. There is a total storage volume of approximately 243,000 cubic metres when the reservoirs are filled to capacity, and the individual volumes are listed in Table 4.3.

The main purpose for the reservoirs on the Coronet Peak Skifield is to store water that can be pumped via a series of subterranean pipes around the skifield, for example, to the base hut, medical centre and the large number of snow guns that operate around the mountain. It is the samples from these five reservoirs that comprise the most evaporated meteoric waters on Coronet Peak, due to the fact that they are exposed to the atmosphere for varied amounts of time, allowing evaporation to

occur. The source of the water held within these reservoirs typically comes from the Big Easy bore and the Hurdles bore (including groundwater sourced from the Elephant, Hurdle and Express bores), therefore the stable isotopic signature of the reservoirs before evaporation takes place should be very close to that of the groundwater of the area. Also some of the spring flows are diverted to reservoirs, again indicating that the initial stable isotopic composition should be comparable to the groundwater. Precipitation contributes a small amount to the reservoir sources, as limited precipitation falls directly into the reservoirs.

Local evaporation lines have been constructed for Coronet Peak on a monthly basis when sampling was undertaken, these being Figures 4.9 (July), 4.10 (August) and 4.11 (September). Their purpose is to identify any variation between these months, and a total LEL (Figure 4.12) has been compiled to give an overall sense of the extent of evaporation of the surface waters on the Coronet Peak Skifield.

The equation of each of these lines is shown on Figures 4.9 to 4.12 inclusive. With slopes between 3.97 (July) and 5.43 (September), they fit well with Craig's (1961) statement that most evaporated meteoric waters plot on a δD and $\delta^{18}O$ graph with a slope of approximately 5. The deuterium excess value is also a useful indicator of evaporation. As stated by Iqbal (2008), most meteoric water has a d-excess value between 0‰ and 20‰, all of the LELs above have d-excess values between –20.68‰ and –38.865‰, this signifies that these waters have been highly affected by evaporation.

The reservoir samples collected in September 2009 are least affected by evaporation, having the highest slope and the lowest d-excess value. This indicates that the amount of evaporation the reservoirs have undergone (or the time they have been exposed to the atmosphere) has been less than the other months that reservoirs were sampled. There is the possibility that cooler temperatures resulted in less evaporation during September 2009, but Table 4.4 shows that the average monthly temperature in September is substantially warmer than both July and August.

Figure 4.4. Local Meteoric Water Line for the Coronet Peak area for the month of July, 2009.

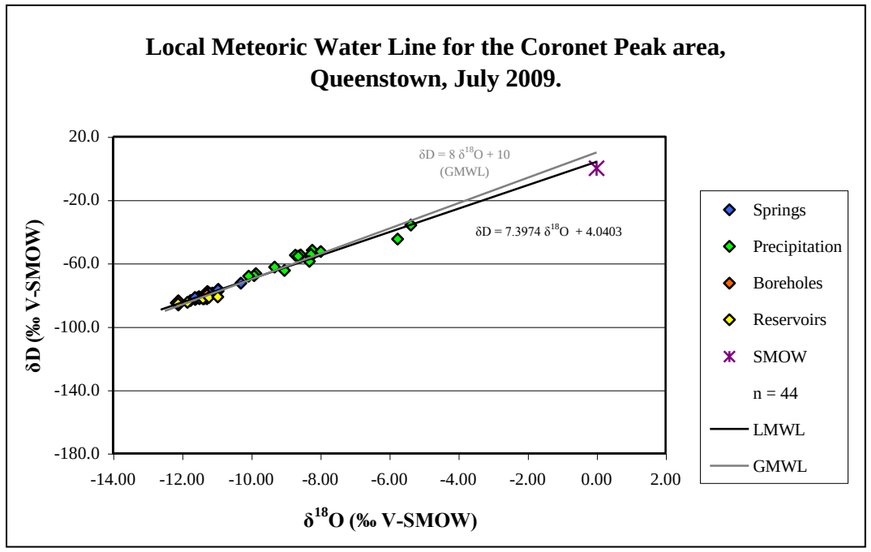

Figure 4.5. Local Meteoric Water Line for the Coronet Peak area for the month of August, 2009.

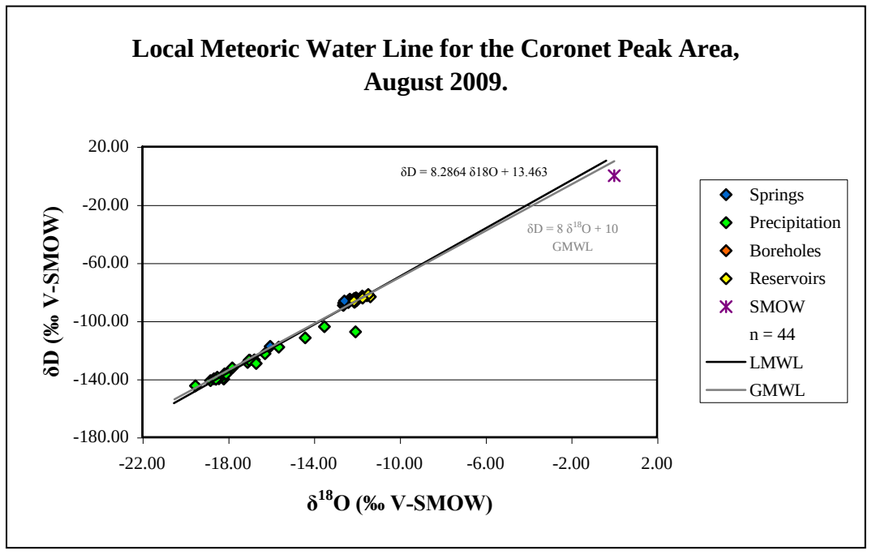

Figure 4.6. Local Meteoric Water Line for the Coronet Peak area for the month of September, 2009.

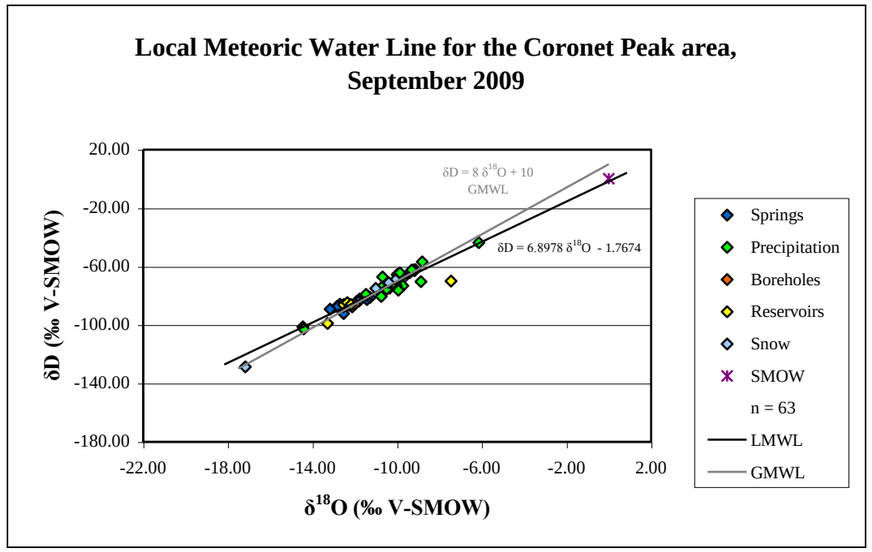

Figure 4.7. The total Local Meteoric Water Line for the Coronet Peak area.

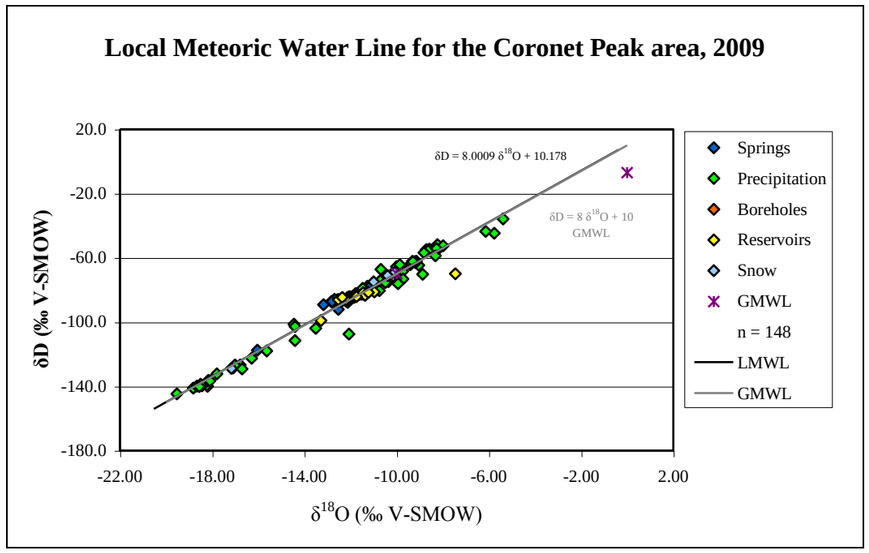

Figure 4.8. Google Earth image of the location of surface reservoirs on the Coronet Peak Skifield. The red icon indicates a settlement pond (not a storage reservoir) and was therefore not sampled for its stable isotopic content.

Table 4.3. Reservoir volumes on the Coronet Peak Skifield.

Reservoir	**Volume (m^3)**
1 - Main	80,000
1b - Elephant Pit	19,000
2 - Lower	4,000
3 - Rocky Gully	93,000
5 - Sarah Sue	47,000
Total	**243,000**

Table 4.4. Average temperatures at the Queenstown Airport for the months where sampling occurred on Coronet Peak (NIWA, 2009).

Month	**Average temperature (° Celsius)**
July 2009	2.8
August 2009	6.4
September 2009	8

Therefore the main factor is most likely the residence times of the water within the reservoirs, indicating that the reservoirs were utilised and refilled with fresh groundwater more often in September than in July and August. Due to the warmer temperatures at this time, the amount of snow that falls is less than in the cooler months previously. It is because of this that the reservoirs have less residence times in September because the water within the reservoirs would have been used in the snow guns to create artificial snow that allows the skifield to improve the reliability of the snow coverage around the mountain and to extend the ski season.

4.5 Local Evaporation Lines correlated with Borehole Data

The individual stable isotopic composition of each reservoir can show which reservoirs had the longer residence times at the time of sampling, and also indicating which reservoirs were in use at this time. This information has been plotted on a δD versus $\delta^{18}O$ graph along with the borehole data that was collected at the same time as the reservoir samples. This allows inferences as to which reservoirs had been filled using which groundwater source (ie the Big Easy or the Hurdles bores) by their stable isotopic compositions. Each month of sampling is graphed with the borehole data in Figures 4.13, 4.14 and 4.15. The reservoir data was collected on my behalf by the staff of Coronet Peak Skifield, therefore the depth of collection is uncertain. However, each reservoir is aerated to stop the top from freezing so there is continuous mixing of the water stored within them. This therefore implies that there should be no isotopic difference within the reservoir, and any sample collected is representative of the reservoir as a whole.

Figure 4.9. The Local Evaporation Line for Coronet Peak, July 2009.

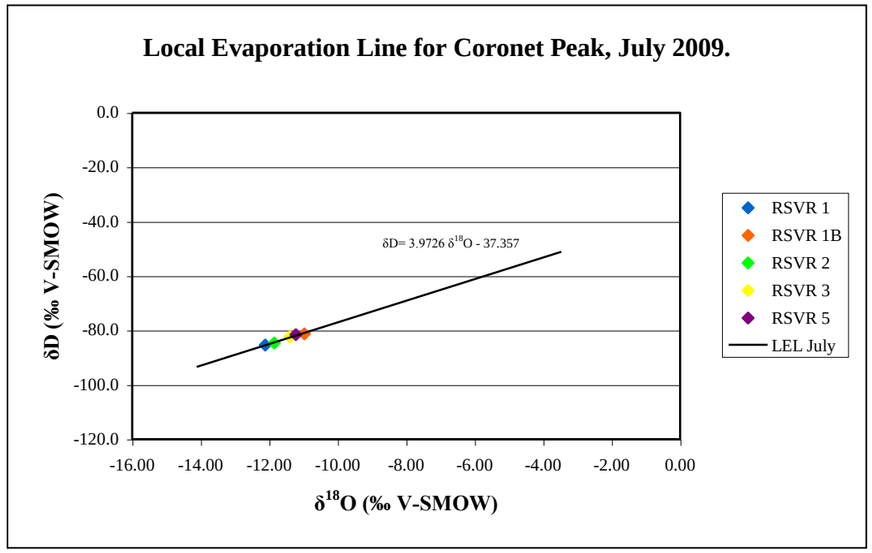

Figure 4.10. The Local Evaporation Line for Coronet Peak, August 2009.

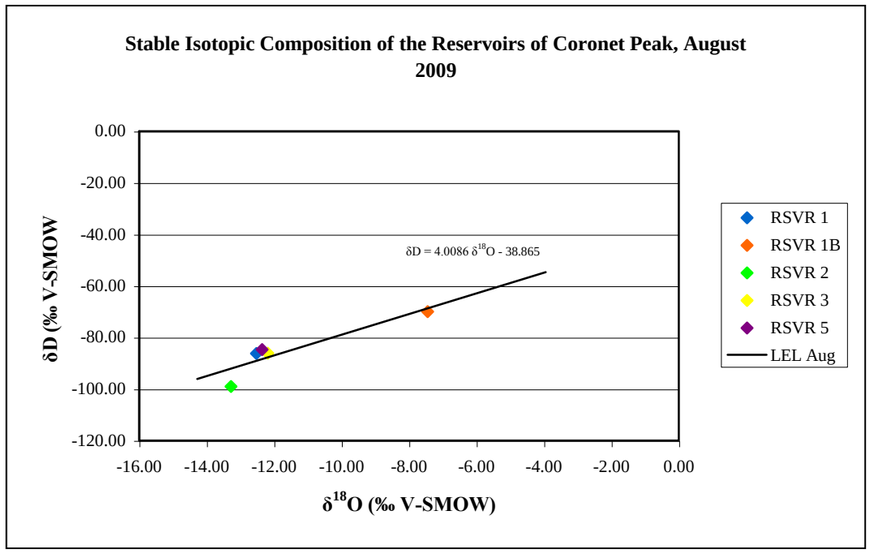

Figure 4.11. The Local Evaporation Line for Coronet Peak, September 2009.

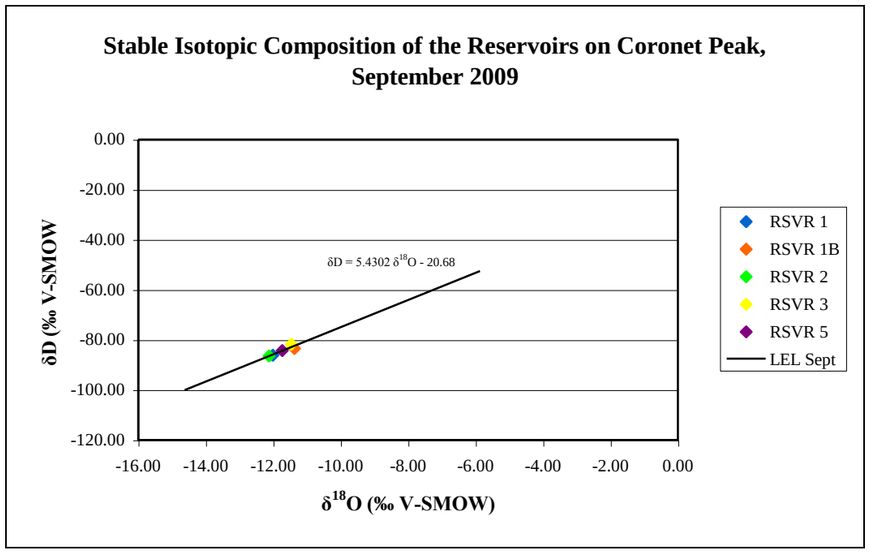

Figure 4.12. The Local Evaporation Line for Coronet Peak, 2009.

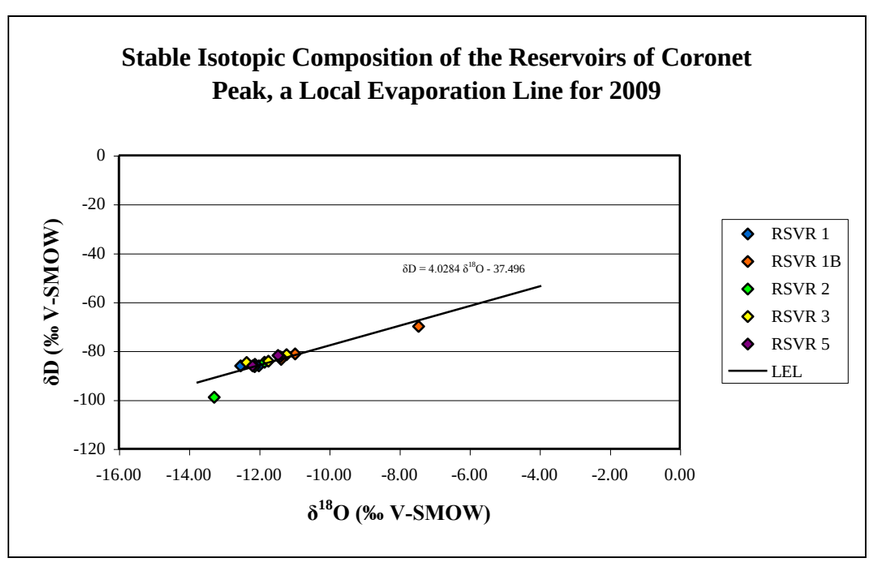

Figure 4.13 shows the reservoir and boreholes stable isotopic data for July 2009, these samples were collected on the 21/07/2009. From this graph, it can be seen that the reservoirs cluster in two areas, and within these two areas a borehole also is plotted. Therefore, from this data RSVR 1 and RSVR 2 are dominated by pumping from the Hurdles bore, as this is the bore that is plotted very near to these two samples. The Big Easy bore plots very similarly to the other three reservoirs, RSVR 1B, RSVR 3, making it their most likely groundwater source. All of the reservoirs plot to the left of both boreholes indicating evaporation. RSVR 5 plots more negatively than the Big Easy bore, but is a lot more positive than the Hurdles bore. It is possible that the stable isotopic composition of RSVR 5 originated from the Hurdles bore, but has been evaporated to plot just behind the Big Easy bore. This could indicate that RSVR 5 had the longest residence time out of all of the other reservoirs. Also, RSVR 1 and RSVR 3 almost plot on top of the Hurdles and Big Easy bores respectively, which could signify that these two reservoirs were utilised the most. Their stable isotopic compositions are certainly the closest to the groundwater sources at the time the samples were collected.

The reservoir and borehole samples for the sampling period in August 2009 have been plotted in Figure 4.14. The stable isotopic compositions of the reservoirs are quite varied, with RSVR 2 being very negative, even compared to the Hurdles bore. This negativity (all reservoirs apart from RSVR 1b are more negative than both boreholes) may be due to the pronounced negativity in the precipitation that fell during the period in which these samples were collected. These samples were collected during the month of August, the reservoirs on the 14/08/2009 and the boreholes on the 28/08/2009. The precipitation that fell during Event D (11/08/2009) averaged –121.70‰ and –15.88‰ for δD and $\delta^{18}O$ respectively, while Event E (12/08/2009) averaged -136.72‰ and -18.11‰ for δD and $\delta^{18}O$ respectively, these values being averaged over all the samples taken for these precipitation events. This could indicate that the reservoirs were affected largely by the precipitation, or that the groundwater pumped to them was influenced by the precipitation that fell at this time.

Figure 4.13. The Local Evaporation Line for Coronet Peak, July 2009, with Borehole Data.

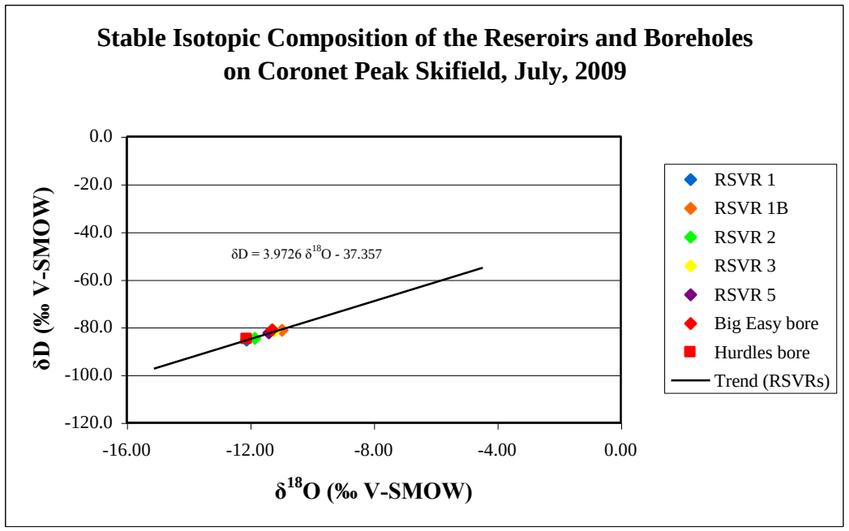

Figure 4.14. The Local Evaporation Line for Coronet Peak, August 2009, with borehole data.

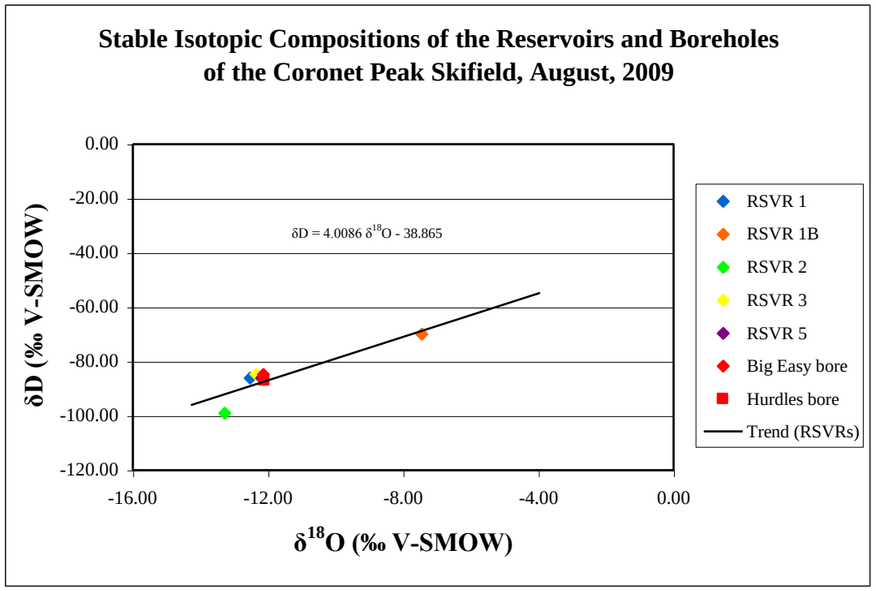

Figure 4.15. The Local Evaporation Line for Coronet Peak, September 2009, with borehole data.

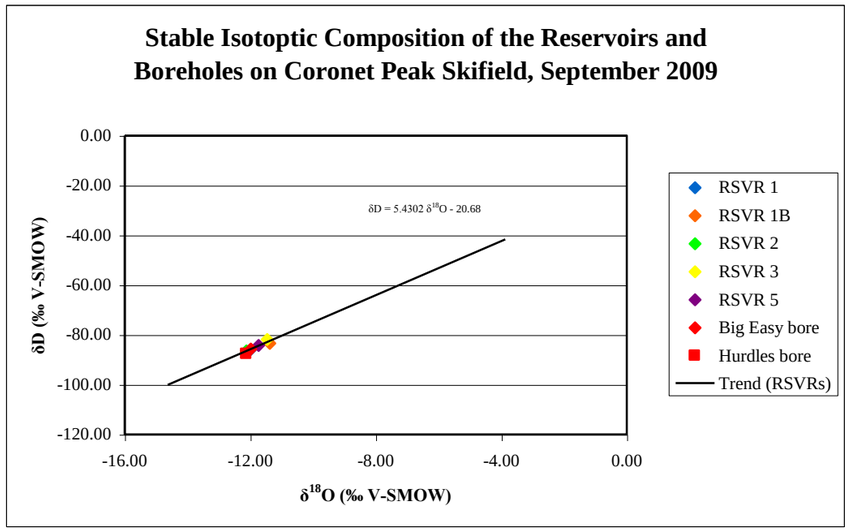

Another possibility is that the groundwater that is continuously filtered down to the aquifers beneath Coronet Peak from previous rainfall events was also very negative, indicating a time in a past environment, most likely within the last five years, as the composition is similar. This indicates that it has taken possibly five years to percolate down through the earth and has only just reached the aquifers where it is pumped to the reservoirs. To determine the age of the groundwater within the aquifers of Coronet Peak, testing would need to be done that is beyond the scope of this thesis. The most likely way to indicate the age is to use the radioactive isotope of tritium (^{3}H), which has been discussed briefly in Chapter Two, where the concentration of tritium within the water sample correlates to the concentration of tritium in the atmosphere at the time the water sample was last exposed to the atmosphere, however it can only be used on modern groundwater, approximately less than 80 years old.

The exception to this high negativity is RSVR 1b. This plotted differently from all the other reservoirs and boreholes, indicating that this reservoir may have undergone a long period of exposure to the atmosphere and therefore evaporation when compared to the other reservoirs and the stable isotopic composition of the groundwater accessed by the two boreholes. It is also possible that this reservoir had not been in use since it was sampled earlier in July and is showing the effects of evaporation on the reservoir for a period longer than a month. Also the difference in the dates of the samples collected for this month may have influenced this data and is therefore not as reliable as the others.

The stable isotope ratios plotted in Figure 4.15 are for the samples collected from the reservoirs and boreholes on the 25/09/2009. Figure 4.15 indicates that RSVR 2 plots on top of the Hurdles bore, signifying that this reservoir had not been exposed to the atmosphere for long, while RSVR 1 plotted above the Hurdles bore but just behind the Big Easy bore, indicating that this reservoir had undergone more evaporation than RSVR 2 (longer residence time). The other three reservoirs all plotted substantially more positively than the Big Easy bore, therefore these three have undergone evaporation to varying degrees. These three reservoirs plot in the order of RSVR 5, RSVR 3 and then RSVR 1b, becoming progressively more positive and indicating that this is the order of shortest to longest residence time.

From the information given in Figures 4.13, 4.14 and 4.15, the likely groundwater sources for each reservoir can be identified. In all of these figures shown RSVR 1 and RSVR 2 give stable isotopic compositions that best fit the Hurdles bore, whilst RSRV 1b and RSVR 3 indicate the Big Easy bore as their groundwater source. RSVR 5 may be a combination of the two.

4.6 Conclusions

In conclusion, the meteoric water samples collected from the Coronet Peak area from precipitation, springs, surface reservoirs and boreholes create a Local Meteoric Water Line (LMWL) for the Coronet Peak area. This LMWL has a slope of 8.0009 and a y-intercept of 10.178, almost falling directly on the Global Meteoric Water Line (GMWL). This similarity indicates that the stable isotopic compositions of the meteoric waters of the Coronet Peak area are typical of global compositions.

Data collected from the surface water of the Coronet Peak Skifield, specifically the five storage reservoirs, give a Local Evaporation Line (LEL) for the area. The slope of this line is similar to the Craig's (1961) observation of evaporated waters plotting on a line with a slope of approximately 5. The LEL of Coronet Peak gave a slope of 4.03, with the deuterium excess value (y-intercept) of –37.5.

When plotting the reservoir stable isotopic data as well as the borehole data for the corresponding sampling month, the dominant groundwater source for each reservoir becomes clear. RSVR 1 and RSVR 2 store water from the Hurdles bore, whilst RSVR 1b and RSVR 3 receive groundwater from the Big Easy bore. The stable isotopic composition of RSVR 5 tends to plot close to one source and then the other, suggesting that this reservoir may store groundwater from both of these sources.

Chapter Five:

Stable Isotopic Variation of Precipitation

5.1. Introduction

The stable isotopic composition of precipitation is dependent on temperature. The five main 'effects' that cause variation within the stable isotopes of precipitation have been described previously in Chapter Two. The altitude effect will be discussed in detail in this chapter with reference to the Coronet Peak area. However, there are other factors that also impact on the precipitation falling at a specific site, and all are in some way a temperature effect. These include the effect that storm duration has on the variation on the stable isotopic composition of precipitation, as well as the impact-specific storm track trajectories effects. The effect that different storm tracks have on the stable isotopic composition of precipitation can also be thought of as a terrain effect and a rain out effect. This is because the amount of terrain an air mass travels over can help to determine the stable isotopic signature of precipitation, and the amount of rain-out that occurs is mainly due to the terrain over which the air mass flows and the changes in temperature that are associated with lower and higher elevations.

5.2. Sample locations

The samples collected to display the effects of altitude, storm duration and storm track trajectory were collected from all (or in some cases only one) of the precipitation sampling sites (Figure 5.1). Samples from all possible sites were used to show the effect that changes in altitude have on the stable isotopic composition of precipitation, whilst only the samples collected at Site 3 were used to determine variations in stable isotopic composition due to storm duration. The samples from site 3 were also the samples used to analyse the effect that different storm track trajectories had on the stable isotopic composition of precipitation on Coronet Peak. The stable isotopic data supplied by the CF-IRMS of every sample collected from the precipitation sampling sites on Coronet Peak are given in Table 5.1 with the date, duration, temperature and wind direction of each storm event. The temperature data

displayed in this table from the Queenstown Airport NIWA monitoring station is not the best indicator of the temperature on Coronet Peak. This is because the airport is located in the Wakatipu Basin, approximately 600 metres below the base hut. Temperature data was not available from the mountain itself due to constraints on time and staff. The wind directions given in Table 5.1 were also not taken directly from the mountain. They were determined using the HYSLIT modelling program, which deduces wind directions of air masses from satellite imagery.

Figure 5.1. Google earth image of the precipitation sampling sites on Coronet Peak that were used in this study.

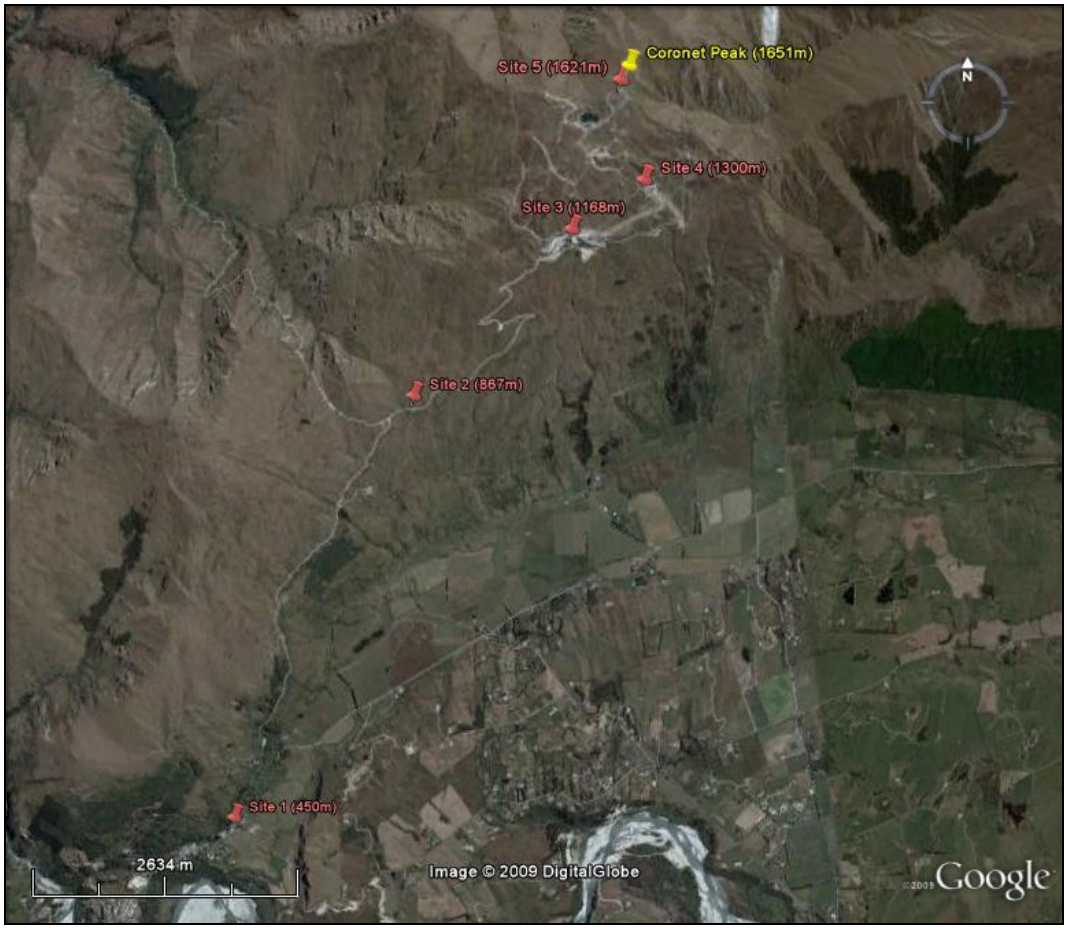

Table 5.1. Event dates, sample numbers, stable isotopic compositions, time period, temperature and wind direction for all samples collected on Coronet Peak 2009.

Event	Sample	δD	$\delta^{18}O$	Time	Temperature	Wind Direction	Event	Sample	δD	$\delta^{18}O$	Time	Temperature	Wind Direction
A (15/07/09)	A1	-35.8	-5.38	02:45-14:45	3.6	**W**	**E (12/08/09)**	E1	-136.67	-18.10	00:00-16:00	5.7	**N/NE**
	A2	-54.9	-8.72	02:45-14:45	3.6	**W**		E2	-136.39	-18.17	00:00-16:00	5.7	**N/NE**
	A3	-55.9	-8.28	02:45-14:45	3.6	**W**		E3	-139.78	-18.43	00:00-16:00	5.7	**N/NE**
	A31	-51.8	-8.23	02:45-06:45	3.6	**W**		E31	-132.28	-17.80	00:00-04:00	6.5	**N**
	A32	-52.5	-7.98	02:45-10:45	3	**SW**		E32	-138.79	-18.50	00:00-08:00	6.7	**N**
	A33	-54.3	-8.27	02:45-14:45	3.6	**SW**		E33	-141.09	-18.81	00:00-12:00	6.2	**N/NE**
	A3a	-54.7	-8.57	02:45-14:45	3.6	**NW**		E34	-139.83	-18.66	00:00-16:00	5.7	**N/NE**
	A3b	-55.5	-8.64	02:45-14:45	3.6	**W**		E4	-139.37	-18.23	00:00-16:00	5.7	**N/NE**
	A5	-44.7	-5.76	02:45-14:45	3.6	**W**		E5	-140.07	-18.20	00:00-16:00	5.7	**N/NE**
						W (overall)							**N/NE** (overall)
B (18-19/07/09)	A4	-58.8	-8.31	19:00-03:00	5.9	**SW**	**F (21-22/09/09)**	F1	-43.63	-6.14	14:00-10:00	7.5	**W**
						SW (overall)		F2	-68.40	-9.74	14:00-10:00	7.5	**W**
C (21/07/09)	C3	-62.4	-9.32	04:00-08:00	7.3	**NW**		F3	-74.37	-10.72	14:00-10:00	7.5	**W**
	C32	-64.6	-9.04	04:00-12:00	8.1	**NW**		F31	-74.89	-10.35	14:00-18:00	9.5	**NW**
	C33	-66.5	-9.86	04:00-16:00	7.9	**W**		F32	-73.20	-9.73	14:00-22:00	8.8	**W/NW**
	C3a	-67.7	-9.91	04:00-20:00	7.5	**W**		F33	-73.81	-10.10	14:00-02:00	8.1	**W/NW**
	C3b	-68.2	-10.07	04:00-20:00	7.5	**W**		F34	-73.02	10.04	14:00-07:00	7.6	**SW**
						N/NW (overall)		F35	-75.50	-10.49	14:00-10:00	7.5	**W**
D (11/08/09)	D1	-103.91	-13.50	07:30-10:30	5.0	**N/NE**		F4	79.08	-11.46	14:00-10:00	7.5	**W**
	D2	-118.04	-15.63	07:30-10:30	5.0	**N/NE**		F5	-104.35	-14.45	14:00-10:00	7.5	**W**
	D3	-126.75	-16.78	07:30-10:30	5.0	**N/NE**							**W** (overall)
	D31a	-126.89	-17.01	07:30-10:30	5.0	**N/NE**	**G (23/09/09)**	G1	-56.81	-8.81	03:00-07:00	1.6	**SE**
	D31b	-129.20	-16.70	07:30-10:30	5.0	**N/NE**		G2	-65.52	-10.00	03:00-07:00	1.6	**SE**
	D31c	-122.56	-16.20	07:30-10:30	5.0	**N/NE**		G3	-64.28	-9.86	03:00-07:00	1.6	**SE**
	D31d	-107.47	-12.06	07:30-10:30	5.0	**N/NE**		G32	-62.97	-9.18	03:00-07:00	1.6	**SE**
	D4	-128.51	-17.09	07:30-10:30	5.0	**N/NE**		G33	-62.14	-9.40	03:00-07:00	1.6	**SE**
	D5	-126.95	-17.00	07:30-10:30	5.0	**N/NE**		G34	-62.33	-9.20	03:00-07:00	1.6	**SE**
						N/NE (overall)		G4	-64.36	-9.41	03:00-07:00	1.6	**SE**
								G5	-67.15	-10.68	03:00-07:00	1.6	**SE**
													SE (overall)

5.3. Variations in stable isotopic composition of precipitation with altitude

5.3.1. *Background*

The "Altitude Effect" is a global trend in the stable isotopic composition of precipitation. It characterises the relationship between decreasing δD and $\delta^{18}O$ values in precipitation with increasing altitude. The increase in elevation above sea level causes the air mass to become depleted in the heavy isotopes of both hydrogen and oxygen. The changes in the behaviour between the light and heavy isotopes are due to the relative decrease in temperature with altitude. The fact that cooler air masses hold less moisture than warmer air masses also has an affect (Sharp, 2007).

The temperature of an air mass is directly related to the amount of energy it has. A cooler air mass has less kinetic energy to allow fractionation to occur compared to an air mass that has a higher temperature. A cold air mass has a lesser ability to change phase from vapour to liquid, whilst the phase change from liquid to vapour is easier. Because of this, as supersaturation occurs in a cold air mass and precipitation transpires, the liquid reservoir becomes depleted.

As the δD and $\delta^{18}O$ values are ratios, and the heavy isotopes of hydrogen and oxygen both preferentially convert to the liquid phase, the remaining vapour in the air mass consists more of the light isotopes than the heavy isotopes. Any further vapour that is condensed then forms negative precipitation (enriched in the light isotopes) in comparison to any precipitation that was formed at a lower elevation, where fractionation is easier in relatively warmer temperatures. Changes in the δD and $\delta^{18}O$ ratios become more pronounced as the amount of vapour and liquid within in the air mass decreases. Therefore the variations in the stable isotopic composition of the precipitation reflect the changes of the stable isotope ratios of hydrogen and oxygen within an air mass as elevation changes (Barrens and Cook, 2006).

5.3.2. *Results and Discussion*

The stable isotopic compositions of the precipitation events collected on Coronet Peak are graphed in Figures 5.2 (a) event A, 5.2 (b) event D, 5.2 (c) event E, 5.2 (d) event F, and 5.2 (e) event G, where the altitude effect is shown.

Precipitation event A occurred on 15th July 2009. Only samples from four sites were analysed for this storm event due to the sample from site 2 being evaporated before it was analysed in the laboratory. Evaporation affected this sample

because there was little precipitation collected at this site. The sample collected from site 5 plots relatively positive to what was expected of it. This sample should be the most negative of the samples collected from this event because it is located at the highest elevation as stated by the altitude effect.

The other samples indicate the altitude effect as they follow the trend of decreasing δD and $\delta^{18}O$ values with elevation. Without including this sample, the other three give a good correlation. The R^2 value of 0.89, shown in Figure 5.2 (a), indicates a very good relationship between the isotope composition and altitude. The equation to calculate the R^2 values is shown in Eq 5.1.

$$R^2 = 1 - \frac{(\Sigma (y_i - \hat{y})^2)}{(\Sigma (y_i - f_i)^2)} \qquad \text{Eq. 5.1.}$$

Where: Σ = the sum of…

y_i = observed values

$\hat{y}$ = mean of observed values

f_i = modelled values

Precipitation events B (18-19/07/2009) could not be analysed for stable isotopic variations with altitude due to event B only having one sample analysed, the others all being evaporated. Samples collected from event C (21/07/2009) were only done from site 3, and also could not be analysed for variations in stable isotopic composition with altitude.

Figure 5.2 (a). Altitude effect for precipitation event A.

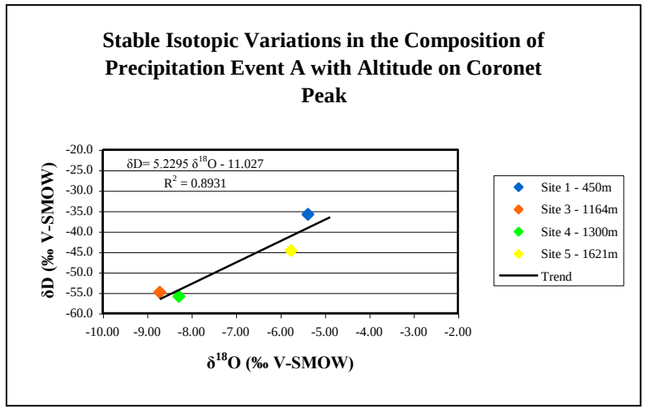

Figure 5.2 (b). Altitude effect for precipitation event D.

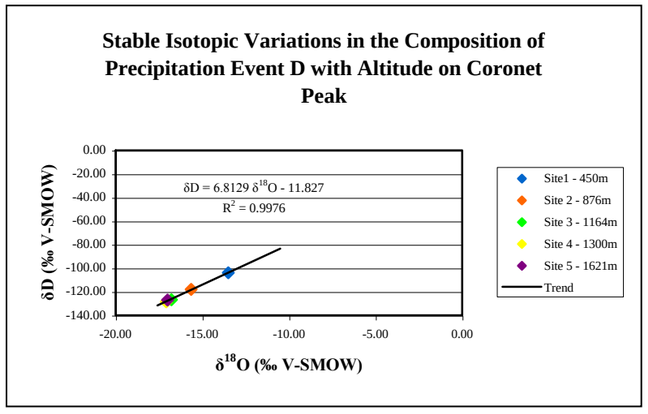

Figure 5.2 (c). Altitude effect for precipitation event E.

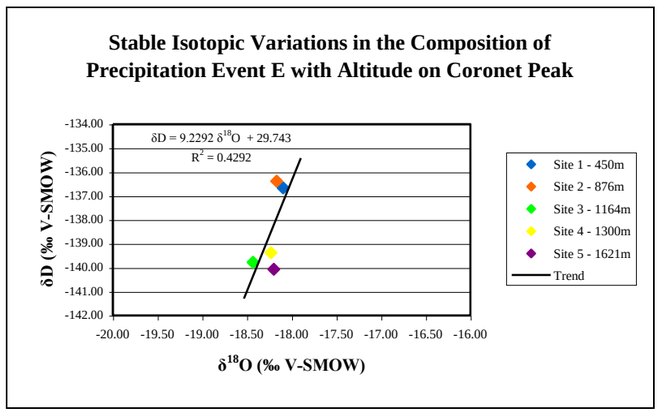

Figure 5.2 (d). Altitude effect for precipitation event F.

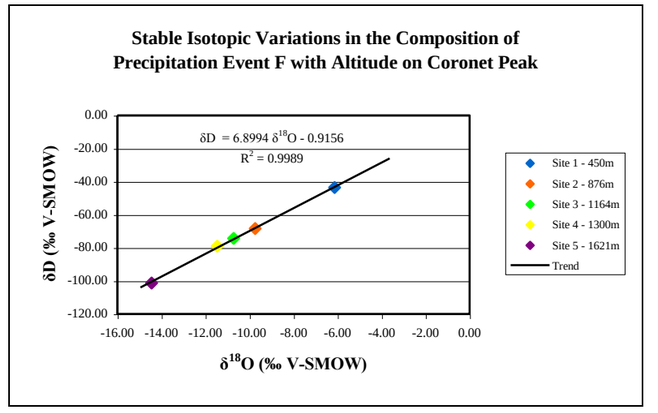

Figure 5.2 (e). Altitude effect for precipitation event G.

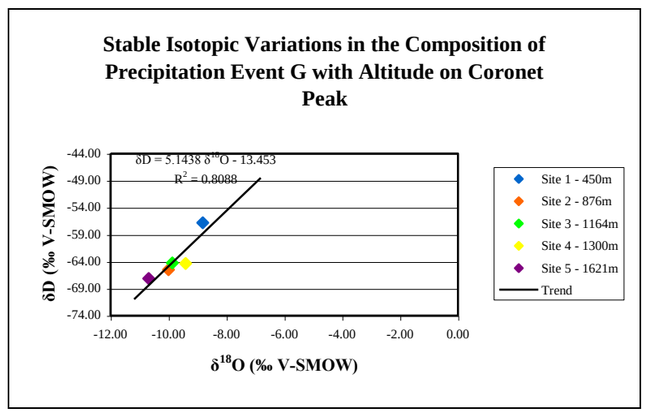

Sampled on 11th August 2009, event D also shows the altitude effect very well, with a correlation between δD and $\delta^{18}O$ having a R^2 value of 0.99. However, again the sample collected at site 5 is more positive than expected. This is most likely due to the effects of evaporation after the rain event whilst the sample was exposed to the atmosphere prior to collection.

Precipitation event E collected on 12th August 2009 does not show a very good relationship between the hydrogen and oxygen stable isotopes with altitude. It does generally indicate the decreasing trend of both isotopes with increasing altitude, however, the samples do not plot in the expected order. This may be due to variations in wind direction during the precipitation event, as seen in Table 5.1 there is little variation in the wind direction during the storm, however this information is taken from satellites and may not reflect the local wind variations correctly, especially in mountainous areas. Evaporation may also have occurred before some samples were collected, some samples could be in the field all night before collection. The samples collected from site 4 and 5 are more positive than the sample collected at site 3, also the sample collected at site 1 is more negative than the site 2 sample. Evaporation of samples collected from sites 2 and 3 may explain these variations.

It must also be noted that for this particular storm event, the variations in the oxygen isotope ratios is very small. This may be due to the amount of rainfall that has occurred during the storm, as the amount of precipitation has been shown to affect the stable isotopic composition of further precipitation, however typically in tropical locations with large quantities of precipitation. Larger precipitation events being isotopically more depleted. Pionke and De Walle observed in 1992 that rapid changes in the oxygen values occurred with increased rainfall intensities. Therefore there may have been very little precipitation from this event causing little variation in the oxygen ratios.

Precipitation event F collected on 21st and 22nd September 2009 gives the best correlation between decreasing hydrogen and oxygen stable isotopes with increasing altitude, with an R^2 value of 0.99. Each site sampled is in the order expected for the correlation, indicating that evaporation is unlikely to have affected any particular sample. From this precipitation event an altitude gradient can be calculated, this is the amount both δD and $\delta^{18}O$ values decrease with every 100 metre increase in altitude, δD decreases by 5.19‰ and $\delta^{18}O$ decreases by 0.71‰ for every 100 metres increased in altitude above sea level.

Precipitation event G was sampled on 23rd September 2009. In Figure 5.2 (e), the stable isotopic data from this event is graphed, displaying the altitude effect. This event gives a good indication of the relationship between δD and $\delta^{18}O$ values and altitude; however, as seen in Figure 5.2 (e) the sample from site 2 plots more negative than the samples from site 3 and 4. This could be due to a local variation in wind pattern or temperature, although these influences were not analysed during this study. The amount of rain that has occurred may have an impact on the stable isotopic composition of precipitation, a rain out effect. This may be the case here, as this site may have experienced a large amount of rainfall compared to the other sites, continually depleting the air mass over this site of hydrogen and oxygen given a more negative value than expected. However, more information is needed to determine the influences on the individual sites, and how much each influence each factor has on the samples collected.

5.4. Stable isotopic variations with storm duration

5.4.1. *Background*

There has been a trend recognised around the world where there are variations in the stable isotopic composition of precipitation as the duration of a single storm event continues (Pionke and De Walle, 1992). The δD and $\delta^{18}O$ values decrease as storm duration lengthens, as long as there is no extra addition of water vapour from a new source. This isotopic trend in water molecules is due to the changes in temperature. As the temperature decreases, the vapour in the air mass reaches the supersaturation point, where the water vapour condenses to form water in its liquid form; this liquid then falls from the air mass as precipitation. In the case of Coronet Peak, the most likely cause for the temperature decreases within the air masses are due to the deflection of the air mass up and over the mountain.

Due to fractionation processes, the heavy isotopes rather than the lighter isotopes of hydrogen and oxygen preferentially condense to form precipitation. This is known as the Rayleigh Distillation Process, whereby as precipitation continues during a single storm event with the same moisture source, the precipitation becomes more and more enriched in the lighter isotopes, making the rain and snow fall become more negative with time. In other words, the reservoir within the air mass of the heavy

isotopes decreases with time, and this causes any future precipitation that occurs to have an even more negative stable isotopic composition as the reservoir of heavy isotopes is continuously depleted. This relationship is only true for air masses that collect no new water vapour as the precipitation event continues, as this would replenish the heavy isotopes in the air mass and change the δD and $\delta^{18}O$ ratios.

5.4.2. *Results and Discussion*

The stable isotopic compositions of the samples collected during the precipitation events sampled on Coronet Peak at site 3 have been plotted on the graphs below in Figures 5.3 (a) event A, 5.3 (b) event C, 5.3 (c) event E and 5.2 (d) event F. In some cases the precipitation event is not represented in this set of results due to the lack of samples, (event B), or due to the short time frame of the storm event, (events D and G). These two events were not long enough to give a good indication of variations of stable isotopic composition with storm duration.

Precipitation event A does not show a good relationship between decreasing hydrogen and oxygen stable isotope ratios with increased storm duration. The samples are in the right order for the hydrogen ratios, but are wrong for the oxygen ratios, with a coefficient of determination value of 0.14 indicating there is no correlation between these two variables. This value indicates that there are other unknown factors affecting these samples, possibly including changes in wind direction (varying between SW and W), temperature or amount of precipitation.

Variations in the stable isotopic composition in event C precipitation samples show the variation with storm duration better, with a R^2 value of 0.5921. However once again the oxygen ratios are not in the correct order expected, with the second sample increasing in $\delta^{18}O$. Therefore there are unknown variables affecting these samples too.

Event E gives the best correlation between hydrogen and oxygen stable isotopes out of all the precipitation events sampled, giving a R^2 value of 0.99, which indicates a very good correlation. However, Pionke and De Walle (1992) indicate that stable isotopic compositions decrease with storm duration, therefore the last two samples plot in the incorrect order in Figure 5.3 (c). The last sample (00:00-16:00 on 12th August 2009) was expected to have the more negative ratio, but this is not the case. Again indicating influences that have not been analysed in detail in this study.

Figure 5.3 (a). Stable isotopic variation of precipitation event A.

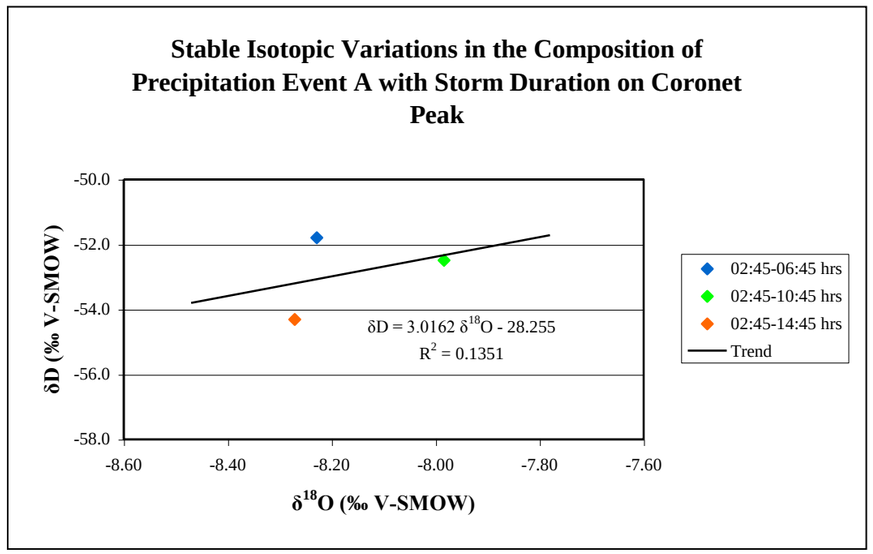

Figure 5.3 (b). Stable isotopic variation of precipitation event C.

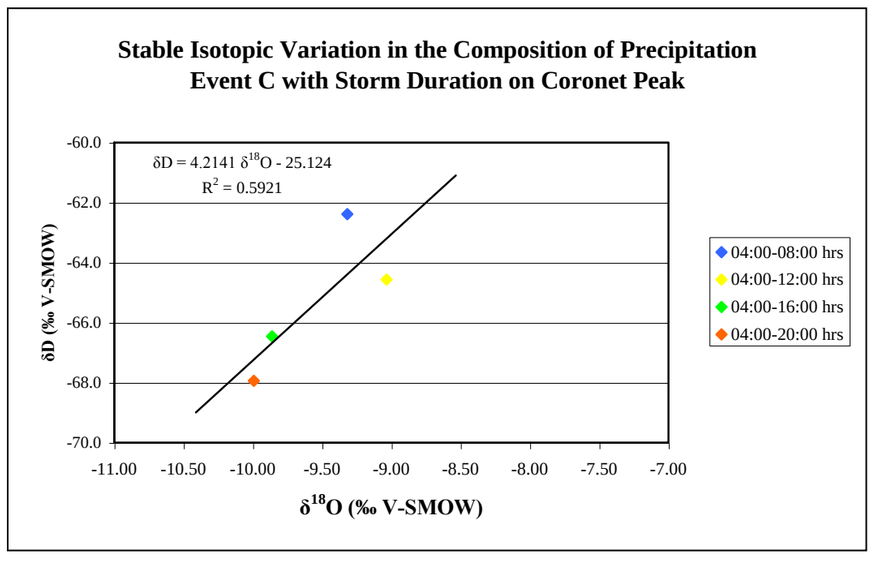

Figure 5.3 (c). Stable isotopic variation of precipitation event E.

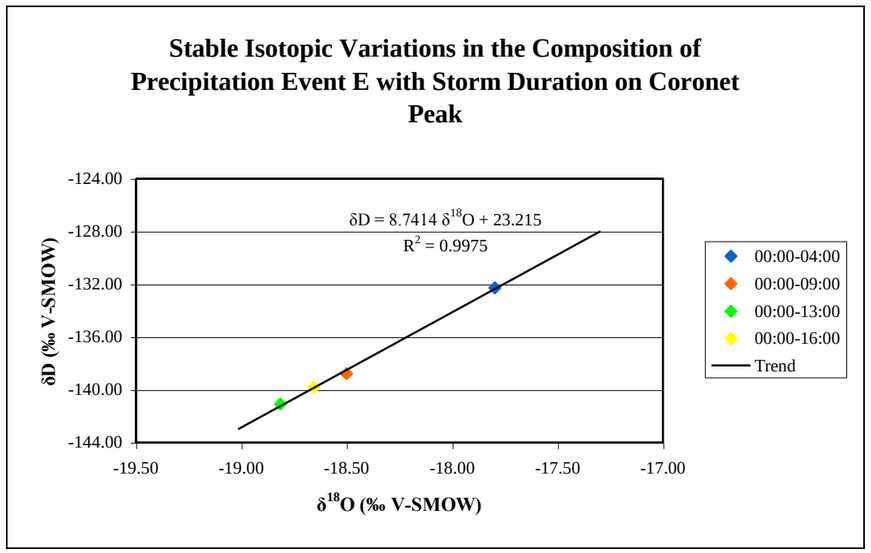

Figure 5.3 (d). Stable isotopic variation of precipitation event F.

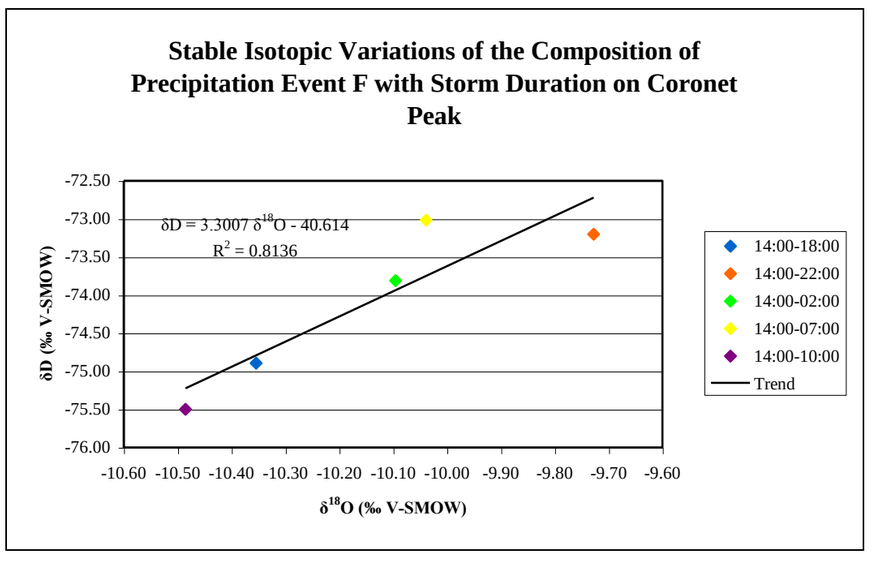

The samples collected during precipitation event F vary. On Figure 5.3 (d) the samples plot in an unexpected order. The most negative sample is correct and the sample collected from 14:00 to 02:00 is also in the expected place stated by the relationship of stable isotopes in precipitation with storm duration. However, the samples from the other time periods do not plot in the expected order. The R^2 value of 0.81 indicates a correlation, but the R^2 value does not take into account the unexpected order of the samples. Giving a false representation of the relationship, as the samples collected do not fit well with the implied correlation of these isotopes with storm duration.

5.5. Stable isotope variations due to storm track trajectory

5.5.1. *Background*

The stable isotopic composition of a specific air mass is related to the environment in which it has flowed over. The movement of air masses around the globe is influenced by four factors; pressure gradients, which provide the stimulus for air motion, the coriolis effect (rotation of the Earth), the curved motion of air (centripetal force) and friction (Sturman and Tapper, 1996). These factors dictate the direction and speed of the large air masses that flow around the Earth. The definition of an air mass from Sturman and Tapper, 1996, (p121), is 'a large body of air which is uniform horizontally with regard to temperature, humidity and lapse rate', the lapse rate referring to the rate at which temperature decreases as the air mass rises. Pressure gradients act as the stimulus for air mass motion because air masses travel from high pressure to low-pressure environments. The changes in pressure also govern the direction of the wind that is blowing. The variations in pressure are basically due to changes in temperature around the globe, the main influence being the influx of solar radiation from the sun. The equator receives more solar radiation than the polar regions because it is closer to the sun, therefore the radiation it receives is stronger, and the ice and snow located in the polar regions help to reflect the solar radiation back out to space, creating a greater difference in the amount of solar radiation received at these two areas (Marshall and Plumb, 2008).

In view of the fact that the composition of the stable isotopes of both hydrogen and oxygen vary considerably within water samples around the world, specifically

precipitation samples in the case of this chapter, it is possible to trace the air mass that has created a precipitation sample at a certain location and to determine its origin.

5.5.2. *Local Atmospheric Circulation*

Coronet Peak Skifield and the adjacent area is located at 45° latitude south of the equator. Figure 5.4 does not show New Zealand on the map, but the trade winds are the same on either side of the Earth, and therefore the dominant wind direction that affects New Zealand is from the west. What can also be seen on this diagram is that the airflow within the cells signifies the greater cycle of air mass movement travelling in a north-south direction, indicating the overall heat and moisture transport of air masses. The trade winds are the large-scale atmospheric circulatory processes, and do not wholly represent the smaller local winds that affect the study area at Coronet Peak.

Figure 5.4. Global atmospheric circulation cells from NASA (b), 2008.

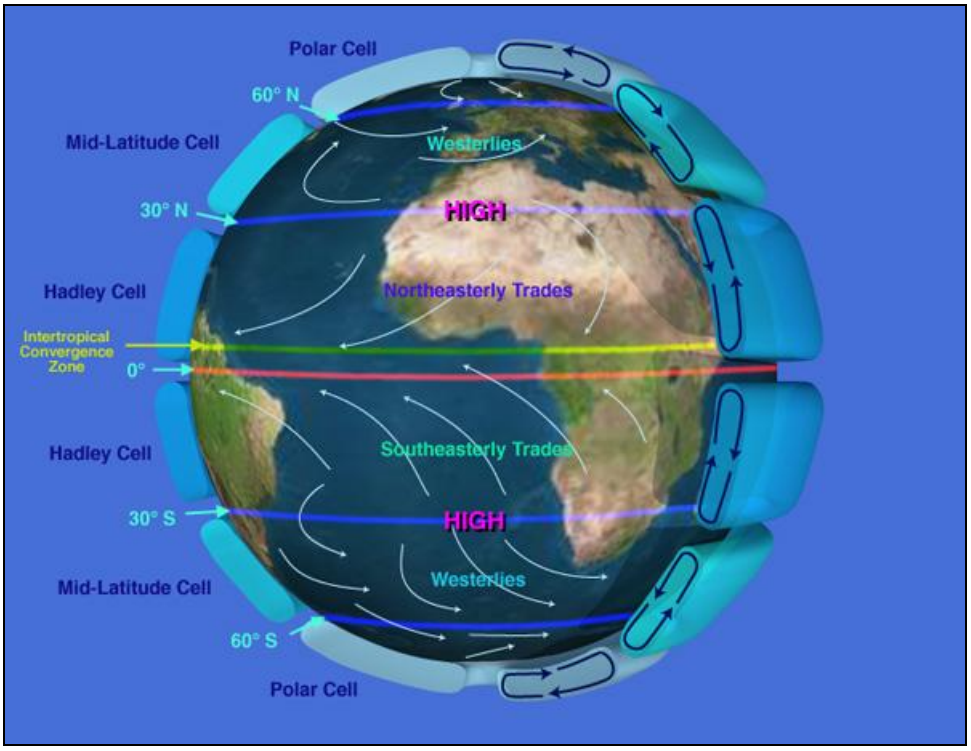

It is the interaction between the cold (from the Southern Ocean) and the warm fronts coming in from the Tasman Sea and the Pacific Ocean, that create a lot of the

storm fronts in New Zealand. This is due to the interaction of the dry and cold air masses from the south and the relatively warmer, moister air masses from the tropical regions. Fronts from the south are dry because little evaporation occurs over the Southern Ocean, (Figure 5.5), and cold air cannot hold has as much moisture because it has less energy than a warmer air mass.

Sturman and Tapper in 1996 differentiated the air masses received by the South Island from the Antarctic region. The Southern Maritime source is derived from latitudes of 35 to 55° south, and the Polar Maritime source comes from the very edge of the Antarctic continent at latitudes between 55 and 68° south. The air masses from the tropical regions are sub-divided into Tropical Maritime and Tropical Continen. Whereas the latter does not affect the South Island of New Zealand greatly, the former does, originating from the Tasman Sea and the Pacific Ocean. Hybrids can occur between any of these, complicating the stable isotopic signatures of storm tracks even further (Sturman and Tapper, 1996).

Figure 5.5. Evaporation rates from the oceans of the world (Lemke, 2009).

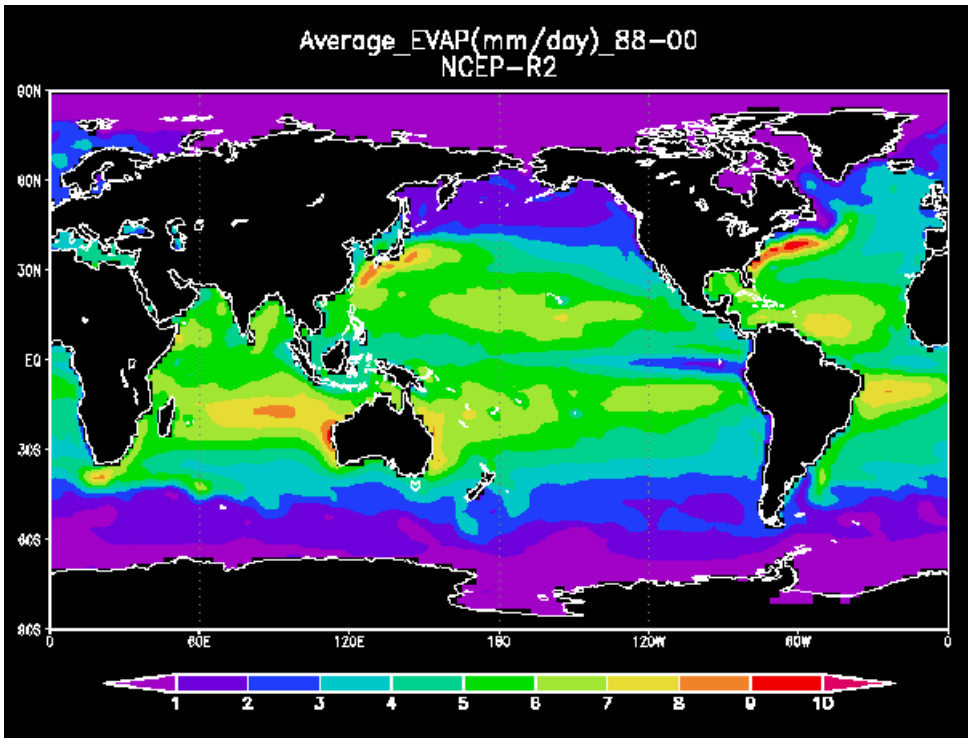

The dominant wind directions for the Queenstown area of New Zealand are displayed below in a ‘rose’ diagram. These diagrams depict the frequency, strength

and wind direction over a period of time for a particular location. The key for the rose diagram (Figure 5.6) shows direction of the winds that blow at the Queenstown Airport, the length of these arms is proportionate to the frequency of wind blown in that direction. Whereas the length of each segment within the arm dictates how often the wind is blown at a particular strength, for example between 1-10 knots (Brenstrum, 1998). For every rose diagram, the length of the arms total 100% for both wind direction frequency and strength for each location. The dominance of the westerly winds can be seen in Figure 5.6, the trade winds of this area of the globe.

Figure 5.6. Rose Diagram of the Wind Direction and Strength of Queenstown, New Zealand, data collected for wind frequencies between the years of 1970 and 1974, with data collected for wind speeds between 1977 and 1981 (Brenstrum, 1998 and New Zealand Meteorological Service, 1983).

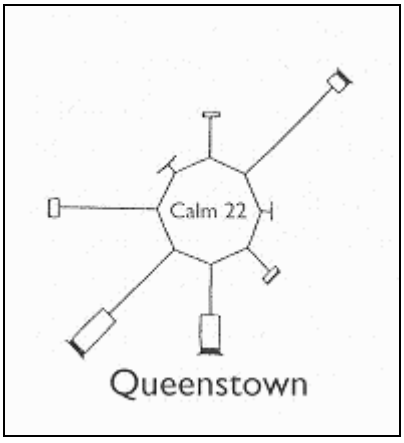

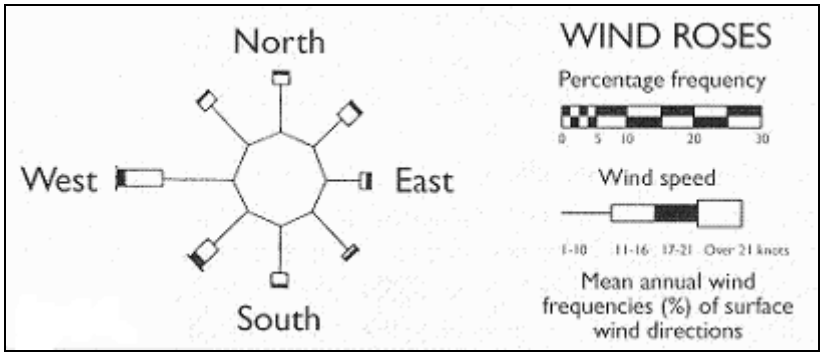

There is also the slight dominance of the north-easterly winds in Queenstown that is shown on the diagram above and in Figure 5.7 below. This can be attributed to

the dominance of easterly winds on the eastern side of the South Island. Not only does global atmospheric circulation include the three main cells of Hadley, Mid-Latitude and the Polar Cells that transport heat in a meriodonal direction (north-south), but within the South Pacific Ocean there are also cells that flow in a general east-west (zonal) direction, known as the Walker Cells or the Walker Circulation. Zonal circulation can only occur when the Coriolis 'deflection' is weak, and these cells link the larger meriodonal cells together. Walker Cells are driven by the differences in ocean surface temperature between the east and west tropical South Pacific Ocean, and are closely associated with ocean circulation and variations with in this cycle. They result in wet easterlies for the east of New Zealand, and decreased rainfall in the Eastern Pacific. Figure 5.7 below indicates the main air masses that affect New Zealand during the winter (July), most notably winds from the west and south, but also from the east. Variations in the Walker Cycle lead to what is known as the El Niño or La Niña cycles (Sturman and Tapper, 1996). The Pacific is in an El Niño cycle at present.

Rose diagrams also indicate the strength of the wind blowing at a specific location. Figure 5.6 demonstrates that Queenstown receives weak winds, dominated by wind speeds of 10 knots or less. This is due to the geographic location of Queenstown, however Coronet Peak is approximately 1200 metres higher than Queenstown. Queenstown is situated inland within a basin surrounded by large mountain ranges (Brenstrum, 1998). The distance from the coast (where winds are the strongest due to there being less friction over water) and the surrounding mountains, which act as "shelterbelts", are the main factors that affect the winds at this location. High winds, greater than 20 knots only occur 0.2% of the time, and in the general directions of the north-east and south-west (New Zealand Meteorological Service, 1983).

The rose diagram is for Queenstown, not for Coronet Peak specifically; therefore the data may not be entirely accurate for Coronet Peak, and just give a general picture of the dominant wind directions for the area. However, it can be assumed that the overall frequencies of wind directions are most likely the same, but there may be some difference with wind speeds. Wind speeds generally increase with height above sea level due to the mountains themselves creating less friction with the air mass than basins do, but the complex terrain within mountainous areas may act to intensify wind speeds in some areas (Whiteman, 2000). Therefore it would be

expected that the wind speeds on Coronet Peak will be higher than those for Queenstown.

Figure 5.7. Air mass distribution in the Australia and New Zealand region during winter (Sturman and Tapper, 1996).

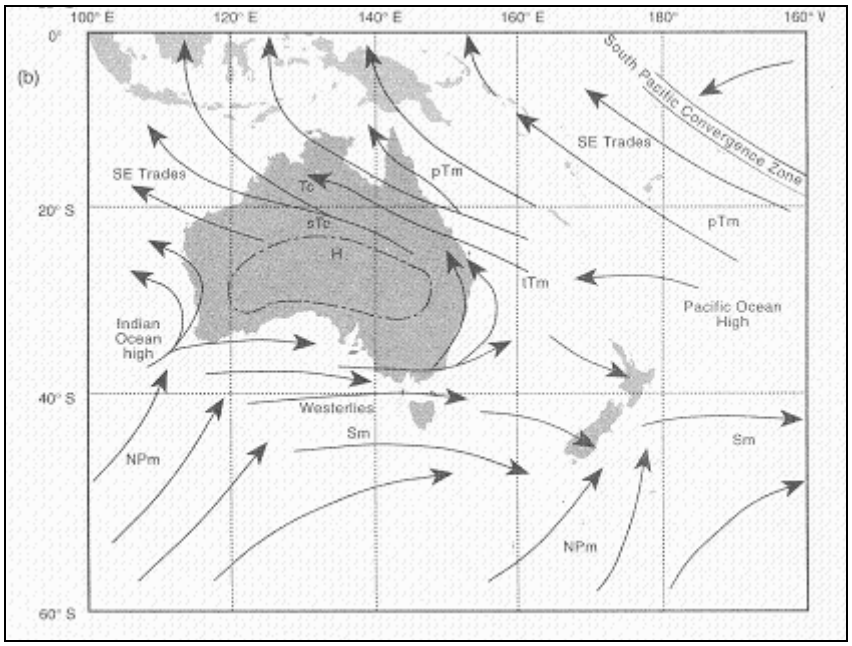

5.5.3. *Results and Discussion*

The precipitation samples used to determine specific stable isotopic signatures for storm tracks are the samples that were collected at sample site 3. These samples collected from each storm event are given in Table 5.1, showing the δD and $\delta^{18}O$ values as well as the wind directions at the time that the sample was collected to establish the over all storm track of the event. Wind directions were found using HYSPLIT models (Hybrid Single Particle Lagranian Integrated Trajectory Model), from which the trajectories of any storm that has occurred on a particular date and time can be shown on a Google Earth image. The stable isotopic values have then been graphed together in Figure 5.8 below to determine whether there is a link between the stable isotopic composition of a precipitation event and the storm track of that event.

The samples collected from events D and G do not show variations in stable isotopic composition with storm duration. In these cases, the stable isotopic data used

is from samples collected at site 3, and are for the whole duration of the storm event. The two end-member samples have been plotted for these two events to analyse their stable isotopic compositions with the storm track given by the HYSPLIT model. Also, the only sample collected for event B has been graphed below to see where it plots in relation to the other events.

Figure 5.8. Stable isotopic composition of all precipitation events sampled on Coronet Peak, 2009.

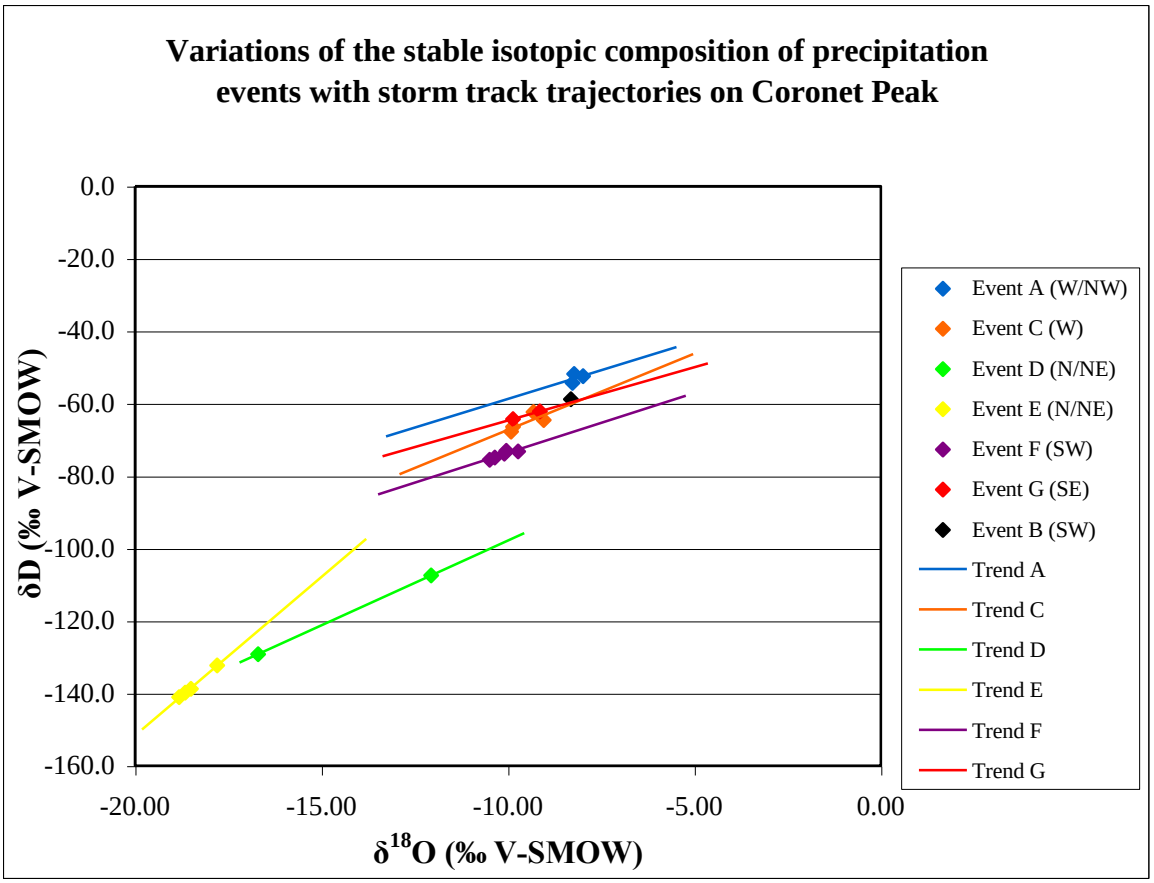

From Figure 5.8 above, it can be seen that there are two distinct groups in which the stable isotope values for each precipitation event plot. Five out of the seven storm events plot with the δD and $\delta^{18}O$ values of approximately –65‰ and –9‰ respectively, whilst events D and F plot with more negative values of approximately –135‰ and –15‰ for δD and $\delta^{18}O$ respectively. These last two events are the only events that have a storm track trajectory from the north and slightly to the east. Each precipitation event sampled on Coronet Peak has be put into the HYSPLIT model, as

shown in Figure 5.9, showing all seven storm trajectories from the time the air mass was first sampled on Coronet Peak and the 72 hours previous to this, indicating the origin of the air mass.

Figure 5.9. Google Earth image of the storm track trajectories sampled on Coronet Peak, 2009. The colours of each track correspond to the colours and events in Figure 5.8, (A-blue, B-black, C-orange, D-green, E-yellow, F-purple and G-red).

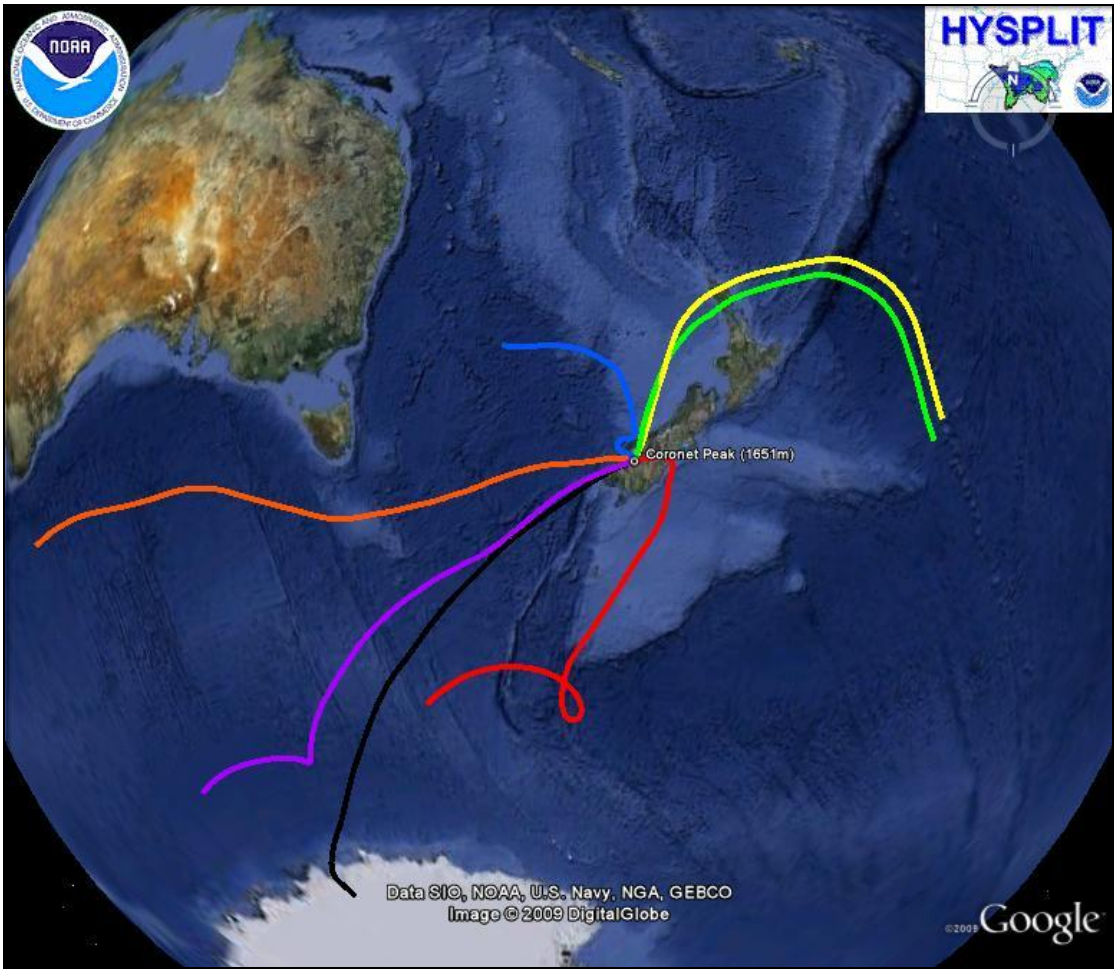

The storm tracks of events D and E (green and yellow lines) can clearly be seen approaching Coronet Peak from the north, originating within the Walker Cells of the Pacific Ocean. They flow north and then travel over the tip of the North Island of New Zealand, where it is very likely that precipitation would occur. From here, the air mass continues to flow to the south where it approaches Coronet Peak. The warm,

moisture-laden air mass as it travels south will be decreasing in temperature, allowing precipitation to occur. It is this precipitation that leads to these air masses becoming very depleted in the heavy isotopes of hydrogen and oxygen in terms their stable isotopic composition. The other precipitation events tend to travel to Coronet Peak on a south-west direction and therefore plot together on Figure 5.8 above, indicating their relatively more positive stable isotopic compositions, enriched in the lighter isotopes of hydrogen and oxygen. This may be because cooler air masses that flow from the Southern Ocean hold less moisture. Due to this characteristic, these air masses produce little precipitation as they move towards New Zealand because of the lack of evaporation from the colder oceans. Therefore, the precipitation that does occur over the Coronet Peak area from these air masses is most likely among the first cycles of rainfall, making the stable isotopic composition less depleted than precipitation coming from the north where there may have been several more cycles of rainfall depleting the isotopic content of the air mass.

The HYSPLIT model also gives information about the elevation at which an air mass flows. For each of the storm tracks sampled, the elevation of the air mass has also been graphed in Figures 5.10 (a – g). The elevations of the air masses for the events D and E will not be analysed in detail here, as it has already been confirmed above that the storm track trajectory is the main determining factor for these events. The figures below show the elevations of the air masses for the 72 hours prior to the air mass reaching Coronet Peak. There is a large amount of variation within these elevations.

The order that the precipitation events plot on Figure 5.8 (from more positive to more negative) is event A, B, G, C and F, with events D and E being the most negative. This order corresponds with the changes in the elevation of the air mass 72 hours before precipitation occurs at Coronet Peak, see table 5.2. 72 hours was chosen to be the period to determine the origin of the air mass because a shorter time period may not show the true origin in enough detail. Whereas a longer time frame may complicate the origin to a point where it may be difficult to deduce the main influences on the stable isotopic composition of the air mass. This may indicate that the height above sea level that the air mass travels at may influence the stable isotopic composition of precipitation. The lower the elevation at which the air mass travels at, the more positive the stable isotopic composition of the precipitation, with the exception of events D and E.

Table 5.2. Elevation of the air masses sampled on Coronet Peak. Elevation is approximate and in metres above sea level.

Event	**Air Mass elevation**	**Air mass source**
A	2000	Tropical Maritime (Tasman)
B	3500	Polar Maritime
C	4500	Southern Maritime
D	2000	Tropical Maritime (Pacific)
E	2000	Tropical Maritime (Pacific)
F	5000 (rising to 6000)	Polar Maritime
G	4500 (rising to 5000)	Polar Maritime

The distance that the precipitation falls before it reaches the ground also seems to impact on the stable isotopic composition of precipitation. From the HYSPLIT elevation images in Figures 5.10 (a – g), excluding events D and E as their stable isotopic signatures are due to storm trajectory, the elevation at which precipitation falls onto Coronet Peak from event A is approximately 1000 metres, and this event is the most positive of all the events sampled on Coronet Peak. The other four events, (B, C, E and F) are at approximately 500 metres elevation above the top of Coronet Peak, 2100 metres, when precipitation occurs. Precipitation event A is the most positive of all events because it has a longer distance to fall until it lands on the ground surface of Coronet Peak and therefore there is more time for evaporation of the raindrops to occur as they fall, leading to a more positive stable isotopic composition for this event.

Figure 5.10 (a). Elevation of air mass for EVENT A.

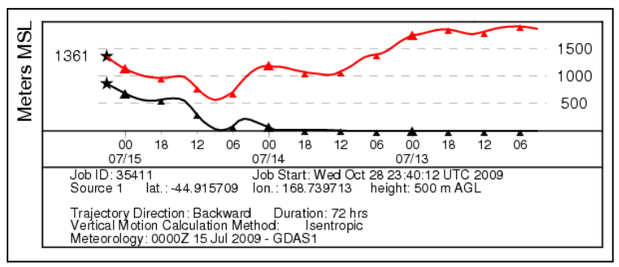

Figure 5.10 (b). Elevation of air mass for EVENT B .

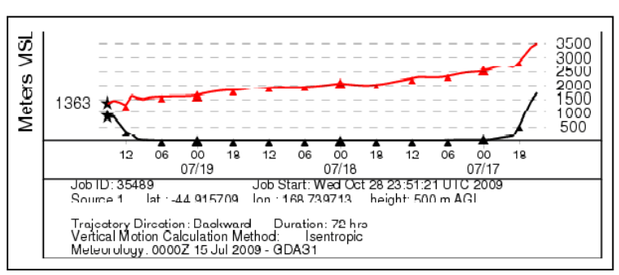

Figure 5.11 (c). Elevation of air mass for EVENT C.

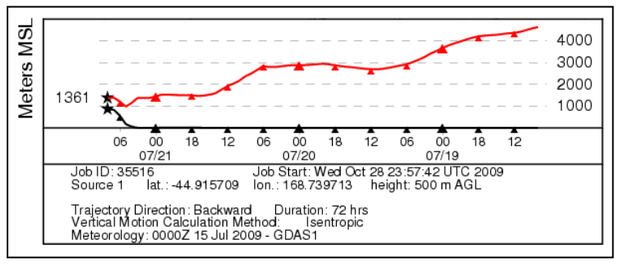

Figure 5.10 (d). Elevation of air mass for EVENT D

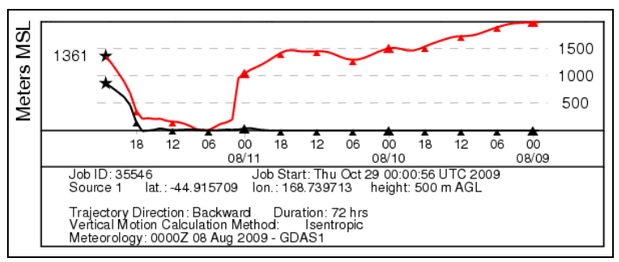

Figure 5.10 (e). Elevation of air mass for EVENT E

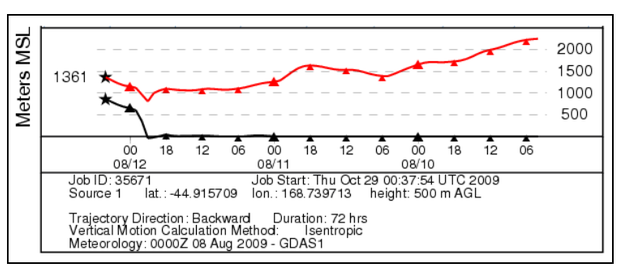

Figure 5.10 (f). Elevation of air mass for EVENT F

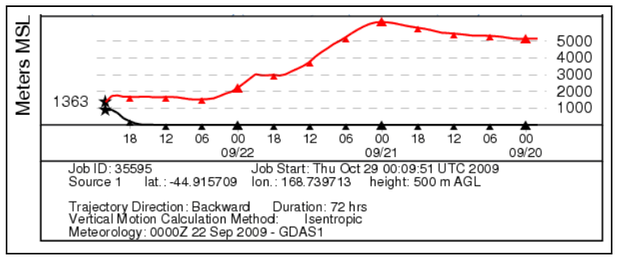

Figure 5.10 (g). Elevation of air mass for EVENT G

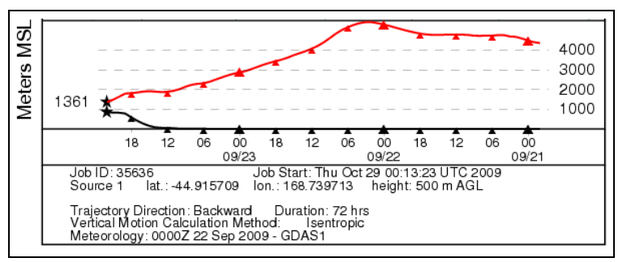

It must be noted that the HYSPLIT images in Figure 10 (a - g) show the height of Coronet Peak to be approximately 900 metres above sea level. This is incorrect, as the height of Coronet Peak is approximately 600 metres higher than what is indicated in the figures. This is due to the meteorological model used HYSPLIT. The samples used in this model to give these elevations are taken from selected points on the earth, which smoothes out valleys and mountains, giving a height for Coronet Peak lower than the actual height for the mountain. A correction can be done to counter this effect, but it is not needed here.

The distance the air mass travels over land (terrain effect) does not have a great influence on the stable isotopic signature of the precipitation falling on Coronet Peak. These distances vary between 87 kilometres and 202 kilometres (Table 5.3). The stable isotopic composition of precipitation is influenced by the terrain that an air mass covers and the distance inland where precipitation occurs (Sharp, 2007). It would be expected to see the stable isotopic composition of the precipitation sampled at Coronet Peak to be more depleted in the heavy isotopes of hydrogen and oxygen in storm events where the air mass travelled the largest distance over land. However, these distances do not correlate with the variations in stable isotope content of precipitation. Event A is the exception to this case, being the most positive and travelling over the least amount of ground. It would be expected that events D and E, being the most negative, would have travelled over the greatest amount of land when compared to the other events, therefore contributing to their negativity. However, these events travel 132 and 150 kilometres on land, an average distance when compared to the other storm events sampled. This gives more evidence that the storm track greatly dominates the stable isotopic composition of precipitation at this location. The terrain of the land in which the air mass travels over has an impact; we know this because of the altitude effect. The elevation of the terrain is also shown in the HYSPLIT images below; however, there is little difference between them.

Table 5.3. Distance and approximate bearing at which the air mass travelled over land to be sampled on Coronet Peak. Distances are noted in kilometres and bearings in degrees of the wind direction.

Event	Distance travelled	Bearing (°)
A	87	302
B	202	243
C	116	272
D	132	012
E	150	018
F	175	249
G	199	081

Temperature of the storm event can also be used to help understand the stable isotopic composition of a particular event, in that cooler temperatures usually indicate an air mass depleted in the heavy isotopes of hydrogen and oxygen. However, in the case of the events sampled on Coronet Peak the only temperature information has been collected not on the mountain itself but from the NIWA (National Institute of Water and Atmospheric Research) monitoring station located at the Queenstown Airport, which is 358 metres above sea level and approximately 12 kilometres from Coronet Peak. Therefore, this temperature information would be inaccurate and this is why there have not been any correlations made between air mass temperature and its stable isotopic composition in this study.

5.6. Conclusions

The precipitation events sampled on Coronet Peak during the months of July, August and September 2009 show large variations within their stable isotopic composition. Events A, D, E, F and G were sampled to determine whether the altitude effect had any impact on the stable isotopic signature of precipitation events on Coronet Peak. Most events showed the expected trend of decreasing δD and $\delta^{18}O$ values as altitude increased, however some of the samples collected plotted in

unexpected places. From precipitation event F an altitude gradient could be established, and this event showed the altitude effect best with the gradient being -5.19‰ δD and -0.71‰ $\delta^{18}O$ for every 100-metre increase in altitude above sea level.

Variations in the stable isotopic composition of precipitation events with storm duration on Coronet Peak gave mixed results. Samples from events A, C, E and F were graphed to determine whether the relationship of decreasing δD and $\delta^{18}O$ values as storm duration increased was true for Coronet Peak. The results obtained were unsatisfactory and inconclusive. Most events showed the expected trend.

Storm trajectories of the precipitation events sampled on Coronet Peak have been shown to have a greater influence on stable isotopic composition than altitude and storm duration. Events D and E originated in the Pacific with a trajectory towards Coronet Peak from the north/north-east, these two events were extremely depleted in the heavy isotopes of hydrogen and oxygen due to their origin. The air masses for the other events sampled were all sourced from the Southern Ocean, with one originating from the Tasman Sea, reaching Coronet Peak on a south-westerly track. These events were isotopically enriched in the heavy isotopes of hydrogen and oxygen when compared to events D and E. This has resulted from the cooler temperature of the Southern Ocean allowing air masses to hold less water vapour and minimising evaporation from the ocean surface. Other factors that affect the stable isotopic composition of the events seem to be the height at which the air mass generally flows above sea level and the height that precipitation condenses from the air mass.

The variations in the stable isotopic composition of the precipitation events sampled on Coronet Peak are due to many factors. However, more confidence needs to be given to this data by sampling a greater number of storm events to build up a larger database for this area. In this way, the relationships between the stable isotopic composition of precipitation events on Coronet Peak with altitude, storm duration and storm track trajectory will be better understood and constrained, giving a greater understanding of the determinants, for example temperature and local wind variations, that affect precipitation for this study area and therefore a better knowledge of these factors in general and how they may impact on other environments.

Chapter Six:

The Springs of Coronet Peak

6.1. Introduction

Springs occur as a concentration of groundwater discharge at the ground surface, and are fed by an aquifer system, either confined or unconfined, within the ground (Todd and Mays, 2005). Spring flow generally indicates a healthy aquifer. There is no minimum flow required to classify between springs from seepage areas, though generally a seepage area is defined as the movement of water through the ground that once it reaches the surface there is no associated flow. Bryan, (1919), defined springs as representing the termination of underground flow systems, and marking the point at which fluvial processes become dominant. Spring discharge magnitudes can be grouped in the following table.

Table 6.1. Spring magnitudes and discharge from (from Meinzer, 1942).

Magnitude	**Mean Discharge**
First	>10 m^3/s
Second	1-10 m^3/s
Third	0.1-1 m^3/s
Fourth	10-100 l/s
Fifth	1-10 l/s
Sixth	0.1-1 l/s
Seventh	10-100 ml/s
Eighth	<10 ml/s

The first complete classification scheme for springs was set down by Bryan (1919), and he first divided springs into two sub-categories, non-gravitational and gravitational. Non-gravitational springs are volcanic in origin and are driven by the heat convection of deep-seated water; a mixture of water from the surface, water entrapped in buried sedimentary rocks, and water expelled during the crystallisation of igneous rocks. Gravitational springs are derived from shallow waters (resulting primarily from precipitation at the Earth's surface), and are driven by hydraulic head (Bryan, 1919). Gravitational springs can be categorised even further as seen below (Fetter, 1994).

Contact Springs: occur when a permeable water-bearing formation overlies a less permeable formation that intersects the ground surface.

Depression Springs: form where the ground surface intersects the water table.

Artesian Springs: result from the release of water under pressure at outcrop or through a confining bed.

Impervious Rock Springs: result in water flow through fractures or tubular channels of impervious rock.

Fault Springs: occur where an impermeable unit is emplaced against an aquifer due to fault movement.

Sinkhole Springs: form in carbonate environments where solution channels create either diffuse or channelised flow.

Joint or Fracture Springs: result where fracture controlled flow is dominant in the rock mass.

The spring types that were most commonly found on Coronet Peak and the adjacent areas were fracture, contact, depression and artesian springs, although some were hybrids between some of these categories. They are depicted schematically in Figure 6.1.

Figure 6.1. Diagrams of the common spring types on Coronet Peak, with water flow indicated by the arrows.

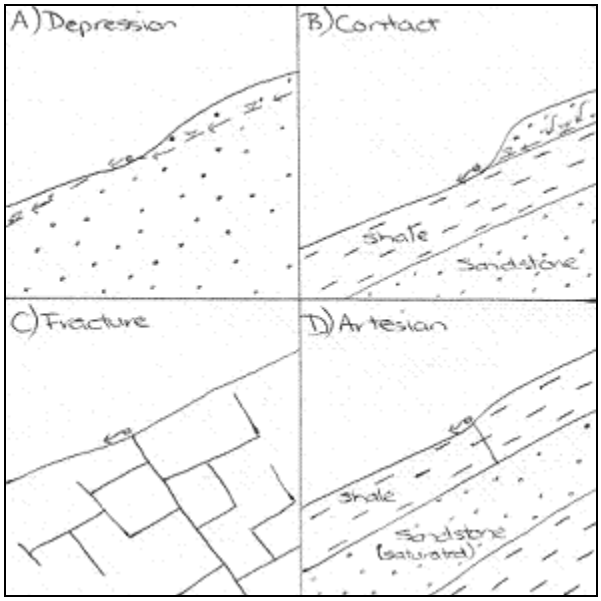

The precipitation of the area where a spring is situated has a large impact on the spring itself. There are cases where this statement is not true, in some environments groundwater can travel large distances, for example karst terrains. The largest karst landscape in the world in the Mammoth Cave System, Kentucky, USA. Where the cave systems explored extend as far as 580 kilometres, with the possibility of 1600 kilometres of cave systems in total (National Park Service, 2006). Aquifers by definition of saturated bodies of water, therefore water travels up towards the surface under pressure, unless it is gravity driven. The movement of groundwater may be helped by fractures or large pore spaces within the rock. Spring flows tend to fluctuate throughout the year depending on the season (ie. evapotranspiration) and amount of recharge, therefore the highest flows in mountainous areas should be in the springtime when the snow and ice begins to melt and the aquifers and water table are recharged. During the summer in mountainous areas it is usually dry and some springs may stop flowing altogether and are termed ephemeral springs, or they may continue to flow but at a lower rate and are known as permanent springs.

6.2. Spring locations

There are 26 springs located on the Coronet Peak Skifield and Recreation Reserve, and they were located using changes in topography and vegetation, studying Google Earth maps, and the knowledge of the Coronet Peak Skifield staff. The springs found in this area vary in locality, nature, formation process and flow rates. There were initially 30 springs to be monitored, however during the timeframe of this thesis some have not shown any flow, though they may still flow at times of very high rainfall or snow melt. It must be noted that the three springs Lunch Rocks, Rocky Gully and Easy Rider, all in the central northern region of the skifield, could not be individually monitored at times due to snow cover. Therefore these springs have been monitored using a pipe that collects the flows from these springs at a location of Heidi's Hut, and it is the flow from this pipe that has been stated for the flow rate of these three springs combined. The location of this pipe is shown on Figure 6.2, together with the locations of the 26 springs on the Coronet Peak Skifield and Recreation Reserve that were monitored. Each letter in this figure corresponds to a name in Table 6.2. The four locations thought to be spring areas are shown in Figure 6.2 also; they are the letters in blue. The springs located on Coronet Peak can be subdivided into five groups determined by their localities, the groups are shown in Table 6.2.

Figure 6.2. Map of all spring sites on Coronet Peak and the adjacent area. Letters correspond to the spring names and localities in Table 6.2. The colour lines also represent the locality division in Table 6.2.

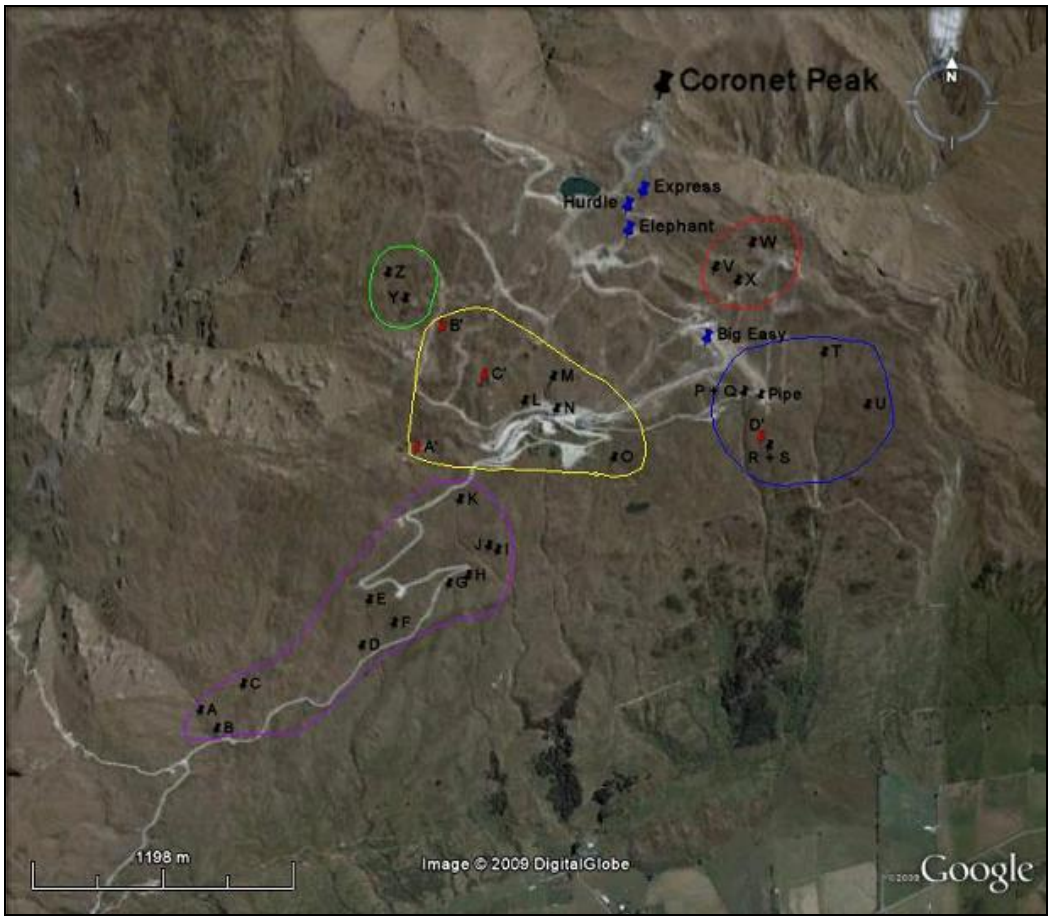

Table 6.2. Spring Locality References.

Group	Symbol	Spring Name	Group	Symbol	Spring Name
Central Eastern:	P	Danni's	**Central Northern:**	V	Lunch Rocks
(Blue)	Q	Heidi's	(Red)	W	Rocky Gully
	D'	McMullans #1		X	Easy Rider
	R	Moss	**Central Western:**	B'	Sarah Sue
	S	McMullans #2	(Yellow)	C'	Tarn
	T	Waterfall		L	Gobblers
	U	Grasshopper		M	Wall St
	Pipe	At Heidi's Hut		N	Water Supply
Long Gully:	Y	Dirty Four		O	Station
(Green)	Z	Dirty Creek		A'	Old Man Rock

Group	Symbol	Spring name
South Western:	K	Tussock
(Purple)	J	Twin
	I	Grassy
	H	Hairpin
	G	Multiple
	F	Coronet Peak Road
	E	Bramble
	D	Pond
	C	Wired
	B	Swamp
	A	Cattlestop

6.3. Monitoring of spring flows

The springs on Coronet Peak Recreation Reserve and Skifield have been monitored throughout the winters of 2008 and 2009, on average once a month. The springs were to be monitored via weirs, and when a weir could not be utilised a simple bucket and stopwatch method was used.

A weir is a structure that provides a restriction on the depth of the flow in a river or stream channel. It does this by being fixed in a position in which the weir blocks the river or stream channel creating a raised water level above the weir, a critical flow as the water above the weir rises to flow over the crest and a super-critical flow downstream of the weir. There are many types of weirs, for example v-notch, rectangular, trapezoidal and broad crested to name a few (Shaw 1994). The weir is a versatile structure for gauging water flow in comparison to a flume-type structure that is often used in river and stream channels, as it restricts the width of a river or stream channel rather than the depth. There are many varieties of weirs that can be used to measure a wide range of flows, from a few litres per second to hundreds of cubic metres per second. Each weir variety has the unique relationship of upstream head to the discharge over the crest where the critical conditions are passed (Shaw, 1994).

The type of weir used on the Coronet Peak Skifield and Recreation Reserve is the v-notch weir, as pictured in both Figure 6.3 and 6.4, they are constructed out of thin sheet metal.

Figure 6.3. V-notch weir with a 90° notch. Photo from Wired Spring on 15/04/2008.

The calculations have already been done for the type and dimensions of this weir and so the flow values can easily be measured and marked on the weir itself for easy monitoring in the field, as can be seen in Figure 6.3. The equation to calculate the flow rates is given in Equation 6.1, the flow rates for specific H (height above the notch in the weir) values are shown in Appendix D.

$$Q = K \tan(\theta/2) H^{5/2} \qquad \text{Eq 6.1.}$$

Where: Q = discharge in litres per second

K = coefficient

θ = angle of v-notch

H = height of water flow above the base of the notch

The angle of the v-notch weir was chosen to be at 90° and installed in all but one spring in which it was possible to fit a weir because it can give flow rates between 0.5 to 35 litres per second accurately, the latter flow rate being the highest flow rate expected from any of the springs on Coronet Peak Skifield and Recreation Reserve. Sheet metal was chosen as the construction material of the weirs because it is light, durable, cost effective and thin. The material needed all these qualities, but it especially needed to be thin because the thinner the material, the more accurate the readings as the water flows over the weir through the v-notch.

The weir that is installed in the Dirty Four Spring in 2006 is different to the other weirs. It is a v-notch weir but the 'v' is cut at 45° instead of 90° and is pictured below, it was installed prior to this project. The flow rates are calculated from the same equation as the 90° weir, and the flow rates are tabulated in Appendix D.

Figure 6.4. V-notch weir with a 45° notch. Photo from Dirty Four Spring on 15/04/2008.

The increments marked on this weir are H, (height) in millimetres above the notch, so the flow rate cannot be read off this weir like all the others. The increments begin at 0mm at the notch and increase to 300mm at the top of the weir. H needs to be

noted, and then matched up with its corresponding flow rate (Q) in the table in Appendix D.

The installation of the weirs within the streams created by the springs present on the Coronet Peak Skifield and Recreation Reserve was a matter of finding the best location near the spring. The location needed to be:

- accessible by foot
- typically within 10 metres of the spring source
- approximately one metre wide so the weir could fit
- collecting all or most of the flow from the spring sources
- in material relatively soft so the weir could be dug into it

There was one case where a spring did not have a location that met these criteria and so was monitored via a stopwatch and bucket, a method not as accurate as using a weir, this was the Grassy Spring. The weir installation involved clearing any vegetation that may impede the impermeability of the weir and digging a small trench across the streambed for the weir to sit in. This involved excavating the sides of the channel or building them up so the weir could fit and remain stable. The weir needed to be installed upright and level. The base of the v-notch needed to be at least 60 millimetres above the flow of the water on the downstream side to allow for the best possible flow through the v-notch and the most accurate readings.

When the trench was dug and the weir placed inside, it was infilled with the material previously excavated and also with bentonite. This is used because in the presence of water the bentonite particles expand and fill in any holes that may be present so that water does not escape under or around the weir. Bentonite is also layered between 500-1000 millimetres upstream of the weir on the channel floor and sides to make the area in which the weir is installed as impermeable as possible, and to allow the maximum flow rate to be measured through the v-notch. The thickness of the bentonite should be between 200-300 millimetres to allow the clay to infiltrate the soil to make an impermeable layer. Making an impermeable layer is difficult as most streams were flowing with water at the time of installation and so the layering of the bentonite may have been uneven, possibly allowing some water to flow under or around the weir. Small schist blocks (approximately 100 millimetres in size) found within close proximity to most springs were then placed on either side of the weir. On

the upstream side the blocks were used to provide some protection to the bentonite and the soft materials where the trench was dug. On the downstream side they were used to act as an energy dissipater as the water flows over the crest of the weir, the blocks were also used here to help to stabilise the weir against the pressure of the water on the upstream side.

After installation the upstream side of the weir begins to fill and flow over the crest, it is important to check for any leaks that may be seeping under or around the weir that will affect the accuracy of the flow rates. The accuracy of weirs themselves is not without variability, they give a reading that can be ± 10 %. Some weirs did not leak at all, whilst others needed to be modified with extra bentonite. Some springs could not have a weir installed due to construction work on the reservoirs of the Coronet Peak Skifield, and so needed to be measured with a stopwatch and bucket. These springs were Sarah Sue and Rocky Gully and the flow was diverted by a series of pipes because of the construction work on the Sarah Sue and Rocky Gully Reservoirs. However, little to no flow was measured at these outlet pipes, but the reasons were not known.

6.4. Recording and data analysis

The recording of the spring flows was done initially when the weirs were installed in April 2008. Recording from then on has been done mostly during the winters of 2008 and 2009, approximately one reading for each weir a month. It was initially planned to monitor the spring flows all year round to obtain a better understanding of how much natural water was available on the mountain that could be utilised for snow making purposes, however, this did not happen due to the lack of staff on the mountain during the warmer seasons of the year. The monitoring itself was carried out by me or by Coronet Peak Skifield staff. If some weirs were leaking when monitoring was conducted, they were fixed as best as could be done, and then when the flow filled the reservoir behind the weir and flow through the weir was stable (after approximately 10 minutes) the flow rates were then noted.

In Table 6.3, the type of each spring found within the Coronet Peak Skifield and Recreation Reserve is shown. These types are based on observations made in the field, and have been noted in detail in Appendix D with photos of each spring and weir. The Water Supply spring does not have a type associated with it, as this spring

has been accessed underground by the staff of Coronet Peak Skifield and the area around the spring has been severely modified with access ways and buildings. Therefore the type of spring could not be determined with confidence. The magnitudes of the springs has also been shown in the table below, they are all either a magnitude 5 or 6 spring, having flows between 1-10 litres pre second and 0.1-1 litre per second respectively.

Table 6.3. Spring types and magnitude, with flow ranges in litres per second.

Spring	Type	Magnitude	Flow Range
Coronet Peak Road	Depression	5-6	0.2-1.6
Wall Street	Depression	6	0.25-1.6
Station	Depression	6	0.1-0.9
Gobblers	Fracture	6	0.3-1.2
Heidi's	Fracture	5	1.0-6.0
Hairpin	Fracture	5	1.5-2.5
Lunch Rocks	Fracture	6	0.2-0.3
Rocky Gully	Fracture	6	0-0
McMullan #2	Contact/Fracture	5	0.5-1.5
Waterfall	Contact/Fracture	5	1.0-2.2
Dirty 4	Contact/Fracture	5	1.6-6.04
Easy Rider	Contact	6	0.1-0.2
Cattlestop	Contact	6	0.05-0.9
Danni's	Contact	6	0.1-1.2
Twin	Contact	6	0.25-0.7
Bramble	Contact	6	0.2-0.6
Tussock	Contact	5	0.25-5.6
Grassy	Contact	5	0.25-2.0
Moss	Contact	6	0.15-2.0
Pond	Contact	6	0.5-2.5
Grasshopper	Contact	5	0.25-1.6
Dirty Creek	Contact	6	0.3-6.0
Wired	Contact	6	0.05-1.0
Swamp	Artesian/Contact	6	0.05-0.6
Multiple	Artesian/Contact	6	0.1-0.6
Water Supply	?	5	2.0-3.2

Table 6.4. Spring flows measured on Coronet Peak. All flows are in litres per second.

Date	**14/04/2008**	**21/04/2008**	**9/06/2008**	**7/07/2008**	**21/07/2008**	**11/08/2008**	**1/09/2008**	**15/09/2008**	**13/07/2009**	**10/08/2009**	**21/09/2009**	**Average**
Spring Name												
Cattlestop	0.25	0.25	0.25	0.05	0.25	0.2	0.25	0.2	0.6	0.4	0.9	**0.33**
Swamp	0.4	0.35	0.25	0.05	0.25	0.2	0.2	0.2	0.4	0.2	0.6	**0.28**
Wired	0.25	0.2	0.05	0.05	0.05	0.1	0.2	0.2	0.5	0.8	1	**0.30**
Pond	0.5	0.6	0.75	0.5	0.5	0.9	1.0	0.7	2.0	2.3	2.5	**1.11**
Bramble	0.6	0.5	0.5	0.2	0.25	0.6	0.2	0.5	0.4	0.5	0.4	**0.45**
Coronet Peak Rd	0.8	0.7	0.5	0.2	0.25	0.7	0.5	0.5	0.7	0.6	1.6	**0.64**
Multiple	0.5	0.4	0.25	0.25	0.1	0.3	0.3	0.2	0.4	n/a	0.6	**0.33**
Hairpin	2.5	2.0	2.0	2.0	2.0	1.8	2.0	1.5	1.5	n/a	1.5	**1.88**
Twin	n/a	0.4	0.25	0.5	0.5	0.7	n/a	0.5	0.5	n/a	0.5	**0.48**
Grassy	n/a	1.0	1.0	1.0	0.25?	1.0	1.0	1.0	2.0	n/a	1.8	**1.12**
Tussock	n/a	1.9	1.0	1.2	0.25?	1.4	0.5?	1.5	4.5	n/a	5.6	**1.98**
Gobblers	0.4	0.5	0.75	n/a	n/a	0.9	n/a	0.3	1.0	0.8	1.2	**0.73**
Wall St	0.4	0.4	0.5	0.75	n/a	0.6	0.25	0.5	1.2	0.5	1.6	**0.67**
Water Supply	n/a	3.2	n/a	n/a	n/a	n/a	n/a	2	n/a	n/a	n/a	**2.6**
Station	0.4	0.3	0.1	0.5	n/a	0.7	n/a	0.5	0.4	0.2	0.9	**0.44**
Danni's	1.2	1.1	1.0	n/a	n/a	0.8	0.3	0.3	0.4	0.1	1.2	**0.71**
Heidi's	2.8	1.5	1.0	n/a	n/a	1.2	n/a	4.2	3.0	1.0	6.0	**2.58**
Moss	0.2	0.15	0.5	1.0	n/a	0.7	n/a	0.9	0.6	0.4	2.0	**0.72**
McMullans #2	0.8	1.0	1.0	0.5	n/a	0.9	n/a	1.1	1.5	1.4	1.5	**1.08**
Waterfall	1.0	1.2	1.0	1.5	n/a	1.5	1.5	1.5	1.2	1.5	2.2	**1.41**
Grasshopper	0.5	0.5	0.5	1.0	n/a	1.2	0.25?	0.9	1.0	1.0	1.6	**0.85**
Lunch Rocks	*0.3*	*0.2*	*n/a*	*n/a*	*n/a*	*n/a*	*n/a*	*n/a*	*n/a*	*n/a*	*n/a*	***0.25***
Rocky Gully	*0*	*0*	*n/a*	*n/a*	*n/a*	*n/a*	*n/a*	*n/a*	*n/a*	*n/a*	*n/a*	***0***
Easy Rider	*0.2*	*0.1*	*n/a*	*n/a*	*n/a*	*n/a*	*n/a*	*n/a*	*n/a*	*n/a*	*n/a*	***0.15***
Pipe @ Heidi's Hut	0.5	0.3	n/a	n/a	n/a	n/a	n/a	n/a	0.5	0.5	0.5	**0.46**
Dirty Four	2.05	1.95	1.6	n/a	3.09	n/a	5.19	6.04	4.8	n/a	6.04	**3.42**
Dirty Creek	0.3	n/a	3.0	n/a	0.5	0.5	2.0	6?	frozen	n/a	1.2	**1.93**
Total Average Flow												**26.5**

The flows measured during the winters of 2008 and 2009 from the springs found on Coronet Peak Skifield and Recreation Reserve are listed in Table 6.4, and the date stated is the Monday of each week of sampling, with the sample being taken during that week. Some flow rates have question marks next to them to indicate lack of confidence in these flows, and all these measurements were taken by the staff on the Coronet Peak Skifield but do not seem to fit with the rest of the flows for those particular springs. Where very small flows have been measured from springs there may have been leaks. The weir should have been checked prior to taking the measurements. Examples where this may have happened are both the Tussock and Grasshopper Springs.

The average flows from each spring are shown above, in litres per second, as well as the total average flow rate. The averages per spring vary, from 0.28 (Swamp Spring) to 3.42 litres per second (Dirty Four Spring), with the total combined average flow rate being 26.50 litres per second. This indicates that if both of these winters were average in terms of spring flows, there should be on average 26.50 litres per second (l/sec) that is available on the mountain at any one time during the winter months. Spring monitoring during the summer months would determine have much this values varies seasonally, and give the base flow of each spring.

Some of these springs have been slightly modified and are diverted or collected so that they can be pumped into the water storage reservoirs on the Coronet Peak Skifield. The most notable ones are Heidi's Spring, Danni's Spring, the pipe at Heidi's Hut (Lunch Rocks, Rocky Gully and Easy Rider Springs), and Waterfall, Gobblers, Wall St and Water Supply Springs. The Water Supply Spring is collected and used to supply water to the main base building on the Skifield. These springs are utilised because of their relatively constant flow rates, usually above one litre per second, and because of their proximity and ease of access to the Skifield.

The Dirty Four has the highest average flow rate in the area and has been monitored since 2006, however it has not been utilised yet because it is in a gully on the western side of Coronet Peak and is hard to access. There are other springs that may be useful from the flow data above that have not been previously exploited, for example, Tussock (1.98 l/sec), Hairpin (1.88 l/sec), Pond (1.11 l/sec), McMullan #2 (1.08 l/sec) and Dirty Creek (1.93 l/sec). The locations of these springs can be seen in Figure 6.2 and from this the best springs that could be utilised by the Coronet Peak Skifield are the Tussock (just below the road) and McMullan #2 (close to Heidi's

Spring collection area) springs. However, these are only winter flow rates and more information is needed, especially over the summer to determine the spring flows all year round. Using this data the springs that could be useful to the Skifield to utilise in artificial snowmaking will be evident.

The spring flows vary, there is no clear trend from this data, and this maybe due to the pumping from the aquifers beneath Coronet Peak. Unfortunately, detailed pump statistics for the whole length of the sampling period were not able to be obtained, which would have led to the probable correlation of decreasing spring flows with times of increased pumping to the reservoirs of the mountain. However, it may still be difficult to determine a correlation towards to end of the ski season because pumping from the aquifers also occurs when the snow begins to melt.

The information from the pumps is for the winter of 2008 only, the months of June, July, and August. During this time the main bores, the Big Easy (PS400) and the Hurdles bores (PS100), were pumped for nearly the whole duration of the winter, with some small breaks at various points in time (see Figures 6.5 and 6.6).

Figure 6.5. Rate of pumping from bore PS100 (the Hurdles bore) during June, July and August 2009.

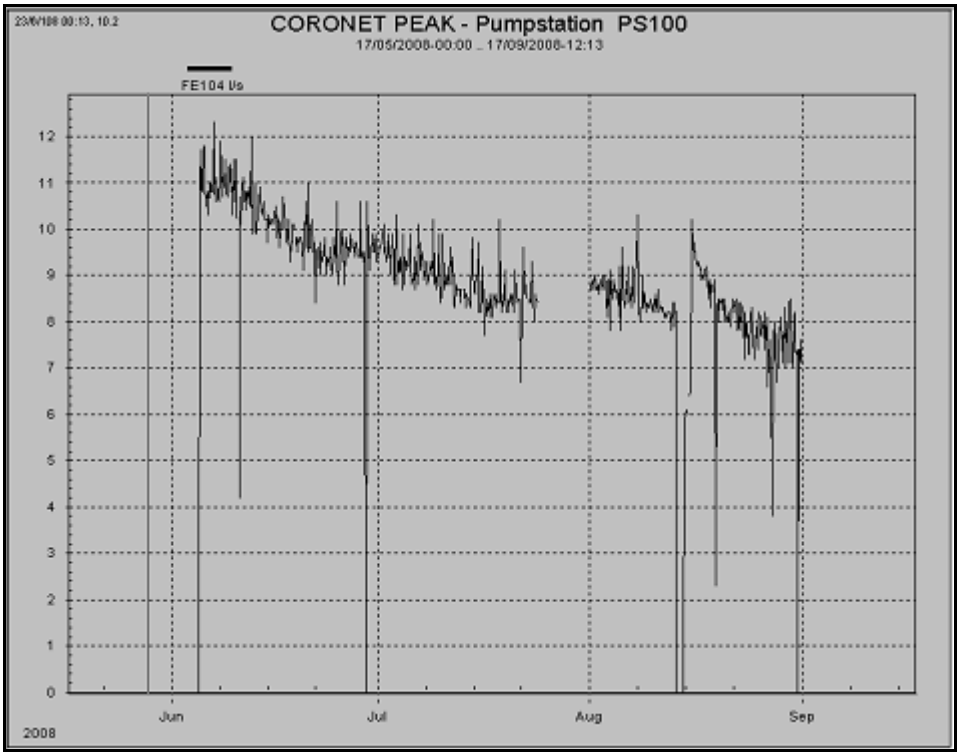

Figure 6.6. Rate of pumping from bore PS400 (the Big Easy bore) during July and August 2009.

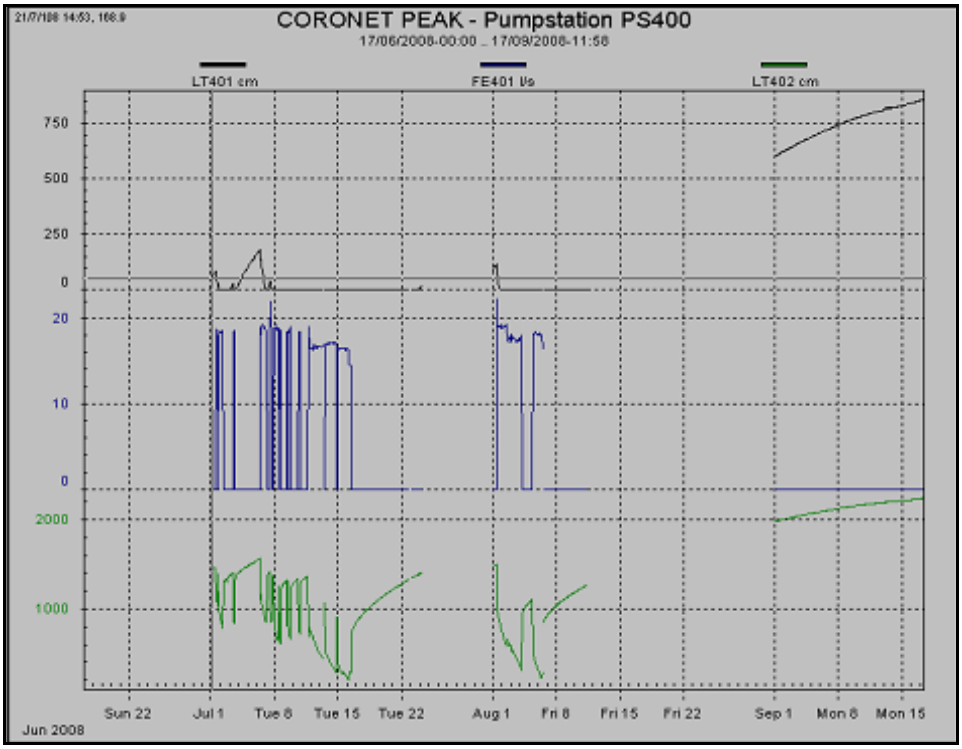

From these two figures, the rate at which pumping has occurred during the winter of 2008 is shown from these two bores in litres per second. The Hurdles bore was pumped continuously, with one break at the end of July and a very short break in the middle of August. The Big Easy bore was pumped nearly on a day-to-day basis from the start of July to mid July, then pumping ceased until the beginning of August, but only for the first week, then pumping stopped completely. It is difficult to see whether this pumping has any impact on the spring flows of Coronet Peak as more information on flow rates is needed on a continuous basis. It would be expected that pumping from the groundwater system would have a large effect, however without data of the spring flows during a season where no pumping occurred and other factors such as rain and snow fall it is hard to determine the causes for the variations in the spring flows that can be seen in Table 6.4.

Some of the springs that had larger flows and are classed as a category 5 in magnitude have shown a considerable decrease in their flow rates from the beginning to the end of winter in 2008, the Heidi's and Tussock springs demonstrate this,

decreasing from 2.8 (April) to 1.3 (August) and 1.9 (April) to 0.5 (September) respectively. This may indicate the influence of the pumping on these springs. Other springs however did not comply with this trend, for example the flows from the Wall St and Cattlestop springs remained similar over the winter, whilst the Pond, Waterfall and Dirty Four springs show increases from the beginning to the end of the winter. These springs may be highly influenced by snow melt that occurs towards the end of the winter, whereas the springs that show little change from this information may not be influenced by pumping or snow melt. It would be expected that pumping would influence all spring flows on Coronet Peak. Without detailed monitoring it is difficult to determine the impact of pumping on spring flows.

6.5. Conclusions

In conclusion, this study has identified 26 permanent springs on the Coronet Peak Skifield and Recreation Reserve. Another four springs were identified, however when monitoring was done none of these were flowing, these areas may be ephemeral springs or not springs anymore (or ever) but still have the physical characteristics of a spring. The flow rates from these 26 springs were observed for the winters of 2008 and 2009, the averages of these flows give a total average spring flow rate of 26.50 litres per second. This is the water available from the surface of the mountain that can be utilised in the snow making endeavours undertaken by the staff on the Coronet Peak Skifield to extend their ski season and guarantee quality skiing. From the flow rate data it can be seen that there are some springs that are not being exploited by the skifield at the moment that perhaps should be, these are the Hairpin, Pond, Dirty Creek Springs, but especially the Tussock and McMullan #2 Springs, as these springs have favourable locations. More data is needed about all of these springs to determine year round flow rates and their utility to the Skifield.

It is possible for the Coronet Peak Skifield to utilise this additional water source of 26.50 litres per second. However, information will need to be obtained relating to the effects on the farmland below the skifield. As this water is being diverted to water storage reservoirs on the skifield, instead of flowing down the mountain has it has done under natural conditions. It may be that only a certain amount of spring flow, perhaps half, can be utilised by the skifield in order to allow some of the water to continue to flow down to the farms below. If all spring water

were to be utilised by the skifield, the farmers may suffer adverse effects, by a lack of water. However, as the skifield only needs additional water during winter when it makes artificial snow, the adverse effects would only occur during the winter months. It is at this time where precipitation is at it's highest, and therefore utilising the spring flows may not significantly impact the farmers in the basin below.

The reasons for the variations within the flow rates of these springs on Coronet Peak are difficult to determine, however the pumping from the aquifers beneath the skifield affects some spring flows where others it does not. There is no relationship that can be seen from the available flow data and pumping records from the winter of 2008. This is most likely due to the fact that in the times when precipitation is at its highest (the end of winter), pumping is being done, therefore it is difficult to deduce any spring flow variations that are wholly due to the dewatering of the aquifers beneath or whether flows decline in some springs due to snow cover and ground freezing. A record of precipitation falling on the mountain would also help this situation. However, what will be shown next in Chapter Seven is that current precipitation has little effect on the stable isotopic composition of the springs located here, therefore the changes in precipitation that has fallen on Coronet Peak in previous years will have an impact on aquifer levels as it percolates through the earth, and consequently the spring flows.

To better understand the flow rates of the springs on Coronet Peak continuous monitoring is needed on a weekly basis. Also detailing observations of the pumping rates from the boreholes is needed. From this information, the pattern with spring flows and dewatering can be seen giving further knowledge of how the surface and ground waters are linked and related. Only then can the effects that the pumping from the aquifers has on spring flows be truly observed. Adding precipitation data to this will only enhance the understanding of this system.

Chapter Seven:

Stable Isotopic Compositions of Springs and Aquifers

7.1. Introduction

Water samples were collected from the springs where possible during July, August and September 2009. To identify the stable isotopic signature of each spring, and to determine the source of the spring flow. Specifically the flow could be dominated by groundwater, or precipitation could be a major contributor. Samples have also been taken from the two pumping bores on the Coronet Peak Skifield, the Big Easy and the Hurdles bores, for similar purposes. These stable isotope results were gathered and collated to identify any relationships within the springs themselves, examining specific spring characteristics and also looking at the borehole data. The sampling of the springs and boreholes, their locations, and the analysis of the water samples using the CF-IRMS, have been described in Chapter Three (Figure 3.2 for locations and 3.9 for basic diagram of a mass spectrometer).

7.2. Spring characteristics and data analysis

7.2.1. *Isotope values*

The results of the water samples collected from the springs on Coronet Peak are tabulated in Table 7.1, where all results are displayed in parts per thousand (‰). It can be seen from these results that the stable isotopic compositions of the springs vary, with a range of 45‰ for the δD values and 2.9‰ for the $\delta^{18}O$ values. This very large range for the hydrogen values is due to the sample collected from the Wall St Spring, which is extremely negative in comparison to all other samples. The August sample from this spring is –117.55‰ and 16.04‰, δD and $\delta^{18}O$ values respectively, whereas the δD and $\delta^{18}O$ values for July and September respectively are –81.8‰ and –11.31‰, and, –82.27‰ and –11.77‰. The large range for this spring may indicate that the sample collected was dominated by snow melt or precipitation, not direct spring flow when it was taken as this sample is very different from the other samples taken from this spring. The elevation of each spring is also shown in Table 7.1 to

determine whether the elevation in metres above sea level has any impact on the stable isotopic composition of the springs of Coronet Peak.

7.2.2. *Springs isotopic trends*

The individual stable isotopic composition of the springs are shown in Appendix E. Each spring is plotted on a δD and $\delta^{18}O$ graph to determine the variations in stable isotopic composition of the individual springs. In these graphs there are two clear trends shown. The first is the decrease in the stable isotopic content in some springs with time, whilst the second is a variation of this trend where the most negative sample was collected during August instead of September.

The decreasing trend in the first group of springs may indicate a trend within the aquifers themselves rather than in the current precipitation. The precipitation data that is shown in Figures 7.4 through to 7.6 indicate little influence of the current precipitation on spring isotopic compositions. However, the second group indicates variation from the other springs due to relatively negative δD and $\delta^{18}O$ values in August. This negativity corresponds with the precipitation sampled in August, indicating there may be some influence on spring stable isotopic compositions by current precipitation. This may occur due to mixing of groundwater and infiltrating precipitation.

7.2.3. *Results with spring type*

Figure 7.1 (b) graphs the spring samples collected during July 2009, Figure 7.1 (d) graphs the samples collected for August 2009 and Figure 7.1 (e) plots samples for September 2009. Figure 7.1 (f) plots the averages of each spring from the data (Table 7.1). Figure 7.1 (a) is the key to these graphs, where each spring has it's own identifying symbol, and the colours indicating the spring type shown in Figure 7.1 (c). From these graphs it can be seen that some of the spring types plot together whilst others do not. Borehole data for the corresponding months have also been graphed with the spring data. Where no values are present for a spring for a specific date, this indicates that sampling was not undertaken from this spring. In the case of the Lunch Rocks, Rocky Gully and Easy Rider springs, no individual stable isotopic data is known, however, combination samples have been taken for the 'pipe at Heidi's Hut', which is the location of the samples for these three springs.

Table 7.1. Stable isotopic composition of spring samples with type and height in metres above sea level. The dashes indicate the spring was not sampled.

Spring	Height	Type	δD-July	δ^{18}O-July	δD-Aug	δ^{18}O-Aug	δD-Sept	δ^{18}O-Sept	Average δD	Average δ^{18}O
Coronet Peak Road	1010	Depression	-81.1	-11.40	-85.78	-12.18	-83.81	-11.85	-83.57	-11.81
Wall Street	1200	Depression	-81.8	-11.31	-117.55	-12.37	-82.27	-11.77	-82.02	-11.54
Station	1133	Depression	-81.1	-11.52	-84.31	-12.01	-86.70	-12.37	-84.03	-11.97
Gobblers	1128	Fracture	-82.4	-11.50	-84.95	-12.33	-83.99	-11.84	-83.78	-11.89
Heidi's	1208	Fracture	-82.9	-11.62	-87.24	-12.54	-87.45	-12.67	-85.87	-12.28
Hairpin	966	Fracture	-81.4	-11.49	-	-	-86.72	-12.41	-84.04	-11.95
Lunch Rocks	1381	Fracture	-	-	-	-	-	-	-	-
Rocky Gully	1368	Fracture	-	-	-	-	-	-	-	-
McMullan #2	1112	Contact/Fracture	-81.9	-11.58	-84.17	-12.04	-85.87	-12.70	-83.99	-12.11
Waterfall	1279	Contact/Fracture	-77.7	-11.26	-86.60	-12.36	-86.04	-12.50	-83.46	-12.04
Dirty 4	1265	Contact/Fracture	lost	lost			-85.63	-12.37	-85.63	-12.37
Easy Rider	1358	Contact	-	-	-	-	-	-	-	-
Cattlestop	913	Contact	-72.6	-10.29	-82.76	-11.52	-81.32	-11.28	-78.90	-11.03
Danni's	1184	Contact	-83.6	-11.75	-87.35	-12.61	-87.29	-12.83	-86.07	-12.40
Twin	982	Contact	-78.7	-11.20	-	-	-86.83	-12.21	-82.79	-11.71
Bramble	1059	Contact	-81.0	-11.39	-84.68	-11.74	-83.92	-11.90	-83.20	-11.68
Tussock	1128	Contact	-76.6	-10.96	-	-	-86.55	-12.42	-81.59	-11.69
Grassy	1003	Contact	-82.3	-11.36	-	-	-92.21	-12.53	-87.27	-11.94
Moss	1120	Contact	-78.8	-11.12	-87.72	-12.61	-86.34	-12.47	-84.27	-12.07
Pond	977	Contact	-81.4	-11.24	-84.56	-12.08	-83.23	-11.76	-83.08	-11.69
Grasshopper	1231	Contact	-79.2	-11.33	-86.22	-12.57	-87.26	-12.79	-84.23	-12.23
Dirty Creek	1380	Contact					-89.22	-13.16	-89.22	-13.16
Wired	968	Contact	-77.6	-10.95			-79.86	-11.41	-78.72	-11.18
Swamp	879	Artesian/Contact	-79.0	-11.25	-82.79	-12.39	-82.70	-11.42	-81.49	-11.68
Multiple	975	Artesian/Contact	-76.5	-10.95			-86.04	-12.25	-81.26	-11.60
Water Supply	1161	?	-81.6	-11.63	-89.26	-12.63	-87.40	-12.54	-86.09	-12.26
Pipe at Heidi's Hut	1223	-	-82.3	-11.60	-85.63	-12.36	-87.15	-12.57	-85.03	-12.18

Figure 7.1 (a). Spring symbols.

Figure 7.1 (b). Spring samples July 2009.

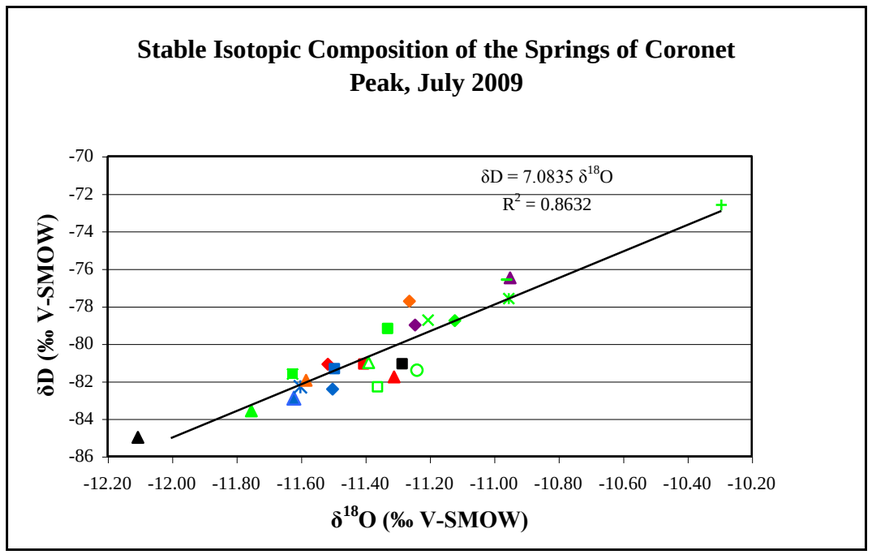

Figure 7.1 (e). Spring samples September 2009.

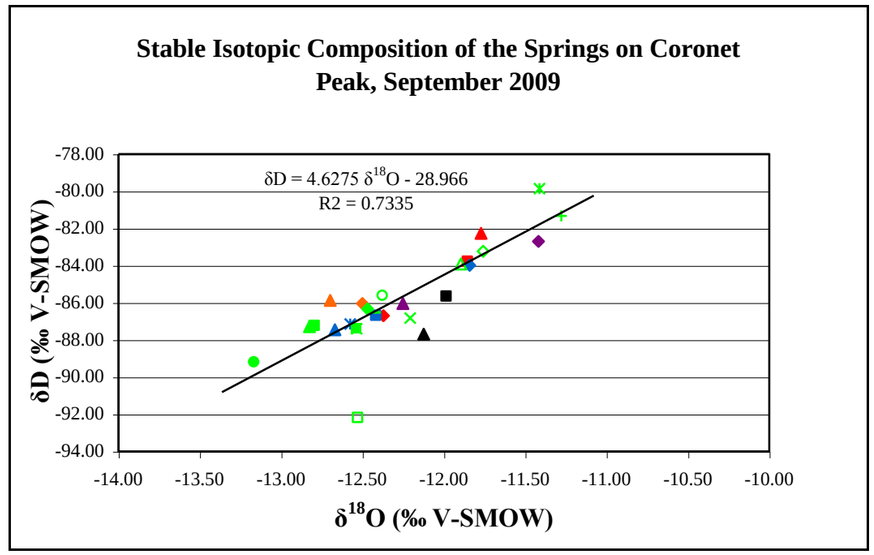

Figure 7.1 (c). Colour code for Figure 7.1.

Symbol Colour	Type
Blue	Fracture spring
Red	Depression spring
Green	Contact spring
Orange	Contact/Fracture spring
Purple	Contact/Artesian spring
Black	Borehole
Navy Blue	Precipitation

Figure 7.1 (d). Spring samples August 2009.

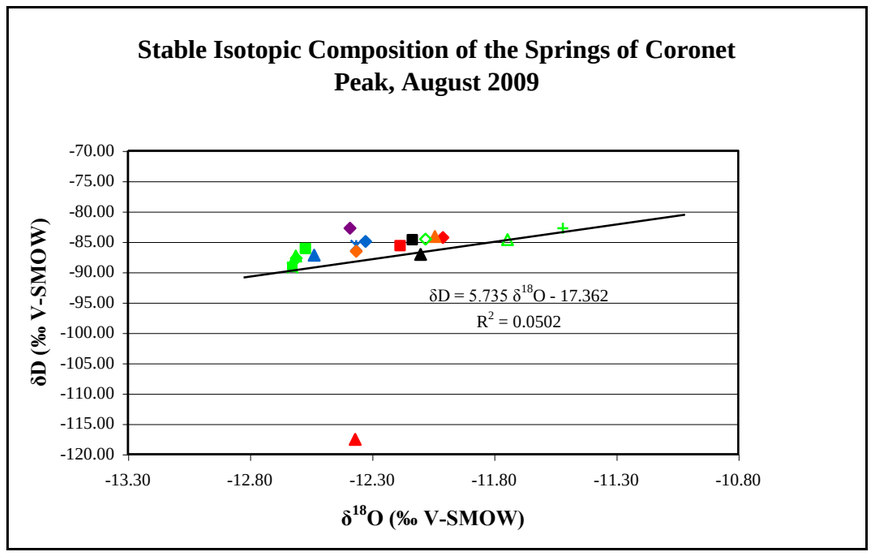

Figure 7.1 (f). Spring samples, average for July, August and September 2009.

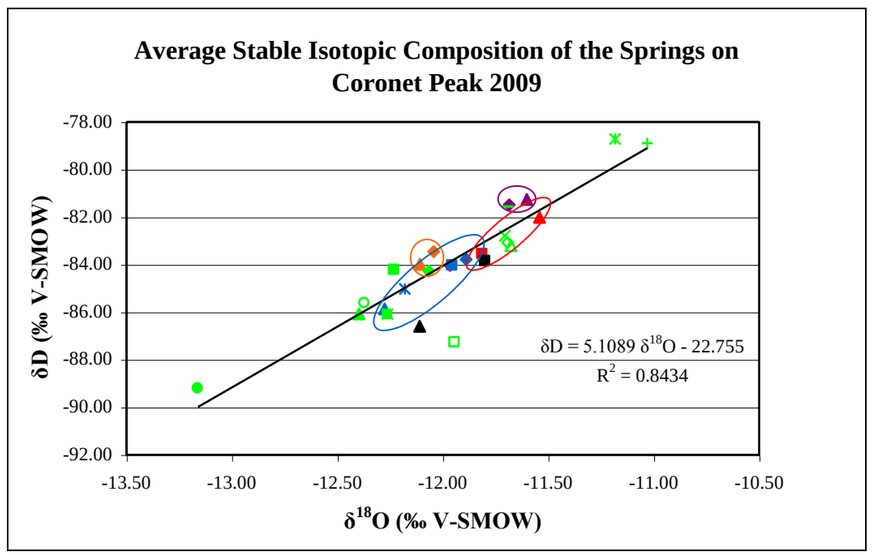

For the month of July 2009, Figure 7.1 (b) indicates that the depression springs plot very closely together and are therefore isotopically similar, and the fracture springs also do this for this time period. However, the contact, contact/fracture and contact/artesian springs do not plot together and have a wide range of stable isotopic values.

The springs sampled in the month of August 2009 (Figure 7.1 (d)) only indicate that fracture springs plot together whilst all the other spring types do not. Although there is a pattern within the contact springs, the solid green symbols represent contact springs from higher elevations than most of the others, and these springs plot more negatively than the contact springs of lower elevations that have the green symbols that are only an outline.

This pattern is also shown in the month of September 2009 (Figure 7.1 (e)), while the contact/fracture springs plot together where all others vary and show a wide range of values. This indicates a possible altitude effect within the springs and will be discussed further in the chapter.

The average stable isotopic values of each spring have been calculated and are shown in Table 7.1, whilst they have been graphed in Figure 7.1 (f). The average stable isotopic content has been used in this case to give an overall indication of the isotopic composition of the springs over the three months of sampling. It can be seen that on average during the months of July, August and September 2009, most spring types do plot together and show similar stable isotopic hydrogen and oxygen values. Indicating a similar water source. Some of the springs plot so similarly that the symbol may cover the symbol of another, this happens to the Station spring symbol being overwritten by the Hairpin symbol, and the Water Supply spring symbol plotting on top of the Heidi's spring symbol. The contact springs however do show the largest range within these samples but also indicate a difference between the lower and higher elevation springs, the elevations of each spring are shown in Table 7.1, in metres above sea level. Indicating an elevation effect in spring stable isotopic composition.

Due to most spring types plotting together in Figure 7.1 (f) indicating a similarity in their stable isotopic compositions, it could be interpreted that the spring formation processes and the mechanism by which groundwater flows to the surface through these springs is very similar for each type of spring, leading to the grouping of spring types in Figure 7.1 (f). Because the borehole data are also plotted with the

spring values above, the average δD and $\delta^{18}O$ values for the Big Easy and Hurdles bores are –83.86‰ and –11.80‰, and –86.60‰ and –12.11‰ respectively. It can be said that the fracture springs, ranging in δD and $\delta^{18}O$ values from –83.78‰ and –11.89‰ (Gobblers spring) to –85 87‰ and –12.28‰ (Heidi's spring) respectively, and access groundwater of both the Big Easy and the Hurdles bores. The depression springs tend to access groundwater from the Big Easy bore alone, however these samples are more positive than the groundwater indicating another possible water source. The δD and $\delta^{18}O$ values of the two end-member of this group are –82.02‰ and –11.54‰ (Wall Street spring) and –84.03‰ and -11.97‰ (Coronet Peak Road spring) respectively. The contact/artesian springs are fed by the Big Easy bore and also signify an additional water source due to their positive values. The Multiple spring has an average δD value of –81.26‰ and a $\delta^{18}O$ value of –11.54‰, whilst the Swamp Spring has δD and $\delta^{18}O$ values of –81.49‰ and –11.68‰ respectively. The contact/fracture springs access water from both boreholes, giving average δD and $\delta^{18}O$ values for the springs Waterfall and McMullan #2 of –83.46‰ and –12.04‰, and –83.99‰ and –12.11‰ respectively.

The stable isotopic composition of the contact springs varies considerably, being the most positive and the most negative samples collected from springs on Coronet Peak. The Cattlestop spring having an average δD and $\delta^{18}O$ values of –78.90‰ and –11.03‰, whilst the Dirty Creek spring has δD and $\delta^{18}O$ values of –89.22‰ and –13.16‰ respectively. This is due to an elevation effect, the higher the elevation, the more negative the stable isotopic values tend to be, as can be seen in Figure 7.2 below, and may be because of the altitude effect in the precipitation that falls on Coronet Peak. Using the averages of the spring stable isotopic compositions, the changes in the oxygen ratios with elevation can be shown by the relationship that $\delta^{18}O$ values decrease by 0.43‰, for every 100-metre increase in elevation. This value is similar to the altitude gradient calculated from precipitation event F in Chapter Five, being a decrease in $\delta^{18}O$ of 0.71‰ for every 100-metre increase in elevation. There may also be additional water sources that influence these springs, possibly from beneath the groundwater accessed by the current boreholes, or from above (current precipitation). The 0.28‰ difference in the $\delta^{18}O$ values between the altitude gradients given above may be due to the fact that the gradient from event F is from current precipitation, whereas the gradient from the springs maybe from other sources of groundwater or from previous precipitation.

Figure 7.2. Variations in the stable isotopic spring compositions with elevation.

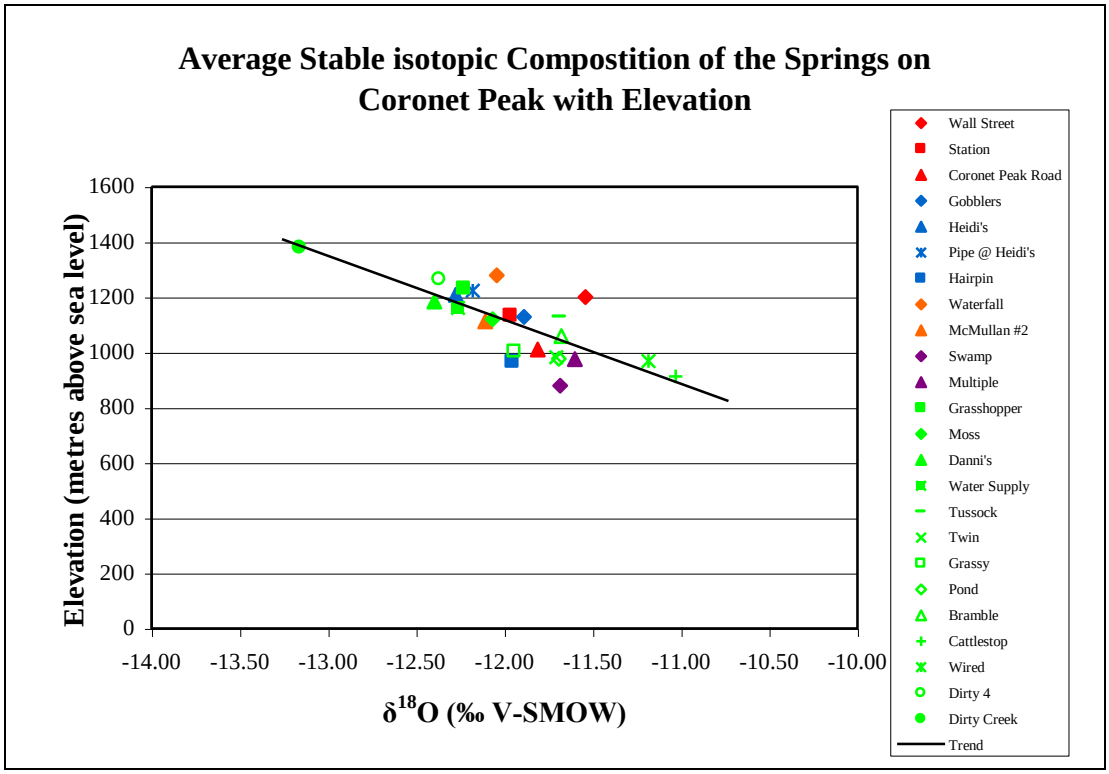

7.3. Spring results and groundwater sources

The two boreholes that have been sampled on the Coronet Peak Skifield, (Big Easy and Hurdles bores), have also been plotted in Figure 7.1 to try to determine the groundwater source for each spring using the stable isotopic content from the springs and boreholes. The stable isotopic composition of the groundwater sampled from the boreholes is graphed in Appendix E (Figures E-25 and E-26). The two graphs do not indicate clear trends within their stable isotopic contents, unlike the springs. The borehole data has also been averaged over the sampling periods of July, August and September 2009 to give an overall indicator of spring flow origin.

The sampling during July 2009 (Figure 7.1 (b)) shows that the groundwater sampled from the Hurdles borehole has little impact directly on the spring flows in the area of Coronet Peak. Most springs plot within the area on the graph where the Big Easy bore plots. However, there are some springs that plot in between these two

groundwater sources and this may indicate mixing between these aquifers accessed by the boreholes, or another water source. Some springs also plot more positive than both boreholes indicating that other factors may play a role in the stable isotopic composition of the springs of Coronet Peak. Springs sampled in August 2009 tend to plot more negatively than the two boreholes, which plot closer together than in July. All of the samples in Figure 7.1 (d) plot slightly more negative than in Figure 7.1 (b). This also indicates other factors involved in determining the stable isotopic composition of the springs. In September 2009 (Figure 7.4), the boreholes plot similarly again, with the Hurdles bore always more negative than the Big Easy bore. There is an indication of mixing between these two groundwater sources, but a lot of the springs once again plot more negatively than both.

In Figure 7.1 (f), the averages of all the spring and borehole stable isotopic data are graphed together. This is the most useful graph of the four as it gives a better idea of the long-term stable isotopic signatures of the springs and boreholes, being a compilation of the data over the three-month period. A group of springs plot around both boreholes, the groundwater accessed by the Big Easy bore from this information seems to feed the Coronet Peak Road (depression), Gobblers (fracture), Hairpin (fracture), Station (depression and on the graph is behind Hairpin), Waterfall (contact/fracture), Bramble (contact), Pond (contact) and Twin (contact) springs, whilst the groundwater accessed by the Hurdles bore feeds the Grassy (contact), Water Supply (unidentified), Heidi's (fracture and on the graph is behind Water Supply), Dirty Four (contact/fracture) and Danni's (contact) springs. The Dirty Creek spring (contact spring) plots more negatively than both bores, indicating another water source. The Pipe at Heidi's Hut (Lunch Rocks - fracture, Rocky Gully - fracture and Easy Rider - contact Springs), as well as the McMullan #2 (contact/fracture) and Moss (contact) springs plot in between the groundwater accessed by the two boreholes. Whilst some springs plot more positively than the groundwater accessed both boreholes, these are the Tussock (contact), Swamp (contact/artesian), Multiple (contact/artesian), Wall St (depression), Cattlestop (contact) and Wired (contact) springs.

There may be other factors involved in determining the stable isotopic composition of the springs located in the Coronet Peak area, these may be the influence of precipitation, which will be discussed below, and the possibility of another groundwater source. Below Coronet Peak Skifield there is evidence of three

aquifers, see Figure 7.3 below, where the cross-section line is shown on the Google Earth image which is also shown in Figure 7.3. The numbers of the boreholes in Figure 7.3 correspond to Table 7.2. The Big Easy bore accesses the shallowest of the three aquifers at approximately 40 metres below ground level, whilst the three Hurdles bores access water from the remaining, deeper aquifers, at approximately 58 and 130 metres below the ground level. The stable isotopic composition of the samples collected from the Hurdles bore are an amalgamation of these two groundwater sources and do not indicate the true stable isotopic signature of either of these two aquifers. Therefore, the springs that are not sourced by the groundwater accessed by the Big Easy bore may be fed by either of these two deeper aquifers. This is very difficult to determine whether this is true or not as the two deeper aquifers cannot be accessed and sampled individually.

Table 7.2. Borehole numbers and corresponding names from Figure 7.3, with the depth that groundwater was found at in metres below ground level. The bore logs can be found in Appendix B.

Number	Name	Depth (metres)
Bore 1	Hurdle	56
Bore 2	Express	63
Bore 3	Elephant	130
PS 4	Big Easy	40

Figure 7.3. Elevations (in metres above sea level) of the aquifers beneath Coronet Peak Skifield. The vertical lines indicate the depth of the borehole (1cm =10m), where the horizontal lines indicate the level at which the aquifer is located. The red dashed line is the approximate depth to the Coronet Peak Landslide interface with in situ bedrock. The Google Earth image indicates the line used to draw the cross-section and the location of the bores. The bore numbers correspond to Table 7.2.

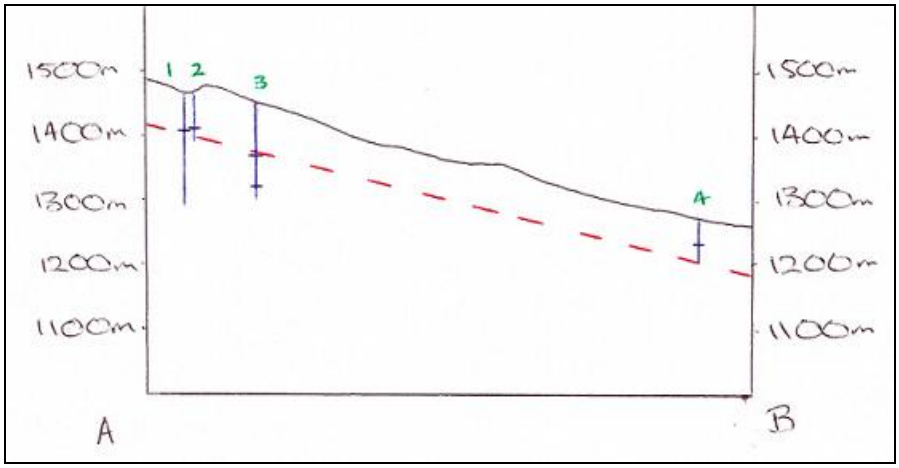

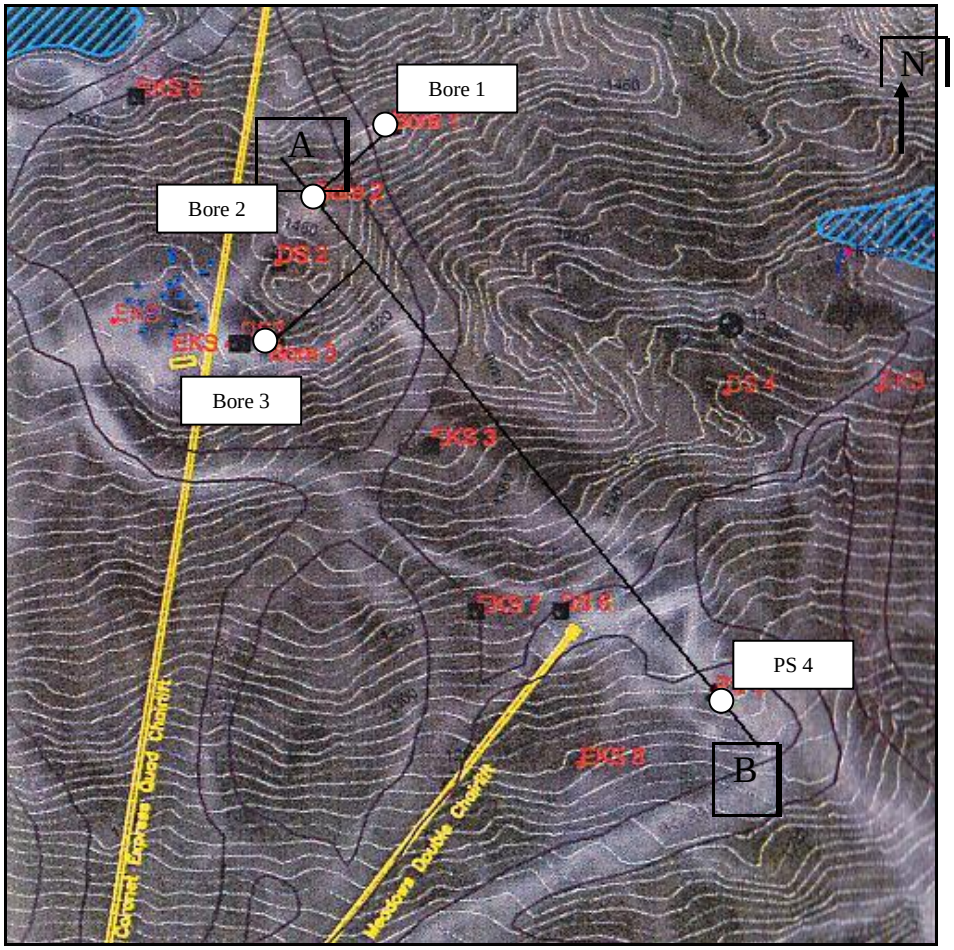

7.4. Influence of precipitation on spring stable isotopic compositions

Current precipitation does not have a large influence on the springs located on the Coronet Peak Skifield and Recreation Reserve as seen by the differences in the stable isotopic contents. Figures 7.4, 7.5 and 7.6 below show the stable isotopic composition of the springs sampled each month, and the precipitation sampled during these periods is also graphed on these figures. In doing so, the impact that current precipitation has on the stable isotopic composition of the springs is identified. The key to these graphs is the same as Figure 7.1 (a).

The spring and precipitation samples collected in July 2009 have been graphed together in Figure 7.4 below. The difference in these two of sample groups can be seen. The precipitation plots very positively in comparison to the spring samples, indicating little to no involvement of the current precipitation affecting the spring compositions. This indicates a residence effect. However, the more negative samples collected from precipitation at Site 3 may have an effect on the springs that exhibit the most positive stable isotope compositions. For example, the green cross represents the Cattlestop spring; this is the most positive spring and plots closer to the precipitation samples than other spring samples. Evaporation may have caused this, however it is unlikely because all the springs samples were filled to the top of their sampling vials to minimise this. It is possible that the sample collected may have been tainted by the precipitation as it fell from above, however this is also unlikely as all samples were collected as close to the springs as possible. Therefore the effect of the precipitation falling from above would be very minimal. The most likely reason for the positivity is that as the precipitation percolates through the surface, it interacts with the groundwater, therefore changing the stable isotopic composition of the spring. Due to the precipitation at this time being more positive than the groundwater, see the groundwater composition collected from the boreholes in Figure 7.4, it may have given rise to the spring stable isotopic composition being more positive. It is also possible that the groundwater in this area is more positive due to the altitude effect on earlier precipitation, giving rise to the positive composition of Cattlestop spring.

Figure 7.4. Spring and precipitation samples from July 2009. The key for this graph is Figure 7.1 (a), and the precipitation samples are navy blue.

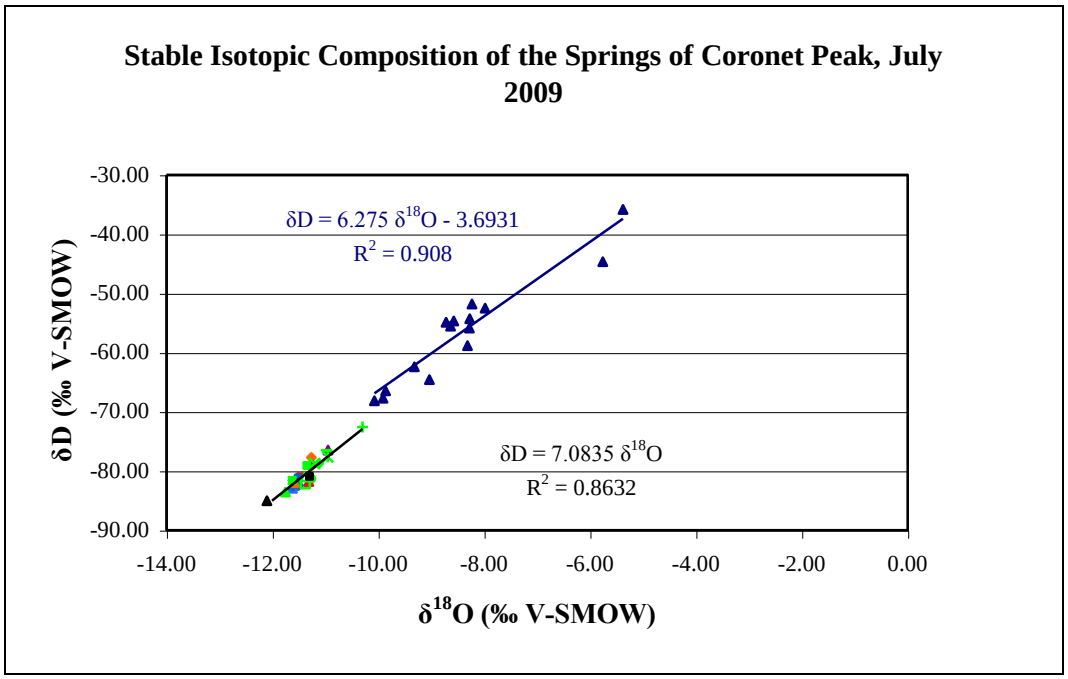

Figure 7.5 graphs both the spring and precipitation samples collected during August 2009 on Coronet Peak. The precipitation during August plots very negatively when compared to the spring samples, with no springs plotting near any of the precipitation values, and this suggests little interaction between the current precipitation and the current spring flows. The exception to this is the Wall St spring; this plots very negatively in the hydrogen and oxygen stable isotopes, having a δD value of –117.55‰ and a $\delta^{18}O$ value of –16.04‰, contrasting with all other spring samples. This is due to the sample collected from this spring being influenced by the negative precipitation (in comparison to the months of July and September) when it was sampled

Figure 7.5. Spring and precipitation samples from August 2009.

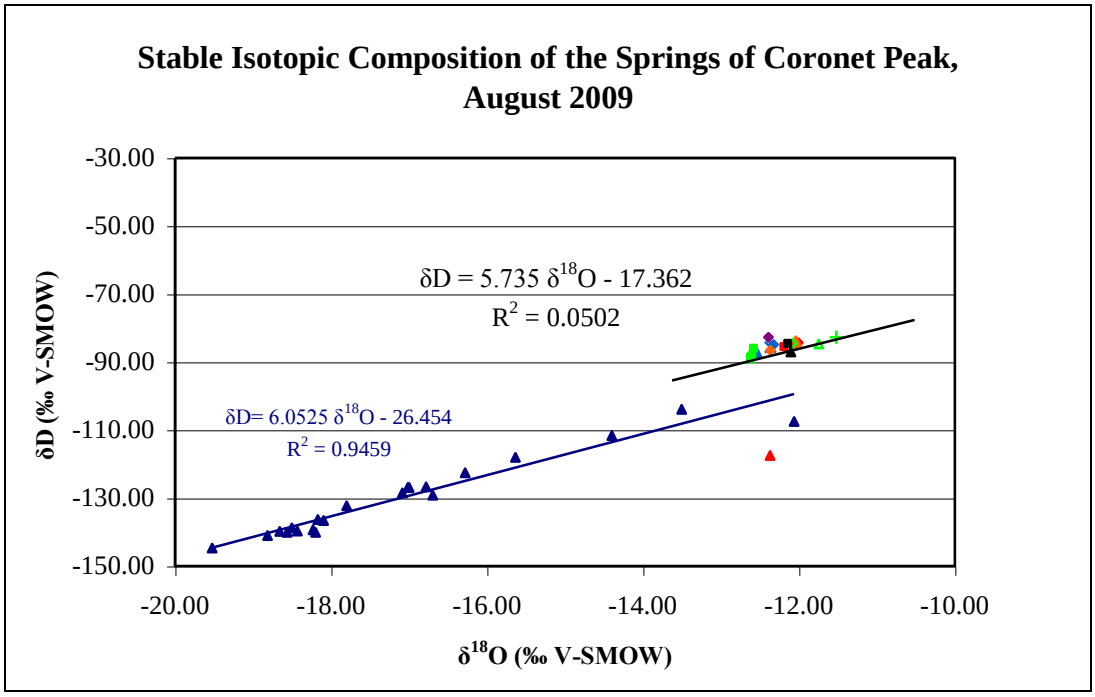

The precipitation and spring stable isotopic compositions sampled during September 2009 are plotted in Figure 7.6. It can be seen from this graph that the precipitation sampled is mostly more positive than the spring samples. The two samples that plot within the spring samples and below were collected from Site 4 (1300 metres above sea level) and Site 5 (1621 metres above sea level) respectively during precipitation event F. From the figure below it would seem that the precipitation sample from Site 4 (F4) has had an influence on the three most positive springs sampled, the Cattlestop, Wired and Swamp springs. However, these three springs are the three that are located at the lowest elevation on the mountain, being 913, 968 and 879 metres above sea level respectively. Therefore the precipitation sampled at Site 4 during precipitation event F would be extremely unlikely to have an affect on these springs because there is an altitude difference of approximately 400 metres, and given the altitude gradient above, there should also be a 1.72‰ decrease in the $\delta^{18}O$ values. It has been proven above that the stable isotopic composition of the springs is a function of the spring's elevation on the mountain, an altitude effect within the springs. Therefore the stable isotopic composition of the current precipitation measured during 2009 vastly contrasts with the spring stable isotopic

contents. The precipitation having minimal affect on the stable isotopic composition of these springs.

Figure 7.6. Spring and precipitation samples from September 2009.

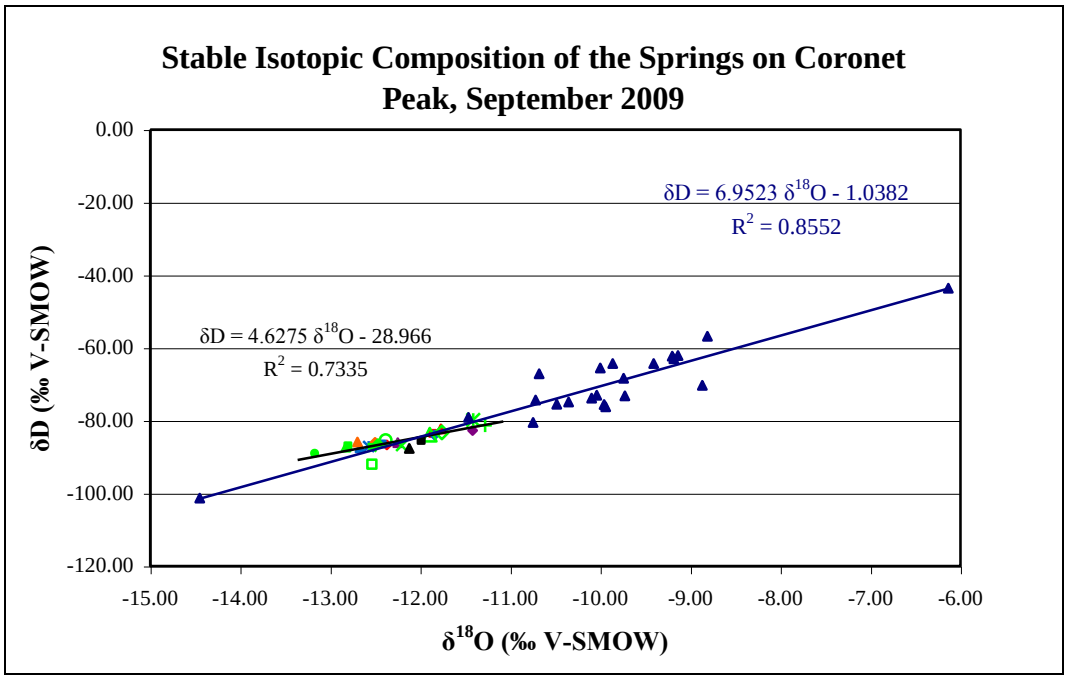

The Cattlestop, Wired and Swamp springs are not affected by the precipitation sampled at Site 4 during event F. Although, it is possible that these springs are affected by precipitation giving their more positive stable isotopic composition when compared to the other springs sampled. The groundwater flowing to these springs may have been influenced by the precipitation percolating through the ground at these spring sites, giving them a more positive composition, the infiltration rate would be very useful here. It is also possible that these springs are the most affected by the current precipitation possibly by the geology surrounding them and by their elevation. The geology within a landslide changes with respect to the distance from the head-scarp, the distance material travels down slope dictates the size of the material. Because these springs are at lower elevations, the schist blocks that comprise the landslide may be smaller than at higher elevations. The smaller debris may allow for easier infiltration of precipitation, and more of an affect on the stable isotopic composition of these springs. The lower elevation of these springs indicates less or no

snow cover on the ground allowing any precipitation that occurs to infiltrate the ground surface easily. This infiltration may not be possible at other spring sites at higher elevations because the ground is covered in a thick snow base, leaving the stable isotopic composition of these springs unaltered and closer to that of the groundwater. It is also possible that the positivity of these springs is due to the altitude effect in previous precipitation, making the groundwater feeding these springs more positive than at higher locations.

7.5. Conclusions

When dividing the springs that are located on the Coronet Peak Skifield and Recreation Reserve into their respective types, the stable isotopic composition of the springs in each type plot similarly, however most springs plot very differently from precipitation. The most varied of these types are the contact springs. However, the spring types do not plot perfectly together and therefore the type of each spring is not the main influence on their stable isotopic compositions. When the spring $\delta^{18}O$ values are plotted against altitude, a trend emerges similar to the altitude effect in precipitation, giving the relationship of 0.43‰ decrease in $\delta^{18}O$ with every 100-metre increase in elevation. Thus indicating that the altitude of the spring is a governing factor in its stable isotopic composition.

The individual stable isotopic trends of the springs indicate that some springs show variation within the groundwater system, whilst others are influenced by precipitation, indicating mixing between current infiltration precipitation and groundwater. Using the average spring and borehole stable isotopic compositions calculated from the samples collected in July, August and September 2009, the likely groundwater source has been indicated for each spring. However, not all springs were fed by the Big Easy and Hurdles bores, some were mixtures between the two, others gave stable isotopic signatures more negative than both. Because there can be no differentiation between the two deeper aquifers, it can only be said that the more negative springs are likely to be fed from either of these sources. Other springs plot more positive than the groundwater, possibly indicating the influence of current precipitation on spring compositions, however these springs are all at lower elevations where the altitude effect may explain this better.

Most of the springs are not influenced by the current precipitation on Coronet Peak. However, the lower springs, namely the Cattlestop spring, are more positive than the other springs. This maybe due to the infiltration of the more positive precipitation during July and September 2009 through the exposed ground surface, the lower the elevation, the less snow cover on the ground. However, during August with very negative precipitation the Cattlestop spring was still very positive, therefore this theory might be incorrect. The more probable theory is that the positive stable isotopic composition is due to the altitude effect in past precipitation, giving rise to the more positive stable isotopic compositions at lower elevations.

The main contributing factor in the stable isotopic composition of the springs located on the Coronet Peak Skifield and Recreation Reserve is the altitude effect in the precipitation falling on the mountain, however in this case not the current precipitation. The groundwater within the aquifers beneath Coronet Peak is not sourced from the present precipitation, as can be seen in the differences between the borehole and precipitation data, and is most likely from precipitation that has occurred in the past, though still modern in general terms but possibly up to five years old, because the stable isotopic compositions are still similar. Hence the recharge mechanisms for the aquifers are complex, and it may take years for the current rainfall to percolate through the ground surface to reach these water bodies. The altitude effect acting on precipitation in the past is the main factor here, whereas the stable isotopic signature of the rain that falls onto the ground surface, (at lower elevations with a more positive stable isotopic content than at higher elevations), is preserved within the ground, as there are no means to modify it, the groundwater then flows to the surface to feed the springs on Coronet Peak giving the stable isotopic composition of past precipitation.

Chapter Eight:

Summary and Conclusions

8.1. Thesis objectives and methodology

The two main objectives of this thesis were to establish the stable isotopic composition and trends of the meteoric water of the Coronet Peak Skifield area during the winter months of July, August and September 2009. And to establish flow rates for the springs on the mountain to determine how much naturally occurring water is available to the Skifield to utilise in artificial snowmaking. This study has led to:

- The creation of the first Local Meteoric Water Line and the first Local Evaporation Line for the area.
- The creation of an Altitude Gradient from the Altitude Effect in precipitation on the mountain.
- The indication of stable isotopic variations in precipitation due to storm duration
- The identification of the variations in stable isotopic composition of precipitation due to storm track trajectory.
- The groundwater sources of the springs in the area being identified.
- The indication of an Altitude Effect among springs.
- An average of 26.5 litres per second of naturally occurring spring water available on the mountain during winter.

Water samples were collected from all water sources in the study area, precipitation, water storage reservoirs, springs and groundwater during the winter of 2009. Spring flow rates were also recorded during both winters of 2008 and 2009. The flow data was examined, whilst the water samples were analysed using a CF-IRMS at the University of Canterbury. The results obtained have led to the conclusions found in this thesis.

8.2 Precipitation

The use of the stable isotopes of hydrogen and oxygen in water to characterise the hydrogeology of the Coronet Peak area has proven valuable. A Local Meteoric Water Line (LMWL) has been constructed for Coronet Peak for the months of July, August and September 2009, combining these results a total LMWL that has a slope of 8 with a y-intercept of 10, this lies exactly on the Global Meteoric Water Line (GMWL). The LMWL indicates that the meteoric water from the Coronet Peak area is average on a global scale. A total Local Evaporation Line (LEL) has also been constructed for Coronet Peak for this time frame, giving a slope of 4 and a y-intercept of –37, indicating that evaporation has had a large impact on the reservoir water samples used to create the LEL. From the information gained from the LEL, it can be seen that the residence times (on a scale of days to months) of the groundwater within the water storage reservoirs is the main factor governing the rate evaporation that occurs from these water bodies.

8.2.1. *Altitude Effects*

The altitude effect on precipitation is shown to occur on Coronet Peak from the precipitation events sampled and analysed. Not all of the events indicated the relationship of the stable isotopic composition of precipitation decreasing with increasing altutde perfectly, however, with more storm events sampled an altitude gradient could be found for the mountain. An altitude gradient has been indicated for precipitation event F, as this event showed the correlation with little variation. The gradient given for this event with every 100-metre increase in altitude is a decrease of 5.19‰ for the hydrogen isotopes whilst the oxygen isotope values decrease by 0.71‰.

8.2.2. *Storm Duration*

The duration of each precipitation event sampled on Coronet Peak has been monitored, with water samples collected at four-hour time intervals during the storm. This data has allowed the variations in the stable isotopic compositions of precipitation to be observed. As the duration of an event continues, the heavy isotopes of both hydrogen and oxygen are ‘rained out’, making the precipitation depleted, as the storm persists, the precipitation becomes more and more depleted. The events sampled on Coronet Peak, show this relationship well, but not perfectly as there are

other factors that impact on the stable isotopic composition of precipitation that have not been monitored, other such factors being the temperature during precipitation and the local wind direction of the storm track from where the precipitation is condensed.

8.2.3. *Storm Trajectories*

The storm trajectories of the precipitation events sampled on Coronet Peak have been found using the HYSPLIT model. With this information enabling the track of the storm to be seen for the time period of 72 hours prior to the storm reaching Coronet Peak, the origins of the air mass can be traced and the stable isotopic compositions of the precipitation that results from that air mass can be analysed. The storm events sampled had varying storm tracks, with five out of the seven arriving at Coronet Peak from a southerly direction. These five had similar stable isotopic compositions due to the Southern Oceans lack of evaporative capacity. The two remaining precipitation events had storm trajectories that originated in the Pacific Ocean, flowing north around the tip of New Zealand and then travelling south down the west coast of New Zealand to arrive at Coronet Peak on a northerly track. These two events had extremely negative stable isotopic compositions when compared to the other events, indicating that these two warmer air masses had picked up evaporated water from the tropical seas north of New Zealand and then as they travelled south precipitation occurred due to the cooling of the air masses, allowing ‘rain out’ to occur and giving rise to their negative compositions. The trajectory of the air mass is an extremely important factor in determining the stable isotopic composition of precipitation on Coronet Peak.

8.2.4. *Key Conclusions*

The stable isotopic composition of precipitation within this study area is extremely variable. The altitude effect, storm duration and storm track trajectories were the three factors examined. From the data obtained, the storm track trajectory has the most influence on the precipitation stable isotopic content in this area.

8.3. Spring investigations

8.3.1. *Spring flows and seasonality*

The flows of the 26 springs located on the Coronet Peak Skifield and Recreation Reserve have been monitored during the winters of 2008 and 2009. The information gathered has given a total of 26.50 litres per second available from the springs that may be used for the purposes of the Skifield during the winter. This data has also allowed the springs with the largest flow rates that are not already utilised by the Skifield to be identified and recommended for further monitoring to discover their base flows during the summer months. If the base flows are satisfactory, they can then be modified to best suit the needs of the Skifield, typically by collection areas for the spring flows and conduits to pump it to the water storage reservoirs to be used in making artificial snow. The springs of interest are the Dirty Four, Dirty Creek, Tussock, Hairpin, Pond and McMullan #2, all indicating flows during the winter months of greater than one litre per second on average.

8.3.2. *Spring Isotope Data*

The water sources of the spring flows on Coronet Peak have been identified using stable isotopic data from springs, groundwater and precipitation. However the extent of each of the aquifers is unknown. Most of the spring stable isotopic compositions correlate well with either the Big Easy or Hurdles bores, some being a mixture of these two groundwater sources, while some may be mixtures between them and precipitation. Some of the springs however plot very negatively compared to all other meteoric water on Coronet Peak and suggest another source. Due to the Hurdles bore sampling groundwater from two of the three aquifers, and these cannot be differentiated, it is possible that these negative springs are fed from one of these two aquifers. The slightly more positive springs may be fed from the other of these deeper aquifers, while the most positive springs being fed from the Big Easy bore which accesses groundwater from an approximate depth of 40 metres.

8.3.3. *Altitude Effect*

The spring samples also show a relationship with altitude, much like the altitude effect in precipitation. The lower altitude springs have a more positive stable isotopic composition than those springs located at higher elevations. This is most

likely due to the altitude effect in the precipitation that has occurred in the past. As precipitation percolates through the ground surface the stable isotopic signature is preserved, as there is no mechanism to change it in this environment. Therefore when the groundwater is released from the aquifers beneath Coronet Peak and flows through the ground to the surface where it appears as springs, the stable isotopic composition of those springs is the same as the precipitation that was precipitated in the past and that has been stored in the groundwater system for a period of time.

8.3.4. *Key conclusions*

The stable isotopic composition of the springs in this study area vary due to their source, whether it be sourced from groundwater or is influenced by precipitation. The groundwater source of the springs is not current precipitation, however, the current precipitation does influence some springs as it infiltrates through the ground and mixes with the groundwater.

8.4. Groundwater and reservoir waters

8.4.1. *Hydrogeological data sources*

The source of the data used to obtain information of the hydrogeological nature of the field area were bore logs that were completed during a drilling program that ended in 2008. The logs are brief, but do provide some information as to the depth to water bearing rock. It is from this data that the three aquifers have been inferred.

8.4.2. *Isotopic variations in groundwater*

The groundwater within the study area varies considerably in its stable isotopic content. The water samples collected from the two pumping bores give different isotopic signatures, indicating different groundwater sources. However, the Hurdles Bores, accesses water from two depths within the ground that could not be differentiated. The isotopic content of these water samples reflect the isotopic composition of two aquifers.

8.4.3. *Reservoir waters*

The five water storage reservoirs on the mountain are filled by groundwater accessed by the two pumping bores, however precipitation also has an impact on the stable isotopic composition as it falls onto the reservoirs. The main influence on the variations within the isotopic contents of the reservoirs is evaporation. Evaporation causes the stable isotopic content to become more positive than the groundwater source.

8.4.4. *Key Conclusions*

The hydrogeological data available has led to three aquifers being identified within the study area. The groundwater is not sourced from the current precipitation, but from older precipitation. The aquifers are accessed by two pumping bores, which are used to fill the water storage reservoirs on the mountain. The stable isotopic composition of the reservoirs is more positive than the groundwater due to the effects of evaporation.

8.5. Further work

Further research into the stable isotopes in the meteoric waters of the Coronet Peak area is needed to reaffirm these conclusions and to give them more confidence. With continued research, a yearlong Local Meteoric Water Line can be composed, as well as a yearlong Local Evaporation Line. With more precipitation events sampled, the altitude effect on Coronet Peak can be further understood and a higher precision given to the altitude gradient proposed in this thesis. Moreover, a larger number of precipitation events sampled would better define the variations in stable isotopes of precipitation with storm duration and storm track trajectories. Whilst for the data of both storm duration and storm track trajectories would be better understood with further information about temperature, local wind directions and possibly the amount of precipitation that has occurred. Furthermore, a longer monitoring period for the springs of the Coronet Peak area is needed, for both flow rates and water samples. This would give both a detailed flow rate for each spring, particular those that are of possible use to the Skifield, and flow rates could also be correlated to the pumping data from the Big Easy and Hurdles bores to determine whether pumping has an effect on the flow rates of the springs associated with each bore, and if it does, what is the acceptable level of pumping and what is the minimum level of spring flow that will

not adversely affect the environment further down-slope. Long-term spring sampling would also add to the stable isotopic analysis of the origins of the springs, identifying groundwater flow paths with certainty. This would be helped by the separation of the two deeper aquifers from the collection tank of the Hurdles bore, allowing them to be monitored individually, and determining which of the negative stable isotopic composed springs are associated with which of these aquifers. Also, the geophysical techniques of resistivity and seismicity can be employed to understand the extent of the groundwater sources and subsurface modelling. In applying these recommendations, the hydrogeology of the Coronet Peak area would be understood to a higher degree, allowing the utilisation of the water resources of the area to be better managed, as this is an integral part to the running of the Coronet Peak Skifield.

References:

Aggarwal, P.K. et al. (2005) "Isotopes in the Water Cycle: Past, Present and Future of a Developing Science", Springer, Dordrecht, The Netherlands.

Araguas-Araguas, L. et al. (2000) "Deuterium and Oxygen-18 Composition of Precipitation and Atmospheric Moisture", in Hydrological Processes, Vol14: 1341-1355.

Barrens, E. and Cook, D. (2006) "Water Vapour and Temperature" Online Posting, Newton BBS Ask a Scientist, Date Accessed 14/09/2009 from http://www.newton.dep.anl.gov/askasci/wea00/wea00016.htm.

Berner, EK and Berner, RA. (1987) "The Global Water Cycle: Geochemistry and Environment", Prentice-Hall, New Jersey, USA.

Brenstrum, E. (1998). "The New Zealand Weather Book", Craig Potton Publishing, New Zealand.

Bryan, K. (1919) "Classification of Springs", in The Journal of Geology, Volume XXVII, The University of Chicago Press, Chicago, Illinois. P 522-561.

Buchachenko, A.L. (2001). "Magnetic Isotope effect: Nuclear Spin Control of Chemical Reactions" in The Journal of Physical Chemistry, Vol105: 9995-10011.

Campbell, H., Hutching, G. (Editors) (2007) "In Search of Ancient New Zealand", 1st Edition, Penguin Group, North Shore, New Zealand.

Coates, G. (2002) "The Rise and Fall of the Southern Alps", Canterbury University Press, New Zealand.

Craig, H. (1961) "Isotopic Variations in Meteoric Waters", Science, Vol133: 1702-1703.

Craw, D. (1984) "Lithogic Variations in the Otago Schist, Mt Aspiring area, NW Otago, New Zealand" in New Zealand Journal of Geology and Geophysics, Vol27: 151-166.

Dansgaard, W. (1961) "The Isotopic Composition of Natural Waters", Bianco Lunos Bogtrykkeri A/S, Copenhagen.

De Hoffman, E. and Stroobant, V. (2002) "Mass Spectrometry: Principles and Applications", 2nd Edition, John Wiley and Sons Inc., England. P1-10

Epstein, S. and Mayeda, T. (1953) "Variation of O^{18} Content from Natural Waters", Geochemica et Cosmochimca Acta, Vol4: 213-224.

Faure, G. (1986) "Principles of Isotope Geology", 2nd Edition, John Wiley and Sons Inc., U.S.A. *1*: 1-10, *5*: 56-65, *24*: 429-459.

Faure, G., Mensing, TS. (2005) "Isotopes: Principles and Applications", 3rd Edition, John Wiley and Sons Inc., U.S.A. *26*: 693-745, *29*: 846-847.

Fetter, CW. (1994) " Applied Hydrogeology", Third Edition, Prentice-Hall Inc. USA.

Friedman, I. (1953) "Deuterium Content of Natural Waters and Other Substances", Geochemica et Cosmochimica Acta, Vol4: 89-103.

Google (2009) "Google Maps - Queenstown", map retrieved on 26/08/2009 from http://www.queenstown-nz.co.nz/information/maps-queenstown/.

Google Earth (2009)

Graham, I.J. (Editor) (2008) "A Continent on the Move", Geological Society of New Zealand in association with GNS Science, Wellington, New Zealand.

Griffiths, H. (Editor) (1998) "Stable Isotopes: Integration of Biological, Ecological and Geochemical Processes". BIOS Scientific Publishers Ltd., U.K. *23*: 397-405.

Heidenreich III, JE. and Thiemens, MH. (1986) "A non-mass-dependent oxygen isotope effect in the production of ozone from molecular oxygen: The role of molecular symmetry in isotope chemistry" in Journal of Chemistry and Physics, Vol 84: 2129-2136.

Hiscock, K. (2005) "Hydrogeology: Principles and Practice", Blackwell Science Ltd., U.K.

Hoefs, J. (2004) "Stable Isotope Geochemistry", 5rd Edition Springer-Verlag, Germany. *1*: 1-29, *3*: 150-153.

IAEA, (2002) "Managing Water Resources using Isotope Hydrology", International Atomic Energy Agency Information Series, retrieved on 01/11/2009 from http://www.iaea.org/Publications/Factsheets/English/water.pdf.

Iqbal, MZ. (2008) "Short-term Variability in Isotopic Composition of Precipitation: A Case Study from the Midwestern United States", Hydrological Processes Vol22: 4609-4619.

Ira, D. et al, (2000) "Groundwater Flow and Contaminant Transport in Carbonate Aquifers", Taylor and Francis Publishers, U.S.A., P 33.

Jager, E. and Hunziker, JC. (1979) Editors, "Stable Hydrogen and Oxygen Isotopes in the Water Cycle" from Lectures in Isotope Geology, Springer-Verlag, Germany. *22*: 264-273.

Kendall, C. and McDonnell, J.J. (1998) Editors, "Isotope Tracers in Catchment Geology", Elsevier Sciences B.V. Amsterdam.

Kenny, DA. (1979) "Correlation and Causation", John Wiley and Sons, Ltd. U.S.A.

Lemke, KA. (2009) "Introduction to the Hydrologic Cycle", www.uwsp.edu/geo/faculty/lemke/geog101/lecture_outlines/07_hydrologic_cycle_intro.html, accessed on 16/10/2009.

McMaster, M., McMaster, C. (2008) "GC/MS: a Practical Users Guide", 2nd Edition, John Wiley and Sons Inc. Publications, U.S.A. P ?.

Marshall, J. and Plumb, RA. (2008) "Atmospheric, Ocean and Climate Dynamics: An Introductory Text", Elsevier Academic Press, USA.

Meinzer, O.E. (1942) Editor, "Hydrology", Dover Publications Inc, New York.

Michener R. and Lajtha K. (2007) Editors, "Stable Isotopes in Ecology and Environmental Science" Second Edition, Blackwell Publishing, United Kingdom. *1*: 1-18

NASA (2006) "Satellite Image of the South Island New Zealand" retrieved on 27/05/2009 from http://en.wikipedia.org/File:Satellite_image_of_South_Island_New_Zealand.jpg.

NASA (2007) "South Island 07/12/2007" taken from the Aqua Satellite, image retrieved on the 26/08/2009 from http://en.wikipedia.org/File:South_Island_2007-12-07.jpg.

NASA (a) (2008) "Overview: Climate – Movement of the Earth through Space", http://sealevel.jpl.nasa.gov/overview/climate-earth.html, accessed on 06/10/2009.

NASA (b) (2008) "Overview: Climate – The Spherical Shape of the Earth: Climatic Zones", http://sealevel.jpl.nasa.gov/overview/climate-climatic.html, accessed on 06/10/2009.

National Park Service (1996) "Cave/Karst Topography", retrieved on the 21/12/2009 from www.gps.gov/maca/naturescience/cave.htm.

Neilson, DM., Neilson, GL. (2007) "The Essential Handbook of Ground-Water Sampling", CRC Press (Taylor and Francis Group), U.S.A. *6*: 160-162.

New Zealand Meteorological Service, (1983) "The Climatology of Queenstown Airport", Government Printer, Wellington, New Zealand.

Nijichoua, R. et al. (1999). "*Variations of the stable isotopic compositions of rainfall events from the Cameroon rain forest, Central Africa*", Journal of Hydrology, Vol 223: 17-26.

NIWA, (2009) "Cliflow", data retrieved on during the months of July through to November 2009 from http://cliflo.niwa.co.nz.

NZSki, (2009) "Queenstown Resort Guide 2009", printed by? New Zealand.

Pionke, HB. And DeWalle, DR. (1992) "Intra- and inter-storm ^{18}O trends for selected rainstorms in Pennsylvania", Journal of Hydrology, Vol 138: 131-143.

Price, M. (1996) "Introducing Groundwater", 2nd Edition, Chapman and Hall, London. *7*: 70-83, *10*: 144-171.

Salkind, NJ. (2007) "Statistics for People who (think they) Hate Statistics", Excel Edition, Sage Publications, U.S.A.

Sharp, Z. (2007) "Principles of Stable Isotope Geochemistry" Pearson Education, Inc. U.S.A. *1*: 1-12 *2*: 15-36, *4*: 64-93.

Shaw, E. (1994) "Hydrology in Practice", 3rd Edition, Chapman and Hall, London, P 121-130.

Sturman, A. and Tapper, N. (1996) "The Weather and Climate of Australia and New Zealand", Oxford University Press, Australia.

Suggate, RP. (1990) "Late Pliocene and Quaternary Glaciations of New Zealand" in Quaternary Science Reviews, Vol 9: 175-197.

Todd, DK., Mays, LW. (2005) "Groundwater Hydrology" 3rd Edition, John Wiley and Sons Ltd. U.S.A. P 67-77.

Thomson, R. (2007) unpublished. Description of core logs of Coronet Peak done in 07 and 08 for NZ Ski Ltd.

Turnbull, IM. (Compiler) (2000) "Geology of the Wakatipu Area" Graphic Press and Packaging Ltd., Levin, New Zealand.

Wood, BL (1978) "The Otago Schist Megaculmination: Its Possible Origins and Tectonic Significance in the Rangitata Orogent of New Zealand" in Tectonophysics, Vol 47:339-368

Willetts, AJ. (2000) "The Geology and the Geomorphology of the Coronet Peak and Arthurs Point Landslide Complexes". Thesis. P 91-116.

Whiteman, CD. (2000) "Mountain Meteorology: Fundamentals and Applications", Oxford University Press, New York, USA.

Appendices

Appendix A:

Stable Isotope Introduction

A.1. Introduction to Stable Isotopes.

The study of isotopes is based on the tendency of certain elements to separate into light and heavy fractions. The separation of isotopes into relatively heavier and lighter fractions is called mass dependent fractionation (Hiscock, 2005). The discovery of isotopes occurred in the late nineteenth and early twentieth centuries; the breakthrough of the detection of radioactivity in 1896 by Henri Becquerel, (for which he shared in the Nobel Prize for physics in 1903), was the catalyst for further research into the areas of atomic and nuclear physics and radiochemistry (Faure, 1986). It was Sir Ernest Rutherford who first successfully 'split the atom' in 1919, where he discovered the structure of the atom; positively charged particles (protons) within the nucleus with negatively charged particles (electrons) orbiting around it, he also speculated that within the nucleus a neutral particle may also exist. It was not until 1932 that Sir Rutherford coined the term neutron and the structural components of the atom were completed; see Figure A.1 below for the components of deuterium (Faure, 1986). The Noble Prize for Chemistry in 1934 was won by H.C. Urey, who is considered "the father of modern stable isotope geochemistry" due to his discovery of 'heavy hydrogen', known as deuterium (Sharp, 2007,p1).

Figure A.1: The basic atomic structure of deuterium (^{2}H), where the black circle indicates the neutron, the white circle with a cross indicates the proton and the white circle shows the electron with a horizontal line through it.

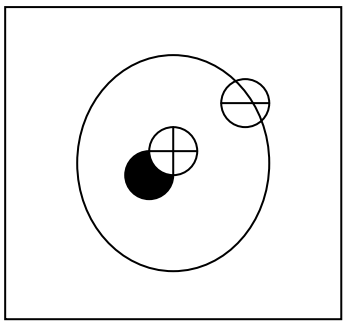

Hydrogen	
Atomic Number	1
Neutron Number	1
Atomic Mass	2

Every atom contains a specific number of protons, electrons and neutrons. The number of protons, positively charged particles, and the number of electrons, negatively charged particles are equal, however, the number of neutrons (no charge/ neutral) can differ. It is these atoms with differing neutron numbers that are known as isotopes (Sharp, 2007). The term 'isotope' comes from Greek and means equal places,

indicating that the isotopes of a specific element occupy the same position in the periodic table, the number of protons remains the same (Hoefs, 2004). Elements are denoted by the number of protons (Z) which is also known as the atomic number, and by the mass number A (where A = Z + N), this can be found by adding the number of protons and the number of neutrons (N) together, A is also be known as the atomic mass. Differing isotopes of the same element have the same atomic number but a varied mass number due to an element being capable of being comprised of differing numbers of neutrons within its nucleus. For example, the element of oxygen has an atomic number of 8 (Z), however oxygen has three naturally occurring isotopes, ^{16}O, ^{17}O and ^{18}O. Where ^{16}O has 8 protons (Z) and 8 neutrons (N), ^{17}O has 8 protons and 9 neutrons, and ^{18}O has 8 protons and 10 neutrons, see Table A.1 below (Sharp, 2007).

Table A.1: The breakdown of the components of the different stable isotopes of oxygen, with the abundances of each isotope in atom percent (Sharp, 2007).

Isotope	Atomic Number (Z)	Neutron Number (N)	Atomic Mass (A)	Abundances
^{16}O	8	8	16	99.7621
^{17}O	8	9	17	0.03790
^{18}O	8	10	18	0.20004

There are two isotopic species in nature; isotopes are characterised into either stable or unstable isotopes. Stable isotopes are defined as isotopes that do not decay and are energetically stable; therefore they are not unpredictable and "do not undergo spontaneous breakdown of their nuclei to form other isotopes," they are not radioactive (Eby, 2004, p165). Unstable isotopes decay and tend to be grouped by their half-lives; because they decay these isotopes are radioactive in nature (Eby, 2004). Typically an isotope will be stable when the Z-value (number of protons) and the N-value (number of neutrons) are similar, normally with a ratio of $Z/N \leq 1.5$ (Michener and Lajtha, 2007). There are over 1500 naturally occurring isotopes, and over 1200 of these are radioactive. The other 300 or so are stable isotopes and of these 21 are monoisotopic. Monoisotopic indicates there is only one stable isotope for that element; the most common of these are phosphorus ($^{31}_{15}P$), aluminium ($^{27}_{13}A$),

sodium ($^{23}_{11}$Na) and fluorine ($^{19}_{9}$F). Of the approximate 300 stable isotopes 6 elements are used for the by far majority of stable isotope applications, they are hydrogen ($_{1}$H), carbon ($_{6}$C), nitrogen ($_{7}$N), oxygen ($_{8}$O), sulphur ($_{16}$S) and chlorine ($_{17}$Cl), this is because they are the most common stable isotopes that occur in nature and are typically known as the traditional light elements. The table below shows a part of the periodic table for both stable and radioactive isotopes for the first ten elements (Michener and Lajtha, 2007).

Table A.2: Isotope table for the first ten elements in the periodic table, (adapted from Michener and Lajtha, 2007).

Z→	0	1	2							
N↓	n	H	He	3	4					
0		^{1}H	^{2}He	Li	Be	5	6			
1	^{1}n	^{2}H	^{3}He	^{4}Li	^{5}Be	B	C	7		
2	^{2}n	^{3}H	^{4}He	^{5}Li	^{6}Be	^{7}B	^{8}C	N	8	
3		^{4}H	^{5}He	^{6}Li	^{7}Be	^{8}B	^{9}C	^{10}N	O	9
4	^{4}n	^{5}H	^{6}He	^{7}Li	^{8}Be	^{9}B	^{10}C	^{11}N	^{12}O	F
5		^{6}H	^{7}He	^{8}Li	^{9}Be	^{10}B	^{11}C	^{12}N	^{13}O	^{14}F
6		^{7}H	^{8}He	9Li	^{10}Be	^{11}B	^{12}C	^{13}N	^{14}O	^{15}F
		7	^{9}He	^{10}Li	^{11}Be	^{12}B	^{13}C	^{14}N	^{15}O	^{16}F
		8	^{10}He	^{11}Li	^{12}Be	^{13}B	^{14}C	^{15}N	^{16}O	^{17}F
			9	^{12}Li	^{13}Be	^{14}B	^{15}C	^{16}N	^{17}O	^{18}F
				10	^{14}Be	^{15}B	^{16}C	^{17}N	^{18}O	^{19}F
					11	^{16}B	^{17}C	^{18}N	^{19}O	^{20}F
						12	^{18}C	^{19}N	^{20}O	^{21}F
							13	^{20}N	^{21}O	^{22}F
								14	^{22}O	^{23}F
									15	^{24}F
										16
										17

Radioactive Half Lives	
	<1 day
	1-10 days
	10-100 days
	100d-10 years
	10-10,000 years
	10k-103m years
	>700million years
	Stable

The varying number of neutrons within an element has no effect on the gross chemical properties of the element or its compounds, the electrons in the atom tend to control the chemical reactions it undergoes and these do not change in number (Michener and Lajtha, 2007). However, within compounds that contain elements that have varying neutron numbers there are subtle changes in the elements

physicochemical properties. It is these small disparities that are the backbone of the study of stable isotopes (Sharp, 2007).

The atomic mass of an atom determines the vibrational energy of the nucleus; the vibrational frequency is defined as being inversely proportionate to the atomic mass of the isotope/atom and therefore the lighter the isotope (having less neutrons), the greater the vibrational energy is. Consequently, the differences found in the reaction rate and bond strength of the nucleus are due to variations in the neutron number and hence the atomic mass. The greatest differences in reaction rates and bond strength between isotopes within the traditional light elements can be seen where the percent change in mass is the greatest. The table below shows the relative mass difference in percent between two isotopes of hydrogen and two isotopes of sulphur, due to the large mass change between ^{2}H (deuterium, D) and ^{1}H relative to the mass change between ^{33}S and ^{32}S, the behavioural difference between these two hydrogen isotopes will be much greater than the behavioural differences during fractionation between the sulphur isotopes. The isotopes are referenced against ^{12}C (Carbon) having an exact relative atomic mass of 12 (Michener and Lajtha, 2007). Changes in physical behaviour of the two isotopes are due to differences in the mass of the individual isotope.

Table A.3: The relative mass difference of the hydrogen isotopes ^{1}H and ^{2}H (deuterium) and the sulphur isotopes of ^{32}S and ^{34}S.

Element	**Isotope**	**Atomic Weight ($^{12}C = 12.$)**	**Relative Mass Difference (%)**
Hydrogen	^{1}H	1.007825	100
Deuterium	^{2}H	2.0140	
Sulphur	^{32}S	31.97207	3
Sulphur	^{33}S	32.97146	

Therefore isotopes within the same environment will have the same kinetic energy; hence an isotope of larger mass will travel at a slower velocity than a lighter isotope (Michener and Lajtha, 2007). Also heavy isotopes and isotopologues (molecules) vibrate more slowly than lighter ones, and so the vibrational energy of the

heavy isotopes is lower, due to this lower vibrational energy heavy isotopes create more stable, stronger bonds. This is due to quantum mechanical effects, where a molecule's energy is restricted to certain discrete energy levels according to quantum theory known as zero-point energy (Hoefs, 2004). Where a molecule even in it's ground state (where all its electrons occupy the lowest possible energy levels in the atom before occupying any higher energy orbits) at a temperature of absolute zero still has vibrational energy. This vibrational energy of a molecule in its ground state is the zero-point energy (Hoefs, 2004).

Vibrational frequency is determined by the mass of the isotopes; therefore molecules of the same chemical formula but with different isotopic species will have different zero-point energies (Hoefs, 2004). Heavy isotopes will have lower zero-point energies because of their lower vibrational frequency and lighter isotopes have higher zero-point energies due to their higher vibrational frequency (velocity) and so will react slightly faster than heavier isotopes.

It is the differences in velocity and bond strength among isotopes and isotopologues that lead to fractionation. For example, the vapour pressure of $^{2}H_2O$ is nearly 40torr (5.333 kilopascals) lower than the vapour pressure of $^{1}H_2O$, this is due to vapour pressure being inversely proportional to intermolecular forces and the bonds between ^{2}H - O are much stronger than ^{1}H – O bonds. Therefore, evaporation will lead to observable fractionation, resulting in relatively light (^{1}H rich, ^{2}H depleted) vapour and relatively heavy (^{2}H rich and ^{1}H depleted) water left behind (Lajtha and Michener, 2007). The table below from Hoefs, 2004 displays the differences in characteristic physical properties of some isotopologues of water.

Table A.4: Characteristic physical properties of $H_2{}^{16}O$, $D_2{}^{16}O$ and $H_2{}^{18}O$. Where Torr is a measure of Pascals. Adapted from Hoefs, 2004.

Property	**$H_2{}^{16}O$**	**$D_2{}^{16}O$**	**$H_2{}^{18}O$**
Density (20 °C, in g cm^{-3})	0.997	1.1051	1.1106
Vapour Pressure (at 100 °C, in Torr)	760.00	721.60	-
Boiling Point (in °C)	100.00	101.42	100.14
Melting Point (760 Torr, in °C	0.00	3.81	0.28

A.2. Stable Isotope Fractionation

"Fractionation is the partitioning of isotopes during physical, chemical and biological processes" (Eby, 2004, P182). The amount of isotopic fractionation in an exchange reaction can be expressed as a fractionation factor (α). The fractionation factor is a ratio of the heavy to light isotopes of one molecular phase (liquid, solid or vapour) compared to the same heavy and light isotopes in another phase (Araguas-Araguas et al, 2000).
So that:

$$\alpha = R_L/R_V > 1 \qquad \text{Eq. A.1}$$

The fractionation factor is temperature dependent as shown in Table A.5 below for both deuterium and oxygen-18 isotopes with the fractionation factor for hydrogen (ε_D), oxygen (ε_{18}) and the total fractionation factor ($\varepsilon_D/\varepsilon_{18}$).

Table A.5: Temperature dependence of the equilibrium isotope fractionation $\varepsilon = \alpha_e - 1$ for both deuterium and oxygen-18 (Araguas-Araguas et al, 2000).

Equilibrium isotope fractionation (‰)	Temperature (ºCelcius)						
	-10	0	5	10	15	20	25
$\varepsilon_D = (\alpha_e - 1) \times 10^3$ ($^1H^2HO$)	129.6	112.6	104.9	97.9	91.3	85.2	79.5
$\varepsilon_{18} = (\alpha_e - 1) \times 10^3$ ($H_2{}^{18}O$)	12.9	11.7	11.2	10.7	10.3	9.8	9.4
$\varepsilon_D / \varepsilon_{18}$	10.0	9.6	9.4	9.1	8.9	8.7	8.5

When α is equal to one, there is no fractionation because the isotopes are distributed evenly between both phases. If α is above one then there is a concentration of the heavy isotope in the first phase (reactant), and if α is less than one, the heavy isotope is depleted in the second phase (product). The example of liquid water and water vapour below shows this effectively.

$$\alpha = \frac{(O^{18}/O^{16})\ \text{liquid}}{(O^{18}/O^{16})\ \text{vapour}} = 1.0098 \qquad \text{Eq. A.2}$$

The above fractionation factor of 1.0098 accounts for the concentration of heavy oxygen isotopes in liquid water relative to water vapour (Michener and Lajtha, 2007). The fractionation factor is only written such that one atom is exchanged, otherwise the equilibrium constant (K) would need to be taken into account. The equilibrium constant when only one atom is exchanged is the same as the fractionation factor and so can be discounted (Hoefs, 2004).

There are two main mechanisms for fractionation in isotopes, kinetic and equilibrium isotope effects, both with the determining factor being the mass of the isotope controlling fractionation (Araguas-Araguas et al, 2000). There are other less common fractionation processes known as mass-independent fractionation effects that have only been observed in a small number of specific isotopes and are briefly explained below.

A.2.1. *Kinetic Fractionation:*

Kinetic isotope effects are normally associated with fast, incomplete or unidirectional processes such as evaporation, diffusion, dissociation reactions and most biological reactions, all of which are irreversible. The reverse reaction is inhibited in some way, for example, evaporation in an open system; as water evaporates to form water vapour, the vapour moves away from the water source and so cannot be condensed back into the water state (Michener and Lajtha, 2007). During diffusion and evaporation the isotope effects are due to the different translational velocities possessed by the different isotopic forms of the molecules (isotopologues) as they move through a phase or across a phase boundary, for example liquid, vapour or solid. Dissociation in isotopologues is where molecules separate or split into smaller molecules or ions, this is due to the lighter isotopes being less stable and so their bonds break easier compared to heavier isotopes that have higher dissociation energies. For example, it is easier to break the bonds between $^{12}C - H$ and $^{32}S - O$ than between $^{13}C - H$ and $^{34}S - O$ (Sharp, 2007). Simply, kinetic isotope effects arise from different isotopes of the same element possessing varying reaction rates that are dependent on the isotopes atomic mass. During this type of reaction there has always been observed a preferential enrichment of the lighter isotope over the heavy isotope in the products of the reaction, otherwise known as the reactants (Hoefs, 2004).

Specifically related to the molecules of water, all kinetic fractionations occur at the water-air interface (evaporation). This is partly due to molecular diffusion in air

of the isotopically different water molecules and also to the humidity above the water surface (Araguas-Araguas et al, 2000).

A.2.2. *Equilibrium Fractionation:*

Equilibrium isotope effects, isotope exchange or thermodynamic reactions are processes in which the distribution of isotopes changes between different chemical substances, between different phases, or between individual molecules when there is no net reaction (Hoefs, 2004). During this reaction isotopes are exchanged and it is the difference in the masses of the exchanged isotopes that creates this type of fractionation because when a heavy isotope is exchanged in place of a lighter isotope the vibrational energy of the molecule is reduced, therefore when a light isotope is exchanged in place of a heavy isotope the vibrational energy is increased.

The reactants and products remain the same in equilibrium isotope reactions, except they have different final masses from their initial masses. This is due to some isotopes forming stronger bonds than others; the difference in the initial and final masses in equilibrium isotope reactions is temperature dependent. Generally, the heavier isotopes tend to accumulate in the denser phase, the compound that has the largest molecular mass, and/or the phase with the highest oxidation state because here the bonds are strongest (Michener and Lajtha, 2007). In Equilibrium reactions, back-reactions can occur. This can be shown in a closed system (see Figure A.2 below) of water and air, where because of evaporation some water particles will move from the surface of the water and evaporate to form water vapour. These vapour particles then move around in the air and come into contact with the sides of the box seen below and they also come into contact with the water's surface again, reforming as water particles through the process of condensation, a back- reaction (Michener and Lajtha, 2007).

Figure A.2: Equilibrium isotope fractionation back-reactions in a closed system. The blue and orange circles represent water molecules and water vapour respectively, with the blue arrows leaving the water surface and the orange arrows entering the water surface indicating evaporation and condensation respectively. The black arrows indicate random movement of the water and vapour particles.

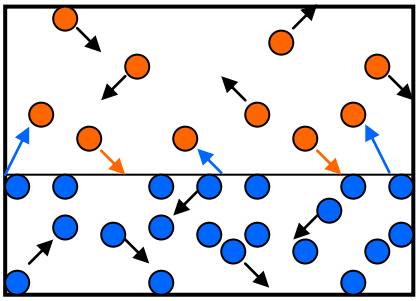

A.2.3. *Mass- independent Isotope Fractionation:*

Mass-independent fractionations are rare in nature or are only just newly discovered (magnetic isotope effect) and can be varied. Traditional non-mass dependent isotope fractionation has been observed in the following atmospheric isotopologues: O_3 (ozone), CO_2 (carbon dioxide), N_2O (nitrous oxide) and CO (carbon monoxide) (Hoefs, 2004). This is an unusual form of fractionation and as yet the mechanisms for this process are not wholly understood. Laboratory experiments run by M. S. Thiemens and J. E. Heidenreich in 1986 first demonstrated mass-independent fractionation in stratospheric ozone (O_3) (Heidenreich III and Thiemens, 1986) 2004). Instead of being attributed to fractionation where mass is the main factor (kinetic and equilibrium isotope fractionation); the isotope fractionation of oxygen (O) during the formation of ozone (O_3) is accredited to "differences in the symmetry of O_2 molecules rather than the differences in the masses of the stable oxygen isotopes" where atomic symmetry refers to the arrangement of the neutrons within the nucleus (Faure and Mensing, 2005, P 846).

A.2.4. *Magnetic Fractionation:*

However, there is another new form of mass-independent isotope fractionation called the magnetic isotope effect. This fractionation occurs due to differences in the nuclear structure among isotopes that leads to preferential reactions depending on

their nuclear spin. Nuclear spin refers to the intrinsic quantum property of spin, where particles rotate on their own axis. Magnetic isotope effect 'monitors the behaviour of angular momentum (spin) of electrons and nuclei in chemical reactions' (Buchachenko, 2001, p9995). This effect is a kinetic process where the dependence of the reaction rate is not determined by chemistry or mass but is determined by physical force of nuclear spin and magnetic forces of atomic particles (Buchachenko, 2001).

A.3. International Reference Standards

The observed isotopic differences in elements due to fractionation via mass-dependent mechanisms (kinetic isotope and equilibrium isotope effects), and non-mass-dependent fractionation methods (both traditional and magnetic isotope effects) between various isotopologues are very small. Therefore the isotopic composition of a molecule is reported relative to an internationally accepted standard. The international reference standards are only available in small quantities; they are not intended for use as 'working' standards. Therefore they are utilised as a reference for workers to establish their own larger supply of secondary reference materials that are a replica of the internationally accepted standard, but that can be used on a daily basis (Sharp, 2007). For example, nitrogen isotopes are compared to Atmospheric Nitrogen (air); carbon is compared to the Vienna Pee Dee Belemnite (VPDB); sulphur is compared to the Vienna Cañon Diablo meteorite troillite (VCDT) whilst hydrogen and oxygen are both compared to the Vienna Standard Mean Ocean Water (VSMOW). V-SMOW is the standard for both hydrogen and oxygen because there are little variations in oceanic isotopic compositions and ocean water constitutes approximately 97% of all water in the hydrosphere, making it the best comparative tool for the constituents of water (Sharp, 2007).

Stable isotope data is expressed as a ratio known as the delta value (lower case, δ), so that small differences can be easily determined (Fetter, 1994).

$$\delta = \frac{R_x - R_{std}}{R_{std}} \cdot 1000 \qquad \text{Eq. A.3}$$

Where R = the ratio of the abundance of the heavy to the light isotope.

$_x$ = denotes the sample.

$_{std}$ = denotes the standard.

For the elements known as the 'light' elements, hydrogen, carbon, nitrogen, oxygen, sulphur and chlorine, the two isotopes used to give 'R' are listed in Table A.6 below. It must also be noted that for hydrogen, the ratio used is D/H, the 'D' is for deuterium, which is another name for ^{2}H, most professionals within the industry prefer using D/H over $^{2}H/^{1}H$ (Sharp, 2007).

Table A.6: Isotopes used when calculating the ratio of heavy to the light isotope in Equation A.5.

R	Element
D/H	Hydrogen
$^{13}C/^{12}C$	Carbon
$^{15}N/^{14}N$	Nitrogen
$^{18}O/^{16}O$	Oxygen
$^{34}S/^{32}S$	Sulphur
$^{37}Cl/^{36}Cl$	Chlorine

The delta values (δ) are presented as parts per mil or parts per thousand with the symbol of ‰. Delta values can be both positive and negative, positive values denote a sample that has a higher ratio of the heavy to the light isotope than the standard (the sample is enriched in the heavy isotope compared to the standard), a negative δ value means that the sample has a lower ratio of the heavy to the light isotope than the standard (the sample is depleted in the heavy isotope compared to the standard) (Sharp, 2007). For example, a sample with an $\delta^{18}O$ value of +19.7‰ has an $^{18}O/^{16}O$ ratio that is 19.7 parts per mil, or 1.97 percent higher than that of the standard.

A.4. The Analytical Technique of Mass Spectrometers

The δ ratios of stable isotopes are found by analysing samples using the Isotope Ratio Mass Spectrometer (IRMS). Mass spectrometers are utilised in the detection and identification of the components of a mixture of compounds, the delta value is deduced by inputting the data produced by the mass spectrometer analysis into a computer that converts the data into the delta values for the sample analysed (McMaster, 2008). Invented in 1912 by J.J. Thompson who called it the parabola spectrograph, it was improved by F.W. Aston who discovered 212 out of the approximate 287 natural stable isotopes and received a Noble Prize in chemistry for his efforts in 1922 by adding velocity focusing to the instrument (de Hoffman and Stroobant, 2002). It was not until 1968 that a data processing unit was coupled with mass spectrometers and throughout recent years mass spectrometry has "evolved into a highly precise and accurate tool for the measurement of isotopic abundances of elements in geological materials" (Faure, 1986, p5).

A.4.1. *CF-IRMS*

Isotope ratio mass spectrometers (IRMS) separate out charged molecules or atoms on the basis of their mass-to-charge (m/z) ratio determined by J.J. Thomson in 1897 (de Hoffman and Stroobant, 2002). There are two main types of IRMS, the Continuous Flow Isotope Ratio Mass Spectrometer (CF-IRMS) and the Duel Inlet Isotope Ratio Mass Spectrometer (DI-IRMS), (Lajtha and Michener, 2007).

Here we will focus on the CF-IRMS as it is more applicable to the specific application of this thesis, however higher precision would be found using the DI-IRMS over the CF-IRMS. The CF-IRMS was chosen over the more precise DI-IRMS because with the CF-IRMS system samples with multiple components can be analysed and the isotopic composition for the individual compounds can be attained (Michener and Lajtha, 2007). There are five main components to the IRMS: the inlet system, ion source, mass analyser, ion detector and the recording system. (The differences between the CF and DI-IRMS are all within the inlet system.) Each component is briefly outlined below.

i. Inlet system: All samples are introduced to the IRMS as a gas, any solid or liquid samples are pyrolised (vapourised to form a gas by heating, combusting) prior to

being put into the inlet system if they are not already in a gaseous form, the auto sampler above is what is used to combust materials in the University of Canterbury Stable Isotope Laboratory. The inlet system is composed of capillary tubes to allow no isotope separation within the IRMS system. Molecules may separate according to molecular flow if the path they travel through is long enough fractionation will occur, this allows heavier isotopes to be left behind whilst the lighter isotopes flow further into the IRMS. The reason capillary tubing is used is because of it's small size it induces viscous flow, where fractionation cannot take place because the molecules are continuously colliding with each other, therefore the sample is well mixed. In a CF-IRMS the samples are transported in a helium (He) stream through the chromatographic column, where the elements of interest are separated and sent through to the mass spectrometer, the other unwanted elements (gases) are sent to waste (Michener and Lajtha, 2007).

ii.Ion Source: after the sample leaves the capillary tubes it enters a high vacuum environment, the ion source box, where electrons are released to bombard the sample gases. This bombardment causes some of the gas molecules to lose an electron this produces positively charged ions. An ion beam is formed by accelerating these ions using a high voltage potential and a series of electric lenses (Sharp, 2007).

iii.Mass Analyser: The ion beam then passes through a strong magnetic field where the ions are deflected in a circular trajectory according to their mass-to-charge ratio (m/z). The charge-to-mass ratio determines their trajectory, light ions are deflected more strongly than heavy ones of the same charge, causing isotopes to physically separate out (Sharp, 2007). The radius of curvature is proportional to the square root of the mass-to-charge ratio ($\sqrt{m/z}$) (Michener and Lajtha, 2007).

iv.Ion Detector: The ion detector is a set of 3 or more faraday cups (collectors) that are positioned specifically to capture certain masses simultaneously. Faraday cups prevent ions from bouncing out of the detector and are long, narrow metal tubes with gold or colloidal graphite coating their internal surfaces to reduce secondary electron emission. Connecting the faraday cups to the ground is a high ohmic resistor; the ion current passes through this resistor creating a magnified voltage that is then fed into the recording system (Michener and Lajtha, 2007).

v.Recording System: A computer records the voltage of the ion current that is proportional to the quantities of the gas being analysed by comparing the signal

strength sent from the resistor to a ratio. The differences in the isotopic composition of the sample and the standard gas are recorded as δ values in parts per mil (Sharp, 2007).

Figure A.3: Schematic of the GC/CF-IRMS System (from Sharp, 2007).

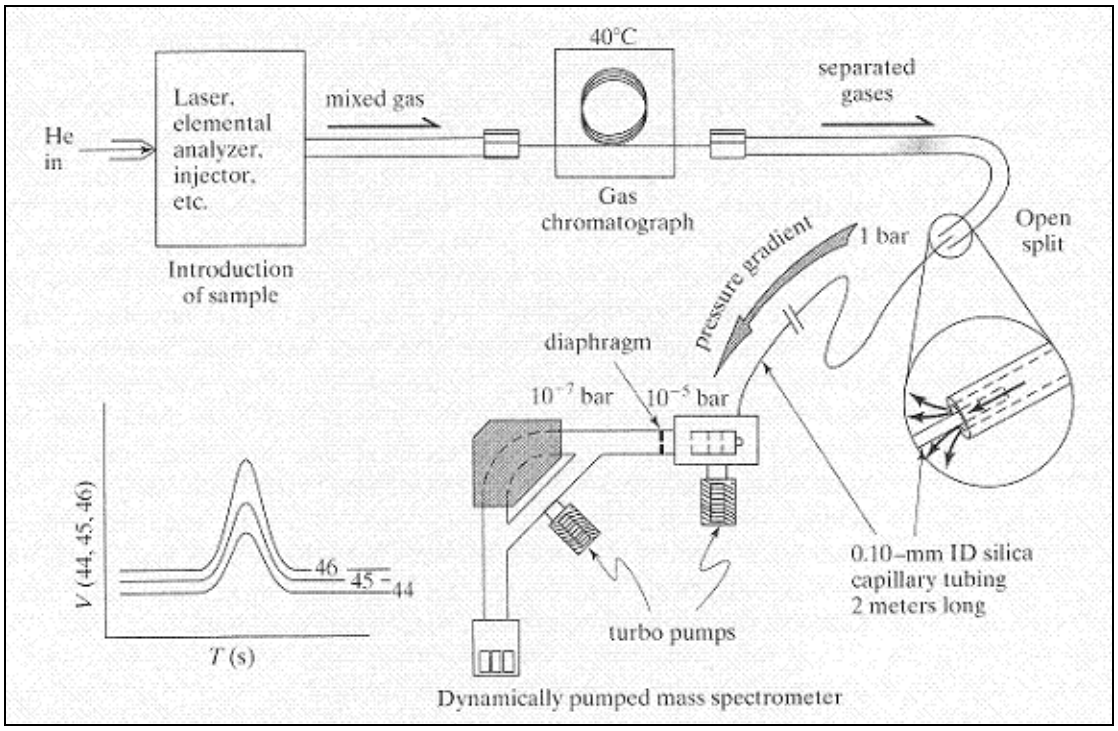

Due to technological advances the current IRMS systems can now process between 60-200 samples per day in comparison to between 2-15 samples per day. Today, smaller sample sizes are needed and the throughput of samples is much faster, additionally the cost of analysing a sample has dropped, allowing IRMS to become a more accessible tool. Also, there has been progress in the area of automated online preparation techniques, for example, depending on the type of sample either combustion, pyrolisis or cryoseparation needs to take place before the sample can be entered as a gas into the IRMS, advances in these fields has also led to greater efficiency in IRMS. (Lajtha and Michener, 2007).

Isotope Ratio Mass Spectrometers are 'rapidly becoming the definitive analytical tool in the research and commercial laboratory' (McMaster, M. and McMaster, C. 2008 p1), and the improvement of this technique has allowed them to be used more prolifically than ever. Stable Isotopes are used regularly in paleoclimatology studies

where carbonates, bones, ice and snail shells have been analysed to help reproduce past climates; stable isotopes can also help to trace fluids, the origin of rocks, contaminants and food sources; and they can also be applied to make distinctions between different types of phases for example, diffusion and recrystallisation, bacterial and thermogenic processes (Sharp, 2007).

Appendix B:

B-1: Rain Data – Coronet Peak Skifield
B-2: Rain Data - NIWA
B-3: Borehole Logs

Table B-1: Rain data collected on Coronet Peak from 01/06/2008 to 05/08/2008.

Date	Rain (mm)	Date	Rain (mm)	Date	Rain (mm)
01/06/2008	0	**23/06/2008**	4	**15/07/2008**	0
02/06/2008	-	**24/06/2008**	2	**16/07/2008**	0
03/06/2008	-	**25/06/2008**	5	**17/07/2008**	0
04/06/2008	-	**26/06/2008**	8	**18/07/2008**	0
05/06/2008	-	**27/06/2008**	2	**19/07/2008**	0
06/06/2008	-	**28/06/2008**	2	**20/07/2008**	0
07/06/2008	6	**29/06/2008**	-	**21/07/2008**	1
08/06/2008	-	**30/06/2008**	-	**22/07/2008**	1
09/06/2008	-	**01/07/2008**	0	**23/07/2008**	-
10/06/2008	0	**02/07/2008**	0	**24/07/2008**	-
11/06/2008	-	**03/07/2008**	17	**25/07/2008**	0
12/06/2008	-	**04/07/2008**	3	**26/07/2008**	0
13/06/2008	-	**05/07/2008**	-	**27/07/2008**	0
14/06/2008	-	**06/07/2008**	0	**28/07/2008**	0
15/06/2008	-	**07/07/2008**	0	**29/07/2008**	2
16/06/2008	-	**08/07/2008**	0	**30/07/2008**	-
17/06/2008	-	**09/07/2008**	0	**31/07/2008**	0
18/06/2008	0	**10/07/2008**	0	**01/08/2008**	6
19/06/2008	0	**11/07/2008**	2	**02/08/2008**	2
20/06/2008	0	**12/07/2008**	8	**03/08/2008**	0
21/06/2008	-	**13/07/2008**	0	**04/08/2008**	5
22/06/2008	1	**14/07/2008**	0	**05/08/2008**	1

Table B-2: NIWA Rain Data from the Queenstown Airport.

Date	Rain	Date	Rain	Date	Rain	Date	Rain
20080101:0800	0	20080216:0800	2.4	20080402:0800	2.8	20080518:0900	0.2
20080102:0800	0	20080217:0800	0	20080403:0800	0	20080519:0900	0
20080103:0800	0	20080218:0800	0	20080404:0800	0	20080520:0900	0
20080104:0800	0.8	20080219:0800	0	20080405:0800	0.2	20080521:0900	0
20080105:0800	0	20080220:0800	0	20080406:0900	0	20080522:0900	6.4
20080106:0800	0	20080221:0800	0	20080407:0900	0	20080523:0900	6.6
20080107:0800	1.8	20080222:0800	0	20080408:0900	0	20080524:0900	10.2
20080108:0800	0	20080223:0800	0	20080409:0900	0	20080525:0900	1
20080109:0800	0	20080224:0800	6.8	20080410:0900	0	20080526:0900	0
20080110:0800	0	20080225:0800	11.4	20080411:0900	0	20080527:0900	0.2
20080111:0800	0	20080226:0800	0	20080412:0900	0	20080528:0900	0
20080112:0800	0	20080227:0800	0	20080413:0900	0	20080529:0900	0
20080113:0800	0	20080228:0800	0.6	20080414:0900	0	20080530:0900	0.5
20080114:0800	0	20080229:0800	0	20080415:0900	0	20080531:0900	0
20080115:0800	13.2	20080301:0800	14.8	20080416:0900	0	20080601:0900	1.6
20080116:0800	0	20080302:0800	4.4	20080417:0900	0	20080602:0900	1.4
20080117:0800	17.6	20080303:0800	4.2	20080418:0900	0.4	20080603:0900	0
20080118:0800	3.6	20080304:0800	0	20080419:0900	0.4	20080604:0900	0.4
20080119:0800	0	20080305:0800	0	20080420:0900	0	20080605:0900	0
20080120:0800	0	20080306:0800	0	20080421:0900	0	20080606:0900	0
20080121:0800	0	20080307:0800	0	20080422:0900	0	20080607:0900	13.2
20080122:0800	3.2	20080308:0800	0	20080423:0900	0	20080608:0900	5.4
20080123:0800	24.6	20080309:0800	0	20080424:0900	0	20080609:0900	0.2
20080124:0800	0	20080310:0800	0	20080425:0900	0	20080610:0900	0
20080125:0800	0	20080311:0800	0.8	20080426:0900	0	20080611:0900	0
20080126:0800	0	20080312:0800	1.4	20080427:0900	0.2	20080612:0900	0.2
20080127:0800	0	20080313:0800	0	20080428:0900	1.2	20080613:0900	8.6
20080128:0800	0	20080314:0800	0	20080429:0900	0	20080614:0900	0.6
20080129:0800	0	20080315:0800	0	20080430:0900	18.8	20080615:0900	0.6
20080130:0800	0	20080316:0800	0	20080501:0900	1.4	20080616:0900	0.2
20080131:0800	0	20080317:0800	0	20080502:0900	3.2	20080617:0900	0.2
20080201:0800	2	20080318:0800	0	20080503:0900	1	20080618:0900	0
20080202:0800	26.6	20080319:0800	0	20080504:0900	0	20080619:0900	0
20080203:0800	0	20080320:0800	0	20080505:0900	0	20080620:0900	0
20080204:0800	0	20080321:0800	0	20080506:0900	0.2	20080621:0900	0
20080205:0800	0	20080322:0800	22.2	20080507:0900	0	20080622:0900	0
20080206:0800	0	20080323:0800	0	20080508:0900	0	20080623:0900	0.8
20080207:0800	0	20080324:0800	0	20080509:0900	11	20080624:0900	3.8
20080208:0800	0	20080325:0800	0	20080510:0900	0.2	20080625:0900	0
20080209:0800	0	20080326:0800	0	20080511:0900	1.4	20080626:0900	6.8
20080210:0800	0	20080327:0800	0	20080512:0900	0	20080627:0900	1.4
20080211:0800	4.4	20080328:0800	0	20080513:0900	0.2	20080628:0900	0.2
20080212:0800	0.4	20080329:0800	5	20080514:0900	0	20080629:0900	1.4
20080213:0800	0	20080330:0800	0	20080515:0900	0	20080630:0900	0
20080214:0800	1.8	20080331:0800	0	20080516:0900	0	20080701:0900	0
20080215:0800	4.8	20080401:0800	0	20080517:0900	0.2	20080702:0900	0

Date	Rain	Date	Rain	Date	Rain	Date	Rain
20080703:0900	8.2	20080819:0900	1	20081005:0800	8.4	20081121:0800	0
20080704:0900	0.4	20080820:0900	0	20081006:0800	0	20081122:0800	0
20080705:0900	3.2	20080821:0900	0	20081007:0800	12.2	20081123:0800	0
20080706:0900	4.8	20080822:0900	10.8	20081008:0800	13.8	20081124:0800	0
20080707:0900	0.2	20080823:0900	4	20081009:0800	1.8	20081125:0800	9.6
20080708:0900	0	20080824:0900	0	20081010:0800	0	20081126:0800	3.4
20080709:0900	0.2	20080825:0900	0.2	20081011:0800	0	20081127:0800	0
20080710:0900	0	20080826:0900	0	20081012:0800	0	20081128:0800	0
20080711:0900	0.4	20080827:0900	0	20081013:0800	0	20081129:0800	0
20080712:0900	18.8	20080828:0900	0	20081014:0800	0	20081130:0800	0
20080713:0900	1.4	20080829:0900	0	20081015:0800	0	20081201:0800	0
20080714:0900	0.2	20080830:0900	0	20081016:0800	0.8	20081202:0800	0
20080715:0900	0	20080831:0900	0	20081017:0800	0	20081203:0800	0
20080716:0900	0	20080901:0900	0	20081018:0800	0.8	20081204:0800	14.8
20080717:0900	0.2	20080902:0900	2.6	20081019:0800	0	20081205:0800	3.4
20080718:0900	0	20080903:0900	0.6	20081020:0800	0.4	20081206:0800	0
20080719:0900	0.2	20080904:0900	6.2	20081021:0800	0	20081207:0800	0
20080720:0900	0.4	20080905:0900	0	20081022:0800	0	20081208:0800	0
20080721:0900	0.4	20080906:0900	0	20081023:0800	0	20081209:0800	20.6
20080722:0900	0	20080907:0900	0	20081024:0800	0	20081210:0800	0
20080723:0900	0	20080908:0900	0	20081025:0800	0	20081211:0800	0
20080724:0900	0	20080909:0900	0.4	20081026:0800	4.4	20081212:0800	1
20080725:0900	0	20080910:0900	10.6	20081027:0800	0	20081213:0800	0
20080726:0900	0	20080911:0900	0.2	20081028:0800	0	20081214:0800	0
20080727:0900	0	20080912:0900	4.6	20081029:0800	4.8	20081215:0800	2.2
20080728:0900	3.4	20080913:0900	1.6	20081030:0800	0.4	20081216:0800	6.6
20080729:0900	2	20080914:0900	0.2	20081031:0800	0	20081217:0800	3.4
20080730:0900	0	20080915:0900	0	20081101:0800	3.6	20081218:0800	0
20080731:0900	0	20080916:0900	0	20081102:0800	0.6	20081219:0800	0
20080801:0900	4.2	20080917:0900	0	20081103:0800	0	20081220:0800	11.2
20080802:0900	0.8	20080918:0900	6.6	20081104:0800	0	20081221:0800	13.4
20080803:0900	0	20080919:0900	0	20081105:0800	3.4	20081222:0800	0
20080804:0900	8.2	20080920:0900	0	20081106:0800	2	20081223:0800	0
20080805:0900	2.8	20080921:0900	5.8	20081107:0800	0.2	20081224:0800	0
20080806:0900	0	20080922:0900	7	20081108:0800	0	20081225:0800	2
20080807:0900	0	20080923:0900	0	20081109:0800	0	20081226:0800	0
20080808:0900	0.2	20080924:0900	23	20081110:0800	0.8	20081227:0800	0
20080809:0900	0	20080925:0900	0	20081111:0800	0	20081228:0800	0.2
20080810:0900	0	20080926:0900	0	20081112:0800	0	20081229:0800	0
20080811:0900	0	20080927:0900	13.6	20081113:0800	0	20081230:0800	0
20080812:0900	0	20080928:0800	25	20081114:0800	0	20081231:0800	0
20080813:0900	0.8	20080929:0800	0	20081115:0800	0	20090101:0800	11.6
20080814:0900	2.6	20080930:0800	5.6	20081116:0800	0	20090102:0800	0
20080815:0900	1.6	20081001:0800	3.6	20081117:0800	22.4	20090103:0800	2.8
20080816:0900	5	20081002:0800	1.2	20081118:0800	0	20090104:0800	0
20080817:0900	7	20081003:0800	0	20081119:0800	0	20090105:0800	0
20080818:0900	0.8	20081004:0800	1.4	20081120:0800	0	20090106:0800	0

Date	Rain	Date	Rain	Date	Rain	Date	Rain
20090107:0800	0.6	20090223:0800	7.6	20090411:0900	0	20090528:0900	0.2
20090108:0800	2.2	20090224:0800	2.5	20090412:0900	0	20090529:0900	0.2
20090109:0800	0.2	20090225:0800	0	20090413:0900	0	20090530:0900	0.2
20090110:0800	15.4	20090226:0800	0	20090414:0900	0.6	20090531:0900	0.6
20090111:0800	0	20090227:0800	0.6	20090415:0900	0	20090601:0900	0
20090112:0800	0	20090228:0800	0	20090416:0900	3.4	20090602:0900	0
20090113:0800	0	20090301:0800	3.8	20090417:0900	0	20090603:0900	0.2
20090114:0800	0	20090302:0800	0.2	20090418:0900	0	20090604:0900	0
20090115:0800	0	20090303:0800	0	20090419:0900	0	20090605:0900	0
20090116:0800	0	20090304:0800	0	20090420:0900	0	20090606:0900	0
20090117:0800	17.4	20090305:0800	0	20090421:0900	0	20090607:0900	0
20090118:0800	0.8	20090306:0800	1.6	20090422:0900	0	20090608:0900	0
20090119:0800	5.4	20090307:0800	1.4	20090423:0900	0	20090609:0900	0.4
20090120:0800	0	20090308:0800	0	20090424:0900	0	20090610:0900	0
20090121:0800	0	20090309:0800	0	20090425:0900	0	20090611:0900	2
20090122:0800	0	20090310:0800	0	20090426:0900	3.2	20090612:0900	4
20090123:0800	0	20090311:0800	2	20090427:0900	4	20090613:0900	0.2
20090124:0800	0	20090312:0800	2.6	20090428:0900	3.6	20090614:0900	0.2
20090125:0800	0	20090313:0800	0	20090429:0900	0	20090615:0900	0
20090126:0800	0	20090314:0800	0	20090430:0900	0.8	20090616:0900	0
20090127:0800	0	20090315:0800	0	20090501:0900	0	20090617:0900	0
20090128:0800	0	20090316:0800	0	20090502:0900	0	20090618:0900	0
20090129:0800	0	20090317:0800	0	20090503:0900	0	20090619:0900	0
20090130:0800	0.4	20090318:0800	0	20090504:0900	0.2	20090620:0900	0
20090131:0800	0	20090319:0800	0.6	20090505:0900	6.2	20090621:0900	0
20090201:0800	1.8	20090320:0800	0	20090506:0900	5	20090622:0900	0
20090202:0800	0	20090321:0800	0.6	20090507:0900	0	20090623:0900	0
20090203:0800	0	20090322:0800	0	20090508:0900	3.6	20090624:0900	0
20090204:0800	0	20090323:0800	0	20090509:0900	0.2	20090625:0900	0
20090205:0800	0	20090324:0800	0	20090510:0900	0	20090626:0900	0.2
20090206:0800	0	20090325:0800	0	20090511:0900	4.8	20090627:0900	0
20090207:0800	0	20090326:0800	0	20090512:0900	4.2	20090628:0900	0
20090208:0800	0	20090327:0800	6	20090513:0900	5.2	20090629:0900	0
20090209:0800	0.4	20090328:0800	8.6	20090514:0900	0.2	20090630:0900	0
20090210:0800	5.4	20090329:0800	0	20090515:0900	9.8	20090701:0900	0
20090211:0800	0	20090330:0800	0	20090516:0900	21.6	20090702:0900	0
20090212:0800	3.2	20090331:0800	0	20090517:0900	42	20090703:0900	0.4
20090213:0800	0.8	20090401:0800	0	20090518:0900	6	20090704:0900	0.4
20090214:0800	0	20090402:0800	0	20090519:0900	5.6	20090705:0900	0
20090215:0800	0	20090403:0800	0	20090520:0900	26.2	20090706:0900	0
20090216:0800	0.6	20090404:0800	0	20090521:0900	1.4	20090707:0900	0
20090217:0800	0.2	20090405:0900	2.2	20090522:0900	1.8	20090708:0900	0.2
20090218:0800	0	20090406:0900	8.8	20090523:0900	0.2	20090709:0900	0
20090219:0800	0	20090407:0900	18	20090524:0900	0.8	20090710:0900	0.2
20090220:0800	2.6	20090408:0900	4.2	20090525:0900	0	20090711:0900	0
20090221:0800	8.2	20090409:0900	2.4	20090526:0900	0	20090712:0900	0
20090222:0800	0.4	20090410:0900	0	20090527:0900	0.2	20090713:0900	0

Date	Rain	Date	Rain				
20090714:0900	0	20090830:0900	0				
20090715:0900	0.4	20090831:0900	5.6				
20090716:0900	0.2	20090901:0900	3.2				
20090717:0900	0	20090902:0900	12				
20090718:0900	0	20090903:0900	0.2				
20090719:0900	0.2	20090904:0900	0				
20090720:0900	0	20090905:0900	0				
20090721:0900	0.4	20090906:0900	0				
20090722:0900	12.4	20090907:0900	0				
20090723:0900	15.4	20090908:0900	0				
20090724:0900	7.4	20090909:0900	0				
20090725:0900	0	20090910:0900	0				
20090726:0900	0	20090911:0900	0				
20090727:0900	0	20090912:0900	0.4				
20090728:0900	0	20090913:0900	0				
20090729:0900	4.8	20090914:0900	0				
20090730:0900	3	20090915:0900	1				
20090731:0900	7.8	20090916:0900	0				
20090801:0900	7.4	20090917:0900	0				
20090802:0900	0.4	20090918:0900	0				
20090803:0900	7.4	20090919:0900	0				
20090804:0900	11.4	20090920:0900	0				
20090805:0900	15.4	20090921:0900	0				
20090806:0900	0	20090922:0900	0.8				
20090807:0900	0	20090923:0900	0.8				
20090808:0900	0	20090924:0900	0				
20090809:0900	0	20090925:0900	0.4				
20090810:0900	0	20090926:0900	0				
20090811:0900	1	20090927:0800	0				
20090812:0900	25.8	20090928:0800	4.2				
20090813:0900	12.8	20090929:0800	0				
20090814:0900	0						
20090815:0900	0						
20090816:0900	0.4						
20090817:0900	0						
20090818:0900	0.8						
20090819:0900	0						
20090820:0900	0						
20090821:0900	0						
20090822:0900	0						
20090823:0900	0.2						
20090824:0900	0						
20090825:0900	0.2						
20090826:0900	8						
20090827:0900	4.2						
20090828:0900	9						
20090829:0900	6.2						

B-3: Borehole Logs.

Bore logs annotated by McNeill Drilling Co. Ltd and Washingtons Exploration Ltd.

Number in Logs	Name	Easting	Northing	Depth	Depth to Groundwater
1	Elephant (Hurdle 1)	2173661	5578722	152	130 to 85
2	Express (Hurdle 3)	2173766	5578925	65	56
3	Hurdle (Hurdle 2)	2173704	5578863	168	63
4	Big Easy	2174065	5578420	66	40
5	Hole 1	2173649	5578805	174	-
6	Hole 2	2173616	5578741	60	-
7	Hole 3	2174054	5578695	102	Dribbles
8	Hole 4	2173239	5578097	174	Dribbles
9	Hole 5	2173912	5578483	118	Dribbles
10	-	2173048	5578039	?	49
11	SS1 (core)	2172782.1	5578223.6	25	21
12	SS2 (core)	2172853.8	5578276.7	49	29
13	RG1 (core)	2174256.3	5578821.2	49	48
14	RG2 (core)	2174175.1	5578805.2	25	23

9. Jan. 2008 17:05 McNeill Drilling INV No. 4282 P. 4

No 1.

883

MCNEILL DRILLING CO. LTD

WATER BORE/WELL SUMMARY FORM

1

CLIENTS NAME: Coronet peak	BORE SIZE: 6inch
FULL ADDRESS:	START DATE: Feb 04
RAPID NO:	FINISH DATE: March 04
GRID REFERENCE: N5578726/E2178664.	
DRILLER: E Pascoe	MACHINE: V8 schramm
MEASURED FROM: ToC	DRILL METHOD: Holts.
TOTAL DEPTH BORE: 151.5m	
TOP LEADER: —	
SWL: 84.3m	
SCREEN: SLOT: —	LENGTH: —
TYPE: —	SIZE: —
PVC SLOTTED: TOP: —	BASE: —
SCREEN/LEADER/SUMP: —	SUMP SIZE: —
TOTAL CASING USED: 128m 6inch	
AIRLIFTED/PUMPED AT:	
DRAWDOWN FROM SWL:	
AIR/PUMP INTAKE:	
BACTERIAL WATER TEST: -	
CHEMICAL WATER TEST: -	
EXTRA NOTES: Drilled to 151.5m but may collapse. To less.	

BORE LOG:

00.000 To 151.5m Brokan shist & rock & silt & Hard shist rock

20/5/04

980

MCNEILL DRILLING CO. LTD

WATER BORE/WELL SUMMARY FORM

(2)

Bore No 2

CLIENTS NAME: Gary Steadman	BORE SIZE: 12"
FULL ADDRESS: Coronet Peak	START DATE: 18.1.05
RAPID NO:	FINISH DATE:
GRID REFERENCE: E/2173760 N/5578926	27.1.05
DRILLER: Even	MACHINE: Schramm T8
MEASURED FROM: Top of casing.	DRILL METHOD: Holes
TOTAL DEPTH BORE: 65m	
TOP LEADER:	
SWL: 46m	
SCREEN: SLOT: 2.5	LENGTH:
TYPE: SS	SIZE:
PVC SLOTTED: TOP:	BASE:
SCREEN/~~LEADER/SUMP~~: 3m	SUMP SIZE:
TOTAL CASING USED: 62.5	
~~AIRLIFTED~~/PUMPED AT: 4.5 Ltrs sec	
DRAWDOWN FROM SWL: 11m	
~~AIR~~/PUMP INTAKE: 60m	
BACTERIAL WATER TEST:	
CHEMICAL WATER TEST:	

EXTRA NOTES:

BORE LOG:

00.000 – 36 Dry Broken Rock + silts.
36 – 64 Wet Broken shist Rock with courts
64 – 66 Dry Rock.

29/4/05 ES

990

3

MCNEILL DRILLING CO. LTD

WATER BORE/WELL SUMMARY FORM

Bore 3-

CLIENTS NAME: Gary Steadman	BORE SIZE: 10" / 6inch
FULL ADDRESS: Coronet Peak	START DATE: 3/2/05
RAPID NO:	FINISH DATE: 2.3.05
GRID REFERENCE: N: 5578859/E: 2173696.	MACHINE: Schramm V8
DRILLER: Evem Pascoe	DRILL METHOD: Holts
MEASURED FROM: Top of casing	
TOTAL DEPTH BORE: 168m	
TOP LEADER:	
SWL: 83.5 T.OC	
SCREEN: SLOT: —	LENGTH:
TYPE: —	SIZE:
PVC SLOTTED: TOP: —	BASE:
SCREEN/LEADER/SUMP: —	SUMP SIZE:
TOTAL CASING USED: 154m 6" 68m 12" 76m 10"	
AIRLIFTED/PUMPED AT:	
DRAWDOWN FROM SWL:	
AIR/PUMP INTAKE:	
BACTERIAL WATER TEST: —	
CHEMICAL WATER TEST: —	

EXTRA NOTES: 10inch hole Drilled To 168
Lined with 6inch To 154m

BORE LOG:

00.000 - 56 Silts e rock Dry.
56 - 66m Silts e rock small amount of water.
66 - 116m Silts e rock Dry.
116 - 168 Silts e rock e Quats water.

14/4/05 ES

08 Jan 2008 11:35 Washingtons Exploration (+) 688263

4

WASHINGTONS EXPLORATION LIMITED

BORE REPORT

Client	SOUTHERN ALPINE RECREATION LTD	Consent No	ORC 2007.063
Address	P O BOX 359	Bore No	
	QUEENSTOWN	Grid Ref	NZMS260 F41:744-787
Driller	Washingtons Exploration Ltd	Rig	R#4
Date completed	23 March 2007	Bore depth	66M
Bore diameter	300mm	Static water level	36.2M

PUMPING DETAILS

Flow rate (gpm)	Drawdown (from top of Csg)	Duration (hrs)
450	47.1M	91 1/2

8" Goulds Pump
set @ 55M

SCREEN DETAILS

Type	Slot size (mm)	Diameter mm	Length (m)	Set from	Set to
Stainless Steel	0.080	300mm	6M	60M	66M
Leader		300mm	1.2M	58.8M	60M

CASING DETAILS

Casing material STEEL Height above ground

Diameter (mm)	Length (m)	Set from	Set to
300mm	60M	0.0	60M

4

WASHINGTONS EXPLORATION LTD - PAGE 2
BORE LOG DETAILS

Depth from surface Top	Bottom	Strata description CORONET PEAK	SWL
0.0	0.2	Top soil	
0.2	3.0	Broken schist	
3.0	24.0	Broken schist firm	
24.0	25.0	Brown sandy soft schist	
25.0	40.0	Brown broken schist	
40.0	48.0	Green schist hard	
48.0	60.0	Green broken schist - H20 1 LPS	
60.0	66.0	Broken schist - firm, small flow H20 into big flow	
66.0		TOTAL DEPTH	

THIS BORE PUMPED 450GPM ON 27 March 2007
BUT MAY VARY OWING TO SEASONAL FLUCTUATIONS
Water level was unstable

PUMP TEST A pumping test is useful to determine the potential yield of the bore following bore development.

	Pumping Rate (l/s) (l/m) (GPM) *(please circle the units)*	Draw Down (m) metres below initial water level	Pumping Duration (hrs)
Step 1	none		
Step 2			
Step 3			
Step 4			
Step 5			
Step 6			

BORE LOG (Please complete this section OR attach the driller's log) **Bore Number**

Your driller will have compiled a log of your bore describing the sequence of different strata encountered during drilling. This information is vital in the compilation of geological cross-sections and groundwater models, and must be included as part of this report.

STRATA

Depth From Surface (metres) Top	Bottom	Colour	Description	Water Level (metres)
HOLE 1			TOP PUMP SHED, 174 m	
0	24		Shist rock broken	
	24		Broken shist, lost circulation	
24	66	Grey-green	Hard shist rock, grey-green layers, 0.5 lt/sec	
66	174		As above, casing pulled	
HOLE 2			AT PUMP SHED, 60m	
0	60		Broken shist rock, no change in formation No water, casing pulled	
HOLE 3			AT LUNCH ROCKS, 102 m	
0	12		Broken shist rock	
12	35		Hard shist rock, pick up dribble H20	
35	102	Grey	Shist grey broken 0.5 lt/sec in dribbles from 35 – 60 m Casing pulled	

5

6

7

Your driller will have compiled a log of your bore describing the sequence of different strata encountered during drilling. This information is vital in the compilation of geological cross-sections and groundwater models, and must be included as part of this report.

STRATA

Depth From Surface (metres)		Colour	Description	Water Level (metres)
Top	Bottom			
HOLE 4			BOTTOM OF HILL, 174 m	
0	65		Shist rock firm to hard	
	65		Broken dribble	8
65	67		Shist rock hard	
67	88		Shist rock hard, broken dribble at 87 m	
88	174		As above, 0.75 lt/sec, casing pulled	
HOLE 5			BESIDE SHORT CHAIR LIFT, 118 m	
0	66	Grey	Broken shist, lost circulation	9
66	118	Grey	Hard shist, fractured dribble	
			Pick up dribbles to bottom of well totalling 1,5 – 2 lt/sec	
			66 m casing left in hole	
			Arrow International Limited	
			Will Fairbairn, Project Manager	
			PO Box 716	
			Queenstown	

Report: 01/02/2008, prepared by Royden Thomson for Hadleys Consultants Ltd who were working for NZ Ski Ltd.

ROYDEN THOMSON, GEOLOGIST

11 Leitrum Street
Cromwell
Phone 03 445 0025
Fax 03 445 0029

1 Feb '08

Will Oswald

Will,

Existing Drill Holes : Miscellaneous Notes

Please find below comment on individual holes to supplement information on the attached register and site plan. Listed numbers refer to those on the plan and not those used by the drilling companies.

(1.) Set up for pumping.

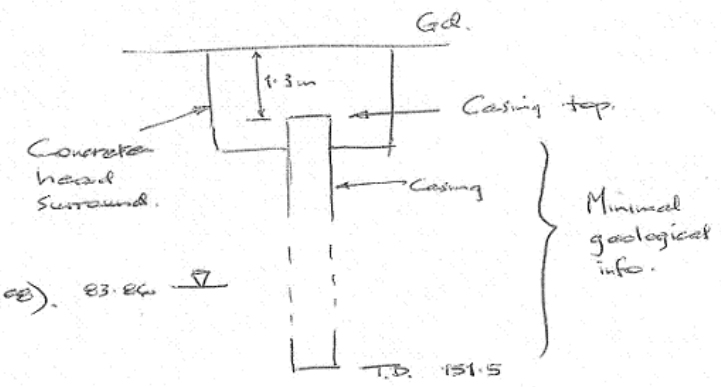

Notes from Geary

- On 14 Jan '08 GWL 83.86 from top of casing. ie. 85.16 below ground.
- Initially encountered water at 130 m. GWL rose to ca. 130 m, then to present level.

Implication Encountered a confined aquifer which is Subartesian. May

have been pump tested but no data available, to my knowledge.

Do

- Accurate survey of hole collar.
- See if pump test info. can be obtained

(2) Set up for pumping.

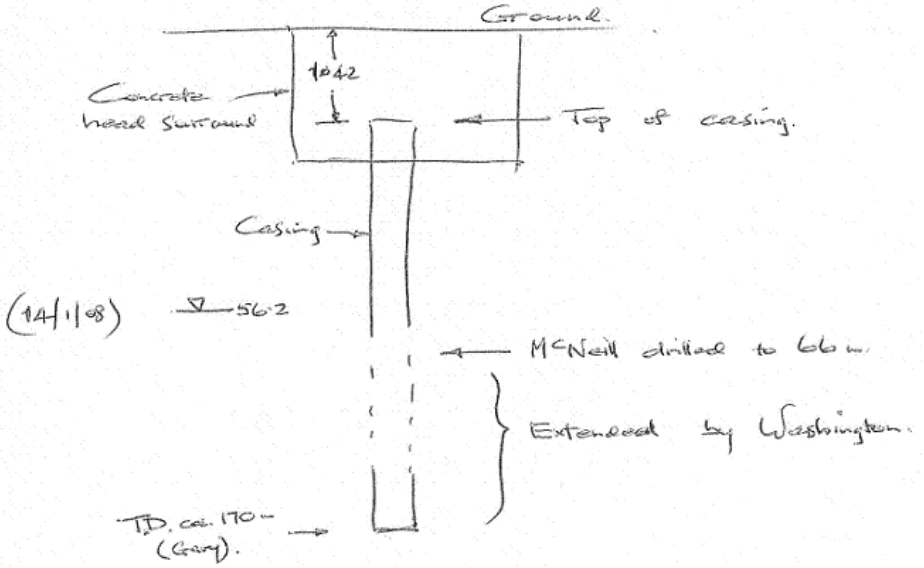

Notes from Gary

- Hole initially drilled by McNeill. Extended to ca 170 m by Washington.
- GWL at 56.2 (from top of casing) on 14 Jan 08.

Comment

McNeill log suggests "moist"/"wet" slide material in interval 36 – 64 m. This "groundwater" is presumably cut off by casing

Do:

- Attempt to acquire log of hole extension

from Washington.

- Enquire about any pump test data.
- Get accurate survey of hole collar.

(3) Set up for pumping

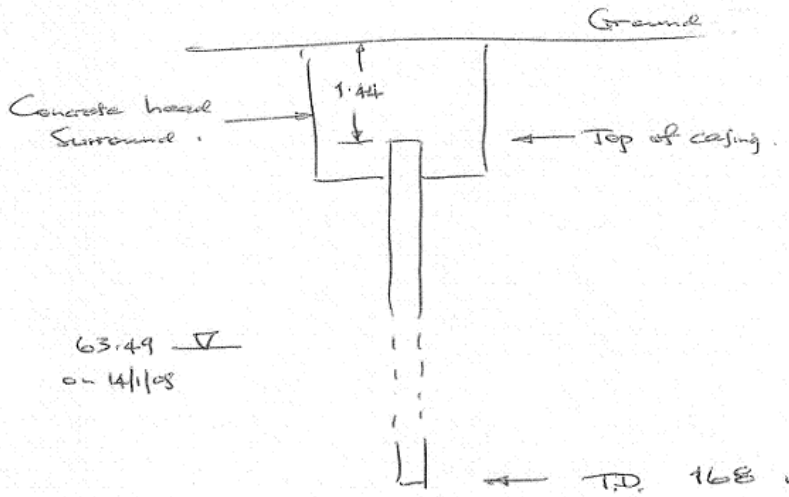

Do

- Acquire and pump test data, if available
- Get accurate survey of hole collar

(4) "The Wall"

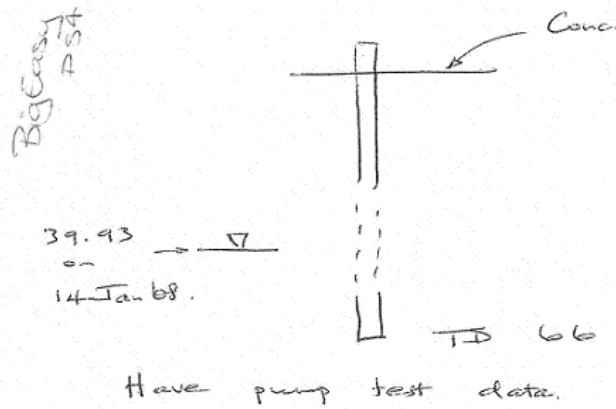

Have pump test data.

Do:

- Get available monitoring data.
- Do an accurate Survey of the top of casing.

(5) Hole abandoned — dry.

Do

- Survey ground at collar position.

(6) As for (5)

(7) " " (5)

(8) " " (5)

(9)

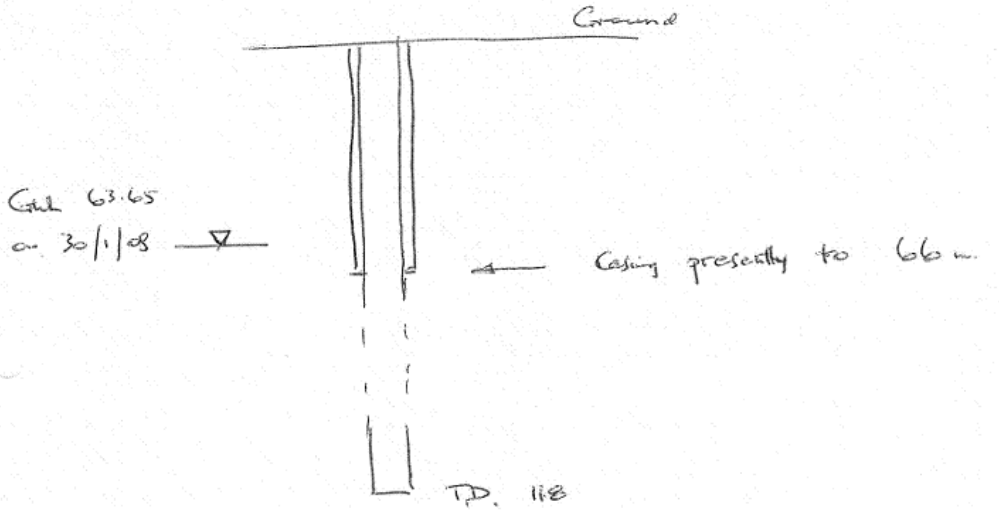

Do

- Survey hole collar
- Acquire any pump test data.
- Check presently open hole depth.

(10) An early McNeill Water Bore — approx early '04.

(5)

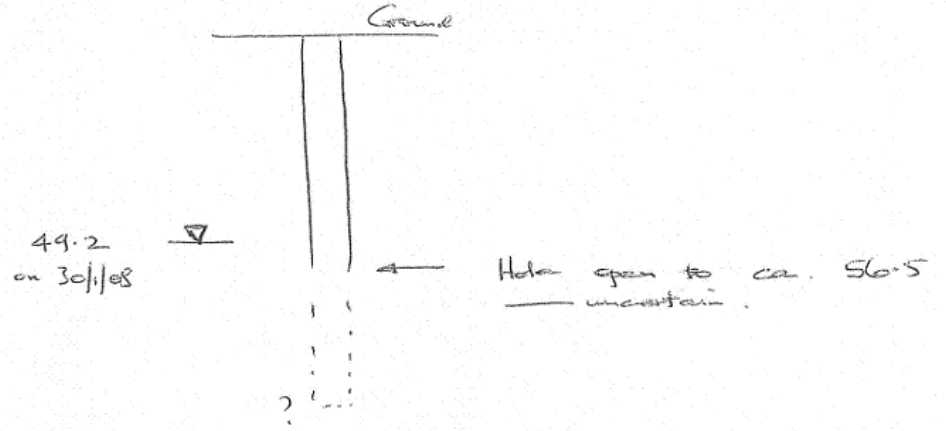

Do
- Acquisition of log in progress — if available.
- Recheck depth to 'blockage'
- Survey hole collar.

(11) SS 1 dry at 22.13 from top of tubing (on 29 Jan '08).

Do nothing.

(12) SS 2

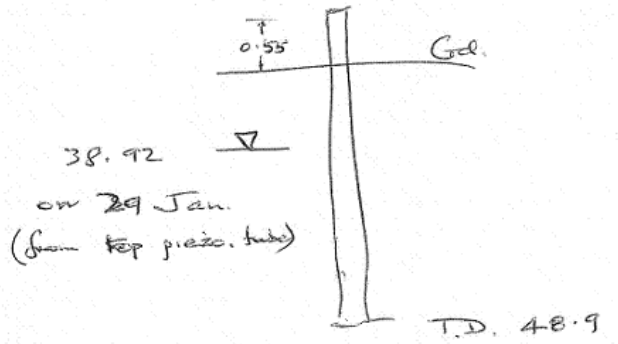

Comment
GWL 10 m lower than when last reading taken on the 3 Dec. '07.

(13) (14)

Holes destroyed by construction.

General Notes

- Need to collate all water level records for each hole to see what changes have occurred over time. — graph levels versus time.
- An accurate survey of all collars of groundwater holes would be desirable to improve cross section construction and understanding.

Trust this advances the knowledge ~~factor~~ significantly.

Cheers,

Rayden

Appendix C:

Stable Isotope Data

Table C-1: All samples collected between the 14-22 of July 2009.

	Sample	δD (‰ V-SMOW)	$\delta^{18}O$ (‰ V-SMOW)
July			
Waterfall	1	-77.7	-11.26
Grasshopper	2	-79.2	-11.33
Moss	3	-78.8	-11.12
McMullan #2	4	-81.9	-11.58
Pipe @ Heidi's Hut	5	-82.3	-11.60
Heidi's	6	-82.9	-11.62
Danni's	7	-83.6	-11.75
Coronet Peak Rd	8	-81.1	-11.40
Bramble	9	-81.0	-11.39
Pond	10	-81.4	-11.24
Wired	11	-77.6	-10.95
Swamp	12	-79.0	-11.25
Cattlestop	13	-72.6	-10.29
Multiple	14	-76.5	-10.95
Hairpin	15	-81.4	-11.49
Station	16	-81.1	-11.52
Tussock	17	-76.6	-10.96
Twin	18	-78.7	-11.20
Grassy	19	-82.3	-11.36
Gobblers	20	-82.4	-11.50
Wall St	21	-81.8	-11.31
Dirty 4	22	lost	lost
Water Supply	23	-81.6	-11.63
Big Easy	29	-81.1	-11.28
Hurdles	30	-85.0	-12.11
A1		-44.7	-5.76
A2		-55.9	-8.28
A3		-54.9	-8.72
A5		-35.8	-5.38
A3a		-54.7	-8.57
A3b		-55.5	-8.64
A31		-51.8	-8.23
A32		-52.5	-7.98
A33		-54.3	-8.27
B4		-58.8	-8.31
C3		-62.4	-9.32
C32		-64.6	-9.04
C33		-66.5	-9.86

C3a		-67.7	-9.91
C3b		-68.2	-10.07
RSVR 5	24	-82.4	-11.39
RSVR 3	25	-81.6	-11.22
RSVR 1B	26	-81.3	-10.97
RSVR 1	27	-85.4	-12.11
RSVR 2	28	-84.7	-11.84

Table C-2: All samples collected between the 10-14 of August 2009.

	Sample	**δD (‰ V-SMOW)**	**$\delta^{18}O$ (‰ V-SMOW)**
August			
Water Supply	31	-89.26	-12.63
Station	32	-84.31	-12.01
Gobblers	33	-84.95	-12.33
Bramble	34	-84.68	-12.12
Coronet Peak Rd	35	-85.78	-12.18
Pond	36	-84.56	-12.08
Swamp	37	-82.79	-11.74
Cattlestop	38	-82.76	-11.52
Wall St	39	-117.55	-16.04
Danni's	40	-87.35	-12.39
Heidi's	41	-87.24	-12.54
Pipe at Heidi's Hut	42	-85.63	-12.37
Moss	44	-87.72	-12.61
McMullan #2	45	-84.17	-12.04
Waterfall	46	-86.60	-12.36
Grasshopper	47	-86.22	-12.57
Hurdle	HURDLE	-87.09	-12.10
Big Easy	PS.4	-84.79	-12.13
	D1	-103.91	-13.50
	D2	-118.04	-15.63
	D3	-126.75	-16.78
	D4	-128.51	-17.09
	D5	-126.95	-17.00
	D31.a	-126.89	-17.01
	D31.b	-129.20	-16.70
	D31.c	-122.56	-16.28
	D31.d	-107.47	-12.06

	E1	-140.07	-18.20
	E2	-139.37	-18.23
	E3	-139.78	-18.43
	E4	-136.39	-18.17
	E5	-136.67	-18.10
	E31	-132.28	-17.80
	E32	-138.79	-18.50
	E33	-141.09	-18.81
	E34	-139.83	-18.66
	E35	-144.68	-19.52
	E36	-140.13	-18.56
	E37	-111.62	-14.40
RSVR 1	RSV.1	-86.15	-12.01
RSVR 1b	RSV.1B	-83.43	-11.37
RSVR 2	RSV.2	-86.49	-12.12
RSVR 3	RSV.3	-81.83	-11.46
RSVR 5	RSV.5	-84.24	-11.73

Table C-3: All samples collected between the 22-25 of September 2009.

	Sample	**δD (‰ V-SMOW)**	**$\delta^{18}O$ (‰ V-SMOW)**
September			
Wall St	55	-82.27	-11.77
Snow - Site 4	56	-71.07	-10.39
Cattlestop	57	-81.32	-11.28
Swamp	58	-82.70	-11.42
Wired	59	-79.86	-11.41
Pond	60	-83.23	-11.76
Bramble	61	-83.92	-11.90
Coronet Peak Rd	62	-83.81	-11.85
Multiple	63	-86.04	-12.25
Hairpin	64	-86.72	-12.41
Tussock	65	-92.21	-12.53
Grassy	66	-86.83	-12.21
Twin	67	-86.55	-12.42
Station	68	-86.70	-12.37
Water Supply	69	-87.40	-12.54
Gobblers	70	-83.99	-11.84
Danni's	71	-87.29	-12.83
Heidi's	72	-87.45	-12.67
Pipe at Heidi's Hut	73	-87.15	-12.57

Moss	74	-86.34	-12.47
McMullan #2	75	-85.87	-12.70
Grasshopper	76	-87.26	-12.79
Waterfall	77	-86.04	-12.50
Dirty Creek	80	-89.22	-13.16
Dirty Four	81	-85.63	-12.37
Snow - Site 5	F5.SNOW	-128.82	-17.16
Snow - Grasshopper	78	-74.95	-11.00
Snow - Heidi's Hut	79	-69.17	-10.08
Hurdle		-87.69	-12.12
Big Easy		-85.68	-11.98
	F1	-43.65	-6.14
	F2	-68.40	-9.74
	F3	-74.37	-10.72
	F4	-79.08	-11.46
	F5	-101.35	-14.45
	F31	-74.89	-10.35
	F32	-73.20	-9.73
	F33	-73.81	-10.10
	F34	-73.02	-10.04
	F35	-75.50	-10.49
	F36	-75.57	-9.96
	F37	-76.18	-9.94
	F38	-70.33	-8.87
	F39	-80.56	-10.75
	G1	-56.81	-8.81
	G2	-65.52	-10.00
	G3	-64.28	-9.86
	G4	-64.36	-9.41
	G5	-67.15	-10.68
	G32	-62.97	-9.18
	G33	-62.14	-9.14
	G34	-62.33	-9.20
	H1	-63.43	-9.36
	H2	-102.83	-14.41
	H3	-62.40	-9.30
RSVR 1	48	-86.17	-12.52
RSVR 2	49	-99.02	-13.28
RSVR 3	50	-84.72	-12.35
RSVR 1b	51	-69.99	-7.45
RSVR 5	52	-86.09	-12.19

Appendix D:

Flow Rates in V-notch Weirs

Spring Descriptions

Table D-1: Flow rates for a 90° v-notch weir.

Q (litres per second)	**H (cm)**
1	5.48
2	7.25
3	8.56
4	9.62
6	11.32
8	12.72
10	13.92
12	14.97
14	15.93
16	16.80
18	17.62
20	18.38
22	19.09
24	19.77
26	20.42
28	21.04
30	21.63
35	23.03

Table D-2: Flow rates of the v-notch weir of the Dirty Four Spring.

H (mm)	**Q (litres per second)**
10	0.01
20	0.03
30	0.08
40	0.16
50	0.28
60	0.45
70	0.66
80	0.92
90	1.23
100	1.60
110	2.04
120	2.53
130	3.09
140	3.72
150	4.42
160	5.19
170	6.04
180	6.92
190	7.85
200	8.92
210	10.08
220	11.32
230	12.65
240	14.07
250	15.58
260	17.16
270	18.86
280	20.69
290	22.59
300	24.58

A) Cattlestop Spring and Weir:

GPS Spring: Northing: 2172763
Easting: 5576563
Height: 913 metres

GPS Weir: Northing: 2171786
Easting: 5576520
Height: 899 metres

Photo D1: Cattlestop Spring, can see scarp where the spring exits the schist block (15/04/2008).

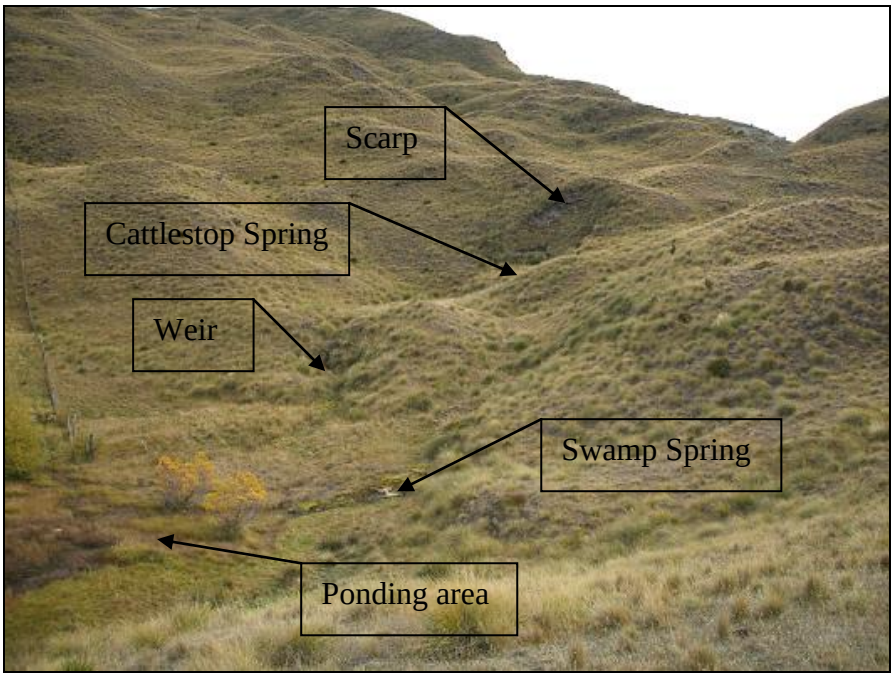

The Cattlestop Spring flows through the base of a large schist block (see photo above). It then flows over a relatively flat area of land and then falls steeply (possibly another schist block) onto another flat area of land creating a ponding area with the nearby Swamp Spring, a good example of typical landslide terrain (hummocky) can be seen at the top of the above photo. The Cattlestop Spring is a contact spring. Groundwater flows downslope where it comes into contact with the schist block, a relatively impermeable barrier, just behind Cattlestop Spring where flow is then diverted to the easiest flow path, which is now under the schist block. Where the block ends, the ground water then begins to flow above ground. In this case, the water flow has eroded away the material where the groundwater flow exits under the schist block, and has created the scarp that can be seen in Photo D1. The Cattlestop Spring is a permanent spring and tends to be roughly linear at the base of the schist block. There is also some flow over/through the schist block, though it is probably better classified as seepage, possibly from water flow over the top of the block or through the block as the water table is diverted behind and below , some water may penetrate through.

The weir is located at the base of the steep bank, see photo above, and was installed on the 15/04/2008, Photo D2 below is a close-up of the weir after it was installed. The material in which the weir was installed was quite soft due to the proximity of the water and tended to be soil with some small schist debris of approximately 5cm in size. The initial flow rate after half an hour was 0.25 litres per second.

Photo D2: Weir at base of steep bank (15/04/2008).

B) Swamp Spring and Weir:

GPS Spring: Northing: 5576500
Easting: 2171821
Height: 879 metres

GPS Weir: Northing: 5576500
Easting: 2171821
Height: 879 metres

The Swamp Spring is located at the base of large bank where there is an outcrop of a schist block. The spring appears to be flowing out from underneath the block at ground level from the entire length of the outcrop (approximately 5 metres), creating a slow flowing stream that leads into a ponding area where it is joined by the Cattlestop Spring. Swamp Spring is an artesian/contact spring. The water released from this spring is due to the pressure of the groundwater beneath pushing up against the schist block and forcing the water to flow along the base on the flow-path of least resistance until it outcrops. Swamp Spring is also classed as a contact spring due to groundwater coming into contact with the relatively impermeable schist block and causing the original flow-path to change. The spring flow is permanent, though at times may be considered a seep and due to the shape of the schist block the flow is linear only approximately five metres of the schist outcrop (see Photo D3).

The weir (see Photo D3 below) was installed approximately 2-3 metres away from where the spring exits the ground and was installed in water-logged mud on the 15/04/2008. The initial flow rate of the Swamp Spring was 0.4 litres per second after half an hour.

Photo D3: Swamp Spring and Weir (15/04/2008).

C) Wired Spring and Weir:

GPS Spring: Northing: 5576637
Easting: 2171871
Height: 968 metres

GPS Weir: Northing: 5576610
Easting: 2171943
Height: 921 metres

Photo D4: Wired Spring (14/04/2008).

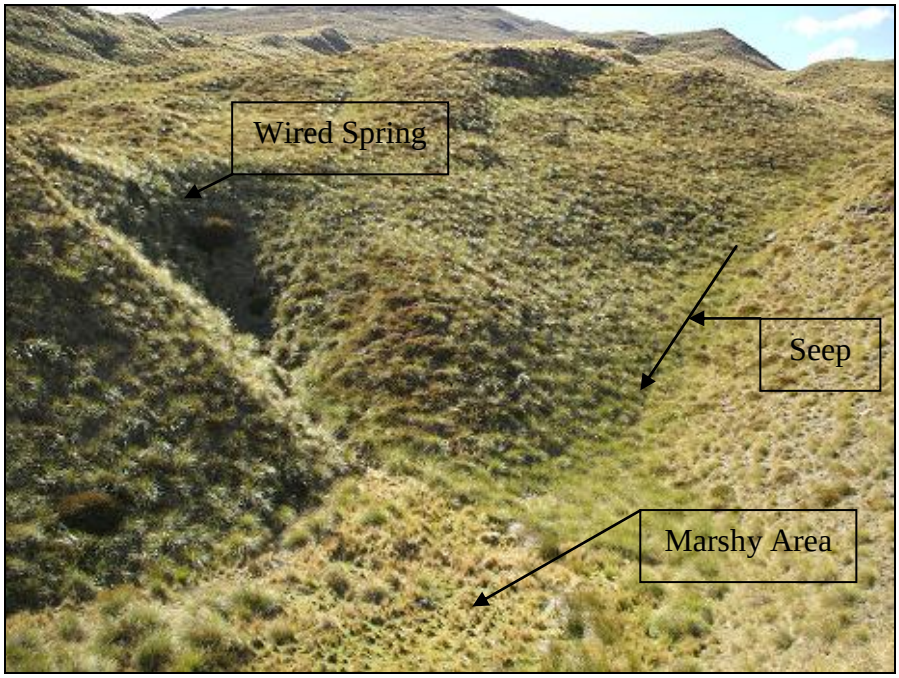

The Wired Spring is a permanently flowing spring and is located in the middle of a steep scarp (block) with possible flow from above occurring as well (see Photo D4 above). This spring is a fracture spring, where the majority of the flow is due to water flowing through the fractures within the schist block, most likely through the natural fabric of the schist itself known as schistocity. The spring flows down-slope in between many steep scarps interpreted as schist blocks before it reaches the site where the weir is located. There are other smaller sources of water (as seen in the above photo) that contribute minimally to the flow rates obtained.

The weir was installed on the 15/04/2008 and seen in Photo D5, and is approximately 50 metres downstream of the Wired Spring and has an initial flow rate of 0.25 litres per second. The weir was installed in soil with schist debris ranging in size from approximately 1-10 centimetres.

Photo D5: Wired Weir (14/04/2008).

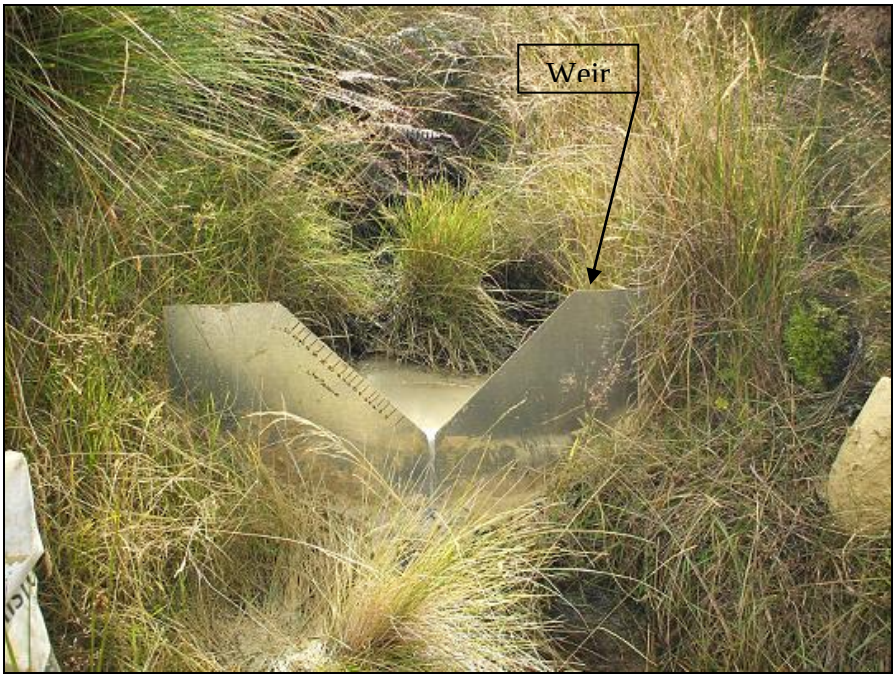

D) Pond Spring and Weir:

GPS Spring: Northing: 5576933
Easting: 2172541
Height: 977 metres

GPS Weir: Northing: 5576882
Easting: 2172550
Height: 965 metres

Photo D6: Pond Spring (14/04/2008).

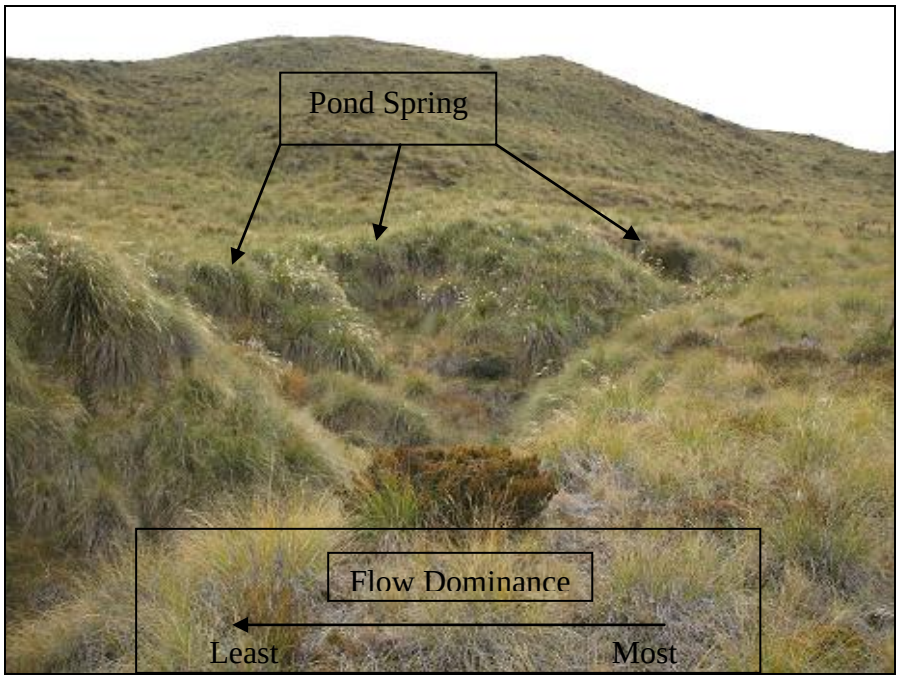

Pond Spring has three lobes where water flow occurs, the right side is dominant whilst the left side has the least flow. Probable flow over top of schist block – a contact spring with permanent 'horizontal' flow, as seen in above in Photo D6.

The weir (seen in Photo D7) was installed in a steep miniature gully that is dominantly comprised of schist debris that made the installation harder as a lot of bentonite was needed to stop leakage underneath the weir via pathways in between the small schist blocks. Flow after half hour from when the weir was installed on the 15/04/08 was 0.5 litres per second.

Photo D7: Pond Weir (14/04/2008).

The Pond Spring, after flowing through the weir then runs under the Coronet Peak Road in a culvert and then onto farm property into a pond on the other side (Photo D8 below).

Photo D8: The pond in which Pond Springs flows into after the road (28/02/2008).

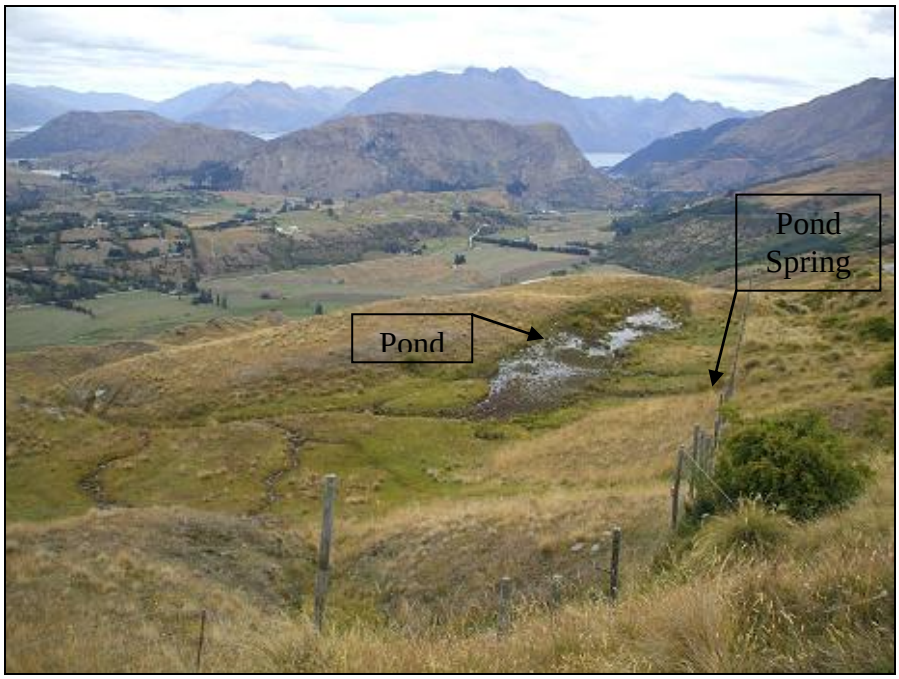

E) Bramble Spring and Weir:

GPS Spring: Northing: 5577230
Easting: 2172520
Height: 1059 metres

GPS Weir: Northing: 5576928
Easting: 2172632
Height: 966 metres

Photo D9: Bramble Spring looking down slope (17/04/2008).

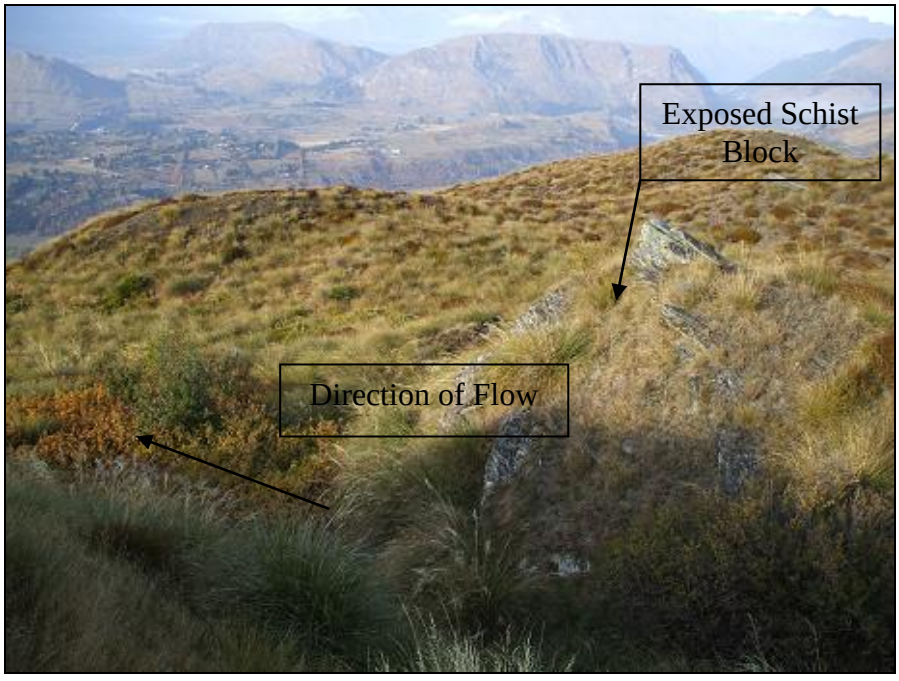

The Bramble Spring looks to begin at the base of a steep bank, a buried schist block, and then flows around an exposed schist block, but it is only damp here in the warmer months (seepage) and if there is flow it probably only occurs in the high flow season of spring with the snow melt. However, flow becomes prominent down slope from this and a clear miniature gully has formed right down to the Coronet Peak Road where it then flows under the road in a culvert and onto farm property. This spring is a contact spring due to the water table coming into contact with the buried schist

block and then was pushed underneath it and re-emerged on the other side of the block where it eroded the landslide debris and began to flow at the grounds surface.

Photo D10: Bramble Weir (16/04/2008).

The weir (Photo D10 above) was installed on the 16/04/2008 just below Coronet Peak Road before it runs onto farm property and had a flow rate of 0.5 litres per second after the initial half an hour after the weir was installed.

F) Coronet Peak Road Spring and Weir.

GPS Spring: Northing: 5577088
Easting: 2172750
Height: 1010 metres

GPS Weir: Northing: 5577012
Easting: 2172749
Height: 985 metres

Photo D11: Coronet Peak Road Spring (28/02/2008).

The Coronet Peak Road Spring (Photo D11 above) creates a bowl shaped depression where it exits the ground. There are no visible explanations for the spring to appear here, that is, there are no obvious schist blocks to impede the flow of the ground water, therefore the spring occurs here due to the outcropping of the water table at this point and so it is termed a 'depression spring' – a spring which is the result of where the water table intersects the ground surface. This spring is a permanent, concentrated point spring.

Coronet Peak Road Weir (Photo D12) was installed on 15/04/2008. There was some initial leakage when checked on one to two days after the installation, but more bentonite was added and the weir became impermeable. The initial flow was 0.8 litres per second and remained steady when further measurements were taken.

Photo D12: Coronet Peak Road Weir (15/04/2008).

G) Multiple Spring and Weir:

GPS Spring: Northing: 5577252
Easting: 2172972
Height: 975 metres

GPS Weir: Northing: 5577241
Easting: 2172973
Height: 973 metres

Photo D13: Multiple Spring (17/04/2008).

The Multiple Spring (as seen in Photo D13 above) flows over the top of a bank, probable schist block, as the spring appears at the base of a very steep bank that has been eroded by the water flow through the spring. This type of spring is known as an Artesian/Contact spring. The spring itself seems to have many sources of water where on site there are small gullies upstream of the weir that have no flow but are damp so they are ephemeral and may only flow in springtime when the water flow is the highest.

Photo D14: Multiple Spring Weir (16/04/2008).

The Multiple Spring weir (as seen above) was installed on the 16/04/2008 where the initial flow was 0.5 litres per second. It was installed in soft soil with small amounts of schist debris.

H) Hairpin Spring and Weir.

GPS Spring: Northing: 5577273
Easting: 2173083
Height: 966 metres

GPS Weir: Northing: 5577254
Easting: 2173093
Height: 962 metres

Photo D15: Hairpin Spring (28/02/2008).

Hairpin Spring (Photo D15) flows over and/or through (fracture spring) a large schist block down onto a relatively flat surface and then down onto the farmland below the Coronet Peak Recreation Reserve. The material in which the weir was constructed in tended to be quite large pieces of schist of approximately 10-15 centimetres with some small schist debris in a matrix of silts. The spring flow is permanent and is concentrated at the base of the schist block, however, there is a small amount of water that seeps down over the front of the block.

The weir was installed on the 16/04/2008 and the initial flow after about half an hour was 2 litres per second, see Photo D16.

Photo D16: Hairpin Weir (16/04/2008).

I) Grassy Spring.

Spring GPS: Northing: 5577489
Easting: 2173246
Height: 1003 metres

Weir GPS: Northing: n/a
Easting: n/a
Height: n/a

Photo D17: Grassy Spring, with Gobblers Stream in foreground and in the upper left area of the photo is Twin Spring (21/04/2008).

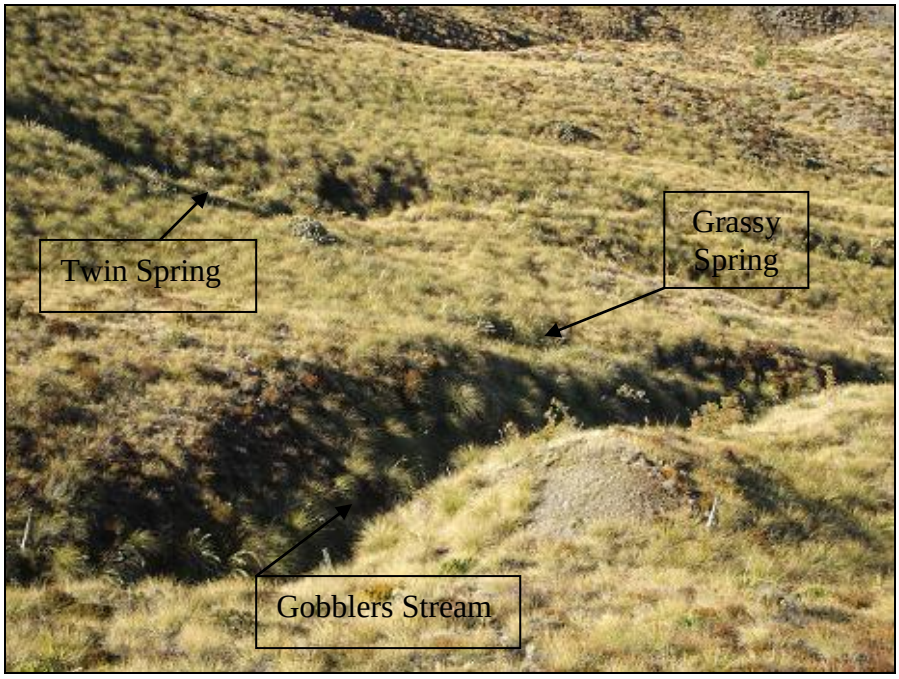

The Grassy Spring may flow over a schist block as the spring flows at the base of a steep bank that then leads into the Gobblers Stream only approximately 10 metres down stream of the spring, therefore it is a contact spring. The large blocks of schist that are seen in the bed of the spring that have impeded the installation of the weir at this site also suggest this. The flow is permanent and concentrated.

There was no weir installed at this spring location as the spring was comprised of schist blocks of a size that would have made making the weir impermeable impossible except with an excavator which would not have been able to have been driven to the spring site. Therefore the spring was monitored via a bucket and stopwatch. This method is not as accurate as using a weir but is the only method available to this site. The initial flow of the spring was approximately one litre per second.

J) Twin Spring and Weir

Spring GPS: Northing: 5577497
Easting: 2173272
Height: 982 metres

Weir GPS: Northing: 5577488
Easting: 2173282
Height: 974 metres

Photo D18: Twin Spring (23/04/2008).

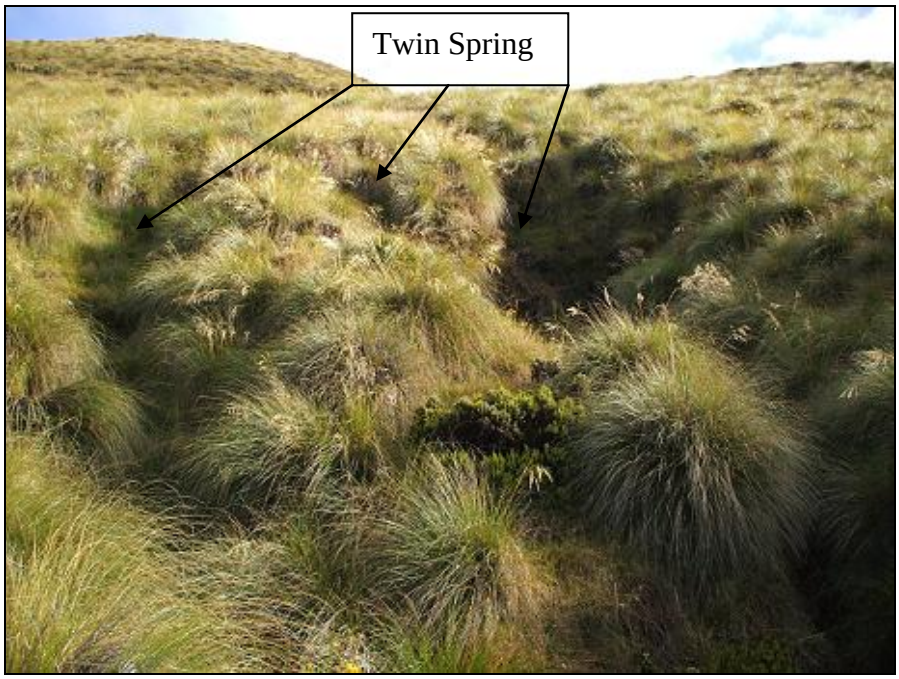

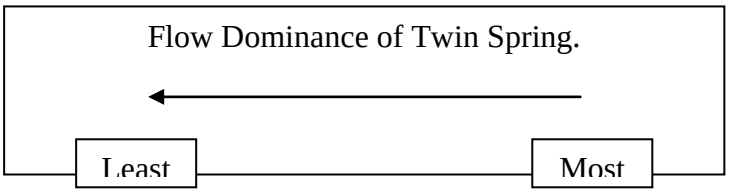

The Twin Spring flows over a schist block, characterising it as a contact spring. It has three sources of water flow; the water source on the right of Photo D18 above is the dominant source, with flow decreasing towards the left. The flow is permanent and is also linear.

The weir was installed on the 23/04/2008, see Photo D19 below, just below where the three water sources converge on each other and had an initial flow of 0.4 litres per second. The material in the streambed was small schist debris ranging from cobble to fine sand sized particles, with some larger schist blocks up to 10 centimetres in length.

Photo D19: Twin Spring weir (21/04/2008).

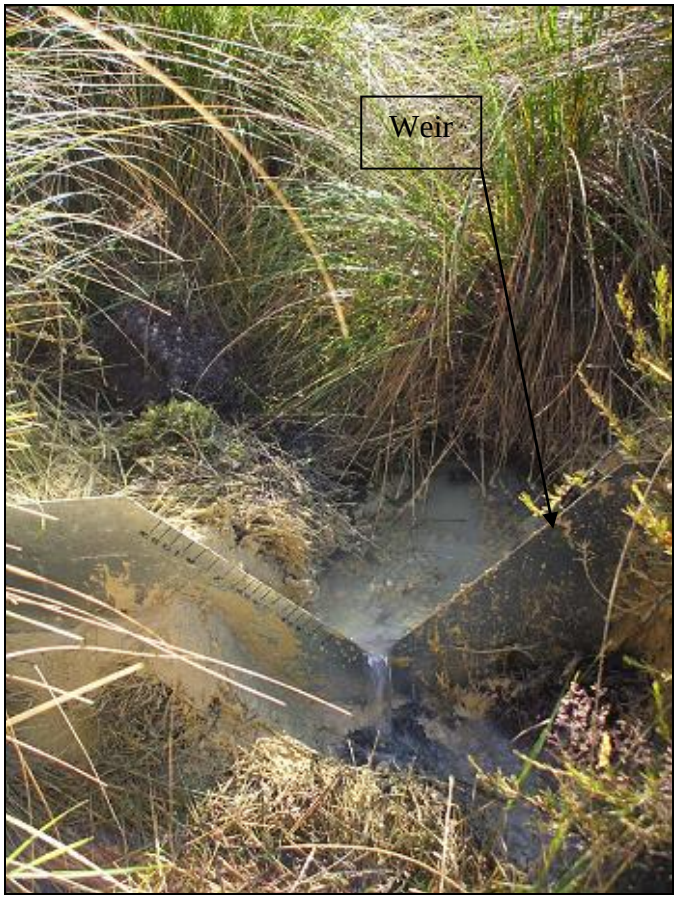

K) Tussock Spring and Weir.

Spring GPS: Northing: 5577653
Easting: 2172992
Height: 1128 metres

Weir GPS: Northing: 5577648
Easting: 2172992
Height: 1125 metres

Photo D20: Tussock Spring (23/04/2008).

Tussock Spring is located at the base of a very steep bank just below the Coronet Peak Road. This spring can be interpreted as a contact spring due to the water flow occurring at the base of the schist block, however the block itself is mossy so there may also be a component of fracture flow through the natural defects within the schist block. The spring itself has four different water sources that converge on each other just above where the weir is placed and then flow in between what looks like the

base of this block and another (in the bottom right-hand corner of Photo D20), and then makes a sharp turn eastward as the latter block ends and the spring cuts a gully into the earth. The dominant water source for the Tussock Spring is the central miniature gully in the above photo.

The weir was installed on the 23/04/2008, see Photo D21, and had an initial flow of 1.9 litres per second. The material in the streambed tended to be small schist blocks of an approximate size between 2-10 centimetres, which is indicative of a schist block being in close proximity to the spring.

Photo D21: Tussock Spring Weir (23/04/2008).

L) Gobblers Spring.

Spring GPS: Northing: 5578104
Easting: 2173238
Height: 1200 metres

Weir GPS: Northing: n/a
Easting: n/a
Height: n/a

Photo D22: Gobblers Spring as at 29/02/2008.

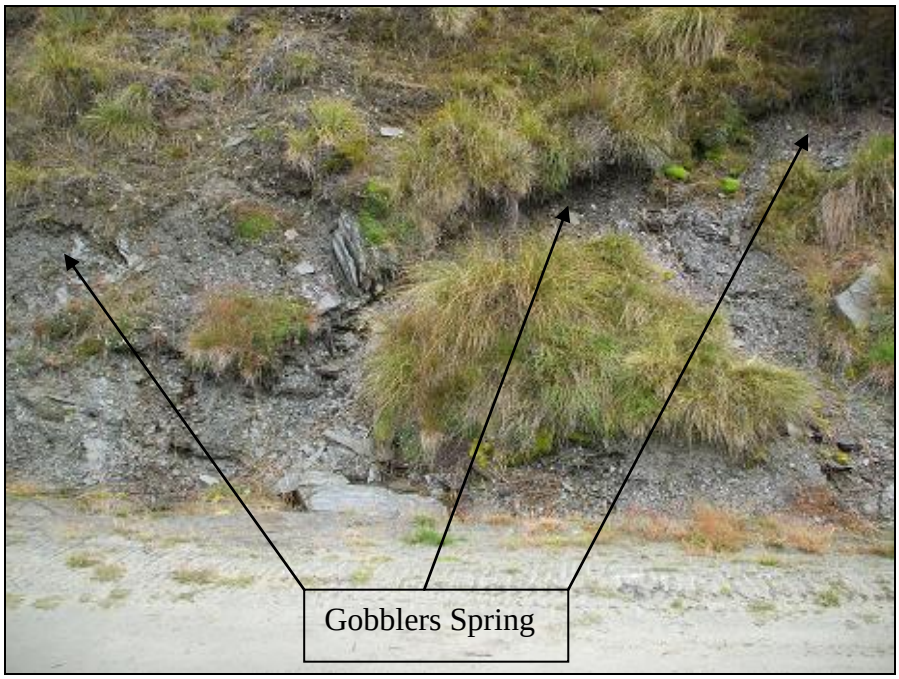

Gobblers Spring is situated just above the access road as seen in the above photo. The spring seeps through a schist block (fracture spring) in many places and then pools in the road drainage where it then runs through a number of culverts until it reaches Reservoir #2 where it is then pumped up to the snow guns on the mountain to make snow. The spring is a fracture flow spring as the ground water flows straight from the schist block; the flow is permanent and diffuse.

There was a weir installed at this site but a new water collection area and pipes were to be laid, so the weir was excavated back up along with some of the schist material (see Photo D23). The initial flow rates from this weir were between 0.4-0.5 litres per second between the time period of the 17/03/2008 to the 20/03/2008. The measuring of the water flow from this spring now has to be monitored via a bucket and stopwatch system down slope before it enters Reservoir 2.

Photo D23: Gobblers Spring (24/04/2008), after the excavation and installation of collection area.

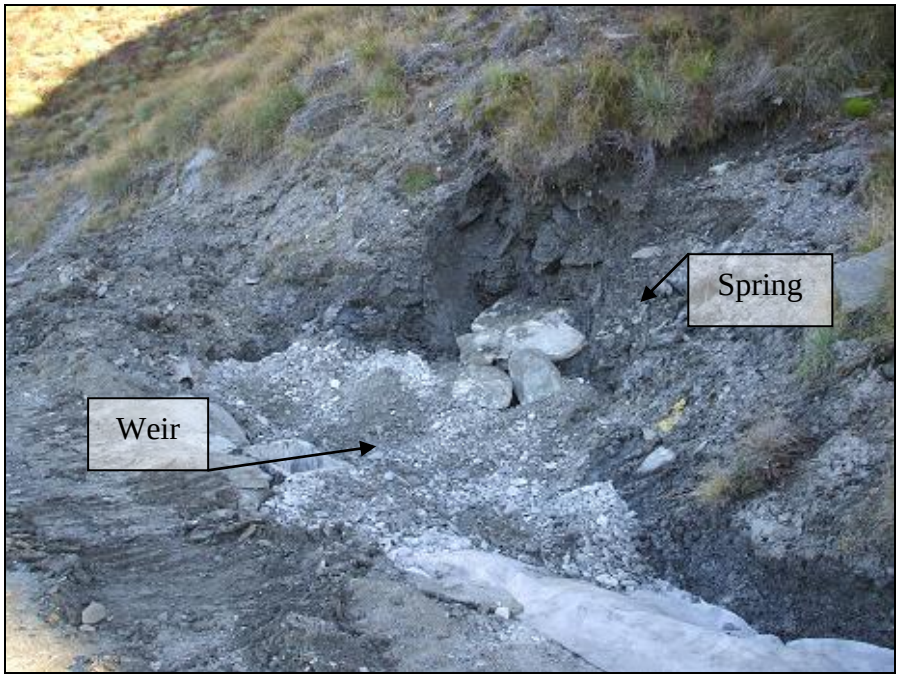

M) Wall Street Spring and Weir.

Spring GPS: Northing: 5578209
Easting: 2173340
Height: 1256 metres

Weir GPS: Northing: 5578176
Easting: 2173351
Height: 1245 metres

Photo D24: Looking up to the Wall St Spring (29/02/2008)

The Wall Street Spring, as seen in Photo D24 above, creates a characteristic depression in the ground surface and is known as a ‘depression spring’, where the water table intersects the ground surface. However there is a steep bank approximately 10-15 metres behind the spring that could be a hidden schist block that is diverting the water table and causing it to make contact with the ground’s surface creating the spring. The bed of the stream created by the Wall Street Spring is dominated by ground up schist debris with small schist blocks. The spring flow is concentrated and permanent.

The Wall Street Weir was installed on the 12/04/2008 and had initial flow rates of 0.4 litres per second half an hour after installation, the location of this is pointed out on Photo D24 above.

N) Water Supply Spring and Weir.

Spring GPS: Northing: 5578112
Easting: 2173440
Height: 1161 metres

Weir GPS: Northing: n/a
Easting: n/a
Height: n/a

Photo D25: Water Supply Spring (21/04/2008).

The Water Supply Spring supplies all the ski buildings with water all year round. It flows permanently and is accessed and collected by the pipe seen in the photo above and then pumped to the buildings to be used. There is less flow data for this spring than for the other springs as there had been no monitoring done until August 2008. What can be seen in the above photo has been updated, and it is now covered with a manhole, but a weir has been installed and the flow rate obtained on the 18/09/2008 was 2 litres per second. As the natural environment of the Water Supply Spring has been modified, the nature of the spring is difficult to define.

This is possibly a fracture spring that the Coronet Peak Skifield staff have dug down into the side of the mountain and tapped into the rock where the groundwater is sourced.

O) Station Spring and Weir.

Spring GPS: Northing: 5577906
Easting: 2173651
Height: 1133 metres

Weir GPS: Northing: 5577888
Easting: 2173658
Height: 1123 metres

Photo D26: Station Spring (13/03/2008).

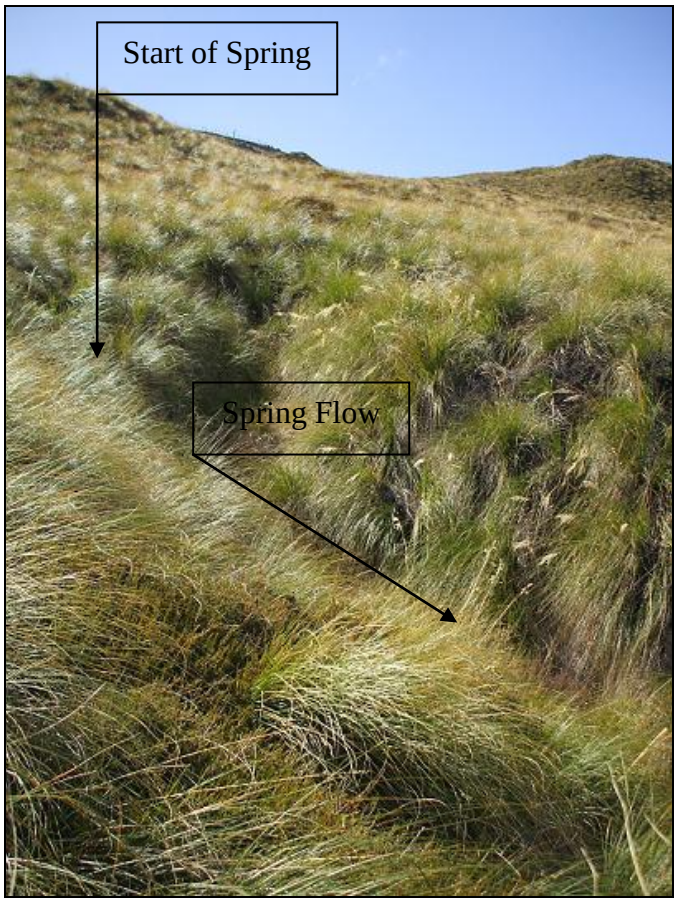

The Station Spring is located below the access road that runs beneath the main building of the Coronet Peak Skifield. The Station Spring creates a bowl shaped impression in the ground and is interpreted as a ‘depression’ spring where the water table intersects the ground surface, see Photo D26 above. The spring flow is permanent and concentrated.

Photo D27: Station Spring Weir (20/04/2008).

The weir was installed on the 20/04/2008 and had an initial flow rate of 0.4 litres per second, see photo above. The weir is predominantly fixed in soil with little schist debris, this fits in with the spring being a depression spring, as it has not formed here due to the presence of a large schist block and therefore lacks the schist debris in it’s bed.

P) Danni's Spring and Weir.

Spring GPS: Northing: 5578163
Easting: 2174223
Height: 1187 metres

Weir GPS: Northing: 5578164
Easting: 2174559
Height: 1184 metres

Image D28: Google Earth image of Danni's Spring.

Danni's Spring is slightly to the west of Heidi's Spring and enters the pool where Heidi's Spring flows in to be pumped to the reservoirs, see the image above. The spring is a contact spring as it flows over a schist block, possibly the same large schist block as Heidi's Spring. The spring flow is permanent and concentrated, unlike Heidi's Spring which is diffuse.

The weir (seen below in Photo D29) was installed on the 17/04/2008 and had an initial flow rate of 1.2 litres per second. The weir is set into soil and schist debris and there are small schist blocks of approximately 15 centimetres in size.

Photo D29: Danni's Weir (17/04/2008).

Q) Heidi's Springs and Weir.

Spring GPS: Northing: 5578196
Easting: 2174249
Height: 1208 metres

Weir GPS: Northing: 5578164
Easting: 2174239
Height: 1175 metres

.

Photo D30: The beginning of Heidi's Springs (17/04/2008).

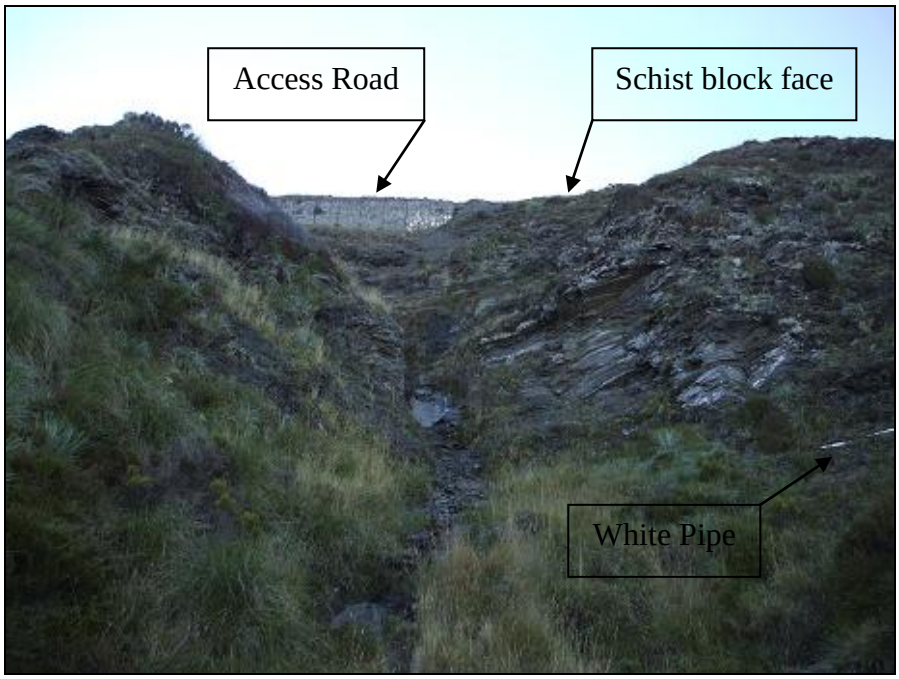

Heidi's Springs are a group of several water sources within the same area that all converge to create the McMullan Stream. The springs are located next to Heidi's Hut and exit the ground surface in the middle of a huge rock face, making it a fracture spring (seen in Photo D30 above). At the base of this rock face is a dam and pump where the spring waters accumulate and are pumped around the ski field to reservoirs for water storage, see PhotoD31 for pump and weir location. The white pipe that can

be seen in the Photo D30 above is directing water here from Waterfall Spring to add to the water source available for the snow guns, however little water actually flow through this pipe. Heidi's Spring has a permanent and diffuse flow due to the several sources of water.

Photo D31: Heidi's Spring, dam and pump (03/03/2008).

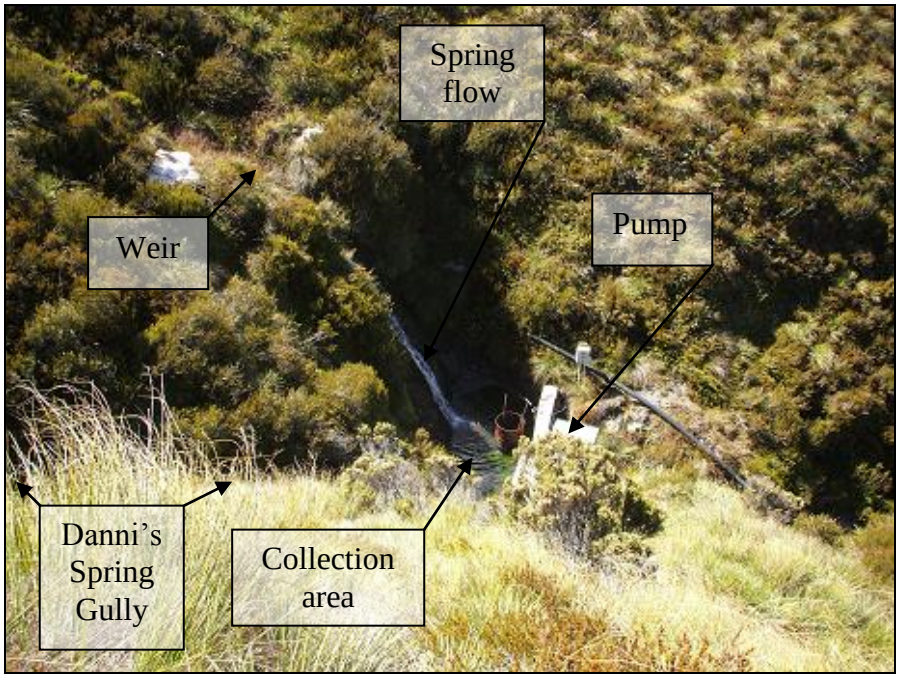

Heidi's weir was installed on the 17/04/2008 and had an initial flow rate of 2 litres per second. The weir is located near the base of the rock face just above the dam and pump (in Photo D31 above) and measures the total flow rate from most of the water sources in this area, Photo D32 below. The material in which the weir was constructed was totally schist debris ranging in size from 2 cm to 25-30 cm.

Photo D32: Heidi's Weir (17/04/2008).

R) Moss Spring and Weir.

Spring GPS: Northing: 5577966
Easting: 2174410
Height: 1120 metres

Weir GPS: Northing: 5577884
Easting: 2174423
Height: 1113 metres

Photo D33: Google Earth image of Moss Spring.

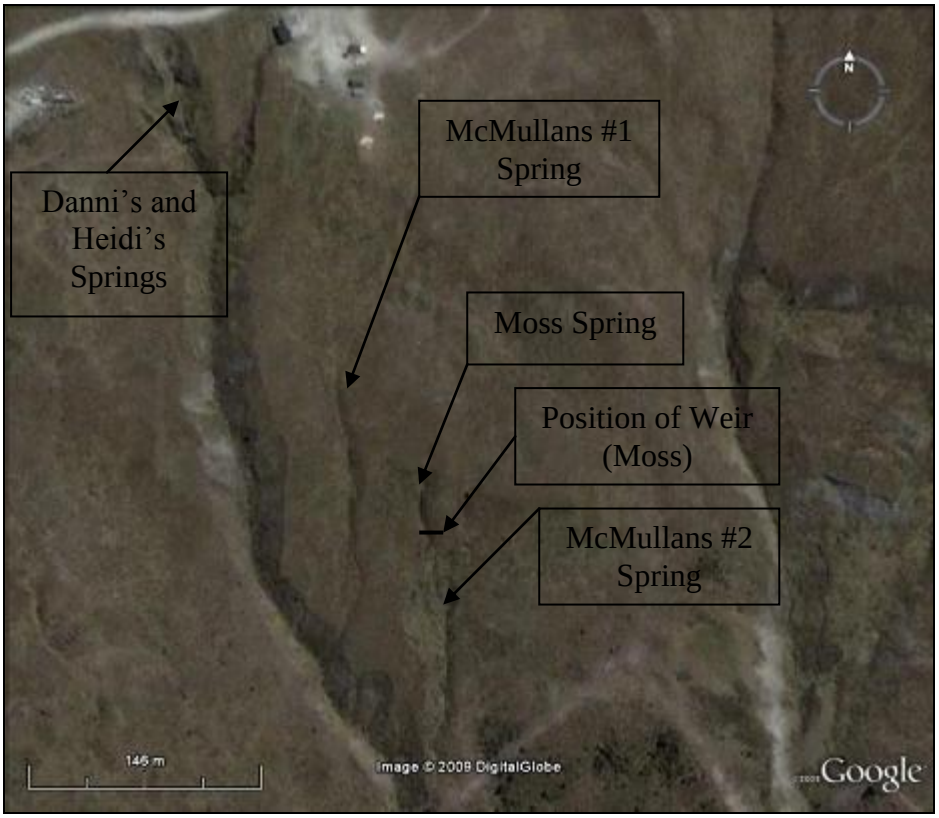

The Moss Spring lies in between the McMullan Springs, (McMullan #1 Spring showing no flow during the times of monitoring) and joins the stream created by the McMullan #2 Spring down slope which in turn flows into the McMullan Stream. The Moss Spring is located at the base of a steep bank and flows over a large schist block and is interpreted to be a 'contact' spring. This spring is a permanent feature.

The weir was installed at the base of the schist block on the 14/04/2008, the location of the weir is shown in Photo D33 above, and was fixed in predominantly schist debris material. The initial flow rate was 0.2 litres per second.

S) McMullan #2 Spring and Weir.

Spring GPS: Northing: 5577961
Easting: 2174405
Height: 1112 metres

Weir GPS: Northing: 5577930
Easting: 2174405
Height: 1107 metres

The McMullan #2 Spring is located to the east of Moss Spring. The spring flows over a large schist block creating a contact spring or possibly a fracture spring as the schist block is broken in places. The McMullan Spring flows downslope into the McMullan Stream and has a permanent flow. The photo below (D34) indicates the spring flow, the spring itself is approximately 15 metres in the opposite direction of flow down to the left of this photo.

Photo D34: McMullans #2 Weir (14/07/2009).

A weir was installed in McMullan #2 spring on the 14/04/2008 that had an initial flow rate of 1 litre per second. The weir sits at the down stream end of a small pond (see Photo D34) created by the spring where part of the schist block has broken away from the main block, possibly due to the spring seeping in through a fracture in the block and widening it through time via erosion. The material in which the weir was installed had a lot of schist debris due to the close proximity of the schist block, as well as silt.

T) Waterfall Spring and Weir.

Spring GPS: Northing: 5578372
Easting: 2174559
Height: 1279 metres

Weir GPS: Northing: 5578372
Easting: 2174559
Height: 1278 metres

Photo D35: Waterfall Spring (03/03/2008).

The Waterfall Spring is located to the east of the Coronet Peak Ski field at the base of a steep bank, a schist block, making this spring a contact or possibly a fracture spring, either the water flows under or through the schist block, or both. This spring water has been utilised in the past as there is an old dam here that used to pool the water behind it and then pump it elsewhere, but there is now a pipe (just out of sight of Photo D35) that takes some of the water here to Heidi's Springs. Further downstream there is evidence of another schist block as there is a small waterfall flowing over a schist block, Photo D36. The flow here is permanent and concentrated.

Photo D36: Waterfall Spring flowing over schist block (03/03/2008).

The Waterfall Weir in Photo D37 below was installed on the 17/04/2008 and had an initial flow rate of 1 litre per second. The weir is set in a bed of schist debris of variable sizes that is typical of the spring being in close proximity to a schist source.

Photo D37: Waterfall Weir (17/04/2008).

U) Grasshopper Spring and Weir:

Spring GPS: Northing: 5578145
Easting: 2174782
Height: 1231 metres

Weir GPS: Northing: 5578127
Easting: 2174775
Height: 1222 metres

Photo D38: Grasshopper Spring (03/03/2008).

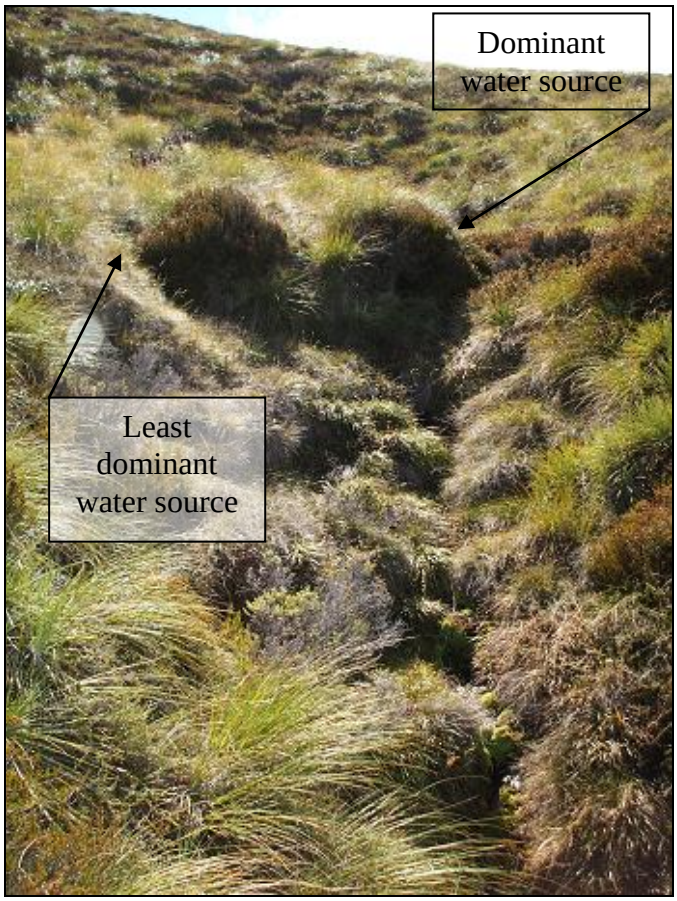

The Grasshopper Spring flows over the top of a schist block and creates a sort of slump in the upper layer of the ground surface. This spring is the eastern most spring on the Coronet Peak Recreation Reserve, with the Waterfall Spring to the west.

There are two sources of water within this spring, the right source in Photo D38 above being the most dominant. This spring is a contact spring where the water table has come into contact with a large schist block and has been diverted over it instead of under it; this is evident in the position of the spring as it begins to flow near the top of a steep slope instead of near the base of it.

The Grasshopper Weir in Photo D39 below was installed on the 17/04/2008 and had and initial flow of 0.5 litres per second, the flow is permanent. The material in which the weir was fixed tended to be mostly soils with some schist debris up to 10 centimetres in length.

Photo D39: Grasshopper Weir (17/04/2008).

V) Lunch Rocks Spring and Weir.

Spring GPS: Northing: 5578726
Easting: 2174057
Height: 1381 metres

Weir GPS: Northing: 5578658
Easting: 2174099
Height: 1364 metres

Photo D40: Lunch Rocks Spring (28/02/2008).

The Lunch Rocks Spring (seen in Photo D40 above) flows over the top but mostly through a large schist block, therefore it is a fracture spring. There are many water sources within this spring (diffuse flow) and the ground surface is damp and

mossy right from the very top of the scarp, with flow beginning approximately halfway down the slope.

The Lunch Rocks Weir (seen below in Photo D41) was installed on the 17/04/2008 and is approximately 50 metres away from the start of the spring flow as the flow is concentrated down in the middle of the valley. The material the weir is fixed in tends to have little schist debris and so is mostly soils, this reflects the distance from the schist block. The initial flow rate here was 0.3 litres per second. The Lunch Rocks Weir also collects water from the nearby spring, Rocky Gully.

Photo D41: Lunch Rocks Weir (18/04/2008).

W) Rocky Gully Spring.

Spring GPS: Northing: 5578718
Easting: 2174076
Height: 1368 metres

Photo D42: Rocky Gully Spring (28/02/2008).

The Rocky Gully Spring (Photo D42 above) is located at the western end of the Rocky Gully Reservoir. It has had to be modified due to the construction and completion of the reservoir, so that now the spring flows into a cut-off drain, where the flow is diverted to the Lunch Rocks area in the next valley. The Rocky Gully Spring is either a contact or fracture flow spring, where the water table either flows over or under a schist block, or through it. The spring is permanent but the flow is diffuse and there are many sources within the scarp it has created.

The flow from the Rocky Gully Spring is diverted to the Lunch Rocks area and so contributes to the flow measurements of the Lunch Rocks Weir, however when checked, no flow was seen from the pipe.

X) Easy Rider Spring and Weir.

Spring GPS: Northing: 5578607
Easting: 2174175
Height: 1358 metres

Weir GPS: Northing: 5578597
Easting: 2174173
Height: 1356 metres

Photo D43: Easy Rider Spring (28/02/2008).

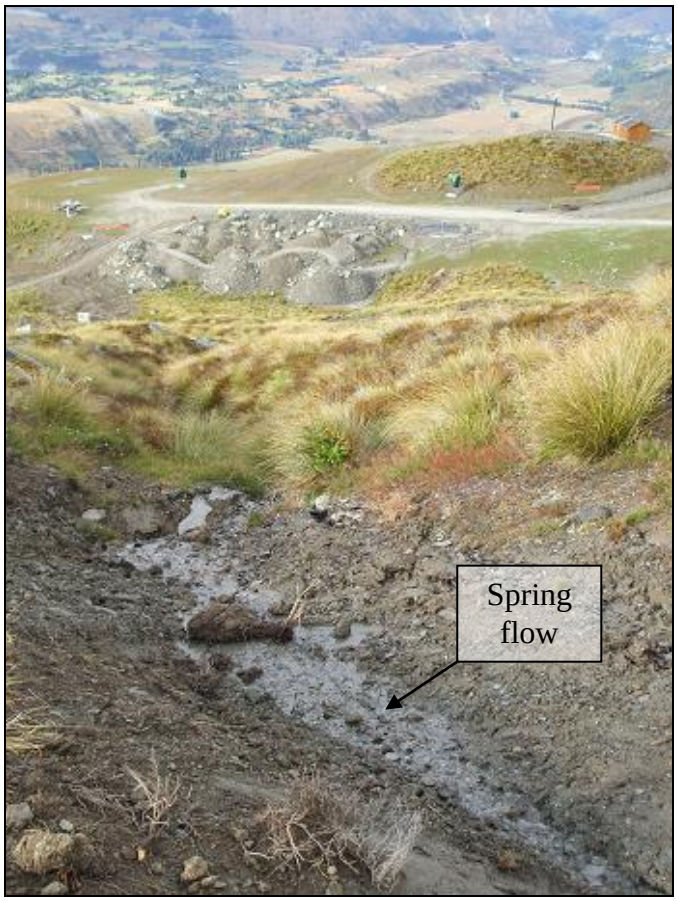

Easy Rider Spring is located to the east of the valley in which Lunch Rocks Spring is found, downslope from the Rocky Gully Reservoir. This slope has been bulldozed (as seen in Photo D43 above), due to the construction of the reservoir

above. Initially the spring flowed approximately 20-30 metres up-slope from where it flows today. Therefore it is difficult to determine the type of spring this is, but there is a large schist block at the top of this slope and so it could be assumed that this is a contact spring, caused by permeable water carrying strata coming into contact with materials that have less permeable characteristics, such as a schist block. The flow is slow, but permanent and concentrated. The natural course of the spring downslope has not been modified to the same extent and the flow creates a small gully that joins with the Lunch Rocks Spring and flows down into McMullans Stream below Heidi's Hut.

The weir was installed here on the 17/04/2008 and had an initial flow of 0.2 litres per second. The weir was fixed in material that has been reworked by construction equipment and so there is no real soil at this location, the material tends to be dominantly schist debris in mud, see photo below.

Photo D44: Easy Rider Weir (17/04/2008).

Y) Dirty Four Spring and Weir.

Spring GPS: Northing: 5578469
Easting: 2172556
Height: 1265 metres

Weir GPS: Northing: 5578483
Easting: 2172587
Height: 1209 metres

Photo D45: Dirty Four Spring (23/09/2009).

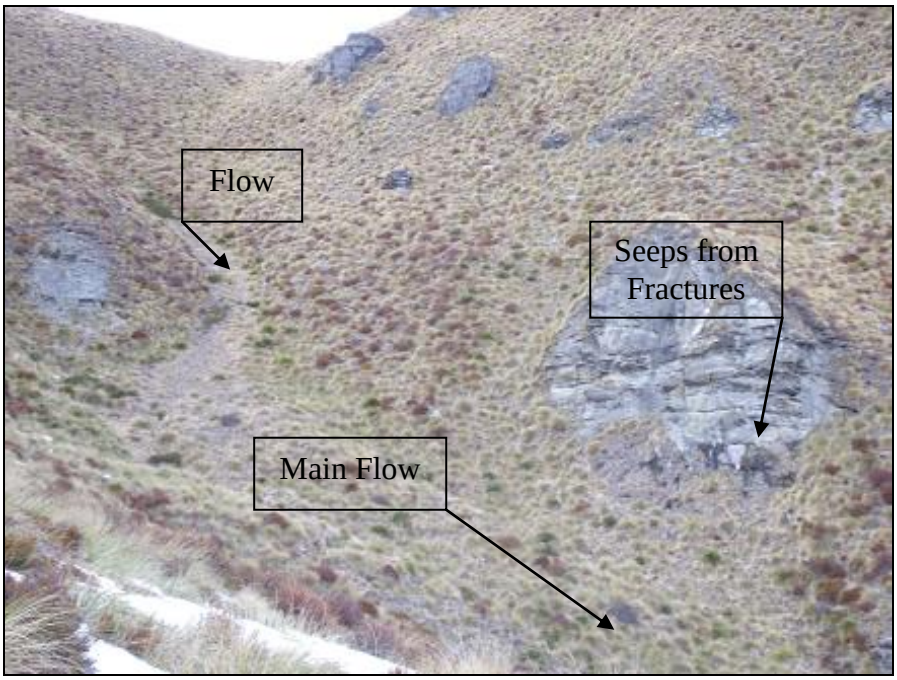

The Dirty Four Spring is a collection of small springs and seeps all in the same small valley system on the far western side of the Coronet Peak Ski Field. All the water sources here seem to either flow at the base of large schist blocks that make up the sides of the valley, or flow over buried schist blocks to become exposed at the surface creating springs, the ground within the valley is very damp and mossy. Therefore, these springs are of a 'contact' type where a permeable water-bearing layer

intersects with a less permeable layer creating a spring or seep at either the top or the base of the impermeable material, schist blocks. However, as seen in the photo above, there are also seeps through the schist blocks.

Photo D46: Dirty Four Weir (04/03/2008).

The weir was installed here in 2006 and is of a different shape to the other weirs used in this study, though it is still a v-notch weir, but of a different angle, 45-degrees instead of 90 (see Photo D46 above). The flow rate on the 16/04/2008 was 2.05 litres per second. The Table D-2 above shows the flow rates in relation to the height of water flow from the intersection of this type of v-notch weir.

Z) Dirty Creek Spring and Weir.

Spring GPS: Northing: 5578726
Easting: 2172595
Height: 1380 metres

Weir GPS: Northing: 5578607
Easting: 2172515
Height: 1309 metres

Photo D47: Looking towards the Dirty Creek Spring (21/04/2008).

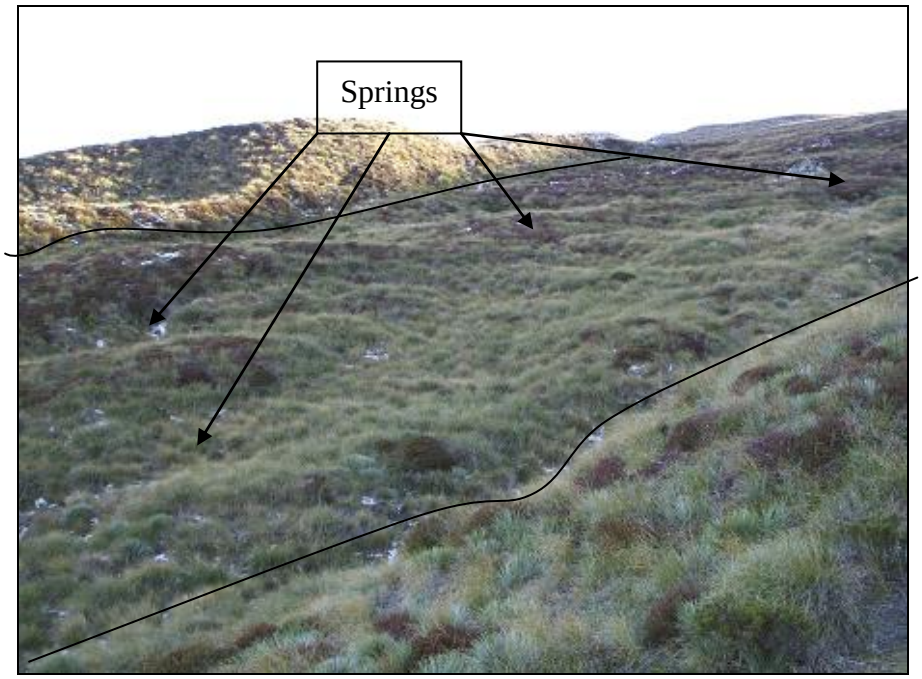

The Dirty Creek Spring is the most western spring found on the Coronet Peak Ski Field. There are many water sources that flow over the top of a large schist block, the area in the centre of Photo D47 is very damp and mossy. This spring is known as a contact spring. The spring flow is very diffuse and covers a large area until further down slope the spring flow concentrates in a small gully.

The Dirty Creek Weir (seen in Photo D48 below) was installed in the small gully created by the spring flow on the 21/04/2008. It was constructed in schist debris and had an initial flow of 0.3 litres per second.

Photo D48: Dirty Creek Weir (21/04/2008).

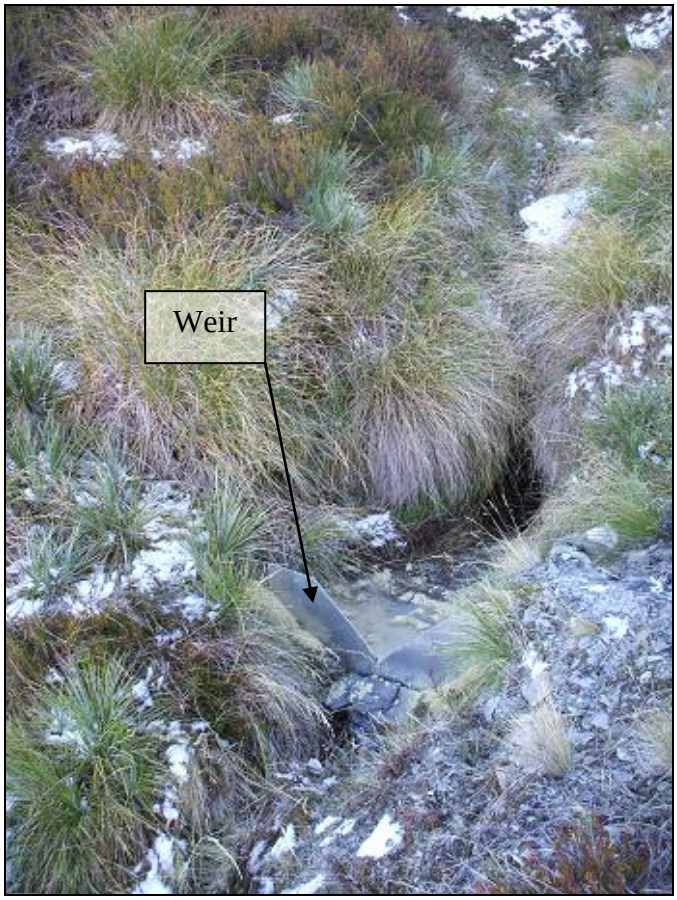

Appendix E:

Spring Stable Isotope Variations

Figure E-1:

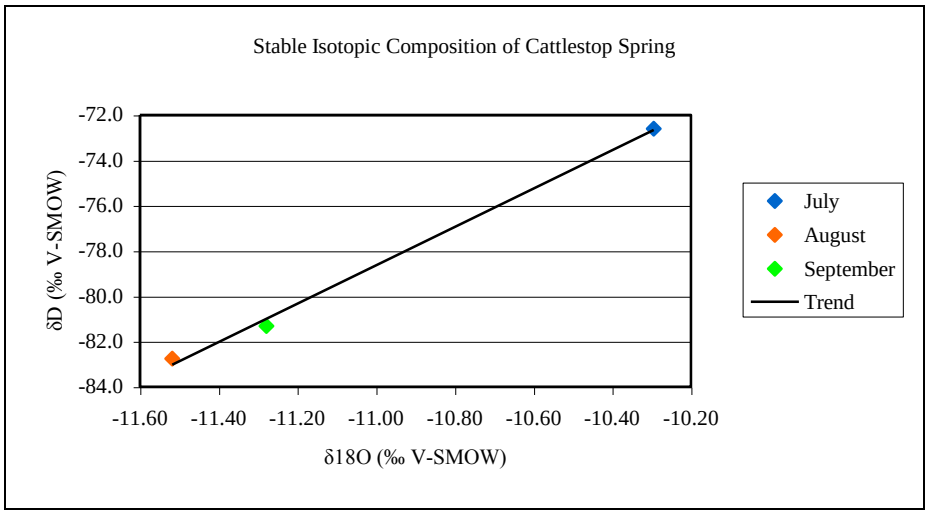

Figure E-2:

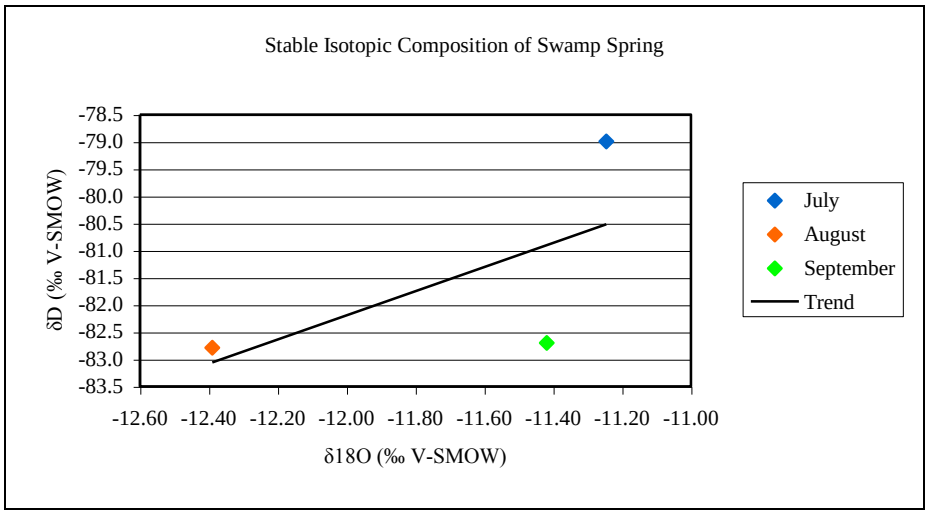

Figure E-3:

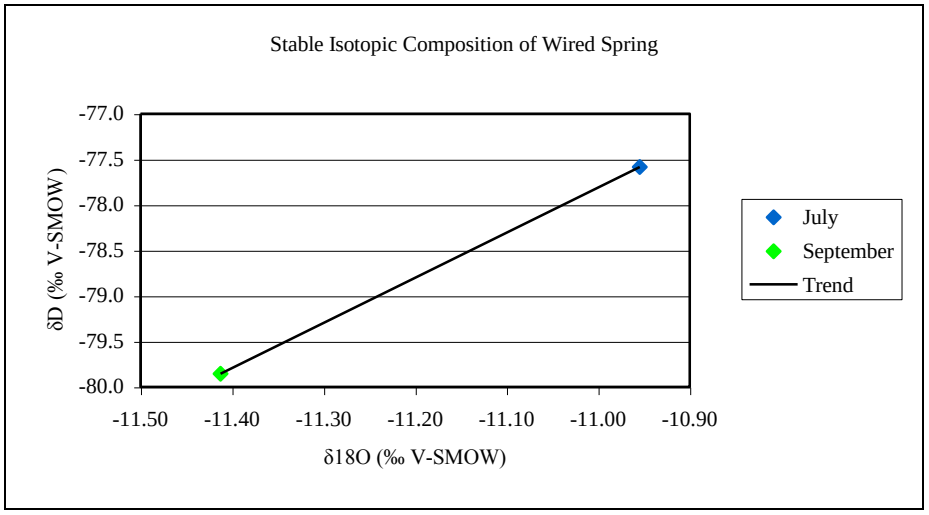

Figure E-4:

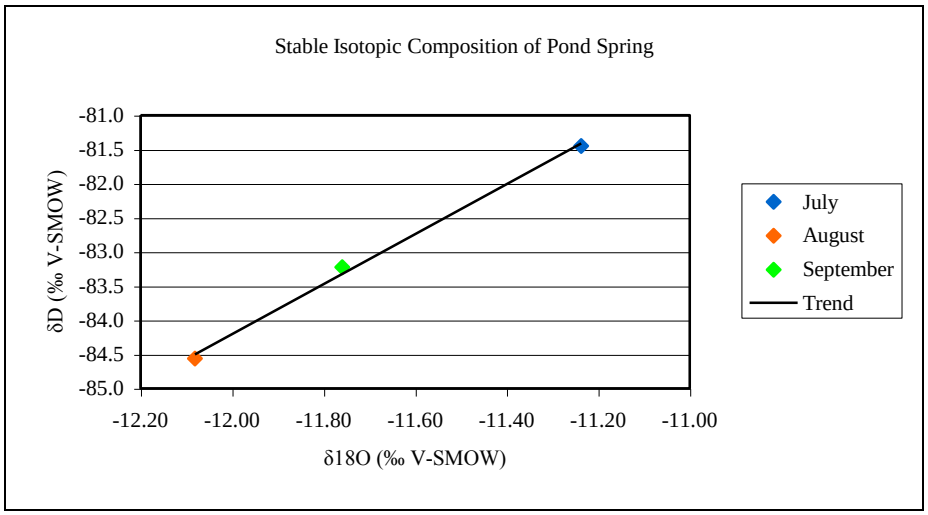

Figure E-5:

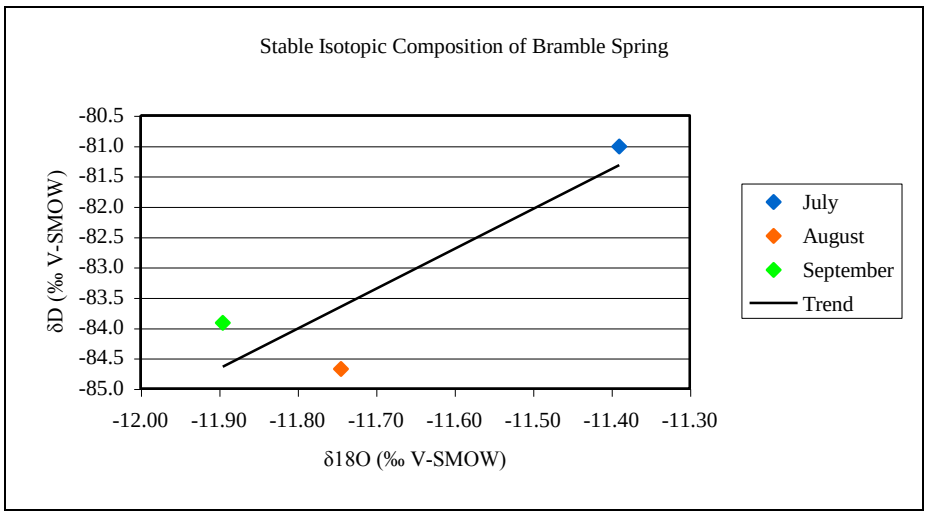

Figure E-6:

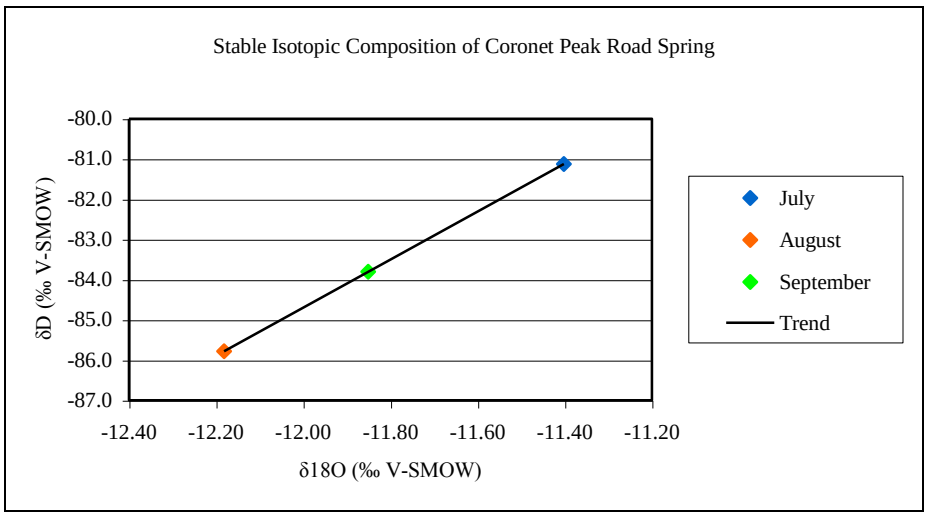

Figure E-7:

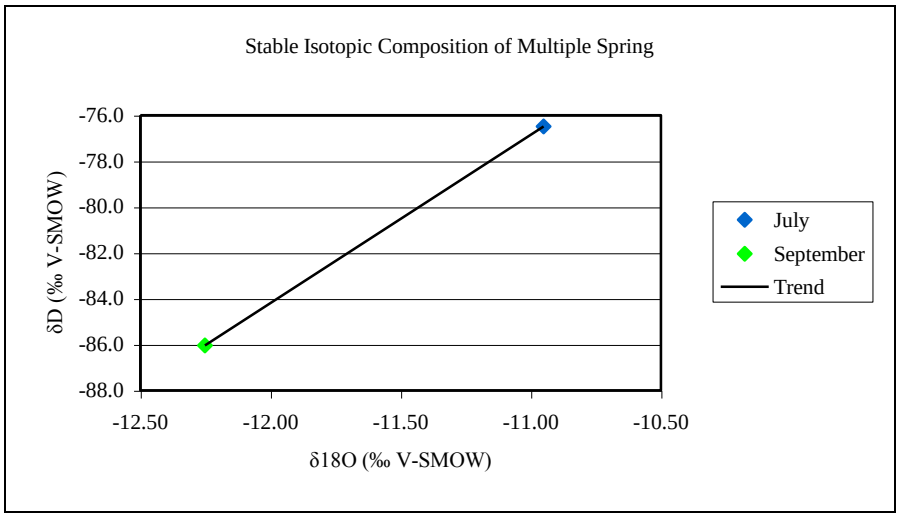

Figure E-8:

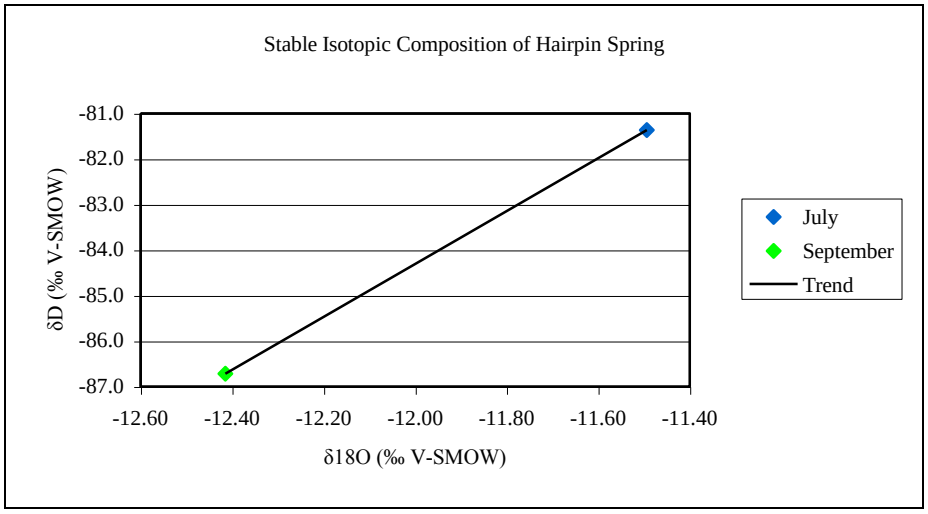

Figure E-9:

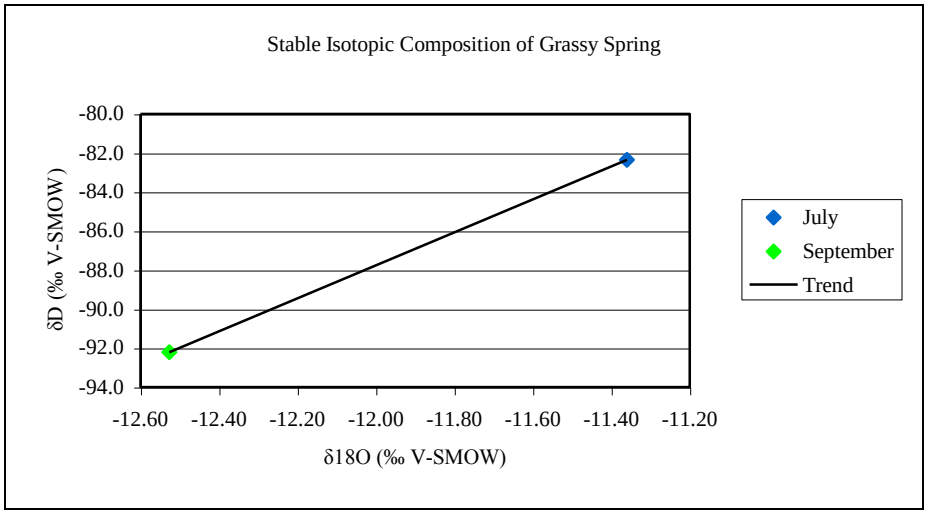

Figure E-10:

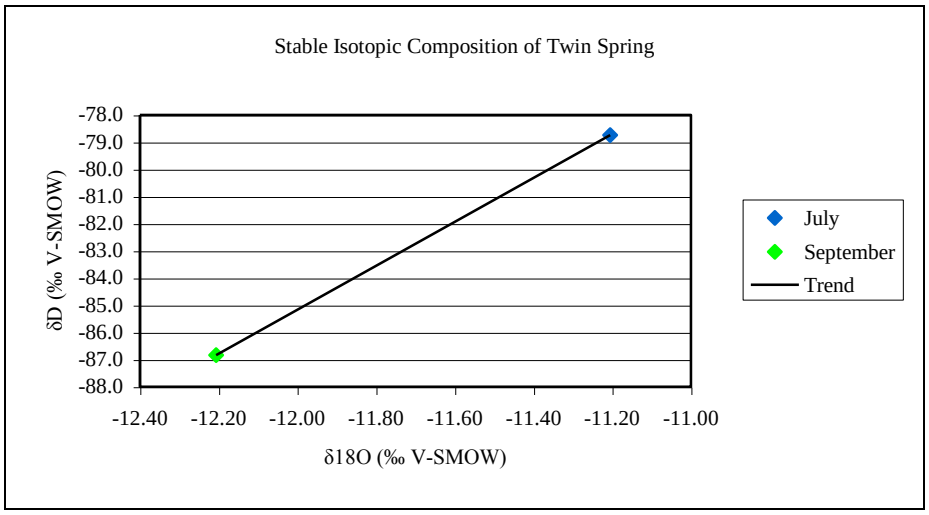

Figure E-11:

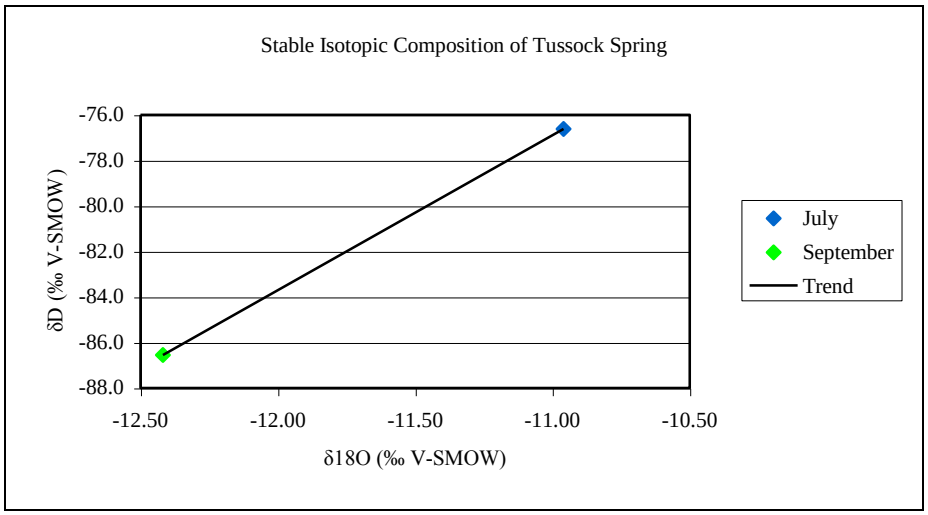

Figure E-12:

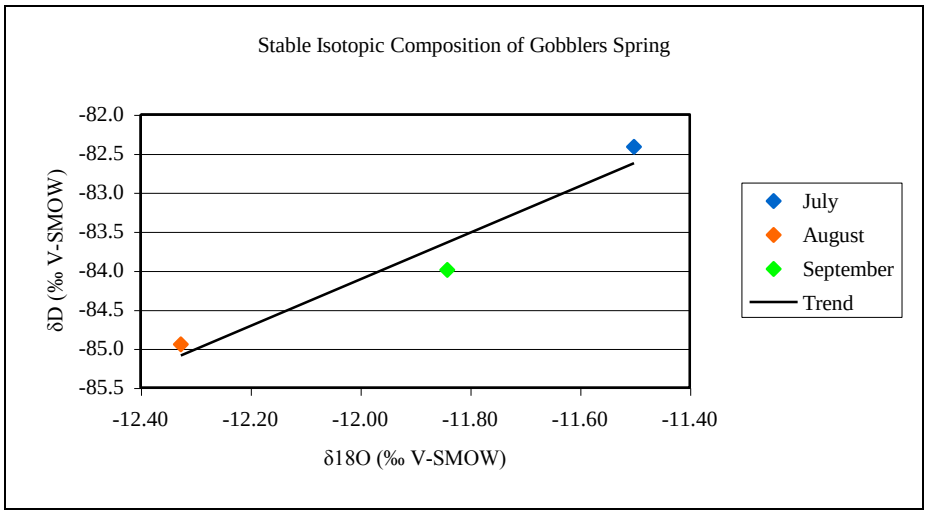

Figure E-13:

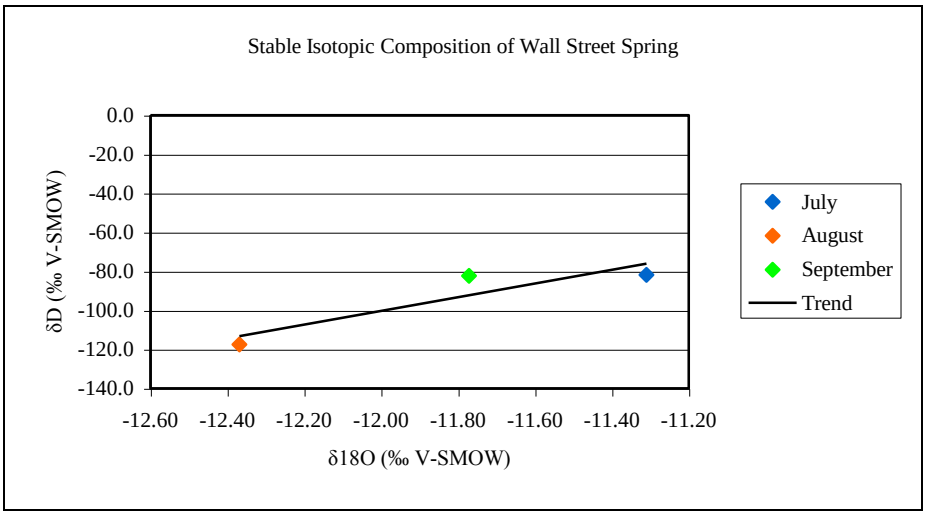

Figure E-14:

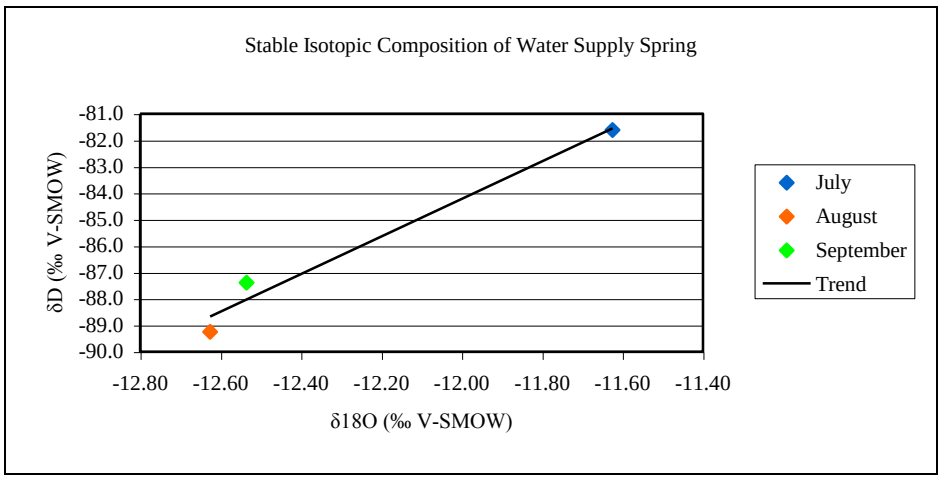

Figure E-15:

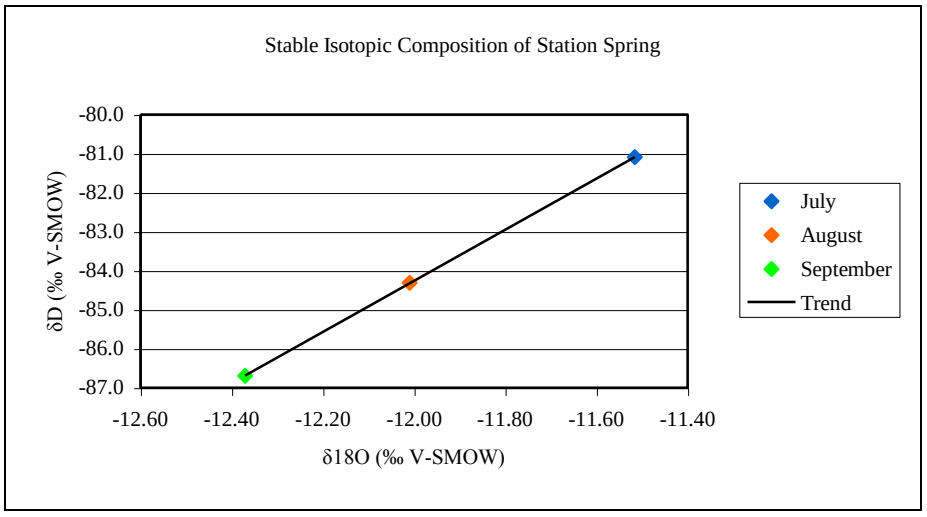

Figure E-16:

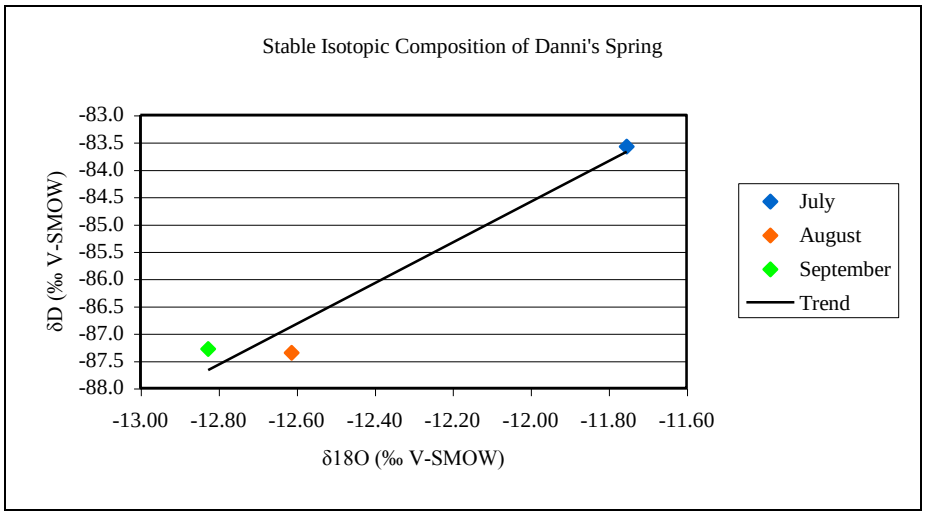

Figure E-17:

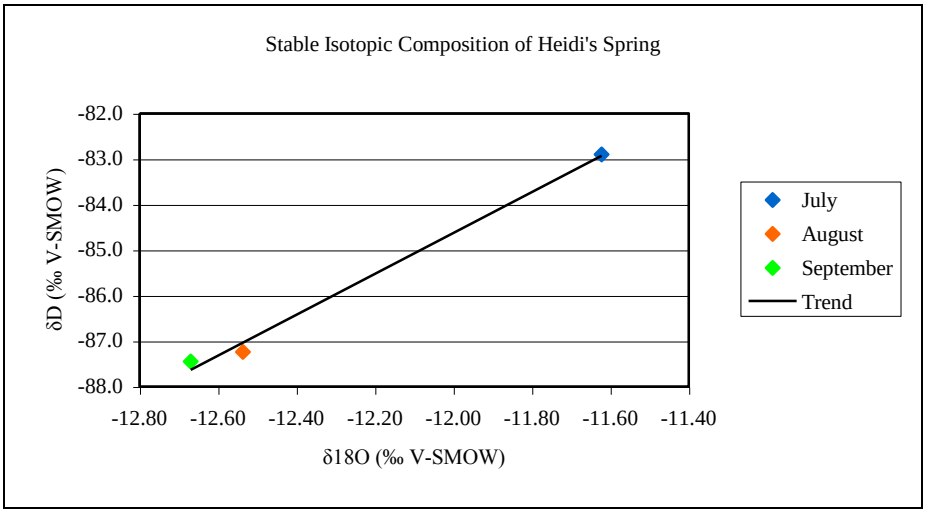

Figure E-18:

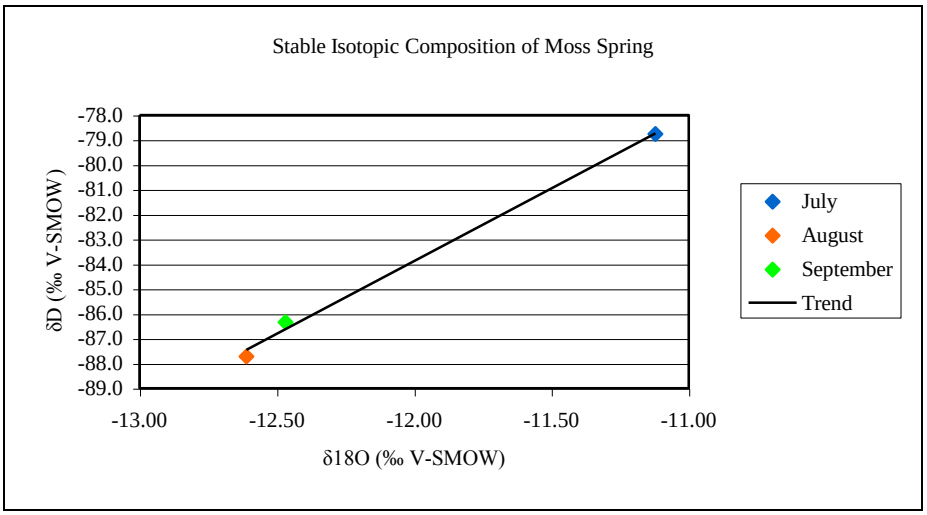

Figure E-19:

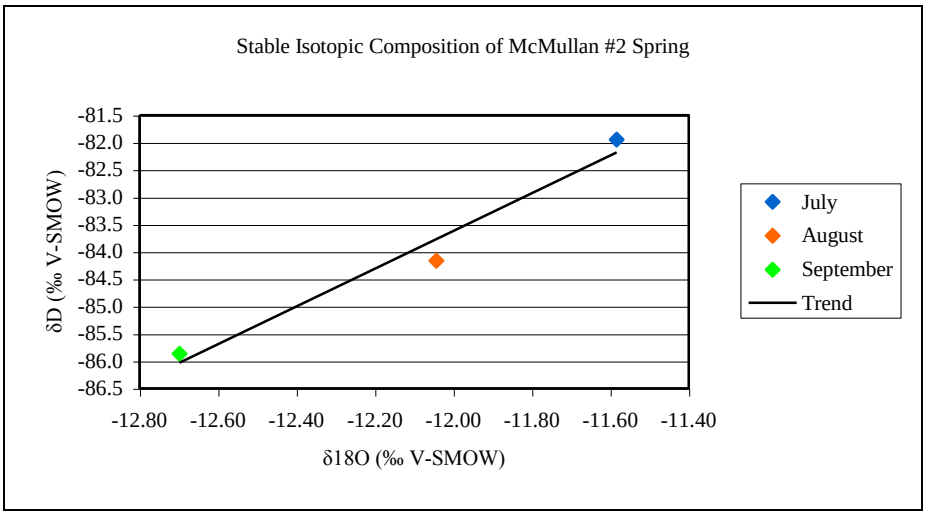

Figure E-20:

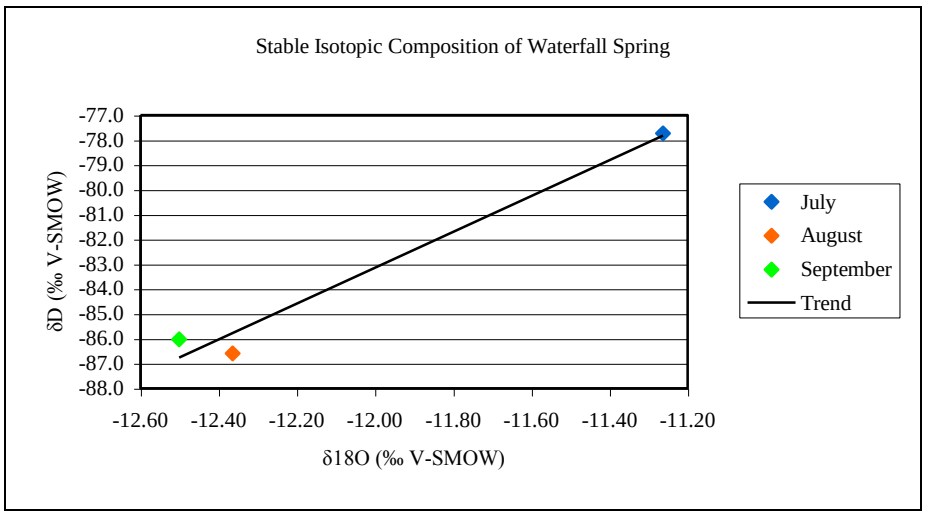

Figure E-21:

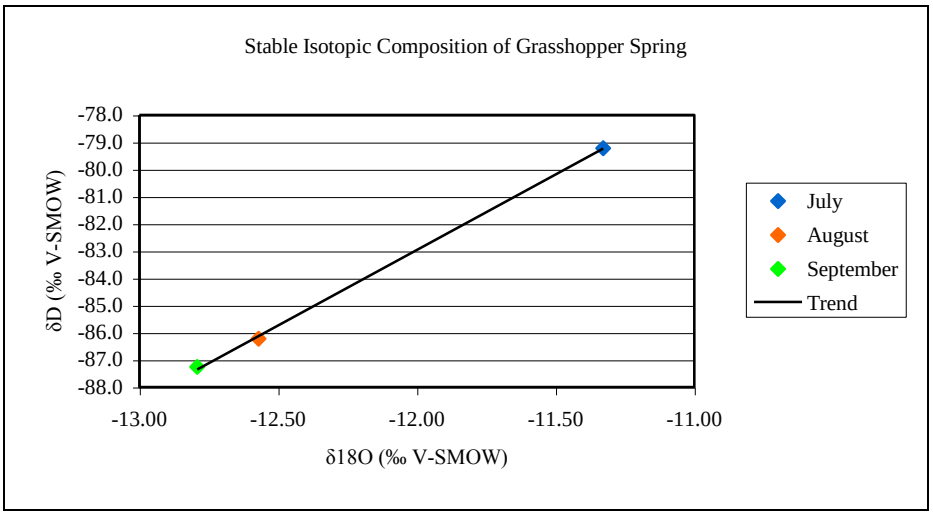

Figure E-22:

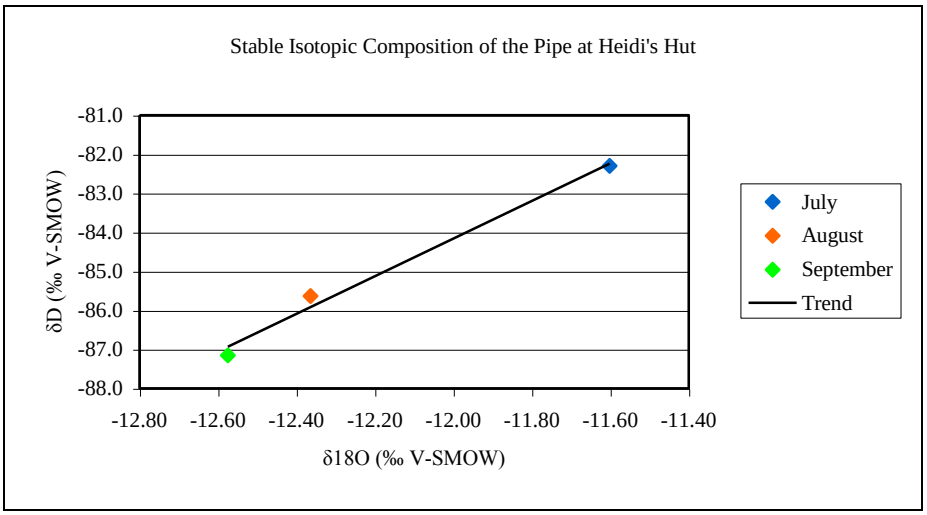

Figure E-23:

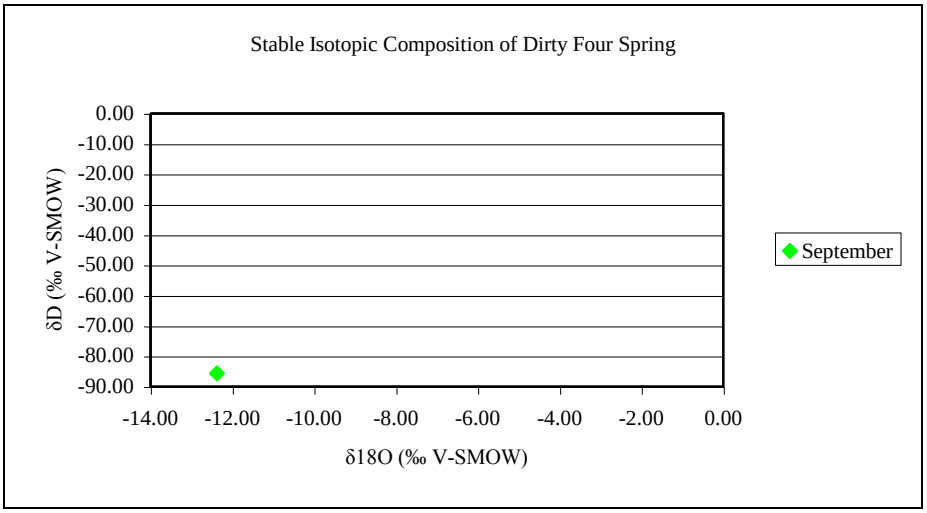

Figure E-24:

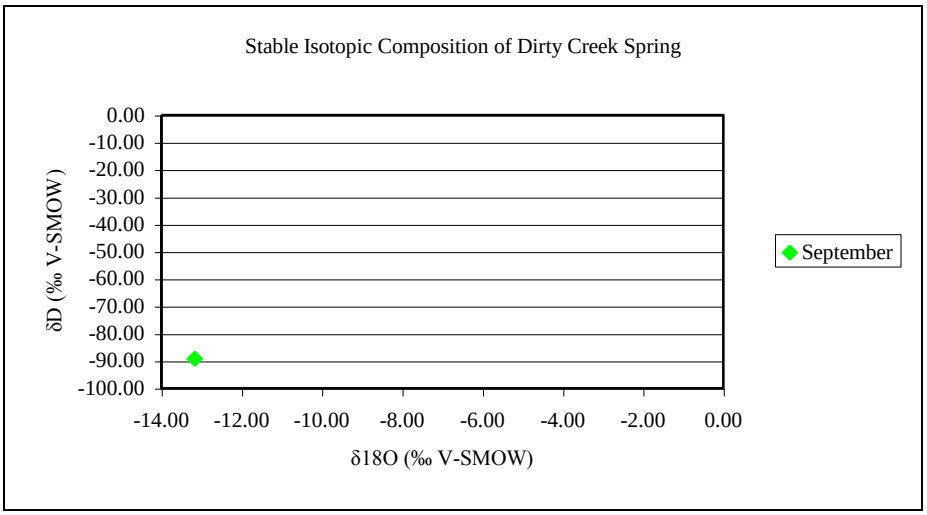

Figure E-25:

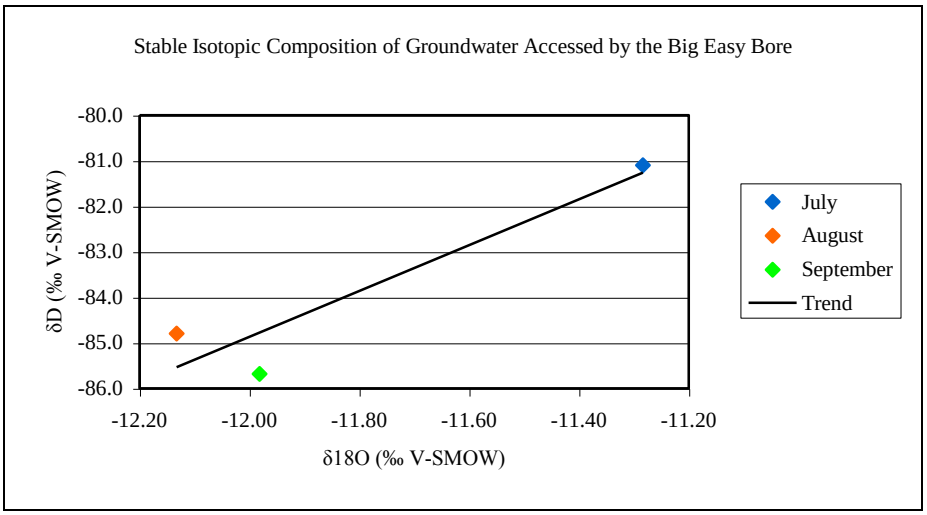

Figure E-26: